Improvement of wave statistics for the prediction of long-term responses of marine structures

Mikulić, Antonio

University of Zagreb
Faculty of Mechanical Engineering and Naval Architecture

Antonio Mikulić

Improvement of wave statistics for the prediction of long-term responses of marine structures

DOCTORAL THESIS

Zagreb, 2023

University of Zagreb
Faculty of Mechanical Engineering and Naval Architecture

Antonio Mikulić

Improvement of wave statistics for the prediction of long-term responses of marine structures

DOCTORAL THESIS

Supervisor: Prof. Joško Parunov, PhD

Zagreb, 2023

Sveučilište u Zagrebu
Fakultet strojarstva i brodogradnje

Antonio Mikulić

Poboljšanje statistike valova za predviđanje dugoročnih odziva pomorskih konstrukcija

DOKTORSKI RAD

Mentor: prof. dr. sc. Joško Parunov

Zagreb, 2023.

BIBLIOGRAPHY DATA

UDC:	629.5:532.5
Keywords:	Marine structures, Ships, Extreme Wave Loads, Extreme Significant Wave Heights, Wave Scatter Diagram, Spatial Correlation, Wave Data Uncertainty, Reliability-based Design, Wave Directionality, Within-Year Wave Climate Variability, Environmental Contours, Adriatic Sea
Scientific area:	Technical sciences
Scientific field:	Naval Architecture
Institution:	University of Zagreb, Faculty of Mechanical Engineering and Naval Architecture
Supervisor:	PhD Joško Parunov, full profesor
Number of pages:	152
Number of figures:	13
Number of tables:	6
Number of references:	69
Date of examination:	November 10, 2023
Evaluation Committee:	PhD Ivan Ćatipović, associate professor PhD Jasna Prpić Oršić, full professor PhD Goran Lončar, full professor
Archive:	University of Zagreb, Faculty of Mechanical Engineering and Naval Architecture

Acknowledgments

Firstly, I would like to express my sincere gratitude to Prof. Joško Parunov for his guidance through my research journey, sharing his experiences and knowledge, and for being a tactful and patient supervisor. Above all, I am thankful for the invested time and his valuable suggestions during pivotal moments, bringing stability and adding value to the final research.

The second thank you goes to the evaluation committee: Prof. Jasna Prpić Oršić, Prof. Goran Lončar, and the chairman Assoc. Prof. Ivan Ćatipović for their valuable time and comments.

I want to thank Assoc. Professors Maro Ćorak and Marko Katalinić, my co-authors in the early stages of the presented research.

Also, I want to thank all my friends and colleagues for their patience, time, and support during the doctoral program.

Since it was a long journey, to keep this reasonably short, I am just going to name some colleagues, hopefully not forgetting anyone, who impacted the presented work. Therefore, in no particular order, I want to thank Ivana Gledić, Ivana Matrić, Andrej Razumić, Andrea Farkas, Andro Bakica, Antun Ivanović, Ivan Batistić, Alen Cukrov, and Space Technology Specialists from the 111 (all current or near-future Dr-s).

I am so thankful for my family, for the love and support, financial and emotional, from my old and young Ivan, and especially my mother Biserka, who sacrifices so much for us and is always there to help.

And my dear Ana... Without her, this would have finished considerably sooner, but it wouldn't be nearly as fun!

Abstract

The aim of the Thesis is to explore possibilities for improvement of the existing long-term wave statistics for the design and analysis of ships and offshore structures. Thus, the effect of spatial correlation among successive sea states along the shipping route, the effects of intra-annual climate variability and wave directionality, the usage of wave data from different sources, and the practical applicability of environmental contours are explored. The introduction of new methods for the improvement of wave statistics is necessary and justified by the appearance and availability of a large amount of data within the hindcast wave databases in the past two decades.

The first goal of the research is to include a spatial statistical correlation between sea states that a ship encounters during a voyage to improve wave scatter diagrams for the analysis of ship structures. The approach consists of the computation of system reliability of a series of partially correlated events, representing sea states that the ship encounters along the sailing route. It was found that a spatial correlation may considerably reduce extreme vertical wave bending moments.

Wave scatter diagrams can be generated from different wave data sources. Hence, a comparative analysis is performed on four different wave data sources collected at the close geographical locations in the Adriatic Sea. Two databases are collected in-situ measurements (RON project and Acqua Alta), while the other two are obtained by wave hindcasting (ERA5 and WorldWaves Atlas).

The extreme significant wave heights predictions often neglect within-year wave climate variability and wave directionality. Depending on a geographical region, local wind patterns and intra-annual climate variability could have an influence on the long-term prediction of waves.

Based on the hindcast wind and wave data, annual extreme significant wave heights generated by different wind patterns and for different months are determined. Combined long-term extremes are then predicted by calculating system probability. It was found that considering the wave directionality, and especially the seasonality of wave climate, leads to a prediction of larger extreme significant wave heights.

Joint distributions consisting of the marginal distribution of significant wave he-

ight and conditional distributions of peak wave periods are used as a basis for the creation of environmental contours using the IFORM and ISORM methods. A possibility of environmental contour practical application to the calculation of global wave loads upon ship structures is presented. Based on the uncertainty assessment performed, conservative environmental contours for the whole Adriatic are developed.

Keywords:
Marine structures, Ships, Extreme Wave Loads, Extreme Significant Wave Heights, Wave Scatter Diagram, Spatial Correlation, Wave Data Uncertainty, Reliability-based Design, Wave Directionality, Within-Year Wave Climate Variability, Environmental Contours, Adriatic Sea

Prošireni sažetak

I Uvod

Opterećenja za projektiranje pomorskih konstrukcija uključuju valove, vjetar, morske struje, led te razinu morske vode. Budući da morski valovi obično predstavljaju dominantan tip opterećenja, predviđanje valova i s njima povezane nesigurnosti presudne su za procjenu opterećenja i odziva pomorskih konstrukcija. Značajke stanja mora ovisne su o regiji i lokaciji te su statistički stacionarni tijekom kratkog vremenskog razdoblja, dok je pretpostavka kako se dugoročna klima valova modelira kao veliki broj uzastopnih stacionarnih, kratkoročnih stanja mora. Za definiranje valnih opterećenja u fazama projektiranja i eksploatacije brodova koriste se statistike valova dobivene iz raznih izvora, koje uglavnom dovode do različitih proračunatih opterećenja pomorskih konstrukcija. Ta se odstupanja u opterećenjima koje nastaju kao posljedica pretpostavki u modeliranju okoliša trebaju uzeti u obzir u postupku racionalnog projektiranja i analize pomorskih konstrukcija u vidu nesigurnosti ili neizvjesnosti.

Prilikom projektiranja i proračuna pomorskih konstrukcija, valno okruženje se obično opisuje pomoću tablice stanja mora koja sadrži združene vjerojatnosti pojavljivanja značajnih valnih visina i prosječnih (ili vršnih) valnih perioda. Za stacionarne pučinske konstrukcije tablice stanja mora su često dostupne za određene lokacije te se izračun dugoročne raspodjele valnih opterećenja ili njihovih ekstremnih vrijednosti može provesti provjerenim inženjerskim metodama [1]. Za brodove je pak problem ponešto složeniji zbog njihove plovidbe različitim akvatorijima te nepredvidivog ljudskog djelovanja [2]. Poznavanje nesigurnosti uslijed proračunskih postupaka za predviđanje odziva pomorskih objekata na valovima i posljedičnih valnih opterećenja osobito je važno danas, kada direktne proračunske metode postaju gotovo standardni inženjerski alat u projektiranju i analizi sigurnosti konstrukcija.

Prilikom analize brodskih konstrukcija, uobičajena praksa nalaže korištenje pomorskog atlasa Global Wave Statistics (GWS) [3] kao izvora podataka o statistici valova. Podaci iz GWS baze sakupljeni su dugogodišnjim promatranjem dobrovoljaca s trgovačkih brodova duž uobičajenih brodskih plovidbenih ruta. Brod prelazi

različite valne zone različitim brzinama, stoga je valne podatke potrebno kombinirati. Postupak spajanja različitih valnih zona u zajedničku tablicu stanja mora dostupan je u IACS-ovim (Međunarodna udruga klasifikacijskih društava) preporukama br. 34. [4].

Podaci o valovima očitani iz IACS tablice stanja mora u Sjevernom Atlantiku zanemaruju mjesečnu i sezonsku varijabilnost jer se odnose na cijelu godinu. Zapravo, nedostaje istraživanja koja bi odredila posljedice na opterećenja brodova ako se dugoročna analiza provede za pojedine mjesece, sezonu ili određeni obrazac vjetra i zatim kombinira u cjelogodišnje rezultate [5].

U analizi valnih opterećenja brodskih konstrukcija koristi se i pretpostavka statističke nezavisnosti kratkoročnih stacionarnih stanja mora s kojima se brod susreće tijekom određenog putovanja. Ova je pretpostavka dvojbena zbog očite korelacije između uzastopnih stanja mora na određenoj ruti. Mogući pristup prevladavanju ovog problema je predložen u [6], gdje se pojedine valne zone na ruti broda razmatraju kao dijelovi probabilističkog lanca. Glavni izazov predstavlja kvantificiranje koeficijenta korelacije takvog sustava.

Tablice stanja mora se mogu definirati koristeći različite izvore podataka. Osim vizualnim opažanjima, podaci o valovima dobivaju se mjerenjima s valnih plutača, nepokretnih oceanografskih tornjeva, radarima, laserima, stereo kamerama itd. [7]. Valne plutače i oceanografski tornjevi smatraju se najtočnijim mjernim izvorom podataka. Međutim, kod primjene na brodskim konstrukcijama imaju nedostatak jer se plutače nalaze van glavnih plovidbenih ruta i često su uslijed kvarova dulje vrijeme izvan upotrebe. Acqua Alta u sjevernom Jadranu predstavlja rijedak primjer neprekinutih dugoročnih mjerenja valova s oceanografskog tornja [8]. Posljednjih desetljeća, satelitska mjerenja su postala važan izvor valnih podataka. Numerički valni modeli treće generacije (WAM, SWAN, ...) koriste se za predviđanje valova na temelju podataka o polju vjetra. Numerički valni modeli prikladno kalibrirani satelitskim mjerenjima smatraju se danas najsveobuhvatnijim izvorom podataka za dugoročni opis klime valova [7]. Numerički podatci dobiveni valnim modelima karakterizirani su značajnim nesigurnostima uzrokovanim različitim prostornim i vremenskim rezolucijama. Odabir tablica valova dobivenih iz raznih izvora rezultira međusobnim odstupanjima u predviđenim dugoročnim odzivima brodova i pučinskih objekata [1]. To može imati posljedice na sigurnost konstrukcije s obzirom na njenu dinamičku izdržljivost i graničnu čvrstoću [9, 10].

Konturni dijagrami valnog okoliša predstavljaju racionalan pristup definiranju ekstremnog stanja mora, opisanog značajnim valnim visinama te vršnim valnim periodima. Konturnim dijagramima valova se opisuju kombinacije visina valova i valnih perioda koje rezultiraju određenom malom vjerojatnošću premašivanja odziva pomorskih konstrukcija. Konturni se dijagrami razmatraju kao alternativa tablicama stanja mora kod analize pouzdanosti i projektiranja pomorskih konstrukcija. Nesigurnosti konturnih dijagrama se javljaju kao posljedica različiti metoda i pretpostavki koje se koriste pri njihovu definiranju [11].

II Cilj i hipoteze istraživanja

Cilj ovog rada je predložiti unapređenje postojeće statistike valova s ciljem poboljšanja analize dugoročnih odziva pomorskih konstrukcija.

Hipoteze:

1. Razmatranje prostorne korelacije između stanja mora na ruti broda može dovesti do pouzdanije analize dugoročnih odziva broda.

2. Usporedna analiza valnih podataka prikupljenih iz različitih izvora te razmatrajući mjesečne i sezonske promjene omogućit će kvantificiranje nesigurnosti dugoročne prognoze odziva.

3. Za područje Jadranskog mora mogu se korištenjem suvremenih simulacijskih postupaka definirati konturni dijagrami valnog okoliša, korisni za karakterizaciju ekstremnih odziva pomorskih konstrukcija.

III Materijali i metode

Učinci prostorne korelacije kratkoročnih stanja mora analizirani su pretpostavljajući značajne visine valova duž plovidbene rute u Sjevernom Atlantiku kao korelirane članove serijskog vjerojatnosnog sustava s pretpostavljenim koeficijentom korelacije. Razdioba vjerojatnosti značajnih valnih visina je modelirana tro-parametarskom Weibullovom razdiobom. Monte Carlo simulacija korištena je za generiranje tablice stanja mora iz zajedničke razdiobe vjerojatnosti valnih visina i perioda.

Dugoročne baze podataka dobivene na temelju satelitskih mjerenja, po-tvrđenih in-situ mjerenjima pomoću valnih plutača i simuliranih numeričkim modeliranjem

valova glavni su izvor podataka korišten u istraživanju. Primjer jedne takve baze je Oceanor World Waves Atlas, koji sadrži podatke za 39 ravnomjerno raspoređenih lokacija u Jadranskom moru. Za svaku lokaciju dostupno je dvanaest fizikalnih parametara vjetra i valova u intervalima od šest sati (četiri na dan). Podatci su dostupni za period od 28 godina počevši od siječnja 1992. do prosinca 2019. Slična baza otvorenog pristupa je ERA5 baza, koja sadrži podatke za svjetska mora.

Komparativna analiza valnih podataka iz različitih izvora je provedena za lokaciju u Jadranskom moru, gdje su dostupne četiri dugoročne baze podataka o valovima. Uz Oceanor i ERA5 baze, in-situ mjerenja za komparativnu studiju dostupna su s valne plutače iz projekta RON te s oceanografskog tornja Acqua Alta.

Nesigurnosti vezane za mjesečne i sezonske varijabilnosti istražene su korištenjem podataka za Jadransko more iz Oceanorove baze podataka. Dugoročna razdioba značajnih valnih visina je određena vjerojatnosnim kombiniranjem ekstremnih vrijednosti određenih za svaki mjesec te uspoređena s konvencionalnom metodom gdje se uzimaju u obzir prosječne godišnje ekstremne vrijednosti stanja mora. Sličan pristup korišten je i za razmatranje učinka uzorka vjetra, gdje su dugoročne raspodjele definirane odvojeno za valove generirane vjetrovima Bure, Juga, Maestrala i Lebića. Metoda je korištena i za procjenu utjecaja mjesečnih varijabilnosti na ekstremne vrijednosti stanja mora uzduž prekooceanskih ruta brodova. Određene su i posljedice koje mjesečne varijabilnosti mogu imati na ekstremna globalna valna opterećenja brodskih konstrukcija.

Koristeći podatke iz Oceanor baze kreirani su konturni dijagrami valova i perioda Jadranskog mora primjenom IFORM i ISORM metoda. Također su istražene nesigurnosti konturnih dijagrama uslijed primjene različitih inicijalnih razdioba vjerojatnosti značajnih valnih visina. Predložen je način kombiniranja konturnih dijagrama i ekstremnih valnih opterećenja brodskih konstrukcija.

Polu-analitički izrazi za prijenosne funkcije, kao i uobičajene metode određivanja kratkoročnih i dugoročnih ekstremnih vrijednosti odziva brodskih konstrukcija, su korišteni za brzo dobivanje procjena odziva broda, što je prikladno za konceptualne analize u okviru predstavljenog istraživanja.

IV Rezultati

Tablice stanja mora koje uzimaju u obzir utjecaj korelacije su određene za različite koeficijente korelacije, od kojih su dvije prikazane u Tablici 3.1 i 3.2 (**Publication I**, [12]). Utjecaj korelacije na ekstremna dugoročna valna opterećenja ispitan je na tankerima za prijevoz nafte različitih veličina. Rezultati sugeriraju smanjenje opterećenja kod porasta korelacije neovisno o veličini broda, što je prikazano na Slici 3.1, gdje se vidi da je smanjenje ekstremnog valnog momenta savijanja 10% - 15% , za koeficijent korelacije 0,8 - 0,9. Rezultati su validirani na način da su izračunate razdiobe vjerojatnosti vizualnih opažanja stanja mora s uključenim utjecajem korelacije uspoređeni s podatcima iz ERA5 baze za isto područje plovidbe, gdje je pokazano da su gustoće vjerojatnosti preklapaju za koeficijent korelacije od 0,8.

Utjecaj izvora podataka na odzive pomorskih konstrukcija je proveden komparativnom analizom stanja mora i odziva za četiri različita izvora podataka o valovima prikupljenih na bliskim geografskim lokacijama u Jadranskom moru (**Publication II**, [13]). Dvije baze podataka dobivene su in-situ mjerenjima (valna plutača RON, oceanografski toranj Aqua Alta), dok su dvije numeričke baze podataka valova (ERA5 i WWA). Utjecaj nesigurnosti na različite aspekte projektiranja pomorskih konstrukcija je značajan. Dugoročne razdiobe valnog opterećenja barže su prikazane na Slici 3.2, gdje se ekstremne vrijednosti za povratno razdoblje od 25 godina razlikuju za 30%. Najveći utjecaj različiti izvori podataka imaju na akumulirani zamor materijala, gdje se procijenjeni životni vijek može razlikovati i do 3,3 puta. Pokazano je i da se ukupni energetski potencijal na nekoj lokaciji može bitno razlikovati, ovisno o valografskoj bazi podataka koja se koristi.

Utjecaj varijabilnosti klime valova unutar godine određen je za različite prekooceanske rute brodova (**Publication III**, [14]) i za Jadransko more (**Publication IV**, [15]). U oba su slučaja dobivene značajne razlike ako se ekstremne vrijednosti prikupljaju za svaki mjesec, pa zatim kombiniraju na godišnjoj razini, u odnosu na slučaj kad se samo godišnje ekstremne vrijednosti analiziraju. U najvećem broju slučajeva su ekstremi veći kad se uzimaju u obzir mjesečne varijacije nego kad se zanemare. Rezultati usporedbe razdiobe značajnih valnih visina za dvije lokacije u Sjevernom Atlantiku su prikazane na Slici 3.5 (**Publication III**, [14]). Utjecaj smjera vjetra je analiziran za Jadransko more i manji je od utjecaja mjesečnih varijacija valova (**Publication IV**, [15]). Analiza raspodjela godišnjih maksimuma po smjerovima nailaska ukazuje na dominaciju valova bure na sjevernoj i duž zapadne

obale Jadrana, dok jugo dominira preostalim područjem. Na najjužnijim lokacijama, u blizini Otrantskog tjesnaca, jak je utjecaj Jonskog mora, što uzrokuje mješavinu različitih sustava vjetrova i valova. Posljedično, na tim mjestima valni ekstremi nisu nužno pod dominantnim utjecajem juga ili bure.

Konturni dijagrami valnog okoliša, opisujući kombinacije značajnih valnih visina i vršnih valnih perioda, definirani su za čitavo područje Jadranskog mora korištenjem IFORM i ISORM metoda. Pokazano je da je ISORM očekivano konzervativnija metoda u svim slučajevima. Primjer kontura je prikazan na Slici 3.9 (**Publication V**, [16]). Pokazano je da na oblik konturnih dijagrama veliki utjecaj ima parametar γ Weibullove 3-parametarske razdiobe, čije je određivanje često nepouzdano. Konturni dijagrami su prikazani zajedno s dijagramima ekstremnih vrijednosti momenata savijanja na valovima, ukazujući na mogućnosti praktične primjene konturnih dijagrama kod određivanja ekstremnih valnih opterećenja.

V Zaključak

U doktorskom radu su istražene napredne metode za poboljšanje statistike valova pri projektiranju i analizi pomorskih konstrukcija, uključujući korelaciju između stanja mora, unutargodišnju promjenjivost klime valova, utjecaj smjera valova te primjenu konturnih dijagrama valnog okoliša. Primjena novih metoda je potrebna zbog dostupnosti baza podataka o valovima visoke prostorne i vremenske razlučivosti, koje se postupno uvode kod projektiranja brodskih i pomorskih konstrukcija.

Korelacija između uzastopnih stanja mora koja brod susreće na ruti je iskorištena za prilagodbu tablica stanja mora, koje vode do značajnog smanjenja maksimalne značajne valne visine te sukladno tome i dugoročne raspodjele valnih opterećenja. Pokazano je da se može očekivati smanjenje ekstremnih vertikalnih valnih momenata savijanja za 10% - 15% za realne koeficijente korelacije.

Utjecaj izvora podataka o valovima na odzive pomorskih konstrukcija može biti značajan, pogotovo na akumulirano zamorno oštećenje, koje se može razlikovati za više od 3 puta ako se koriste različite baze s podatcima o valovima prikupljenima na istoj lokaciji. Ekstremne vrijednosti globalnog valnog opterećenja mogu međusobno odstupati do 30%, a različiti izvori podataka mogu rezultirati i bitno drugačijim procjenama energetskog potencijala valova na datoj lokaciji.

Ukoliko se uključi u analizu, utjecaj varijabilnosti klime valova unutar godine

može promijeniti ekstremne dugoročne valne momente savijanja brodova do 10 %, a najčešće dolazi do povećanja valnog opterećenja. Rezultati dobiveni za prekooceanske rute su potvrđene i za specifični akvatorij Jadranskog mora, za koji je određen i utjecaj usmjerenosti valova na ekstremne vrijednosti značajnih valnih visina. Utjecaj smjera valova na ekstremne vrijednosti je primjetan, ali manji od utjecaja mjesečnih varijabilnosti.

Konturni dijagrami valova i perioda definirani su za čitavo područje Jadranskog mora, i mogu se preporučiti za primjenu u inženjerskoj praksi. Konture za povratno razdoblje od 25 godina su primjenjive za projektiranje brodskih konstrukcija, a one za povratno razdoblje od 100 godina za projektiranje odobalnih pomorskih konstrukcija. Jednogodišnje konture su primjenjive za planiranje posebnih pomorskih operacija (npr. prijevoz teških tereta). ISORM metoda je preporučena za definiranje konturnih dijagrama jer je konzervativna u odnosu na IFORM metodu.

VI Izvorni znanstveni doprinos

Izvorni znanstveni doprinosi provedenog istraživanja:

1. Unaprijeđena je tablica stanja mora za analizu brodskih konstrukcija, definirana uzimjaući u obzir korelaciju između stanja mora koje brod susreće tijekom plovidbe.

2. Kvantificirane su nesigurnosti dugoročnih razdioba vjerojatnosti stanja mora i pripadajućih odziva pomorskih konstrukcija, uzrokovanih korištenjem podataka o valovima iz različitih izvora te razmatranjem mjesečne i sezonske varijabilnosti klime valova.

3. Definirani su konturni dijagrami valova za Jadransko more te predložena njihova primjena za predviđanje ekstremnih odziva pomorskih konstrukcija.

Ključne riječi:
Pomorske konstrukcije; Brodovi; Ekstremna valna opterećenja; Ekstremne značajne valne visine; Tablica stanja mora; Prostorna korelacija; Nesigurnost podataka o valovima; Projektiranje na osnovi pouzdanosti; Usmjerenost valova; Unutargodišnja varijabilnosti valne klime; Konturni dijagrami okoliša; Jadransko more

Abbreviations

3D Three Dimensional
ASSM All sea state method
C&C Carter and Challenor
CDF Cumulative distribution function
CE Closed-form expression
DM Directional maxima
DSSM Design sea state method
EC Environmental contour
ECMWF European Centre for Medium-Range Weather Forecasts
GWS Global Wave Statistics
IACS International Association of Classification Societies
IFORM Inverse first-order reliability method
ISORM Inverse second-order reliability method
LSQ Least squares fit
MC Monte Carlo
MLE Maximum likelihood estimation
MM Monthly maxima
NA North Atlantic
PDF Probability density function
SWH Significant wave height
VWBM Vertical wave bending moment
WWA World Waves Atlas

Contents

List of figures

List of tables

1. Introduction

Loads relevant for the design of marine structures include waves, wind, current, sea water level, and ice. Since sea waves usually represent the dominant load source, wave prediction, and associated uncertainties are crucial for the assessment of loads and responses of marine structures. Characteristics of a sea state are region- and location-dependent, and for a limited period, they vary in a stationary way, while the long-term wave environment is assumed to consist of a large number of stationary, short-term sea conditions. Different wave data sources are used for defining design and operational criteria for ships, and also, different uncertainties are related to them. Significant efforts have been made to explain the consequences of uncertainties in wave data on the prediction of wave-induced motions and loads of marine structures [17].

The wave environment for the design and analysis of marine structures is commonly described using scatter diagrams (e.g., Figure 1.1). A wave scatter diagram is a table containing probabilities of the occurrence of sea states described by a combination of significant wave heights and mean zero-crossing (or peak) wave periods. For fixed offshore structures, wave scatter diagrams are often available for specific locations, and the computation of the long-term distribution of wave loads or their extreme values may be done by well-established engineering methods [1]. For ships, however, the problem is more complicated because of their mobility and because of the unpredictable human actions [2]. This is particularly important nowadays when direct computation methods of wave loads gradually replace simplified rule formulations in the design of ship structures.

There are two methods recommended by the literature [18] for the analysis of extreme wave loads. The design sea state method (DSSM) performs wave loads analysis on a selected short-term sea state condition called design sea state, while the all sea state method (ASSM) calculates the most probable extreme value considering the probability of occurrence of all sea states. The former method is usually used in the design of offshore structures, while the latter is recommended by the International Association of Classification Societies (IACS) for the analysis of ship structures [4]. However, even in cases when ASSM is used, knowledge of extreme sea

states corresponding to long return periods is useful to describe the severity of the wave environment where marine structure operates. The return period of extreme sea states for the design of offshore structures is very often 50, 100, or even 1000 years, while the return period of sea states for ship structural design reads 25 years.

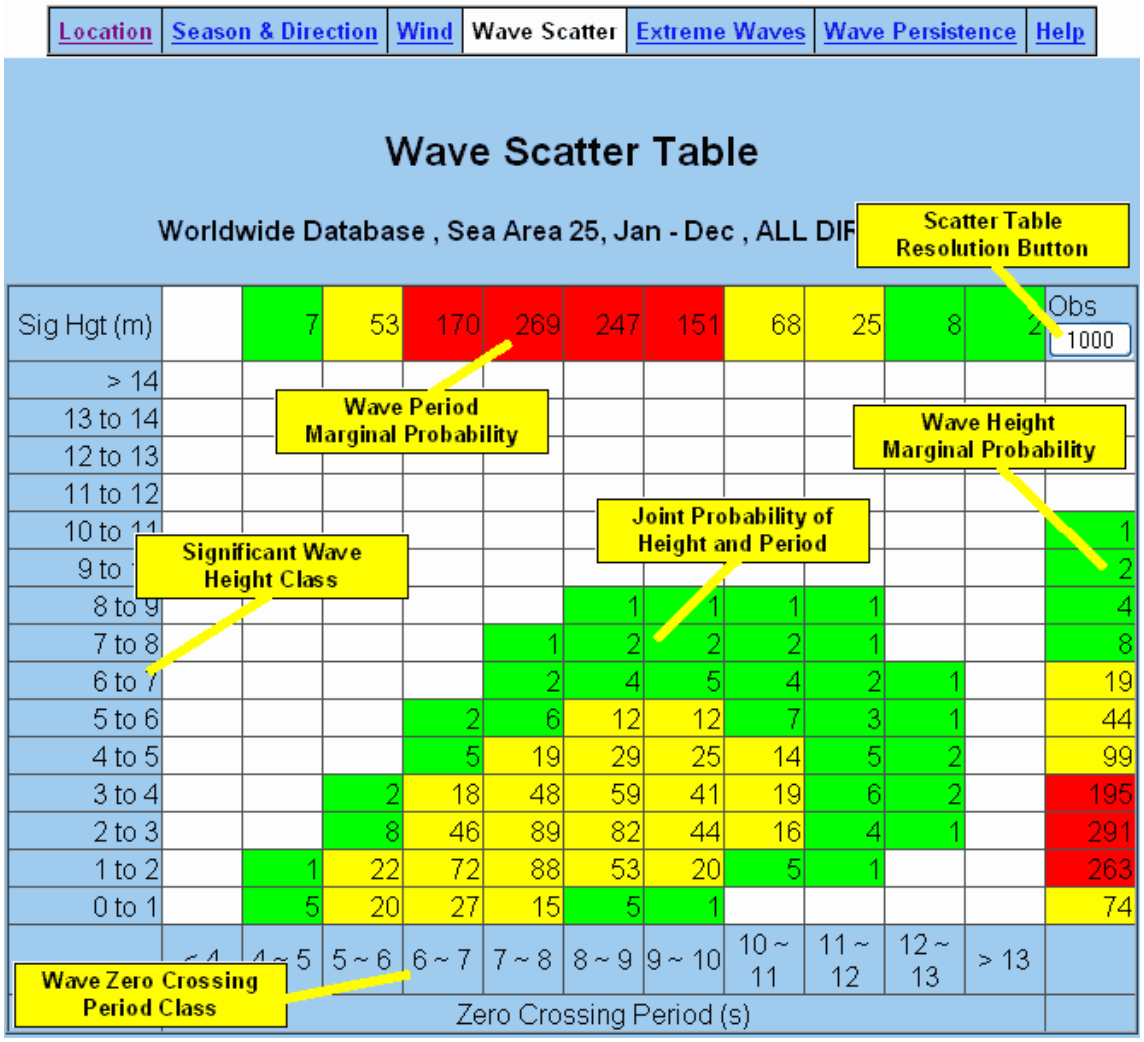

Figure 1.1. The wave scatter diagram. Source: Global Wave Statistics Online

Environmental contours (ECs) represent a rational approach for defining an extreme sea state condition, described by environmental variables (e.g., Figure 1.2). The idea of environmental contours is to provide combinations of wave heights and periods that could result in the marine structures' response with a certain exceeding probability. The environmental contour method has the goal of summarizing the tail of the joint distribution of environmental variables to capture the distribution of extreme structural response within a prescribed return period [1].

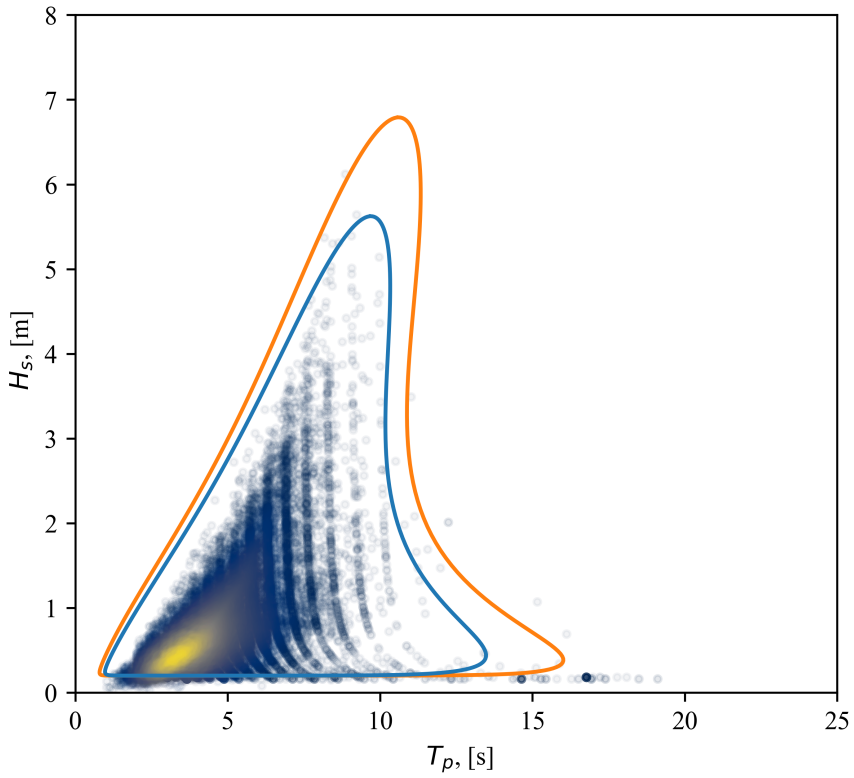

Figure 1.2. Environmental contours. The 25-year IFORM (blue) and ISORM (orange) contour. Heat-map circles represent wave data density. (Source: Publication V [16])

Closed-form expressions (CFEs) developed by Jensen et al. [19] represent a simple method for calculating transfer functions of wave-induced motions and global loads of the monohull ship. CFEs are particularly suitable for seakeeping predictions in the conceptual design, enabling a rapid sensitivity analysis regarding the operating profile and the wave scatter diagram [20]. As the extensive comparison with other seakeeping methods and experiments showed that CFEs provide seakeeping responses with reasonable accuracy, they are used in the present study [21].

The present Thesis combines these methods aiming to provide a rational basis for the definition of long-term wave statistics. The work is primarily oriented toward the improvement of the existing wave statistics for ship structures, although most of the methods are general and can be used for site-specific offshore structures as well.

1.1. State of the Art

For the analysis of ship structures, a common practice has been using probabilities of occurrence of sea states from the wave atlas Global Wave Statistics (GWS) [3]. Data in GWS are obtained by observations of volunteers from merchant ships on the usual shipping routes. As elaborated firstly by [22] such choice is more rational compared to using data from fixed measurements since those data implicitly account for the worldwide practices of shipmasters operating along the main shipping routes. Using data measured on stationary wave buoys tends to overestimate wave loads on ship structures since the effect of heavy weather avoidance is not explicitly accounted for [23]. Another drawback of wave buoys is that they are often out of service for an extended period. A rare example of uninterrupted long-term wave measurements from a fixed oceanographic tower is Aqua Alta in the North Adriatic Sea [8]. In the past decades, satellite measurements have become an important source of wave data. Numerical wave models of third generation (WAM, SWAN, ...) are used to model waves based on the wind field data. Wave data hindcasting is the process of running a wave model backward and calibrating it based on available measurements. Numerical wave models appropriately calibrated by satellite measurements are considered as the state-of-the-art source of data for long-term description of wave climate [24]. Hindcast data obtained by wave models are characterized by uncertainties caused by different spatial and temporal resolutions. Selecting data from different sources in the construction of the wave diagram results in differences in predicted long-term responses of ships and offshore structures [17]. This can have consequences on the structural safety regarding fatigue and ultimate limit states [9]. The latest revision of the IACS Recommendation note. No.34 [25] uses wave hindcast database to define standard North Atlantic (IACS NA) wave scatter diagram for analysis of wave-induced loads on ships [26].

To analyze the influence of data from different sources on the responses of marine structures, data availability for the same locations and long-term measurement periods are crucial. The Fugro Oceanor World Waves Atlas (WWA) and ERA5 databases are obtained by numerical wave model hindcasting based on satellite measurements and validated by in-situ measurements from wave buoys [27, 28]. They contain data for 39 uniformly distributed locations across the Adriatic Sea, with wave and wind parameters provided at each location (Figure 1.3). A detailed description of the two databases is available in Section 2.6. The WWA database was

subjected to extensive analysis in the recent past. First, wave statistics based on WWA are developed in [29] for one location in the middle of the Adriatic Sea. The analysis is extended in [30] modeling joint probability distribution of significant wave heights and peak spectral periods for three geographical locations along typical sailing route in the Adriatic and defining extreme sea states. Finally, the analysis of extreme values is extended for all 39 grid points in the Adriatic basin [31]. In-situ measurements for comparative study are available from the RON project and Acqua Alta oceanographic tower. Within RON, four wave-buoys along the western Adriatic coast off the cities of Monopoli, Ortona, Ancona, and Venezia were operational during the period 2009 - 2014 with occasional breaks due to failure or service intervals [32]. Acqua Alta is one of the oldest and most comprehensive wave datasets in the world. The measuring tower is located 16 km off the coast of Venice (lat./long. 45.3°N - 12.5°E) at a depth of 16 meters. Measurements include 39 years of data (438 912 measurements) at three-hour time intervals starting from 1979 to 2017 [33]. It is to be noted that the existence of multiple data sources at the same geographical location makes them convenient for the comparative analysis of the long-term wave-induced responses of ships and offshore structures. As wave statistics from several sources are available for the location in the north Adriatic Sea, it is used to assess consequences on the design and analysis of marine structures. Also, because of the rich previous experience with the analysis of wave conditions in the Adriatic Sea using the WWA database provided by Fugro Oceanor, these data are used in the definition and comparison of the environmental contours and to demonstrate their applicability in the design of marine structures. Furthermore, as the Adriatic Sea is an important sea region with intense maritime activities, the results presented in the Thesis could have direct practical implementation for the design and analysis of marine structures operating in the Adriatic.

The pioneering research of wave statistics in the Adriatic region was performed by Tabain in [34] and later revised and updated in [35], developing so far the most commonly used Tabain's wave spectrum. Tabain's spectrum is a single-parameter modification of the JONSWAP spectrum based on the limited number of wave measurements and observations from merchant and meteorological ships. A collection of wave data from visual observation across the Adriatic is collected inside the Atlas of Climatology of the Adriatic Sea [36] published by the Republic of Croatia Hydrographic Institute. The data, obtained by observations from the merchant and

meteorological ships for the period from 1949 to 1970, is presented in the form of wave roses. Fifteen years of wave observations from [36] are fitted using the 3-parameter Weibull distribution in [37] to develop extreme wave statistics. However, the data from [36] suffers from uncertainties due to the lack of extremes caused by heavy weather avoidance and visual wave observation inaccuracies. The results presented by Parunov et al. [37] are applicable for ships, while their usage has a large uncertainty for the analysis of offshore structures. Ultimately, an optimized wave spectrum based on the JONSWAP wave spectrum optimized together with the parameters of Tabain's modal frequency was proposed [38].

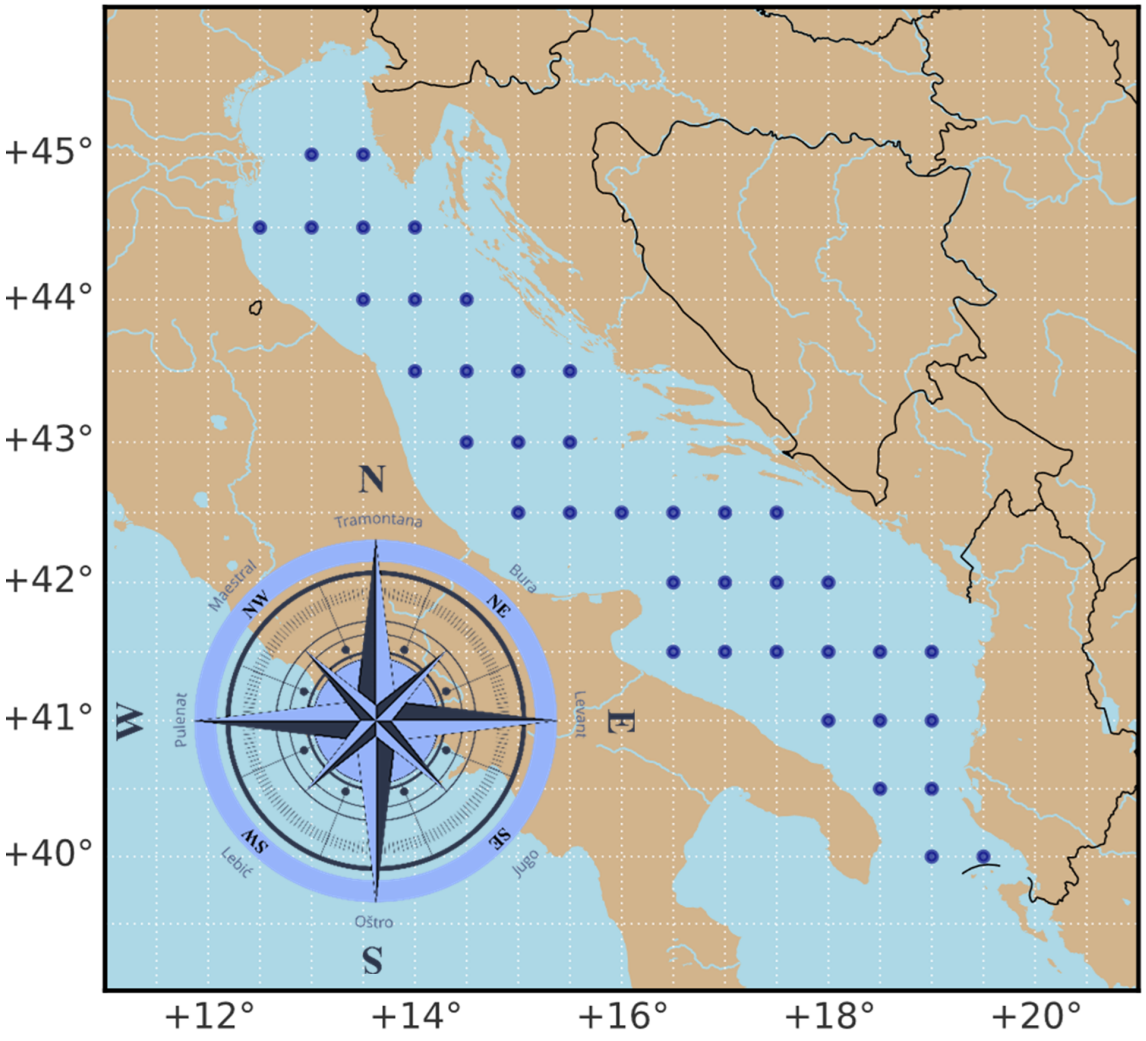

Figure 1.3. The Adriatic Sea map. The offshore grid of 39 available locations for wave data extraction from the WWA and ERA5 database. Lat-lon grid resolution is 0.5 degrees. The wind rose is presented in the lower-left corner. (Source: Publication IV [15])

Wave data in IACS NA scatter diagram neglect monthly and seasonal variability, as they refer to the whole year. There is a lack of research showing what could happen if the long-term analysis is performed for individual months, seasons, or specific wind patterns and then combined in the results for the whole year [5]. This question of seasonal variability of the wave climate was originally raised by Carter and Challenor [39], showing, theoretically, that neglecting seasonality of the wave climate introduces unconservative bias to the estimated long-term extreme values. The within-year variability of wave climate has not been accounted for in the analysis of extreme wave heights because a number of observations were not sufficient to fit theoretical probability distribution with enough confidence. This is especially true for wave statistics used for ship structural design as such data are collected by visual observations, suffering from lack of quality and consistency [40]. However, the situation changed dramatically in the past few decades with the availability of long-term, high-quality wave hindcast databases, offering the possibility to account for many additional effects, intra-annual climate variability being one of them [41].

By assuming that the stochastic process of structural response to sea waves is narrow-banded, it is generally accepted that amplitudes of wave loads in the short-term sea state follow Rayleigh distribution. Short-term ship responses are then combined with the probabilities of occurrence of sea states in order to obtain the long-term probability distribution of the wave-induced loads. Short-term sea states are assumed to be statistically independent and hence uncorrelated in the standard procedure for the long-term response analysis [1]. This assumption is obviously doubtful because of the mutual statistical dependence between successive sea states, i.e., temporal correlation alone for site-specific offshore structures and temporal-spatial correlation for ocean-going ships. The effect of temporal correlation is illustrated by McKay et al. [42], by the simple example of 100-year time series of significant wave height, in which there is one storm that exceeds the wave height of 10 m, and all other storms are milder. In the largest storm, there are several hours that exceed 10 m. If each hour is treated as an independent event, then the empirical estimate would be that 10 m is exceeded several times in 100 years. However, because exceedances are correlated, there was only one event in 100 years that exceeded 10 m.

Different types of correlation that are present in the real wave environment are neglected in the IACS procedure for long-term response analysis. The first correla-

tion that may be observed is between individual wave peaks, as large wave peaks come in clusters. The way how this can be included in short-term response analysis is presented by [43]. Another assumption implicitly adopted in the IACS NA scatter diagram is that wave zones on the ship sailing route are statistically independent, as well as consecutive short-term sea states within each of the wave zones that a ship encounters on her voyage. Considerable effects of correlation among wave zones that a ship encounters during a voyage in commercial shipping routes on extreme sea states are presented by Mansour and Preston [6]. By considering wave zones along a shipping route as members of a serial probabilistic system, they showed how correlation leads to the reduction of the extreme sea states that a ship encounters during its lifetime. The main challenge is the quantification of the correlation coefficient to be used in the correlated series system. Another, albeit mathematically more challenging approach to consider the effects of the spatial correlation for the estimation of significant wave height is the random field modeling, fitted to Satellites wave measurements [44]. The approach is recently extended as a basis for the fatigue analysis in [45].

Various approaches for deriving an EC from a metocean dataset have been proposed in the literature. Although ECs are considered as the alternative to wave scatter diagrams for application in structural reliability assessment and design of marine structures, there are uncertainties in their definition. The process of creating ECs generally includes the estimation of the joint distribution of the environmental variables and contour construction based on the defined joint distribution. A joint distribution can be defined by global hierarchical models [46], copula models [47], non-parametric models (for example, kernel density estimates) [48, 49], or conditional extremes models [50]. Additionally, a method for the estimation of model parameters can vary between maximum likelihood estimation (MLE), method of moments, or least squares fit(LSQ), weighted or not. The contour construction methods can be classified based on the variable space used for creation and associated exceedance probability. The EC can be created in standard normal space (inverse first-order reliability method (IFORM) [51], inverse second-order reliability method (ISORM) [52], and inverse directional simulation [50]) or directly in physical variable space (direct sampling method [53], direct IFORM [54], and highest density contour method [55]). Based on a target exceedance probability, EC can be evaluated based on marginal exceedance probability or total exceedance probability [56].

Two environmental contour approaches recommended by [1] are IFORM and constant probability density approach. The first comprehensive overview of EC methods in general, with a special dedication to structural reliability analysis applications, is given by Ross et al. [11] while a comparison framework for evaluating ECs of extreme sea states is developed by Eckert et al. [57]. A detailed benchmark on the robustness of EC methods and sampling uncertainty was carried out by Haselsteiner et al. [58]. The results showed significant discrepancies in both maximum significant wave height (SWH or H_S) predictions and the amount of data points occurring outside of a given contour caused by variability from different joint distribution models and different contour construction methods.

1.2. Objective and hypotheses of the research

The objective of the thesis is to propose modifications of existing wave statistics aiming to improve the long-term response analysis of marine structures.

The research is based on the following hypotheses:

1. Accounting for the spatial correlation between successive sea states along the sailing route can lead to the improvement of the long-term ship response analysis.

2. Comparative analysis of wave data acquired from different sources will enable quantification of the uncertainty of long-term response prediction.

3. Environmental contours can be formulated for the Adriatic Sea and used to efficiently characterize extreme wave-induced responses of marine structures.

1.3. Scope of work

A spatial statistical correlation between sea states that a ship encounters during a voyage to improve wave scatter diagram for the analysis of ship structures is included in **Publication I**. The method consists of the computation of system reliability of a series of partially correlated events, representing sea states that the ship encounters along the sailing route. The North Atlantic wave scatter diagram is modified to account for such spatial correlation, and new scatter diagrams for partially correlated sea states are constructed. Based on such "correlated scatter

diagrams", long-term distribution of vertical wave bending moments is performed and compared to the results following from an "uncorrelated scatter diagram".

Four different wave data sources collected at close geographical locations in the Adriatic Sea are described and compared in **Publication II**. Two databases are composed of collected in-situ measurements, while two databases are obtained by hindcasting. The consequences that differences in collected wave data could have on the design of marine structures are presented in three examples: assessment of the wave energy that can be used for the selection of wave energy converter, prediction of extreme wave loads for structural strength assessment, and computation of the accumulated fatigue damage.

The effect of within-year wave climate variability on the predicted extreme significant wave heights for the design of ship structures is examined in **Publication III**. The significant wave height data is taken from ERA 5 database along frequent shipping routes. Monthly and annual extreme significant wave heights are extracted, and Gumbel distributions are fitted, respectively, using Maximum Likelihood Estimation. Monthly extreme wave heights are then combined, using the method proposed by Carter and Challenor (C&C) [39], to account for the effect of intra-annual climate variability. Long-term extreme values by two methods are compared for individual locations and shipping routes. Consequences on the extreme wave bending moments are explored, comparing the results to the IACS rules.

The extreme significant wave height predictions accounting for within-year wave climate variability and wave directionality in the Adriatic Sea are analyzed in **Publication IV**. The 24-year hindcast wave data extracted from the WorldWaves database are used in the analysis. Annual extreme significant wave heights generated by different wind patterns and for different months are fitted by Gumbel distribution using maximum likelihood estimation. Combined long-term extremes are then predicted by calculating system probability.

The environmental contours describing significant wave heights and peak wave periods are created in **Publication V** for the whole Adriatic Sea. The environmental contours are established based on 24 years of hindcast wave data extracted from the WorldWaves database. Joint distributions consisting of the marginal distribution of significant wave height and conditional distributions of peak wave periods are used as a basis for the creation of environmental contours using the IFORM and ISORM methods. Return periods of 1 year, 25 years, and 100 years are considered

relevant for the marine operation, design of ships, and offshore structures, respectively. A possibility of environmental contour practical application to the calculation of global wave loads upon ship structures is presented.

1.4. Scientific contribution

Scientific contribution of proposed research includes:

- New scatter diagrams for the analysis of ship structures accounting for correlation among successive sea states that ship encounters during the voyage.
- Quantification of the uncertainty in the long-term distributions of sea states and responses of marine structures caused by using wave data from different sources and by considering monthly and seasonal variability of the wave climate.
- Definition of the environmental contours for the Adriatic Sea and their application for prediction of extreme responses of marine structures.

2. Materials and methods

2.1. Joint probabilistic model of environmental parameters

The environmental variables are described by the joint probability distribution model. The model used in the presented study (2.1), the so-called hierarchical conditional model, factorizes the joint density into the product of a marginal probability density function (PDF) $f_{H_S}(h)$ describing the distribution of H_S and a conditional PDF $f_{T_P|H_S}(t \mid h)$ describing the peak wave period T_P (or zero-crossing T_Z if defined).

$$f_{H_S,T_P}(h,t) = f_{H_S}(h) f_{T_P|H_S}(t \mid h) \tag{2.1}$$

In Equation 2.1, H_S and T_P indicate random variables, while h and t represent their realizations. The three-parameter Weibull distribution (2.2) is used for the marginal PDF of H_S where α, β, and γ represent the scale, shape, and location parameters.

$$f_{H_S}(h) = \frac{\beta}{\alpha}\left(\frac{h-\gamma}{\alpha}\right)^{\beta-1} \exp\left(-\left(\frac{h-\gamma}{\alpha}\right)^{\beta}\right) \tag{2.2}$$

The conditional PDF of T_P is modeled by a log-normal distribution described by Equation 2.3.

$$f_{T_P|H_S}(t \mid h) = \frac{1}{\sigma(h)t\sqrt{2\pi}} \exp\left(-\frac{[\ln t - \mu(h)]^2}{2\sigma(h)^2}\right) \tag{2.3}$$

The mean value $\mu(h)$ and standard deviation $\sigma(h)$ of $\ln(T_P)$ are conditional on H_S as follows.

$$\begin{aligned} \mu(h) &= E\left[\ln\left(T_P\right)\right] = a_0 + a_1 h^{a_2} \\ \sigma(h) &= Var\left[\ln\left(T_P\right)\right] = b_0 + b_1 e^{b_2 x} \end{aligned} \tag{2.4}$$

The parameters of the distributions are determined by applying the MLE and LSQ method on the available data, or it can be found in the literature.

2.2. The correlation among successive sea states

The sea states (and wave zones) along the sailing route are considered as members of a series system of partially correlated events. Therefore, a non-encounter of specific wave height (or a sea state) occurs only if mutual non-encounter takes place in all members of a system. The probability of non-exceeding different significant wave heights along the route is modeled by a 3-parameter Weibull cumulative distribution function 2.5.

$$F_{H_S}(h) = 1 - \exp\left(-\left(\frac{h-\gamma}{\alpha}\right)^{\beta}\right) \tag{2.5}$$

The Weibull's parameters α, β, and γ are available in [59] for the wave zones along the route

The system probability of non-encounter for equally correlated members of a series system can be modified (2.6) to define a probability of non-exceeding a specific H_S for equally correlated sea states [60].

$$P_{H_S,ne}(h) = \int_{-\infty}^{\infty} \left[\prod_{i=1}^{N} \Phi\left(\frac{\beta_i(h) + z\sqrt{\rho}}{\sqrt{1-\rho}}\right)\right] \phi_Z(z)\, dz \tag{2.6}$$

The correlation coefficient is represented by ρ, while $\phi_Z(z)$ and Φ denote the probability density and distribution function of the standard normal variate z. It is implicitly assumed, in the present study, that there is an equal average correlation between sea states, represented by ρ. The reliability index β_i, is an argument of the standard normal distribution Φ, which yields one minus the probability of non-exceeding H_S (2.5) described by equation $\beta_i(h) = -\Phi^{-1}\left(1 - F_{H_S}(h)\right)$.

The Monte Carlo (MC) simulation is then conducted, creating 100 000 random samples to produce a scatter diagram according to the hybrid joint environmental model consisting of the initial distributions of H_S, derived from Eq. 2.6 and distributions of T_Z. The distribution of T_Z is not considered directly by the procedure yet taken from the joint model for the North Atlantic, available in [1].

2.3. Combined extreme value distributions

The annual extreme significant wave heights are extracted from the relevant databases each month throughout every year available. For the seasonality study, H_S monthly maxima (MM) are extracted for each month of every year available, resulting in a subset of MM records easily visualized as a matrix containing years as rows and 12 columns as months. Equivalently, subsets of directional maxima (DM) are extracted from each direction to study directionality effects. According to the recommendations of [1], a year is defined from July of the concerned year to the June of the following year.

The maximum SWHs are described using type-I generalized extreme value distribution, also known as Gumbel distribution [1]. The cumulative distribution function (CDF) is defined as:

$$F_{H_S}(h) = 1 - \exp\left(-\exp\left(-\frac{h-A}{B}\right)\right) \tag{2.7}$$

where A and B are, respectively, the location and scale parameters of the Gumbel distribution. Fitting of Gumbel distribution is performed by the MLE method, using algorithms provided by `scipy.optimize` and `scipy.stats` packages in Python [61]. The location parameter represents the most probable annual extreme significant wave height either for a month, direction, or the whole year combined.

From individual CDFs of directional or monthly maxima, combined 'annual maxima' (AM) is calculated by the Equation 2.8 expression proposed by Carter and Challenor (C&C) [39].

$$P_{H_S}(H_S < h) = \prod_{i=1}^{N} F_i(h) \tag{2.8}$$

Unless distributions of directional or monthly extremes are identical, the resulting distribution from Eq. 2.8 is not a Gumbel distribution. Thus, results must be calculated numerically.

2.4. Methods for the environmental contours construction

The procedure for deriving an EC includes the estimation of the joint distribution (Equation 2.1) of the environmental variables (H_S and T_P) and contour construction based on the obtained joint model.

The IFORM and ISORM are the two considered construction methods. Using the Rosenblatt transformation, the joint distribution of environmental variables is transformed to independent standard normal variables $\mathbf{u} = \{u_1, u_2\}$, for the presented case. The probability of failure (P_f) is then calculated in the standard normalized U-space. To solve the equation, the IFORM method assumes a linear approximation to the failure surface at the design point, while the ISORM assumes a quadratic failure surface. The distance from the U-space origin to the design point corresponds to the reliability index (β_F for the IFORM) and can be calculated as Eq. 2.3 suggests.

$$\beta_F = \Phi^{-1}(1 - P_f) \tag{2.9}$$

Instead of a tangent (hyper-)plane at the design point, Chai and Leira [52] propose a (hyper-)sphere passing through the design point and centered at the origin of the U-space, thus calculating reliability index β_S as 2.10.

$$\beta_S = \sqrt{\chi_n^{-1}(1 - P_f)} \tag{2.10}$$

Based on the reliability index for the selected return period, the circle/sphere is established in U-space. Finally, the EC is obtained by transforming the circle/sphere from the U-space into a contour in the environmental parameter space using the inverse Rosenblatt transformation.

To determine maximum responses corresponding with the ECs, the contours of the most probable extreme (vertical wave bending moment) VWBM at midship in short-term conditions are produced relative to the value of VWBM required by the IACS Rules [62].

2.5. Extreme ship responses

Transfer functions of VWBM at midship are calculated using the semi-analytical approach proposed and validated by Jensen and Mansour [20], which is particularly useful in conceptual studies such as the present one. The approach approximates a ship hull by a pontoon of equal length, equivalent breadth, and draught, while speed and block coefficient are accounted for through correction factors. The long-term distribution of VWBM is calculated by the standard procedure described, e.g., by Ćorak et al. [63], among others.

The accuracy of closed-form expressions is verified by comparison to the model-scale measurements and more complex strip theory and 3D panel hydrodynamic computations in [19, 21, 64]. It was found that considering the simplicity of the method, closed-form expressions give a surprisingly good estimate of vertical ship responses.

The response analysis in **Publication I**, **Publication III**, and **Publication V** is performed on four classes of oil tankers, Panamax, Aframax, Suezmax, and VLCC, representing the actual size range of oil tankers operating worldwide. The average dimensions of a typical ship, i.e., a class representative presented in Table 2.1, are provided in [65]. A reduced ship speed of 5 knots is recommended for the evaluation of the design wave loads for strength assessment [25].

Tablica 2.1. Main dimensions of four representative oil tankers representing the range of actual sizes.

Ship class	Length [m]	Breadth [m]	Draught [m]
Panamax	174.4	31.4	11.3
Aframax	229.7	41.9	13.1
Suezmax	260.8	45.8	15.9
VLCC	318.6	58.4	21.1

Barges for the transportation of heavy cargo are frequently operating in the northern part of the Adriatic Sea because of the intensive industrial activities in that region. Therefore, extreme wave bending moments and fatigue analysis are conducted in **Publication II** for the barge with particulars specified in Table 2.2. Besides, the uncertainty assessment of the wave energy that can be used for the selection of wave energy converter is detailed in **Publication II**.

Tablica 2.2. Barge main particulars.

Length [m]	Breadth [m]	Draught [m]
113.0	36.6	4.5

2.6. Materials - Wave data

The significant wave height data used throughout the research originates from two high-resolution hindcast wave databases.

The wave extracted from ERA 5 database account for waves generated and directly affected by local winds and the ones generated by the wind at a different location and time, also called swell. The ERA5 is the fifth generation ECMWF (The European Centre for Medium-Range Weather Forecasts) reanalysis, produced by combining advanced forecasts modeling and data assimilation systems with vast amounts of observations [28]. For the model data calculation, the ECMWF's Integrated Forecast System (IFS) combines the atmospheric model, the land-surface model (Revised land surface hydrology, HTESSEL), and the third-generation ocean wave model (Wave Modeling Project, WAM). Complete ERA5 data covers the period from 1979 until now, providing hourly estimates for many atmospheric, land-surface, and ocean-wave climate variables, with a lat-lon grid resolution of approximately 0.5 degrees.

The WWA is the collective name for a series of comprehensive high-resolution atlases developed by Fugro Oceanor, providing wind and wave climate statistics/data for any region worldwide [66]. The data derived from the European Centre for Medium-Range Weather Forecasts (ECMWF) wave models are calibrated by Fugro Oceanor against satellite altimetry measurements gathered from eight different satellite missions: Geosat (1986–1989), Topex (1992–2002), Topex/Poseidon (2002–2005), Jason (2002–2008), Geosat Follow-On (2000–2008), EnviSat (2002–2010), Jason-1s (2009–2012), and Jason-2 (2008–on-going). The WWA database for the Adriatic covers a period of 28 years from January 1992 until December 2019 in 6 h intervals giving a total of 40,900 records per parameter at each location. Data are available at a lat-lon grid resolution of 0.5 degrees creating the offshore grid of 39 points across the Adriatic, as shown in Figure 1.3. Available data include wind speed and direction, integral spectral wave parameters (e.g., significant wave height, peak spectral period, mean wave period), and wave direction for wind waves

and swell, considered separately and combined, offering, in total, 12 wind and wave parameters. The WWA model data are calibrated against the long-term satellite data in order to provide bias-free homogeneous long-term model data of the highest quality. Thus, representing a state-of-the-art comprehensive and systematic source of wave data as input to coastal models and studies for the Adriatic region.

Uncertainties of different wave data sources are examined by comparing with two additional databases obtained by in-situ measurements, i.e., RON wave buoy and Acqua Alta oceanographic tower.

Data from the ERA5 wave database is used to study the effect of neglecting within-year wave climate variability (**Publication III**) and the effect of spatial correlation (**Publication I**) at locations along typical shipping routes in the Atlantic and Pacific oceans.

The WWA database is the data source for the Adriatic Sea case studies as suggested by [13], i.e., **Publication II**. The effect of directionality and seasonality, as well as the ECs construction, are done for all available locations across the Adriatic displayed in Figure 1.3.

3. Selected results with discussion

3.1. New correlation wave scatter diagrams

The method used for creating new scatter diagrams accounting for correlation is presented in Section 2.2., and details are available in **Publication I**. The scatter diagrams, modified to account for spatial correlation, are obtained for different values of correlation coefficients. Samples of generated scatter diagrams are illustrated in Tables 3.1 and 3.2 for $\rho = 0$ and $\rho = 0.8$.

Tablica 3.1. Scatter diagram for uncorrelated sea states ($\rho = 0$) [12].

$H_s \backslash T_z$	1	2	3	4	5	6	7	8	9	10	11	12	13	14	15	Sum
1	0.0	0.0	0.0	1.6	116.0	1332.8	3653.2	3682.8	1956.8	643.8	153.8	29.0	5.4	0.6	0.2	**11576**
2	0.0	0.0	0.0	0.0	24.4	712.4	4392.8	9021.8	8680.6	4791.8	1778.4	495.4	121.6	20.2	3.6	**30043**
3	0.0	0.0	0.0	0.0	1.8	137.4	1504.4	4989.8	7231.4	5596.8	2853.0	1019.0	291.8	65.4	14.2	**23705**
4	0.0	0.0	0.0	0.0	0.4	24.4	407.2	2076.6	4055.6	4285.6	2767.4	1208.2	419.0	116.6	28.0	**15389**
5	0.0	0.0	0.0	0.0	0.1	4.4	112.7	766.7	1997.7	2619.9	2046.6	1062.5	414.2	131.3	46.9	**9203**
6	0.0	0.0	0.0	0.0	0.0	0.7	27.5	247.2	818.7	1335.4	1267.0	758.3	350.1	128.2	43.9	**4977**
7	0.0	0.0	0.0	0.0	0.0	0.5	6.3	83.2	317.4	633.1	707.4	492.3	253.7	94.6	44.5	**2633**
8	0.0	0.0	0.0	0.0	0.0	0.2	2.3	20.9	121.2	271.9	357.6	284.5	154.2	72.0	32.2	**1317**
9	0.0	0.0	0.0	0.0	0.0	0.0	0.5	6.4	44.6	113.4	163.2	146.3	91.6	44.0	22.2	**632**
10	0.0	0.0	0.0	0.0	0.0	0.0	0.1	1.5	14.4	41.9	66.5	71.7	48.8	24.3	14.1	**283**
11	0.0	0.0	0.0	0.0	0.0	0.0	0.0	0.5	4.6	17.2	31.6	32.4	26.5	14.7	8.8	**136**
12	0.0	0.0	0.0	0.0	0.0	0.0	0.0	0.1	1.4	5.6	11.4	14.6	11.2	7.0	5.7	**57**
13	0.0	0.0	0.0	0.0	0.0	0.0	0.0	0.0	0.4	2.5	5.3	7.2	6.3	4.2	3.0	**29**
14	0.0	0.0	0.0	0.0	0.0	0.0	0.0	0.0	0.4	0.8	2.4	3.2	3.3	2.5	2.3	**15**
15	0.0	0.0	0.0	0.0	0.0	0.0	0.0	0.0	0.0	0.2	0.8	1.0	1.3	0.9	0.8	**5**
Sum	0.0	0.0	0.0	1.6	142.7	2212.8	10106.9	20897.6	25245.2	20359.9	12212.2	5625.5	2199.1	726.4	270.3	100000

Tablica 3.2. Scatter diagram for partially correlated sea states ($\rho = 0.8$) [12].

$H_s \backslash T_z$	1	2	3	4	5	6	7	8	9	10	11	12	13	14	15	Sum
1	0.0	0.0	0.0	8.2	919.0	10664.4	29152.8	29630.8	15620.4	5170.0	1222.4	219.2	34.8	3.2	0.8	**92646**
2	0.0	0.0	0.0	0.0	2.3	86.1	533.5	1117.6	1066.5	577.8	208.1	58.3	12.4	2.0	0.4	**3665**
3	0.0	0.0	0.0	0.0	0.0	8.9	97.4	311.7	454.4	360.5	181.4	68.4	18.2	4.0	1.1	**1506**
4	0.0	0.0	0.0	0.0	0.1	1.2	22.8	116.2	231.3	238.8	153.8	68.7	23.4	5.9	2.0	**864**
5	0.0	0.0	0.0	0.0	0.0	0.4	6.6	46.6	119.0	155.1	122.1	62.3	25.6	7.8	2.8	**548**
6	0.0	0.0	0.0	0.0	0.0	0.1	2.3	14.1	46.0	77.0	73.6	43.1	20.4	7.4	3.2	**287**
7	0.0	0.0	0.0	0.0	0.0	0.0	0.6	7.3	27.4	50.4	57.8	38.8	19.2	7.6	3.1	**212**
8	0.0	0.0	0.0	0.0	0.0	0.0	0.1	2.0	11.0	24.2	32.3	24.7	14.4	5.2	3.3	**117**
9	0.0	0.0	0.0	0.0	0.0	0.0	0.0	0.8	4.3	11.9	17.5	16.2	10.2	4.4	2.7	**68**
10	0.0	0.0	0.0	0.0	0.0	0.0	0.0	0.2	1.8	5.5	9.4	9.0	6.7	3.3	2.0	**38**
11	0.0	0.0	0.0	0.0	0.0	0.0	0.0	0.1	0.8	3.0	5.3	5.9	4.6	2.6	1.7	**24**
12	0.0	0.0	0.0	0.0	0.0	0.0	0.0	0.0	0.4	1.8	3.2	3.7	3.5	1.9	1.5	**16**
13	0.0	0.0	0.0	0.0	0.0	0.0	0.0	0.0	0.1	0.4	1.0	1.5	1.3	0.8	0.9	**6**
14	0.0	0.0	0.0	0.0	0.0	0.0	0.0	0.0	0.0	0.2	0.3	0.5	0.5	0.3	0.3	**2**
15	0.0	0.0	0.0	0.0	0.0	0.0	0.0	0.0	0.0	0.1	0.1	0.2	0.2	0.2	0.2	**1**
Sum	0.0	0.0	0.0	8.2	921.4	10761.1	29816.0	31247.3	17583.2	6676.6	2088.3	620.3	195.4	56.4	25.9	100000

The severity of the scatter diagram is inversely proportional to the spatial correlation between sea states along the route. As the correlation increases, most MC simulation outputs occur in the lowest H_S class. Thus, for $\rho = 0$, five occurrences of $H_S = 15$ m are observed, while for $\rho = 0.8$, only one. For perfectly correlated sea states ($\rho = 1$), the highest encountered H_S reads just 12 m (see **Publication I**). It is interesting to notice that an operational envelope for bulk carriers and oil tankers in full load conditions reads about 12 m, according to Moan et al. [67], which corresponds to the scatter diagram obtained for perfect correlation.

The effect of correlation on the most probable extreme value (MPEV) of VWBM in a ship lifetime of 25 years is presented in Figure 3.1. Results for various correlation coefficients are presented relative to the uncorrelated VWBM. It may be seen that trend is similar irrespective of the ship size and that there is a clear tendency toward reducing bending moments with ρ coefficient increase.

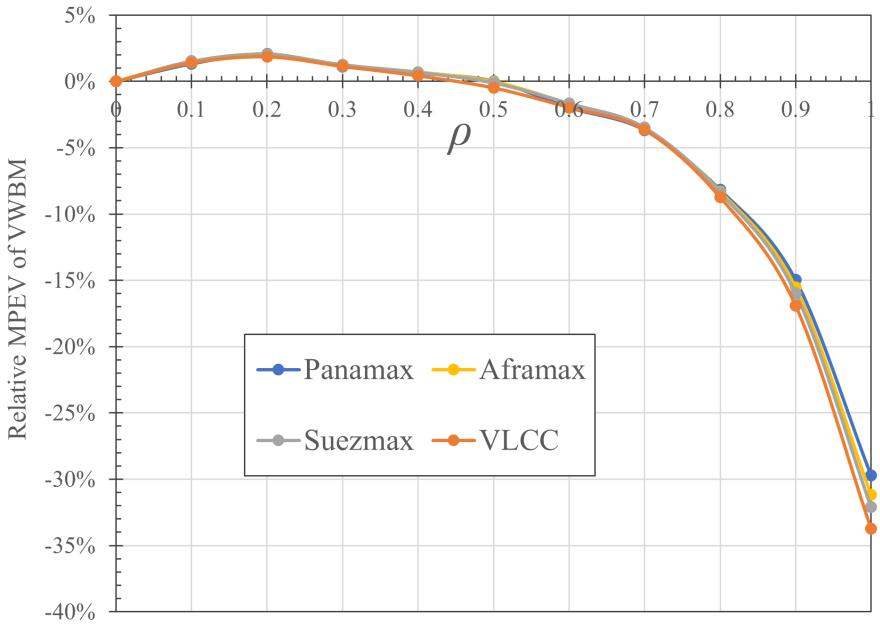

Figure 3.1. MPEV of VWBM maximum relative to uncorrelated case in respect to correlation coefficient for different oil tanker sizes [12].

The MPEV is approximately unaffected for $\rho < 0.6$, while for higher values, an appreciable reduction is observed reaching, 30-35% for perfect correlation ($\rho = 1$). The comparison of correlated results with hindcast data in **Publication I** indicates that correlation coefficients of about 0.8 are in agreement with the visual observations, in which case a reduction of VWBM of about 10% is expected.

3.2. Uncertainties of different wave data sources

Comparative analysis of four different wave data sources collected at close geographical locations in the Adriatic Sea is conducted. Two databases are assembled from collected in-situ measurements (wave buoy - RON and oceanographic tower Acqua Alta), while two databases are obtained by wave hindcasting (ERA5 and WWA). The consequences on the design of marine structures are examined in three different cases. Detailed results are available in **Publication II**, while highlights are presented here. Long-term distributions of VWBM are presented in Figure 3.2.

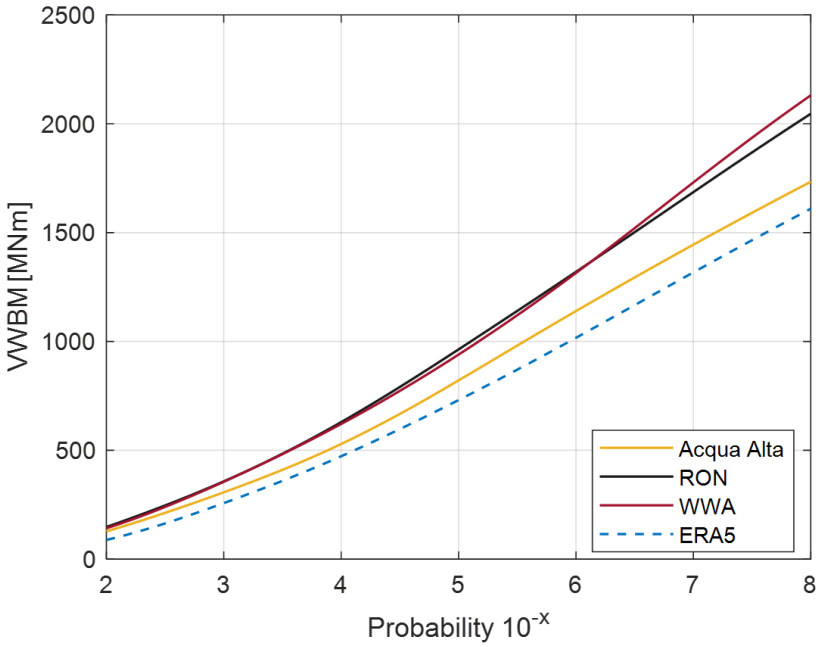

Figure 3.2. Long-term distribution of VWBM for different wave databases [13].

The ratio between the highest and the lowest estimated MPEV of VWBM for the return period of 25 years reads 1.3. Expectedly, extreme values resulting from WWA and RON databases are higher than those resulting from Acqua Alta and ERA5, considering the long-term distribution of H_S presented in Figure 3.3.

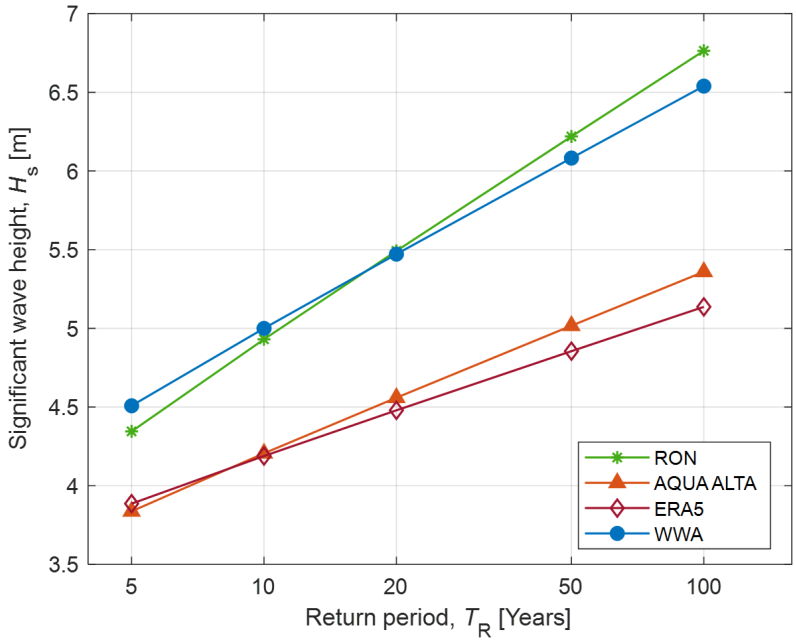

Figure 3.3. Comparison of the extreme significant wave heights for different return periods among different wave databases [13].

Results of the fatigue analysis are given in Table 3.3. It may be seen that the ratio of the largest (RON) and the lowest (ERA 5) accumulated fatigue damage reads 3.3.

Tablica 3.3. Barge Fatigue Damage D due to different wave data sources.

Acqua Alta	WWA	ERA5	RON
0.26	0.42	0.13	0.43

A diagram representing available wave energy potential from the WWA database is displayed in Figure 3.4. The highest energy potential is achieved during sea states with H_S between 1.0 – 2.0 m and T_P between 4.0 – 6.0 s.

Total wave energy potential for location in the Northern Adriatic Sea for different wave databases are presented in Table 3.4.

Tablica 3.4. Yearly total wave energy potential E_{tot}, [MWh/m].

Acqua Alta	WWA	ERA5	RON
11.44	14.39	8.80	12.71

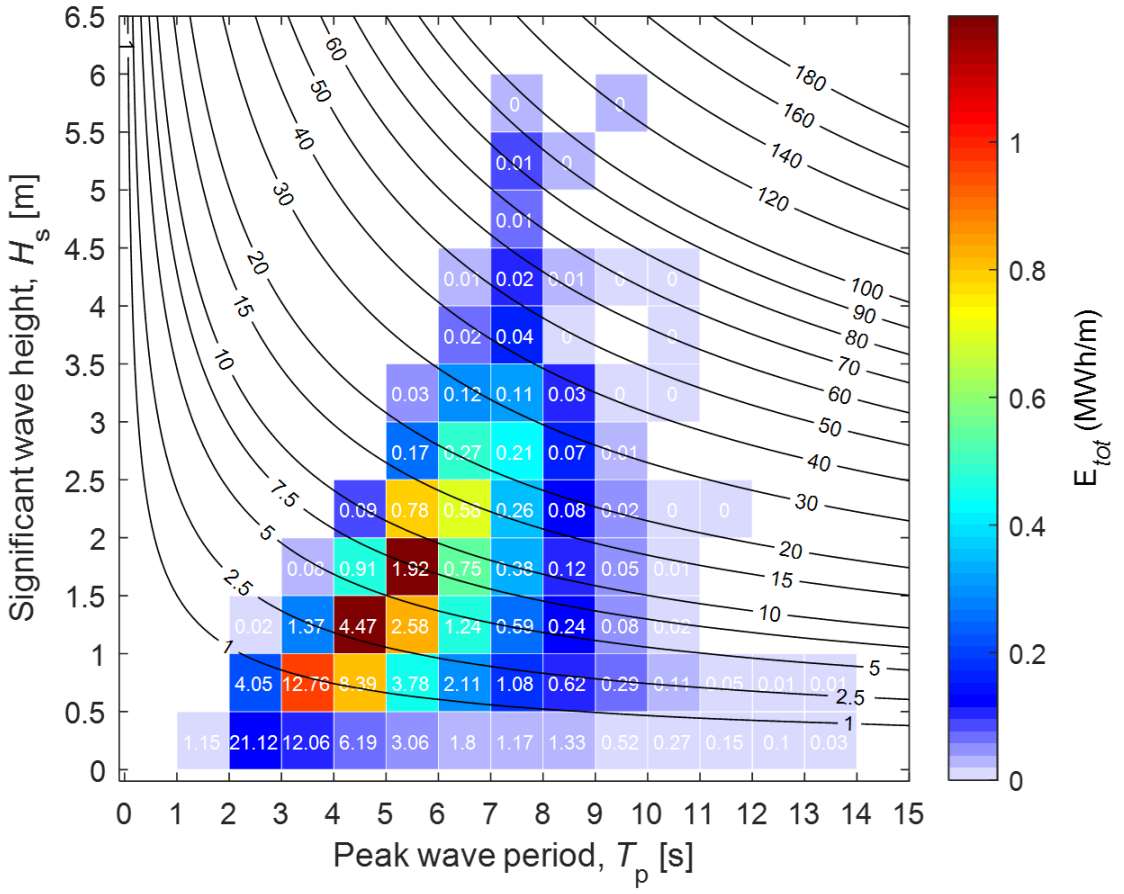

Figure 3.4. Wave energy potential diagram from WWA data (E_{tot} is a total potentially produced yearly wave energy for each sea state. Black lines are curves of a constant wave power P [kW/m] and white numbers are the probabilities of occurrence of a sea state [%].) [13]

3.3. The effect of a Wave Directionality and a Within-Year Wave Climate Variability

A comparison of return significant wave heights obtained by employing C&C method and return values from Gumbel distributions fitted to the yearly extreme values for two locations in the North Atlantic is presented in Figure 3.5. Values from Gumbel yearly extremes are lower in all cases. For both locations, those differences are intensified with the increase of the return period. As expected northern location has higher values of H_S. Similar trends are observed for locations on the Pacific routes (details in **Publication III**).

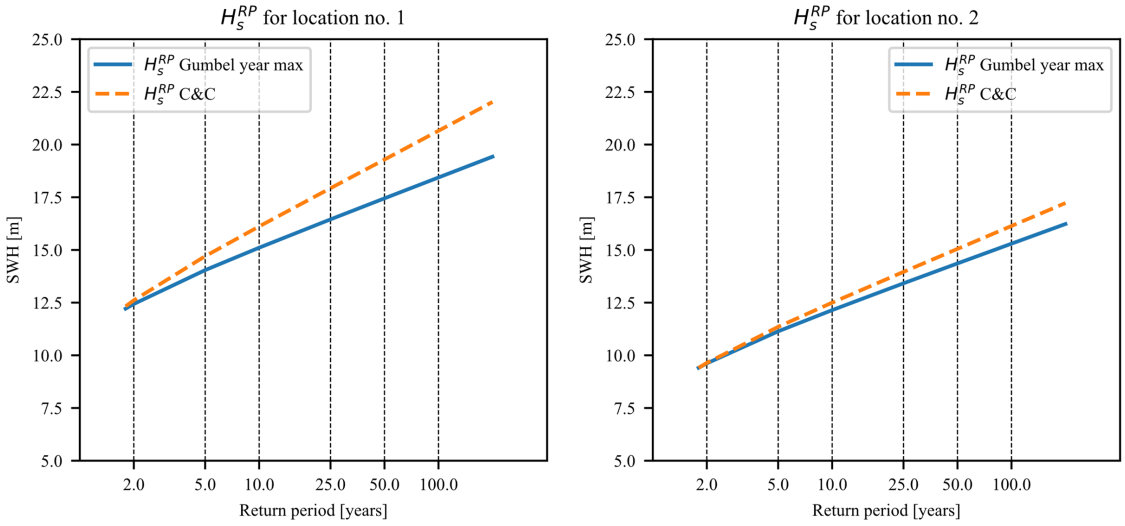

a) NA loc. 54.0°N 33.5°W b) NA loc. 38.5°N 42.0°W

Figure 3.5. The distribution of the return SWHs for mid-locations [14].

The yearly prediction difference between the C&C method and conventional extreme value estimate on an annual basis is around 9% for loc. 1, while for other is approximately halved. The results for two locations in Pacific are available in **Publication II**.

Results for a single location at the midway of each route are more appropriate for offshore structures than for ocean-going ships. To obtain results relevant for the design and analysis of ships, 7 equally spaced locations along each of four routes are considered. The resulting extreme value distribution along the shipping route is obtained by statistically combining extreme value distributions at individual locations. For 25 years return period, North Atlantic routes have 6-10 % (1.1 to 1.4 m) lower SWH values compared to their midway locations. The values for the Northern North Pacific route have negligible difference (0-2%) in contrary to the Southern route in the North Pacific with around 50% higher values. However, a clear conclusion can be made that results from one location are not sufficient to represent the whole shipping route.

Applying the same approach, extreme significant wave height statistics are developed for the Adriatic region by considering different wind patterns and within-year climate variability (**Publication IV**). The extreme SWHs summarized in Figures 3.6 and 3.7 are calculated for the return periods of 25 and 100 years, respectively, at 39 locations across the Adriatic. The dashed lines on the upper graph represent

the extreme value resulting from the system probability approach (C&C method, Equation 2.8). The blue dashed line accounts for different directions combining probability distributions of DM, while the orange dashed line combines probability distributions of MM. The red line displays results from the conventional method using AM, neglecting both effects. Lower graphs on both figures highlight deviations of C&C using DM and MM from the AM. Locations on the left side of the graphs in Figures 3.6 and 3.7 correspond to the southern part of the Adriatic Sea, moving to the locations in the northern Adriatic as we move to the right side of the graphs. The exact position of locations could be easily identified using the map presented in Figure 1.3.

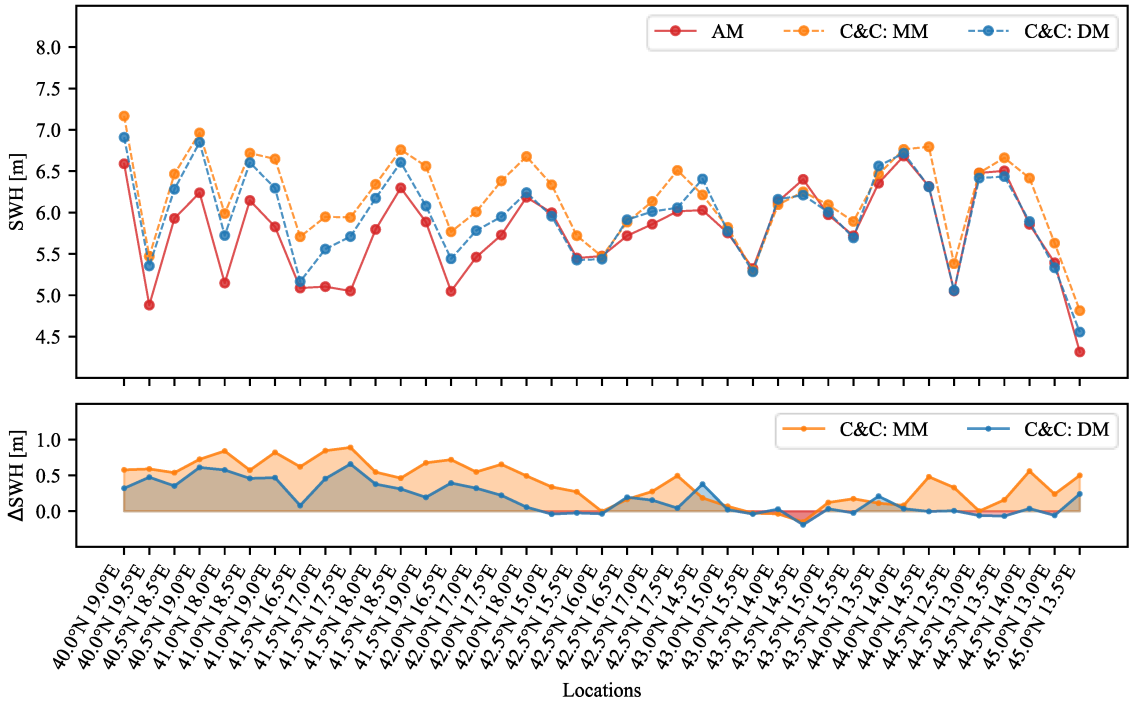

Figure 3.6. The extreme SWHs for the return period of 25 years. The lower graph displays the differences between the given C–C and the AM approach [15].

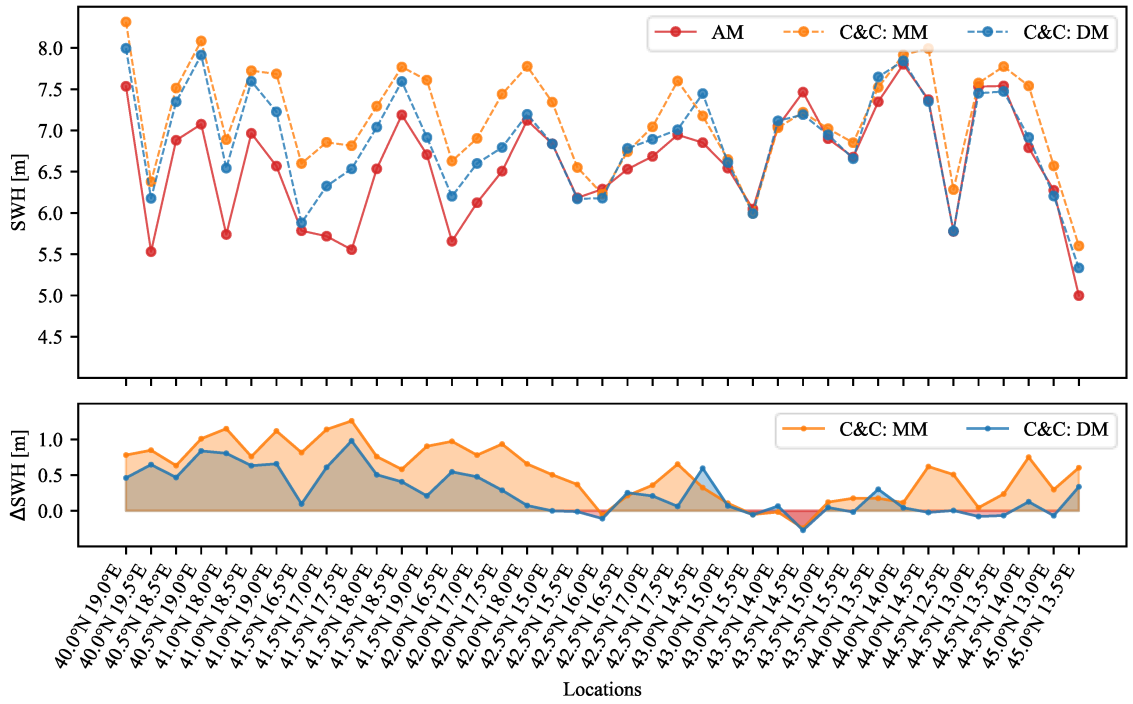

Figure 3.7. The extreme SWHs for the return period of 100 years. The lower graph displays the differences between the given C–C and the AM approach [15].

Relations between extreme values from C&C and AM are qualitatively similar for both months and directions. Throughout locations, C&C MM produces the most conservative results for almost all locations, with few exceptions where it is equal to or slightly exceeded by the other two. These exceptions occur in the middle part of the Adriatic, where the wave climate is the mildest. The C&C DM produces evidently smaller differences, offering predictions close to AM for almost half of the studied locations. Extending the return period from 25 to 100 years amplifies differences while trends remain unchanged. For both return periods, southern locations observe higher differences, yielding the highest values for 41.5°N 17.5°E. The lowest deviations are displayed for locations in the middle Adriatic (43.0°N 15.5°E), whereas for some locations, C&C MM and DM predict SWHs even lower than the standard AM approach. Several locations are found in the northern Adriatic, where Bura has the highest influence yielding results equal to or higher than the AM.

Directionality effects across the Adriatic Sea are also examined in Figure 3.8, revealing the distribution of the number of yearly maxima across four studied directions. Each location is represented by a blue dot and four quadrants suggesting the direction of the waves. The color scale presented in the upper left corner indicates

the number of yearly maxima that occurred in a direction.

Analysis suggests domination of Bura waves in the north and along the west coast of the Adriatic, while Jugo dominates the remaining locations across the basin. In the southernmost locations, close to the Strait of Otranto, there is a strong influence of the Ionian Seas, causing a mixture of different wind and wave systems. Consequently, in those locations, it could be that extreme waves are not predominantly influenced by Jugo or Bura.

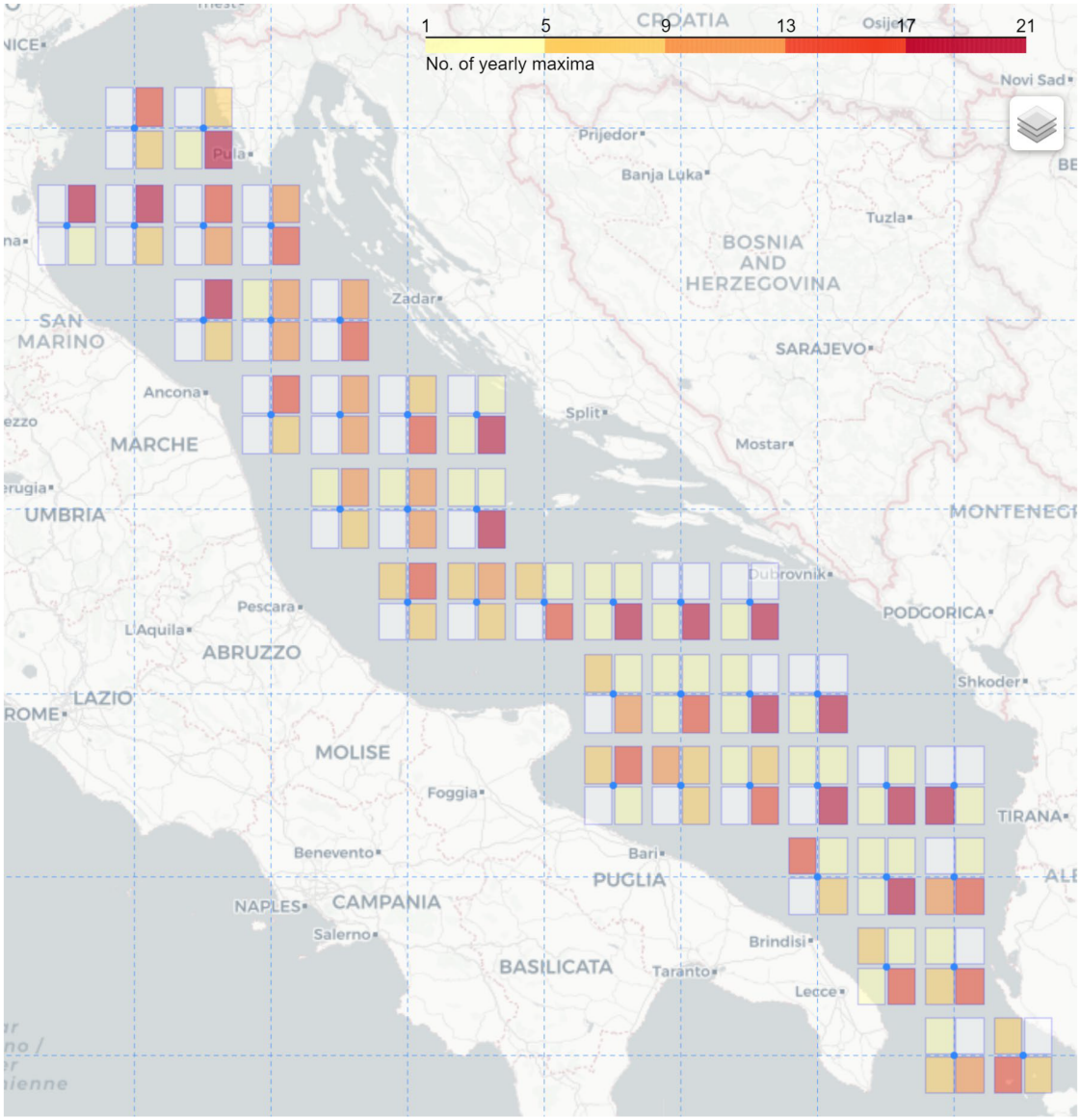

Figure 3.8. Distribution of yearly maxima from four main quadrants across the Adriatic Sea [15].

This part of the study presents results of the extreme value analysis of wave

heights in the Adriatic Sea by considering simultaneously physically similar processes, i.e., waves generated by bora and waves generated by Jugo for directional analysis and waves generated in each month for within-year variability analysis. The main advantage of the proposed method lies in having directional and seasonal maxima that, as we could observe, can sometimes exceed the ones derived from the whole dataset. Also, extreme values obtained by system probability, i.e., combining distributions from individual directions, are always conservative. The approach is slightly more complex than the conventional analysis and requires a large dataset containing many years of uninterrupted records with high temporal resolution. Since a lot more fitting is performed compared to the conventional method, the proposed methodology is more sensitive considering distribution fitting uncertainty.

3.4. Environmental Contours for the Adriatic Sea

Joint hierarchical models are fitted to data for all 39 locations as a base for contour creation. The 25- and 100-year contours have been created applying both IFORM and ISORM approaches. A comparison of contour creation methods for a typical location in the north Adriatic is displayed in Figure 3.9. A 100-year contour is distinguished with a dashed line, while a full line signifies a 25-year return period. Orange and gray differentiate the IFORM and ISORM approaches, respectively, while blue circles represent hindcast wave data.

The goodness of fit of marginal Weibull PDF of H_S is presented on the right, Figure 3.9b. Except for small deviations at the highest quantiles, a rather good fit is obtained, as fitted marginal distributions of H_S seem to slightly underestimate the highest value. As expected, ISORM displays more conservative results yielding the largest variations at the marginal values, i.e., peaks of H_S and T_P. At the extremes, ISORM predicts around 20% higher H_S.

Although the current study has not explored other contour methods and joint models, generated contours seem to describe data well. There is a slight underestimation from IFORM, whereas an overestimation of the ISORM contour on the other end may be noticed. The conservative trends of the ISORM approach are supported by a plain overview of the presented Equations 2.9 and 2.10 for reliability index calculations. There are also in line with the results and conclusions published in the literature [52]. However, the ECs are sensitive to the initial joint probability

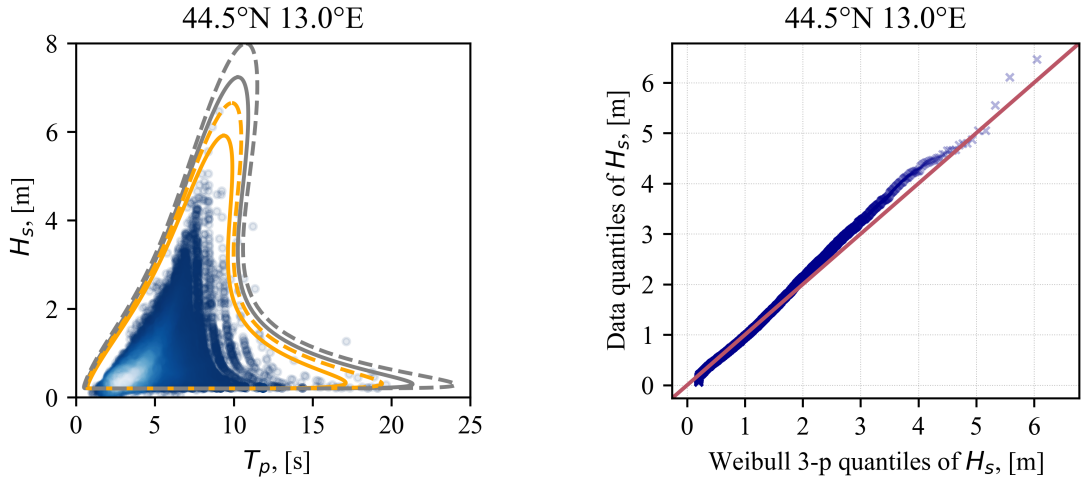

a) The comparison of IFORM and ISORM corresponding 25-year and 100-year contours

b) Q–Q plot comparing H_S data to the corresponding fitted Weibull distribution

Figure 3.9. A comparison of EC for three characteristic locations [16].

distribution. The location parameter γ is the most uncertain when fitting the Weibull 3P distribution. Namely, the physical interpretation of this parameter is the minimum significant wave height representing permanent sea activity. A comparison of IFORM and ISORM ECs for various choices of γ is shown in Figure 3.10, where large uncertainty may be observed. The reason for these discrepancies s in the fitting of the tail of the marginal distribution of H_S, which may be seen in the Q-Q plots presented in Figure 3.10b. One can conclude from Figures 3.10a and 3.10b that the Weibull 2P (Weibull 3P with location parameter equal to zero, $\gamma = 0$) distribution is completely inappropriate as the long-term distributions of H_S lead to unconservative ECs. Therefore, the ISORM contour obtained from the joint model with fixed $\gamma = 0.2$ is used in the response analysis available in **Publication V**.

The ECs for all 39 locations in the Adriatic are presented in Appendix A of **Publication V** for three characteristic return periods of 1, 25, and 100 years. The 1-year ECs are used for planning marine operations in the Adriatic, e.g., transportation of heavy cargoes or installation of offshore platforms, while those for return periods of 25 and 100 years are useful for the design of ships and offshore structures, respectively. Although more detailed information for specific locations is required for commercial purposes, presented contours may be used for preliminary identification of extreme sea states.

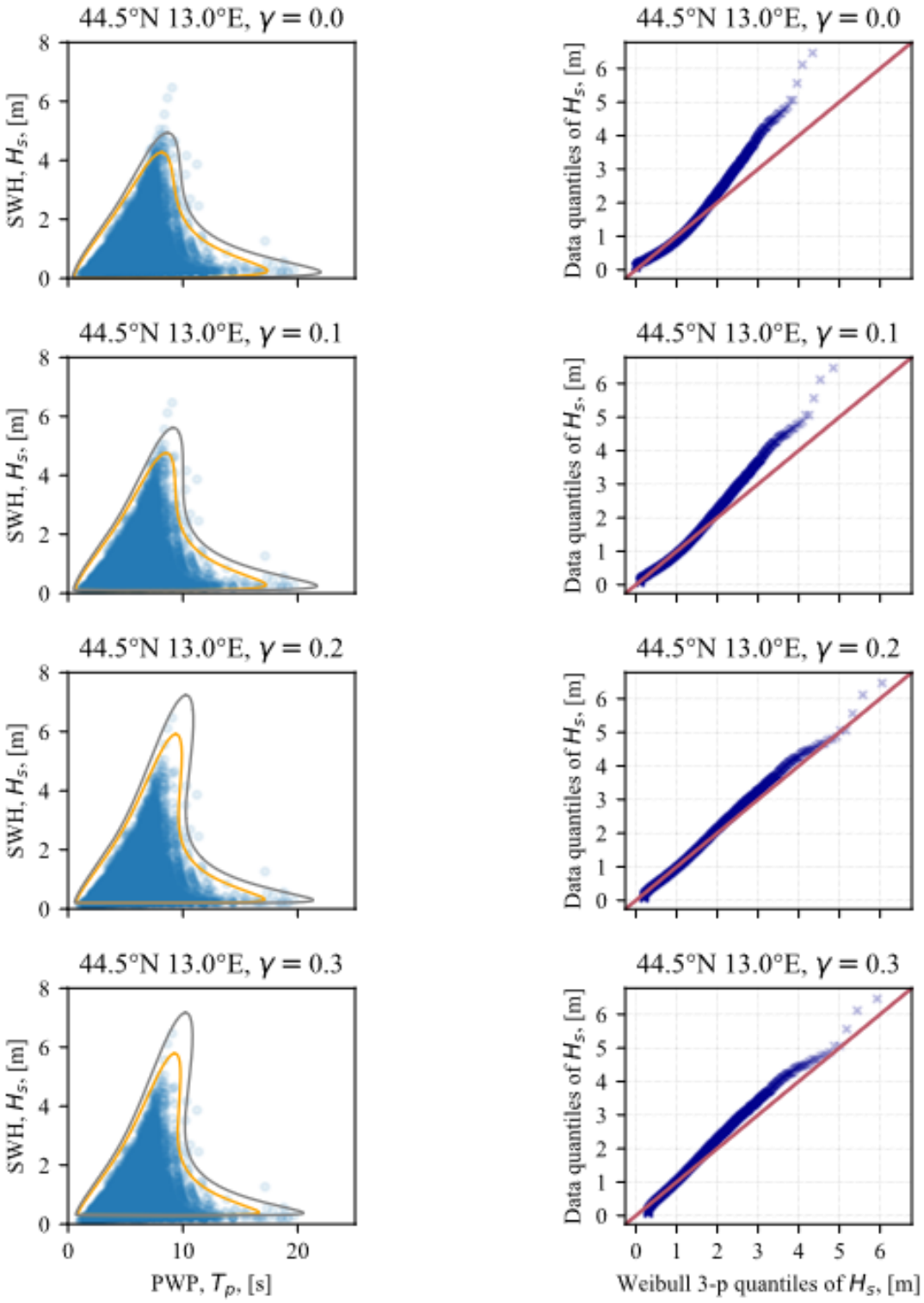

a) The 25-year IFORM (orange) and ISORM (gray) contour, wave data (blue circles)

b) The Q–Q plots of SWH data to the corresponding fitted Weibull distribution

Figure 3.10. Influence of γ variation on joint model fit and ECs [16].

4. Conclusions

The Thesis investigates advanced methods for the improvement of wave statistics for the design and analysis of marine structures that are usually not considered in practice. These methods include correlation among sea states, intra-annual and directional variability, and application of environmental contours. Their usage is enabled nowadays when large hindcast databases are gradually introduced in the offshore and shipping industry.

The first aim of the study is to improve the IACS NA wave scatter diagram by including the spatial statistical correlation between sea states along the ship's route. The successive sea states that ship encounters along the sailing route in NA are represented by a series of partially correlated events. Standard IACS NA wave scatter diagram is modified to account for this correlation and later used to perform long-term analysis of VWBMs for oil tankers of different sizes. It was found that both the extreme H_S that ships encounter and the extreme VWBM are significantly reduced for large correlation coefficients.

The method is verified by considering data from the ERA5 wave database along the route in the North Atlantic. It was shown that extreme significant wave heights that a ship encounters for the reference period on one voyage are lower compared to the results obtained by the commonly used assumption of the statistical independence of sea states along the shipping route. Consequently, for an equivalent correlation coefficient of 0.8, found in the present study, lifetime extreme VWBM may be reduced by about 8%.

The second aim of the Thesis is to investigate the effects of using wave data from different sources, wave directionality, and within-year climate variability on the extreme values. Large uncertainties of wave data from different sources are found even if they refer to the same geographical location. Uncertainties of wave data have the largest consequence on the accumulated fatigue damage of marine structures, where predicted fatigue life based on studied databases can differ by a factor larger than 3. The ratio between the highest and lowest total wave energy potential predicted at the location reads 1.63, while the extreme global wave loads can differ by 30%. Different databases provide similar trends regarding time-series of

significant wave heights and storm predictions, but their extreme values are different. This is the case even if the same time resolution is used.

Extreme significant wave height statistics are developed for the Adriatic region by considering wind patterns and within-year climate variability. The extreme value prediction considering wave directionality is, on average, 4% larger compared to the predictions when this effect is neglected. The extreme values predictions from individual directions can overshoot the ones derived from the whole dataset, i.e., by neglecting directionality. However, extreme values obtained by system probability, combining distributions from individual directions, are always conservative. The extreme value prediction considering within-year climate variability appears as a more important effect, leading to, on average, 8% larger extremes compared to the prediction when this effect is neglected.

The final aim of the study is to obtain ECs for the Adriatic Sea. The ECs are developed based on the joint probability distribution of significant wave heights and peak wave periods using data contained in the WWA database. By comparing ECs obtained using IFORM and ISORM methods, it is found that the latter method leads to the conservative estimate of extreme sea states for the same choice of the joint probability distribution parameters. It is also found that ECs are highly sensitive to the joint probability model, especially to the selection of the location parameter γ of Weibull 3P distribution.

5. Future work

The main direction of the continuation of the presented research is the comparative analysis of the results from the Thesis to the recently published IACS North Atlantic (NA) scatter diagram from the revised IACS Rec No.34 [25], intended for strength and fatigue assessment of sea-going ships. The revised recommendation, appearing in parallel with the present Thesis, represents a step forward in rational ship structural strength design and analysis, as the detailed wave hindcast databases are used instead of visual observations, while weather routing is explicitly accounted for by combining wave databases and Automatic Identification System (AIS) [26]. However, the revised recommendation already faced some criticism. Namely, wave data should be compared to the sea states actually experienced by sea-going ships to assess the credibility of the new IACS NA scatter diagram. Interestingly, a similar reduction of the extreme wave loads is obtained by employing spatial correlation along the shipping route in the present study, as using the new IACS NA scatter diagram [68]. It is also to be mentioned that the IACS NA scatter diagram is obtained by neglecting within-year variability and wave directionality, which also deserves consideration in future research.

The effect of spatial-temporal correlation among successive sea states along the shipping route may be used for the prediction of sea states that ships would encounter in the near future. Except for conventional ships, this prediction could be particularly important for autonomous ships where realistic estimates of sea states that a ship could encounter in the next few hours are required. The initial research for the Adriatic Sea is presented in [69], which should be expanded and examined in more detail in future research.

Environmental contours (EC) could be used as a tool to visually compare different versions of wave scatter diagrams, as the comparison based on the numerical values in tables is difficult. It was indicated in the present study how to combine EC and short-term ship extreme responses (Figures 3 and 4 in **Publication V**). However, more research is required to compare short-term extreme wave loads to the long-term extreme responses obtained by all sea-state method and the expansion of the ECs to include the failure probability of the ship hull. Map of the ECs

for the whole Adriatic presented in **Publication V** can have practical applications for the design of marine structures, special marine operations, and extension of the lifetime of the offshore objects in the Adriatic, which is also a potential topic of future research.

Bibliography

[1] Det Norske Veritas. Recommended Practice DNV-RP-C205: Environmental Conditions and Environmental Loads. Oslo; 2019. Available from: www.dnv.com.

[2] Temarel P, Bai W, Bruns A, Derbanne Q, Dessi D, Dhavalikar S, et al. Prediction of wave-induced loads on ships: Progress and challenges. Ocean Engineering. 2016;119:274-308.

[3] Hogben N, Dacunha NMC, Oliver GF. Global Wave Statistics. Feltham: British Maritime Technology Ltd.; 1986.

[4] IACS. Rec. No. 34. Standard Wave Data (North Atlantic Scatter Diagramm); 2000.

[5] Leder N, Smirčić A, Vilibić I. Extreme values of surface wave heights in the northern Adriatic. Geofizika. 1998;15:1-13.

[6] Mansour AE, Preston DB. Return periods and encounter probabilities. Applied Ocean Research. 1995;17(2):127-36.

[7] Bitner-Gregersen EM, Dong S, Fu T, Ma N, Maisondieu C, Miyake R, et al. Sea state conditions for marine structures' analysis and model tests. Ocean Engineering. 2016;119:309-22. Available from: https://www.sciencedirect.com/science/article/pii/S0029801816300105.

[8] Pomaro A, Cavaleri L, Papa A, Lionello P. 39 years of directional wave recorded data and relative problems, climatological implications and use. Scientific Data. 2018;5.

[9] Schirmann ML, Collette MD, Gose JW. Impact of weather source selection on time-and-place specific vessel response predictions. Trends in the Analysis and Design of Marine Structures - Proceedings of the 7th International Conference on Marine Structures, MARSTRUCT 2019. 2019:33-41.

[10] Schirmann ML, Collette MD, Gose JW. Significance of wave data source selection for vessel response prediction and fatigue damage estimation. Ocean Engineering. 2020;216:107610. Available from: https://www.sciencedirect.com/science/article/pii/S0029801820306144.

[11] Ross E, Astrup OC, Bitner-Gregersen E, Bunn N, Feld G, Gouldby B, et al. On environmental contours for marine and coastal design. Ocean Engineering. 2020;195(July 2019):106194.

[12] Mikulić A, Katalinić M, Ćorak M, Parunov J. The effect of spatial correlation of sea states on extreme wave loads of ships. Ships and Offshore Structures. 2021;0(0):1-11.

[13] Ćorak M, Mikulić A, Katalinić M, Parunov J. Uncertainties of wave data collected from different sources in the Adriatic Sea and consequences on the design of marine structures. Ocean Engineering. 2022:112738. Available from: https://www.sciencedirect.com/science/article/pii/S0029801822020212.

[14] Mikulić A, Parunov J. Bias in estimates of extreme significant wave heights for the design of ship structures caused by neglecting within-year wave climate variability. Ships and Offshore Structures. 2022;0(0):1-14. Available from: https://doi.org/10.1080/17445302.2022.2082104.

[15] Mikulić A, Parunov J. A Wave Directionality and a Within-Year Wave Climate Variability Effects on the Long-Term Extreme Significant Wave Heights Prediction in the Adriatic Sea. Journal of Marine Science and Engineering. 2023;11(1). Available from: https://www.mdpi.com/2077-1312/11/1/42.

[16] Mikulić A, Parunov J. Environmental Contours in the Adriatic Sea for Design and Analysis of Marine Structures. Journal of Marine Science and Engineering. 2023;11(5). Available from: https://www.mdpi.com/2077-1312/11/5/899.

[17] Parunov J, Guedes Soares C, Hirdaris S, Wang X. Uncertainties in modelling the low-frequency wave-induced global loads in ships. Marine Structures. 2022;86:103307. Available from: https://www.sciencedirect.com/science/article/pii/S0951833922001435.

[18] Mansour, Alaa; Liu D. Paulling JR, editor. Principles of Naval Architecture Series - Strength of Ships and Ocean Structures. Jersey City: Society of Naval Architects and Marine Engineers; 2008.

[19] Jensen JJ, Mansour AE, Olsen AS. Estimation of ship motions using closed-form expressions. Ocean Engineering. 2004;31(1):61-85. Available from: `http://www.sciencedirect.com/science/article/pii/S0029801803001082`.

[20] Jensen JJ, Mansour AE. Estimation of ship long-term wave-induced bending moment using closed-form expressions. RINA Transactions. 2002;144:41-55.

[21] Petranović T, Mikulić A, Gledić I, Parunov J. Comparative analysis of closed-form expressions and other commonly used seakeeping methods. Ocean Engineering. 2023;281:114977.

[22] Guedes Soares C. On the definition of rule requirements for wave induced vertical bending moments. Marine Structures. 1996;9(3):409-25. Reliability methods for ship structural design. Available from: `https://www.sciencedirect.com/science/article/pii/095183399500033X`.

[23] Parunov J, Senjanović I, Pavičević M. Use of vertical wave bending moment from hydrostatic analysis in design of oil tankers. International journal of maritime engineering. 2004;146:.

[24] Bitner-Gregersen EM, Waseda T, Parunov J, Yim S, Hirdaris S, Ma N, et al. Uncertainties in long-term wave modelling. Marine Structures. 2022;84:103217. Available from: `https://www.sciencedirect.com/science/article/pii/S0951833922000569`.

[25] IACS. Rec. No. 34. Rev.2 Standard Wave Data (North Atlantic Scatter Diagramm); 2022.

[26] de Hauteclocque G, Maretic NV, Derbanne Q. Hindcast based global wave statistics. Applied Ocean Research. 2023;130:103438. Available from: `https://www.sciencedirect.com/science/article/pii/S0141118722003674`.

[27] Barstow S, Mørk G, Lønseth L, Schjølberg P, Machado U, Athanassoulis G, et al. WORLDWAVES: Fusion of data from many sources in a user-friendly

software package for timely calculation of wave statistics in global coastal waters. In: Proceedings of the 13th International Offshore and Polar Conference and Exhibition, ISOPE2003. Honolulu, Hawaii, USA; 2003. p. 136-43.

[28] Hersbach H, de Rosnay P, Bell B, Schepers D, Simmons A, Soci C, et al. Operational global reanalysis: progress, future directions and synergies with NWP; 2018. 27.

[29] Farkas A, Parunov J, Katalinić M. Wave Statistics for the Middle Adriatic Sea. Journal of Maritime & Transportation Science. 2016;52:33-47.

[30] Katalinić M, Parunov J. Wave statistics in the Adriatic Sea based on 24 years of satellite measurements. Ocean Engineering. 2018;158(April):378-88. Available from: `http://www.sciencedirect.com/science/article/pii/S0029801818304414`.

[31] Katalinić M, Parunov J. Uncertainties of estimating extreme significantwave height for engineering applications depending on the approach and fitting technique-adriatic sea case study. Journal of Marine Science and Engineering. 2020;8(4).

[32] Bencivenga M, Nardone G, Ruggiero F, Calore D. The Italian Data Buoy Network (RON). WIT Transactions on Engineering Sciences: Advances in Fluid Mechanics IX. 2012;74:321-32.

[33] Pomaro A, Cavaleri L, Lionello P. Climatology and trends of the Adriatic Sea wind waves: analysis of a 37-year long instrumental data set. International Journal of Climatology. 2017;37(12):4237-50. Available from: `https://rmets.onlinelibrary.wiley.com/doi/abs/10.1002/joc.5066`.

[34] Tabain T. The proposal for the standard of sea states for the Adriatic. Brodogradnja. 1974;25(3-4):251-8.

[35] Tabain T. Standard wind wave spectrum for the Adriatic Sea revisited (1977-1997). Brodogradnja. 1997;45(4):303-13.

[36] HHI. Klimatološki atlas Jadranskog mora (1949.-1970.). Hydrographic Institute of the Republic of Croatia; 1979.

[37] Parunov J, Ćorak M, Pensa M. Wave height statistics for seakeeping assessment of ships in the Adriatic Sea. Ocean Engineering. 2011;38(11):1323-30. Available from: https://www.sciencedirect.com/science/article/pii/S0029801811001120.

[38] Katalinić M, Ćorak M, Parunov J. Optimized Wave Spectrum Definition for the Adriatic Sea. NAŠE MORE: znanstveni časopis za more i pomorstvo. 2020;67(1):19-23.

[39] Carter DJT, Challenor PG. Estimating return values of environmental parameters. Quarterly Journal of the Royal Meteorological Society. 1981;107(451):259-66.

[40] Organization WM. Guide to Wave Analysis and Forecasting. 2nd ed. 702. Geneva: Secretariat of the World Meteorological Organization; 1998.

[41] Perrault DE. Probability of sea condition for ship strength, stability, and motion studies. Journal of Ship Research. 2021;65(1):1-14.

[42] Mackay E, de Hauteclocque G, Vanem E, Jonathan P. The effect of serial correlation in environmental conditions on estimates of extreme events. Ocean Engineering. 2021;242:110092.

[43] Cramer EH, Hansen PF. Stochastic modeling of long term wave induced responses of ship structures. Marine Structures. 1994;7(6):537-66.

[44] Baxevani A, Borgel C, Rychlik I. Spatial models for variability of significant wave height in world oceans. International Journal of Offshore and Polar Engineering. 2008;18:1-7.

[45] De Gracia L, Wang H, Mao W, Osawa N, Rychlik I, Storhaug G. Comparison of two statistical wave models for fatigue and fracture analysis of ship structures. Ocean Engineering. 2019;187(March):106161. Available from: https://doi.org/10.1016/j.oceaneng.2019.106161.

[46] Bitner-Gregersen EM. Joint met-ocean description for design and operations of marine structures. Applied Ocean Research. 2015;51:279-92. Available from: http://dx.doi.org/10.1016/j.apor.2015.01.007.

[47] Montes-Iturrizaga R, Heredia-Zavoni E. Environmental contours using copulas. Applied Ocean Research. 2015;52:125-39. Available from: https://www.sciencedirect.com/science/article/pii/S0141118715000747.

[48] Haselsteiner AF, Ohlendorf JH, Thoben KD. Environmental contours based on kernel density estimation; 2017.

[49] Eckert-Gallup A, Martin N. Kernel density estimation (KDE) with adaptive bandwidth selection for environmental contours of extreme sea states. In: OCEANS 2016 MTS/IEEE Monterey; 2016. p. 1-5.

[50] Jonathan P, Ewans K, Randell D. Non-stationary conditional extremes of northern North Sea storm characteristics. Environmetrics. 2014;25(3):172-88. Available from: https://onlinelibrary.wiley.com/doi/abs/10.1002/env.2262.

[51] Winterstein S, Ude TC, Cornell CA, Bjerager P, Haver S. Environmental parameters for extreme response: inverse FORM with omission factors. Proc of Intl Conf on Structural Safety and Reliability (ICOSSAR93). 1993 01.

[52] Chai W, Leira BJ. Environmental contours based on inverse SORM. Marine Structures. 2018;60:34-51. Available from: https://www.sciencedirect.com/science/article/pii/S0951833917304707.

[53] Bang Huseby A, Vanem E, Natvig B. A new approach to environmental contours for ocean engineering applications based on direct Monte Carlo simulations. Ocean Engineering. 2013;60:124-35. Available from: https://www.sciencedirect.com/science/article/pii/S0029801812004532http://dx.doi.org/10.1016/j.oceaneng.2012.12.034.

[54] A New Approach for Environmental Contour and Multivariate De-Clustering. vol. Volume 3: of International Conference on Offshore Mechanics and Arctic Engineering; 2019. Available from: https://doi.org/10.1115/OMAE2019-95993.

[55] Haselsteiner AF, Ohlendorf JHH, Wosniok W, Thoben KDD. Deriving environmental contours from highest density regions. Coastal Engineering. 2017;123(December 2016):42-51. Available from:

http://dx.doi.org/10.1016/j.coastaleng.2017.03.002https://www.sciencedirect.com/science/article/pii/S0378383916304446.

[56] Mackay E, Haselsteiner AF. Marginal and total exceedance probabilities of environmental contours. Marine Structures. 2021;75(September 2020):102863. Available from: https://doi.org/10.1016/j.marstruc.2020.102863https://www.sciencedirect.com/science/article/pii/S0951833920301568.

[57] Eckert A, Martin N, G Coe R, Seng B, Stuart Z, Morrell Z. Development of a Comparison Framework for Evaluating Environmental Contours of Extreme Sea States. Journal of Marine Science and Engineering. 2021;9(1):1-24. Available from: https://www.mdpi.com/2077-1312/9/1/16.

[58] Haselsteiner AF, Coe RG, Manuel L, Chai W, Leira B, Clarindo G, et al. A benchmarking exercise for environmental contours. Ocean Engineering. 2021;236:109504. Available from: https://www.sciencedirect.com/science/article/pii/S0029801821009033.

[59] Bitner-Gregersen EM, Cramer EH, Løseth R. Uncertainties of load characteristics and fatigue damage of ship structures. Marine Structures. 1995;8(2):97-117.

[60] Rao SS. Reliability-based design. New York: McGraw-Hill; 1992.

[61] Virtanen P, Gommers R, Oliphant TE, Haberland M, Reddy T, Cournapeau D, et al. SciPy 1.0: Fundamental Algorithms for Scientific Computing in Python. Nature Methods. 2020;17:261-72.

[62] IACS. UR S11 Longitudinal Strength Standard; 2021. p. 1-31.

[63] Ćorak M, Parunov J, Guedes Soares C. Long-term prediction of combined wave and whipping bending moments of container ships. Ships and Offshore Structures. 2015;10(1):4-19.

[64] Đigaš A, Ćorak M, Parunov J. Comparison of Linear Seakeeping Tools For Containerships. In: Simpozij Teorija i prakda brodogradnje (20; 2012); 2012. .

[65] Michel RK, Osborne M. Oil Tankers. In: Lamb T, editor. Ship Design and Construction. New Jersey, USA: SNAM0E; 2004. p. 29.1 29.41.

[66] Barstow S, Mørk G, Lønseth L, Mathisen J. WorldWaves wave energy resource assessments from the deep ocean to the coast. J Energy Power Eng. 2011;5.

[67] Moan T, Shu Z, Wu MK, Amlashi H. Comparative reliability analysis of ships – considering different ship types and the effect of ship operations on loads. Transactions SNAME. 2006;114(16–54).

[68] Austefjord HN, de Hauteclocque G, Johnson MC, Zhu TY. Update of wave statistics standards for classification rules. In: Ringsberg JW, Soares CG, editors. Advances in the Analysis and Design of Marine Structures. 1st ed. London: CRC Press; 2023. p. 10.

[69] Mikulić A, Parunov J, Katalinić M. The effect of spatial correlation of sea states on predicted extreme significant wave heights along ship sailing routes. In: Soares CG, editor. Maritime Technology and Engineering 5 Volume 2. 1st ed. London: CRC Press; 2021. p. 37-43.

Curriculum Vitae

Antonio Mikulić, mag. ing. nav. arch. was born on September 30, 1991, in Ljubljana, Slovenia. He finished high school in Biograd na Moru and completed his undergraduate studies at the Faculty of Mechanical Engineering and Naval Architecture, University of Zagreb, in 2014. He obtained his master's degree from the same institution in 2016, completing both programs with the highest honors and faculty medals for excellence. During the graduate program, he spent five months at Instituto Superior Técnico in Lisbon as an exchange student, where he worked on the master's thesis titled "Assessment of global vertical loads in damaged ship".

After graduation, he worked as a CAD and PLM consultant. Since July 2018, he has been working as a research and teaching assistant at the Chair for Ship Structure Design, Department of Naval Architecture, and Ocean Engineering at the Faculty of Mechanical Engineering and Naval Architecture, University of Zagreb. He has published 13 articles in international peer-reviewed journals and participated in a number of specialised conferences (**CROSBI profile: 35016**).

His research interests include wave loads, reliability-based design, structural reliability, seakeeping, data analysis, etc.

Summary of publications

Publication I The effect of spatial correlation of sea states on extreme wave loads of ships

Antonio Mikulić, Marko Katalinić, Maro Ćorak and Joško Parunov
Ships and Offshore Structures 2021, 16(sup1), 22-32
doi.org/10.1080/17445302.2021.1884817

Publication II Uncertainties of wave data collected from different sources in the Adriatic Sea and consequences on the design of marine structures

Maro Ćorak, **Antonio Mikulić**, Marko Katalinić and Joško Parunov
Ocean Engineering 2022, 266(1), 112738
doi.org/10.1016/j.oceaneng.2022.112738

Publication III Bias in estimates of extreme significant wave heights for the design of ship structures caused by neglecting within-year wave climate variability

Antonio Mikulić and Joško Parunov
Ships and Offshore Structures 2022, 18(4), 582-595
doi.org/10.1080/17445302.2022.2082104

Publication IV A Wave Directionality and a Within-Year Wave Climate Variability Effects on the Long-Term Extreme Significant Wave Heights Prediction in the Adriatic Sea

Antonio Mikulić and Joško Parunov
Journal of Marine Science and Engineering 2023, 11(1), 42
doi:10.3390/jmse11050899

Publication V Environmental Contours in the Adriatic Sea for Design and Analysis of Marine Structures

Antonio Mikulić and Joško Parunov
Journal of Marine Science and Engineering 2023, 11(5), 899
doi:10.3390/jmse11050899

Publication I

Preprint of the published journal article.

The effect of spatial correlation of sea states on extreme wave loads of ships

Antonio Mikulić[a], Marko Katalinić[b], Maro Ćorak[c], Joško Parunov[a,*]

[a]*University of Zagreb, Faculty of Mechanical Engineering and Naval Architecture, Ivana Lučića 5, Zagreb 10000, Croatia*
"bUniversity of Split, Faculty of Maritime Studies, Ruđera Boškovića 37, Split 21000, Croatia"
[c]*University of Dubrovnik, Maritime Department, Ćira Carića 2, Dubrovnik 20000, Croatia*

Abstract

The purpose of the study is to include a spatial statistical correlation between sea states that ship encounters during a voyage to improve wave scatter diagram for the analysis of ship structures. The methodology consists of computation of system reliability of a series of partially correlated events, representing sea states that ship encounters along the sailing route. The IACS North Atlantic wave scatter diagram is modified to account for such spatial correlation and new scatter diagrams for partially correlated sea states are constructed. Based on such "correlated scatter diagrams", long-term distribution of vertical wave bending moments is performed and compared to the results following from an "uncorrelated scatter diagram". It was found that a spatial correlation may considerably reduce extreme vertical wave bending moments. Verification of the methodology is performed by simulating shipping route in the North Atlantic using ERA5 wave database.

Keywords: wave scatter diagram; spatial correlation; extreme wave loads; reliability-based design

1. Introduction

Selecting the appropriate wave scatter diagram is one of the crucial steps in the analysis of the long-term response of marine structures to wave action that is required for the prediction of extreme wave-induced loads and fatigue analysis. Wave scatter diagram contains probabilities of occurrence of sea states, described by a combination of significant wave heights and mean zero-crossing (or peak) wave periods. By assuming that the stochastic process of ship response to sea waves is narrow banded, it is generally accepted that amplitudes of the wave loads in the short-term sea state follow Rayleigh distribution. Short-term ship responses are then combined with the probabilities of occurrence of sea states in order to obtain the long-term probability distribution of the wave-induced loads. Short-term seas states are assumed to be statistically independent and hence uncorrelated in the standard procedure for the long-term response analysis (IACS 2000). This assumption is obviously doubtful because of the mutual statistical dependence between successive sea states that ship encounters during the voyage.

As may be seen from the literature review presented in Section 1.1, wave scatter diagrams currently in use for ship structural strength analysis are based on data from Global Wave Statistics (GWS, Hogben et al. 1986). The way how these data were collected, i.e. mostly by visual observations by volunteers from merchant ships, did not allow to consider correlation between sea states along the shipping route. However, availability of long-term high-quality wave databases, obtained by hindcasting using numerical wave models (WAM, WAWATCH-III, SWAN), enables analyzing time series of sea states along common shipping routes and thus to identify correlation that may exist between sea states that ship encounters. The proposal for improvement of scatter diagrams based on the extensive information accessible in the wave databases is the main contribution of the present study.

This work is organized in the following way. Literature review on wave scatter diagrams for ship design and analysis is given as a part of the Introduction. In the first section after Introduction, the actual ship sailing route in the North Atlantic is described, voyage duration and time spent in each of wave zones along sailing route is determined. After that, probability density functions of significant wave height are determined assuming different levels of correlation between successive sea states

* Corresponding author.
E-mail address: jparunov@fsb.hr

along the sailing route. In the following section, consequences on the extreme vertical wave bending moment for return period of 25 years is estimated for four oil tankers of different sizes. In verification section, the correlation coefficient for the sailing route in the North Atlantic is determined using ERA5 wave database obtained by numerical wave modelling calibrated by satellite measurements. At the end of the paper, corresponding conclusions and directions for future researches are provided.

1.1 Literature review on wave scatter diagrams for ship design and analysis

The problem of selecting an appropriate scatter diagram in the computation of the long-term distribution of vertical wave bending moment (VWBM), as the most important wave load component, is identified already during development of IACS Rule formulation (Nitta et al. 1992). Comparative analysis of classification societies has shown significant differences in the predicted extreme VWBM because they have utilized different wave data. For the exceeding probability of 10^{-8}, the calculated design wave bending moments varied by even 80% because of the different choices of wave scatter diagrams. It is interesting to note that all the classification societies claimed to had used data for the North Atlantic with only slight modifications according to their own experience (Nitta 1995). The influence of the choice of wave data on the lifetime VWBM has also been studied by Guedes Soares (1991, 1996 and 1999). Comparative study of various scatter diagrams that may be used in ship design resulted in characteristic values from the long-term distributions differing by up to 50%.

For fixed offshore structures, wave scatter diagrams are often available for specific locations, and the computation of the long-term distribution of wave loads or their extreme values may be done by well-established engineering methods (DNVGL-RP-C205 2017). For ships, however, the problem is more complicated because of their mobility, and because of the unpredictable human actions (Moan 2006). Two different issues were identified in the long-term prediction of extreme wave loads on ships, namely, how to choose the source of the wave data, and within the chosen source of the wave data how to select a representative ship route (Parunov and Senjanović 2003).

For the analysis of ship structures, it is a usual practice to use probabilities of occurrence of sea states from the wave atlas Global Wave Statistics (GWS, Hogben et al. 1986). Data in GWS are obtained by observations of volunteers from merchant ships on the usual shipping routes. As elaborated by (Guedes Soares 1996) such choice is more rational compared to using data from fixed measurements since these data implicitly account for the world-wide practices of shipmasters operating along the main shipping routes. Using data measured on stationary wave buoys leads to too conservative estimates of wave loads on ship structures, since the effect of heavy weather avoidance is not explicitly accounted for (Parunov et al. 2004). Data from GWS provide a reasonably accurate estimate of significant wave height, but it was found that they tend to underestimate actual wave periods, i.e. to overestimate wave steepness of sea states. In order to describe realistic periods of sea states, data from GWS need to be "smoothed" before practical application (Bitner-Gregersen et al. 1995). "Smoothed" joint probability distributions of significant wave heights and mean zero-crossing periods for all wave zones in GWS are provided in DNVGL-RP-C205 (2017).

There is a tendency nowadays to use wave databases derived by numerical models in addition to databases from voluntary observing ships (Vettor and Soares 2016). There are some discrepancies among significant wave heights predicted by these databases, especially between numerical models and visual observations. Schirmann et al. 2019 found that different wave data sources could significantly affect wave induced loads and cumulative fatigue damage of ship structural details.

Since most ships are designed for global, unrestricted service, the North Atlantic (NA) has been chosen as the reference operational area for calculating extreme wave loads on ship structures. Several scatter diagrams originated from GWS have been proposed in the past to describe navigation in the North Atlantic. One of them was proposed by some of the leading classification societies and ship research institutions within the European project SHIPREL (Reliability Methods for Ship Structural Design) (Guedes Soares et al. 1996). The SHIPREL scatter diagram is obtained by combining information from zones Nos. 8, 9, 11, 15, 16, and 17 assuming the probability of occurrence of each of the wave zones proportional to their relative size (Guedes Soares 1999). SHIPREL wave scatter diagram was defined up to a significant wave height of 11.5m and normalized by 10 000 observations. This is because, in the written version of GWS, the probabilities are rounded to four decimal places. Thus, the sea states of a very low probability of occurrence are removed from the scatter diagram.

Different definitions of scatter diagrams used in the past resulted in large differences in extreme VWBM. Such discrepancies are unacceptable, as they could not assure a consistent level of ship structural integrity. To reduce these differences, IACS proposed a standard wave scatter diagram in

IACS Rec. no.34 (2000). The IACS scatter diagram describes the wave data of the North Atlantic, covering the areas 8,9,15 and 16, as defined in GWS. The IACS diagram includes significant wave heights up to 16.5m and contains 100 000 observations. IACS NA scatter diagram was obtained by numerical simulation using the joint probability distribution of significant wave heights and mean zero-crossing periods, obtained by combining distributions of individual wave zones. The simulation is performed based on theoretical distribution fitted to the empirical data set from the written version of GWS. This procedure may introduce numerical errors as there is uncertainty regarding the type and parameters of fitted distributions. Details of resulting distributions for the IACS NA scatter diagram are available in DNVGL-RP-C205 (2017).

The ICAS NA scatter diagram should be used together with zero or small ship forward speed. For some ship types, as bulk carriers and oil tankers it is a justified assumption that in the extreme storms ship speed is considerably reduced. For some ship types, however, as ultra-large container ships (ULCS), this assumption is inappropriate as slamming and whipping are reduced with reduced ship speed. Therefore, by assuming zero speed, these effects, crucial for large container ships cannot, be accounted for. This indicates that specific scatter diagrams, reflecting operational features of individual ship types, may be more appropriate than using generic wave data common for all ships.

Another aspect deserving attention is rerouting, as for voyages of long duration without the opportunity to seek shelter, ships may change route upon additional information based on on-board monitoring of response and sea state forecasting. It is known that weather routing is performed more often by container ships than oil tankers and bulk carriers, so the IACS NA scatter diagram is more appropriate for latter ship types. An example of rerouting for long voyage duration is presented by (Moan et al. 2006), while an example of heavy weather avoidance for a short-term voyage of ULCS is presented by Prpić-Oršić et al. (2014). Modelling approaches to account heavy weather avoidance in the computation of long-term probability distribution of wave loads is provided by Moan et al. (2006) and employed on practical examples of container ships of different sizes by Ćorak et al. (2015).

A one potentially un-conservative aspect of the currently used wave scatter diagram is related to global warming due to human activities, leading to changes in ocean environmental conditions (Bitner-Gregersen et al. 2016). GWS Atlas was published in 1986, so the missing last 30 years data seem to have an impact on extreme values of significant wave height. The 100-year H_s using visual observations up to 2006 is about 2m higher compared to the value given by the IACS scatter diagram. These figures are expected to become even worse in the future years because of global warming. Bitner-Gregersen et al. 2013 reviews effects of climate change on the wind and wave conditions and their impact on ship and offshore structure design. The increase in significant wave height has been noticed, comparing the data from 1950ies up until 2010s. Research also predicts future increases more pronounced for the extremes than for the mean values of the wind speeds and wave heights. Therefore, the exactness of the data from GWS database has been questioned, how reliable will it be and how long will it be in use.

Rogue waves have attracted considerable attention during the past two decades. These waves are very steep and much larger than the surrounding waves, commonly defined by the criterion that the wave height exceeds twice, while the wave crest exceeds 1.25 times the significant wave height. Although responsible for several accidents of ships and offshore structures, rogue waves are not explicitly included in classification society rules and offshore standards yet (Bitner-Gregeren and Gramstad 2015). As rogue waves have different statistical distribution than standard waves included in scatter diagrams, they are considered for the future ship rules as loads for the Accidental Limit State (ALS), with the objective to prevent impairing main safety function of the ship encountering such waves (IACS, 2009). Next generation wave-structure interaction codes with nonlinear waves generated by higher order spectral method, are being developed for design purposes (Bitner-Gregersen 2017). Another way to prevent marine accidents because of rogue waves is to develop warning criteria and systems for ships to avoid such dangerous situations (Bitner-Gregersen and Gramstad 2015). As rogue waves are not predictable by long-term statistics of wind waves and swell, they are outside the scope of the present study.

Different types of correlation that are present in the real wave environment are neglected in the IACS procedure for long-term response analysis. A first correlation that may be observed is between individual wave peaks, as large wave peaks come in clusters. The way how this can be included in short-term response analysis is presented by Cramer and Hansen (1994). Another assumption implicitly adopted in IACS NA scatter diagram is that wave zones on the ship sailing route are statistically independent as well as consecutive short-term sea states within each of wave zones that ship encounters on her voyage. Considerable effect of correlation among wave zones that ship encounters during a

voyage in commercial shipping routes, on extreme sea states is presented by Mansour and Preston (1995). They showed how correlation leads to the reduction of the extreme sea states that ship encounters during the lifetime in different sailing routes. Consequences of spatial correlation among successive sea states on different locations that ship encounters on extreme values are studied by Mikulić et al. (2020), using a database containing 23 years of continuous wave measurements and numerical simulations for the Adriatic Sea. A comparison of statistical predictions and long-term measurements clearly indicated that the assumption of statistical independence leads to the conservative estimate of extreme seas states that ship would encounter along the assumed route. This also could be one of the reasons why extreme wave loads calculated by direct methods often exceed Rule wave loads Parunov et al. (2004). Another, albeit mathematically more challenging approach to consider effects of the spatial correlation for the estimation of significant wave height is the random field modelling, fitted to satellites wave measurements (Baxevani et al. 2008). The approach is recently extended as a basis for the fatigue analysis in De Gracia et al. 2019.

2. Description of the shipping route in the North Atlantic

Overlaying the IACS NA quadrant map and a ship traffic density map provided by vessels tracking services (Figure 1) it is possible to conclude that the northernmost clearly distinguishable and frequent shipping route across the North Atlantic passes through quadrants 15 and 16 (while in quadrants 8 and 9 there is significantly less traffic).

The vessel tracking service (in this case “MarineTraffic”) uses data from on-board transponders, a part of the Automatic identification system (AIS), for tracking vessels in real-time and cumulating historical data. AIS provides unique identification, position, course, and speed for each vessel on which it is installed, and its primary purpose is to assist the vessel’s watchkeeping officer and to allow marine authorities to track vessels. The International Maritime Organization (IMO), in its convention Safety of life at sea (SOLAS), requires AIS to be fitted on-board ships for the international voyage with 300 gross tonnage or more, and all passenger ships regardless of size.

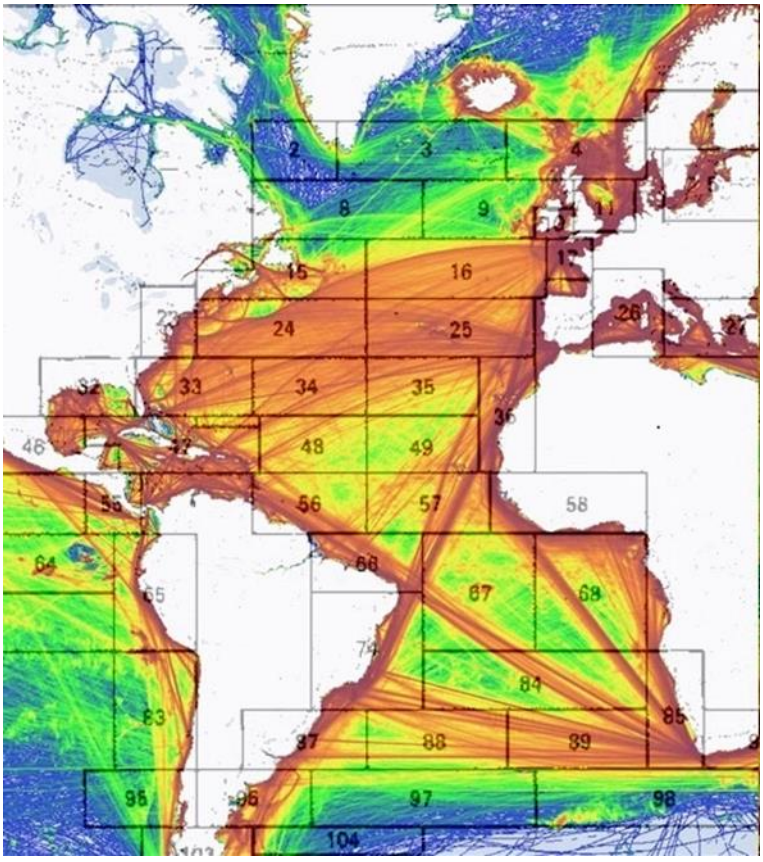

Fig. 1. Vessel traffic density map by “Marine Traffic” and IACS wave quadrants https://www.marinetraffic.com/en/ais)

This identified shipping lane (the northern most, red line in Figure 1) connects the English Channel in the east and North America on the west up to the area where separation starts for the Great Lakes and major east coast ports. The route planned for the case study, across the two IACS quadrants 15 and 16, follows a loxodrome (also called "rhumb line") which appears as a straight line on a map and does not employ the Earth's curvature to optimize distance because it would not be significantly beneficial for the considered route. The total distance travelled equals 2360 nautical miles (nm).

It is common to assume that the sea surface is stationary for duration of 20 minutes to 3-6 hours (DNVGL-RP-C205 2017). In the present study, it is assumed that the sea state is stationary for 3 hours. With the assumed average ship speed of 12 nm/h, and a 3-hour sea state duration interval, the ship travels:

- 36 consecutive 3-hour (sea state) intervals in quadrant 16 (N_{Q16}); corresponding to 108 hours total time spent or 1292 nm travelled within quadrant 16,
- 30 consecutive 3-hour (sea state) intervals in quadrant 15 (N_{Q15}); corresponding to 89 hours total time spent or 1068 nm travelled within quadrant 15,

during one voyage. The number of voyages over the course of one year (N_Y) can be set to 35, considering that oil tankers generally spend no more than one or two days in port.

3. Definition of scatter diagrams accounting for correlation between short-term sea states

The GWS data have been fitted by a joint environmental model in the Bitner-Gregersen et al. (1995) assuming 3-parameter Weibull probability density function defined by (1), adequate for the marginal description of significant wave height H_s.

$$f_{H_s}(h) = \frac{\beta}{\alpha} \cdot \left(\frac{h-\gamma}{\alpha} \right)^{\beta-1} \cdot \exp\left[-\left(\frac{h-\gamma}{\alpha} \right)^{\beta} \right] \tag{1}$$

For Weibull distribution, α represents the scale parameter, β is the shape parameter, γ is the location parameter, and h is the random variable of the H_s. The zero-crossing wave period (T_z), is modeled by a conditional lognormal distribution conditional on H_s:

$$f_{T_z|H_s}(t|h) = \frac{1}{\sigma t \sqrt{2\pi}} \cdot \exp\left\{ -\frac{[\ln(t)-\mu]^2}{2\sigma^2} \right\} \tag{2}$$

where the distribution parameters μ and σ are functions of the H_s defined by expressions (3).

$$\begin{aligned} \mu &= E\left[\ln(T_Z)\right] = a_0 + a_1 h^{a_2} \\ \sigma &= std\left[\ln(T_Z)\right] = b_0 + b_1 e^{h b_2} \end{aligned} \tag{3}$$

The parameters a_0, a_1, a_2, b_0, b_1, and b_2, are specific for wave zone and have been determined from the actual data by least squares technique.

The sea states (and wave zones) along the sailing route are considered as members in a series system. Therefore, a non-encounter of specific wave height (or a sea state) occurs only if mutual non-encounter takes place in all members of a system. The probability of non-exceeding different significant wave heights along the route is modeled by a 3-parameter Weibull cumulative distribution function (4). The Weibull's parameters α, β, and γ are available in Bitner-Gregersen et al. (1995) for the wave zones along the route:

$$F_{H_s}(h) = 1 - \exp\left[-\left(\frac{h-\gamma}{\alpha} \right)^{\beta} \right] \tag{4}$$

The system probability of non-encounter for equally correlated members of a series system can be modified (Eq. (5)) to define a probability of non-exceeding a specific H_s for equally correlated sea states (Rao 1992).

$$P_{H_s,ne}(h) = \int_{-\infty}^{\infty} \left[\prod_{i=1}^{N} \Phi\left(\frac{\beta_i(h) + z\sqrt{\rho}}{\sqrt{1-\rho}} \right) \right] \phi_Z(z) dz \tag{5}$$

The correlation coefficient is represented by ρ, while $\phi(z)$ and Φ denote the probability density and distribution function of the standard normal variate z. It is implicitly assumed, in the present study, that there is an equal average correlation between sea states, represented by ρ. The reliability index β_i, defined in (6), is an argument of the standard normal distribution (Φ), which yields one minus the probability of non-exceeding H_s described by equation (4).

$$\beta_i(h) = -\Phi^{-1}\left(1 - F_{H_s}(h)\right) \tag{6}$$

The probability of non-exceeding a specific H_s during one voyage ($P_{Hs,ne}$) is calculated by (5) for the number of the encountered sea states (N) defined in (7) and ρ ranging from 0 to 1.

$$N = N_{Q15} + N_{Q16} \tag{7}$$

For the ρ=0, the equation (5) provides the same results as the calculation assuming statistically independent sea states (8), while for the ρ=1, it converges to expression (9) assuming a full correlation of sea states.

$$P_{H_s,SI}(h) = \prod_{i=1}^{N} F_{Hs,i}(h) \tag{8}$$

$$P_{H_s,FC}(h) = \min_{i} F_{H_{s,i}}(h) \tag{9}$$

The cumulative distribution functions, i.e. probabilities of non-exceedance of extreme H_s, are calculated using Eq. (5), ranging the ρ values from 0 to 1. A portion of the results is displayed in Figure 2 and suggests a significant reduction in the probability of exceedance of selected H_s as the correlation increases. The curves representing fully correlated (ρ=1) and statistically independent (ρ=0) sea states are steeper, compared to others, suggesting smaller variance, more clearly presented in Figure 3, where probability density functions are displayed.

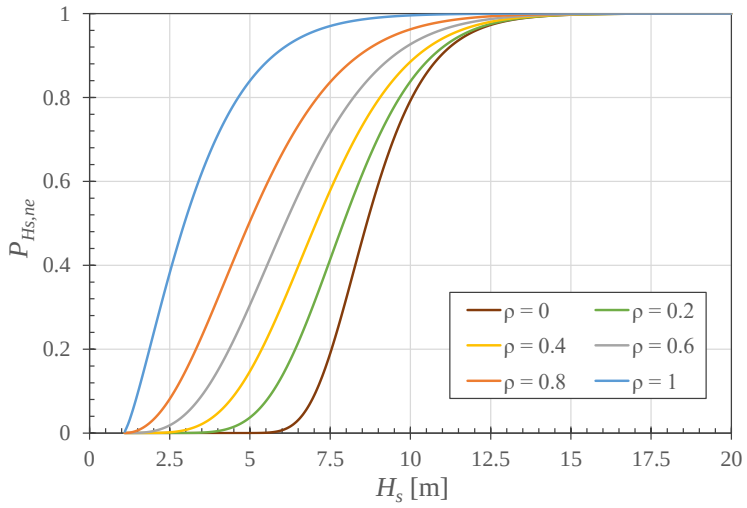

Fig. 2. Probability of non-exceedance of extreme significant wave heights for the one-journey return period.

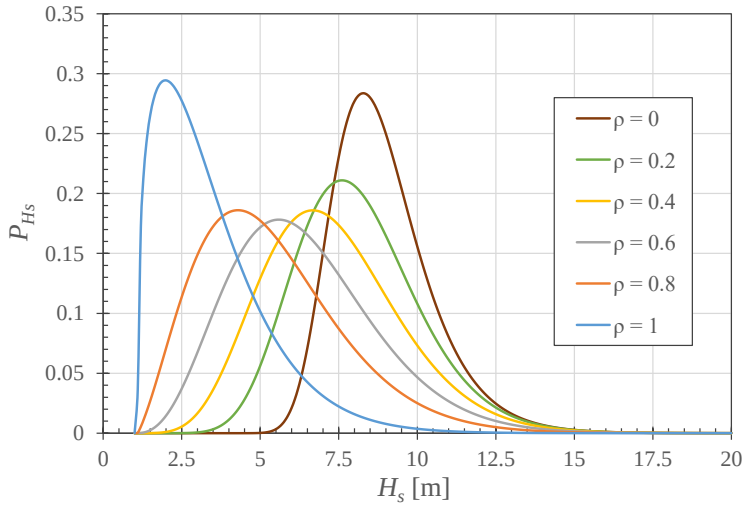

Fig. 3. Probability density functions of extreme significant wave heights for the one-journey return period.

The initial distributions of H_s, for correlated sea states (P_I), are created by a slightly modified and reversed hitherto defined procedure. Extreme value distributions ($P_{Hs,ne}$), calculated by Eq. (5) and presented in Figures 1, are used to compute the initial distributions, assuming the independence between successive sea states as defined in Eq. (10).

$$P_{H_s,ne}(h) = \left(P_I(h)\right)^N \Leftrightarrow P_I(h) = \left(P_{H_s,ne}(h)\right)^{\frac{1}{N}} \tag{10}$$

The results are presented in Figure 4. As may be seen in the Figure 4, results are limited by γ=1m. A physical interpretation of γ, i.e. of the location parameter of 3-parameter Weibull distribution, is the permanent activity of sea waves that is always present. Therefore, the initial distributions do not describe sea states below H_s=1m, since the studied wave zones have γ value around 1. Also, by including sea states (i.e. H_s values) below γ value into the calculation, Eq. (4) would result in complex numbers, and consequently, a numerical problem. Considering the purpose of the present study, the exact distribution of such small values is mostly irrelevant and hence, neglected. The correlated P_I-s

have extremely high starting gradient, signaling, at already very small values of H_s, a very high probability of non-exceedance.

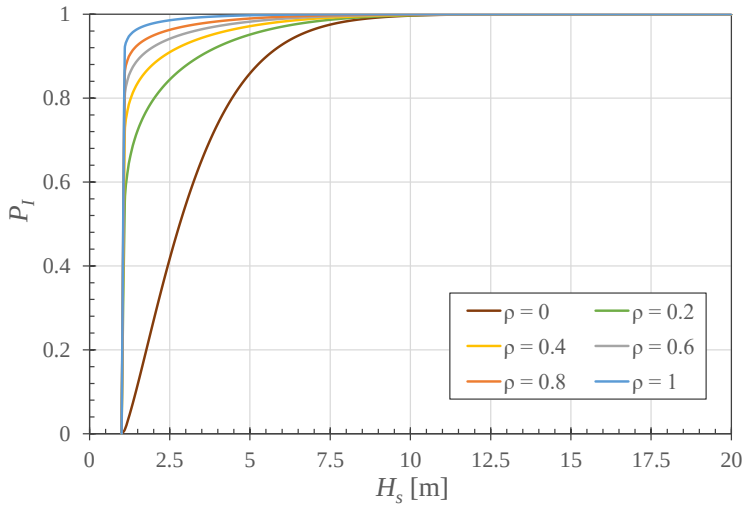

Fig. 4. Probability of non-exceedance of extreme significant wave heights for the one-journey return period.

The distribution of T_z is not considered directly by the procedure yet taken from the joint model for the North Atlantic, available in DNVGL-RP-C205 (2017).

The MC simulation is then conducted, creating 100 000 random samples to produce a scatter diagram according to the hybrid joint environmental model consisting of the initial distributions of H_s, defined by Eq. (10) and distributions of T_z, as already described, using Eq. (2) and (3). Thus, the scatter diagrams, modified to account for spatial correlation, are obtained for different values of ρ. Samples of generated scatter diagrams are illustrated in Tables 1 to 4 for ρ=0, 0.6, 0.8, and 1.

The severity of the scatter diagram is inversely proportional to the spatial correlation between sea states along the route. As the correlation increases, most MC simulation outputs are occurring in the lowest H_s class. Thus, for ρ=0, 5 occurrences of H_s=15m are observed, while for ρ=0.6 and 0.8, such extreme H_s appears 3 and 1 time, respectively. For perfectly correlated sea states (ρ=1), the highest encountered H_s reads just 12m. It is interesting to notice that an operational envelope for bulk carriers and oil tankers in full load conditions reads about 12m, according to Moan et al. (2006), which corresponds to scatter diagram obtained for perfect correlation.

Table 1. Scatter diagram for uncorrelated sea states (ρ=0).

H_s\T_z	1	2	3	4	5	6	7	8	9	10	11	12	13	14	15	Sum
1	0.0	0.0	0.0	1.6	116.0	1332.8	3653.2	3682.8	1956.8	643.8	153.8	29.0	5.4	0.6	0.2	**11576**
2	0.0	0.0	0.0	0.0	24.4	712.4	4392.8	9021.8	8680.6	4791.8	1778.4	495.4	121.6	20.2	3.6	**30043**
3	0.0	0.0	0.0	0.0	1.8	137.4	1504.4	4989.8	7231.4	5596.8	2853.0	1019.0	291.8	65.4	14.2	**23705**
4	0.0	0.0	0.0	0.0	0.4	24.4	407.2	2076.6	4055.6	4285.6	2767.4	1208.2	419.0	116.6	28.0	**15389**
5	0.0	0.0	0.0	0.0	0.1	4.4	112.7	766.7	1997.7	2619.9	2046.6	1062.5	414.2	131.3	46.9	**9203**
6	0.0	0.0	0.0	0.0	0.0	0.7	27.5	247.2	818.7	1335.4	1267.0	758.3	350.1	128.2	43.9	**4977**
7	0.0	0.0	0.0	0.0	0.0	0.5	6.3	83.2	317.4	633.1	707.4	492.3	253.7	94.6	44.5	**2633**
8	0.0	0.0	0.0	0.0	0.0	0.2	2.3	20.9	121.2	271.9	357.6	284.5	154.2	72.0	32.2	**1317**
9	0.0	0.0	0.0	0.0	0.0	0.0	0.5	6.4	44.6	113.4	163.2	146.3	91.6	44.0	22.2	**632**
10	0.0	0.0	0.0	0.0	0.0	0.0	0.1	1.5	14.4	41.9	66.5	71.7	48.8	24.3	14.1	**283**
11	0.0	0.0	0.0	0.0	0.0	0.0	0.0	0.5	4.6	17.2	31.6	32.4	26.5	14.7	8.8	**136**
12	0.0	0.0	0.0	0.0	0.0	0.0	0.0	0.1	1.4	5.6	11.4	14.6	11.2	7.0	5.7	**57**
13	0.0	0.0	0.0	0.0	0.0	0.0	0.0	0.0	0.4	2.5	5.3	7.2	6.3	4.2	3.0	**29**
14	0.0	0.0	0.0	0.0	0.0	0.0	0.0	0.0	0.4	0.8	2.4	3.2	3.3	2.5	2.3	**15**
15	0.0	0.0	0.0	0.0	0.0	0.0	0.0	0.0	0.0	0.2	0.8	1.0	1.3	0.9	0.8	**5**
Sum	0.0	0.0	0.0	1.6	142.7	2212.8	10106.9	20897.6	25245.2	20359.9	12212.2	5625.5	2199.1	726.4	270.3	100000

Table 2. Scatter diagram for partially correlated sea states (ρ=0.6).

$H_s \backslash T_z$	1	2	3	4	5	6	7	8	9	10	11	12	13	14	15	Sum
1	0.0	0.0	0.0	6.6	875.2	10262.2	27885.2	28669.8	14994.8	4977.8	1197.6	202.0	31.0	4.4	1.4	**89108**
2	0.0	0.0	0.0	0.1	3.9	120.3	725.9	1501.3	1449.3	795.8	300.1	86.6	20.1	3.6	1.0	**5008**
3	0.0	0.0	0.0	0.0	0.1	12.8	142.5	496.1	705.5	559.2	277.3	103.4	32.5	6.0	1.6	**2337**
4	0.0	0.0	0.0	0.0	0.0	1.6	36.4	172.7	341.0	367.2	239.8	106.9	32.5	9.6	3.3	**1311**
5	0.0	0.0	0.0	0.0	0.0	0.6	10.7	71.9	185.0	237.6	188.6	100.8	37.6	11.7	4.7	**849**
6	0.0	0.0	0.0	0.0	0.0	0.2	2.9	27.0	90.6	150.6	139.2	85.5	42.0	15.1	4.1	**557**
7	0.0	0.0	0.0	0.0	0.0	0.0	0.9	9.8	39.6	82.0	84.0	62.4	30.0	12.1	5.5	**326**
8	0.0	0.0	0.0	0.0	0.0	0.0	0.3	3.9	19.2	43.7	56.2	45.8	27.9	11.8	5.4	**214**
9	0.0	0.0	0.0	0.0	0.0	0.0	0.0	1.5	8.6	20.5	31.2	29.6	18.1	7.9	4.8	**122**
10	0.0	0.0	0.0	0.0	0.0	0.0	0.0	0.5	3.5	11.2	18.6	19.7	13.8	6.6	4.1	**78**
11	0.0	0.0	0.0	0.0	0.0	0.0	0.0	0.2	1.3	4.8	8.5	11.2	7.7	4.7	2.5	**41**
12	0.0	0.0	0.0	0.0	0.0	0.0	0.0	0.1	0.4	2.4	4.8	6.6	5.2	3.0	2.5	**25**
13	0.0	0.0	0.0	0.0	0.0	0.0	0.0	0.0	0.2	1.2	2.9	4.1	4.2	2.5	2.0	**17**
14	0.0	0.0	0.0	0.0	0.0	0.0	0.0	0.0	0.0	0.3	0.7	0.9	0.8	0.8	0.5	**4**
15	0.0	0.0	0.0	0.0	0.0	0.0	0.0	0.0	0.0	0.2	0.4	0.7	0.6	0.6	0.4	**3**
Sum	0.0	0.0	0.0	6.7	879.2	10397.6	28804.7	30954.5	17839.0	7254.5	2549.8	866.1	304.0	100.3	43.7	100000

Table 3. Scatter diagram for partially correlated sea states (ρ=0.8).

$H_s \backslash T_z$	1	2	3	4	5	6	7	8	9	10	11	12	13	14	15	Sum
1	0.0	0.0	0.0	8.2	919.0	10664.4	29152.8	29630.8	15620.4	5170.0	1222.4	219.2	34.8	3.2	0.8	**92646**
2	0.0	0.0	0.0	0.0	2.3	86.1	533.5	1117.6	1066.5	577.8	208.1	58.3	12.4	2.0	0.4	**3665**
3	0.0	0.0	0.0	0.0	0.0	8.9	97.4	311.7	454.4	360.5	181.4	68.4	18.2	4.0	1.1	**1506**
4	0.0	0.0	0.0	0.0	0.1	1.2	22.8	116.2	231.3	238.8	153.8	68.7	23.4	5.9	2.0	**864**
5	0.0	0.0	0.0	0.0	0.0	0.4	6.6	46.6	119.0	155.1	122.1	62.3	25.6	7.8	2.8	**548**
6	0.0	0.0	0.0	0.0	0.0	0.1	2.3	14.1	46.0	77.0	73.6	43.1	20.4	7.4	3.2	**287**
7	0.0	0.0	0.0	0.0	0.0	0.0	0.6	7.3	27.4	50.4	57.8	38.8	19.2	7.6	3.1	**212**
8	0.0	0.0	0.0	0.0	0.0	0.0	0.1	2.0	11.0	24.2	32.3	24.7	14.4	5.2	3.3	**117**
9	0.0	0.0	0.0	0.0	0.0	0.0	0.0	0.8	4.3	11.9	17.5	16.2	10.2	4.4	2.7	**68**
10	0.0	0.0	0.0	0.0	0.0	0.0	0.0	0.2	1.8	5.5	9.4	9.0	6.7	3.3	2.0	**38**
11	0.0	0.0	0.0	0.0	0.0	0.0	0.0	0.1	0.8	3.0	5.3	5.9	4.6	2.6	1.7	**24**
12	0.0	0.0	0.0	0.0	0.0	0.0	0.0	0.0	0.4	1.8	3.2	3.7	3.5	1.9	1.5	**16**
13	0.0	0.0	0.0	0.0	0.0	0.0	0.0	0.0	0.1	0.4	1.0	1.5	1.3	0.8	0.9	**6**
14	0.0	0.0	0.0	0.0	0.0	0.0	0.0	0.0	0.0	0.2	0.3	0.5	0.5	0.3	0.3	**2**
15	0.0	0.0	0.0	0.0	0.0	0.0	0.0	0.0	0.0	0.1	0.1	0.2	0.2	0.2	0.2	**1**
Sum	0.0	0.0	0.0	8.2	921.4	10761.1	29816.0	31247.3	17583.2	6676.6	2088.3	620.3	195.4	56.4	25.9	100000

Table 4. Scatter diagram for fully correlated sea states (ρ=1).

$H_s \backslash T_z$	1	2	3	4	5	6	7	8	9	10	11	12	13	14	15	Sum
1	0.0	0.0	0.0	7.6	963.8	11062.2	30321.6	30969.8	16258.8	5375.2	1303.8	223.6	32.2	6.2	0.2	**96525**
2	0.0	0.0	0.0	0.0	1.7	47.4	297.9	620.3	586.8	325.9	126.5	34.1	8.3	0.7	0.4	**2050**
3	0.0	0.0	0.0	0.0	0.0	4.3	47.6	157.4	220.2	170.5	91.0	31.8	8.6	2.4	0.5	**734**
4	0.0	0.0	0.0	0.0	0.0	0.5	8.3	44.1	86.3	87.3	56.6	25.9	9.0	2.5	0.8	**321**
5	0.0	0.0	0.0	0.0	0.0	0.1	1.9	15.1	34.1	48.0	39.4	21.6	8.2	2.0	0.9	**171**
6	0.0	0.0	0.0	0.0	0.0	0.0	0.6	4.5	16.8	27.9	24.0	15.0	7.3	2.0	0.8	**99**
7	0.0	0.0	0.0	0.0	0.0	0.0	0.0	1.5	5.2	10.9	12.6	7.7	4.6	1.7	0.8	**45**
8	0.0	0.0	0.0	0.0	0.0	0.0	0.0	0.5	3.1	6.3	7.5	6.9	3.7	1.5	0.5	**30**
9	0.0	0.0	0.0	0.0	0.0	0.0	0.0	0.3	0.8	2.9	4.4	3.3	2.2	1.2	0.8	**16**
10	0.0	0.0	0.0	0.0	0.0	0.0	0.0	0.0	0.3	1.0	1.3	1.3	1.2	0.6	0.3	**6**
11	0.0	0.0	0.0	0.0	0.0	0.0	0.0	0.0	0.1	0.3	0.5	0.5	0.3	0.3	0.1	**2**
12	0.0	0.0	0.0	0.0	0.0	0.0	0.0	0.0	0.0	0.1	0.3	0.3	0.2	0.1	0.1	**1**
13	0.0	0.0	0.0	0.0	0.0	0.0	0.0	0.0	0.0	0.0	0.0	0.0	0.0	0.0	0.0	**0**
14	0.0	0.0	0.0	0.0	0.0	0.0	0.0	0.0	0.0	0.0	0.0	0.0	0.0	0.0	0.0	**0**
15	0.0	0.0	0.0	0.0	0.0	0.0	0.0	0.0	0.0	0.0	0.0	0.0	0.0	0.0	0.0	**0**
Sum	0.0	0.0	0.0	7.6	965.5	11114.4	30677.9	31813.4	17212.5	6056.0	1667.7	371.8	85.9	21.1	6.2	100000

4. Consequences of correlation on the long-term extreme ship responses

2-parameter Weibull probability distribution of peaks of linear VWBM is calculated by a computer program developed by Jensen and Mansour (2002), using closed-form expressions of response amplitude operators (RAOs), derived by Jensen et al. (2004). Closed-form expressions for transfer functions of VWBM at midship section are formulated according to the linear strip theory, assuming constant sectional added mass equal to the displaced water and by decoupling heave and pitch motions. Required input information for the procedure, is restricted to the main dimensions: length, breadth, draught, block coefficient, and waterplane area together with speed and heading. The formulas make it simple to obtain quick estimates of the wave-induced motions and VWBM and to perform a sensitivity study of the variation with main dimensions and operational profile. The method is, therefore, suitable for conceptual studies, like the present one. Accuracy of closed-form expressions is verified by comparison to the model-scale measurements and more complex strip theory and 3D panel hydrodynamic computations in Jensen et al. (2004) and Đigaš et al. (2012). It was found that considering the simplicity of the method, closed-form expressions, give a surprisingly good estimate of vertical ship responses.

In the present study, the analysis is performed for four oil tankers, representing the actual range of sizes of oil tankers operating worldwide, namely Panamax, Aframax, Suezmax, and VLCC. The average dimensions of typical ships representing each class are given by Michel and Osborne (2004) and presented in Table 5. Ship speed is taken as 12 knots for lower sea states, while it is reduced to 5 knots for sea states higher than 11m. All heading angles are taken as equally probable.

2-parameter Weibull distributions describing the probability of exceedance (P_e) of maximum VWBM calculated for different correlation coefficients, i.e for different scatter diagrams are presented in Figure 5. It may be seen that trend is similar irrespective of the ship size and that there is a clear

tendency toward reducing bending moments with ρ coefficient increase. Results for perfectly correlated seas states along the shipping route are obviously separated from all other results, leading to the lowest VWBM. This indicates that reduction of wave loads is gradual for lower ρ values, while a steep reduction in extreme wave loads occurs for very strong correlation of sea states.

Table 5. Main dimensions of typical oil tankers

Ship class	Length [m]	Breadth [m]	Draught [m]
Panamax	174.4	31.4	11.3
Aframax	229.7	41.9	13.1
Suezmax	260.8	45.8	15.9
VLCC	318.6	58.4	21.1

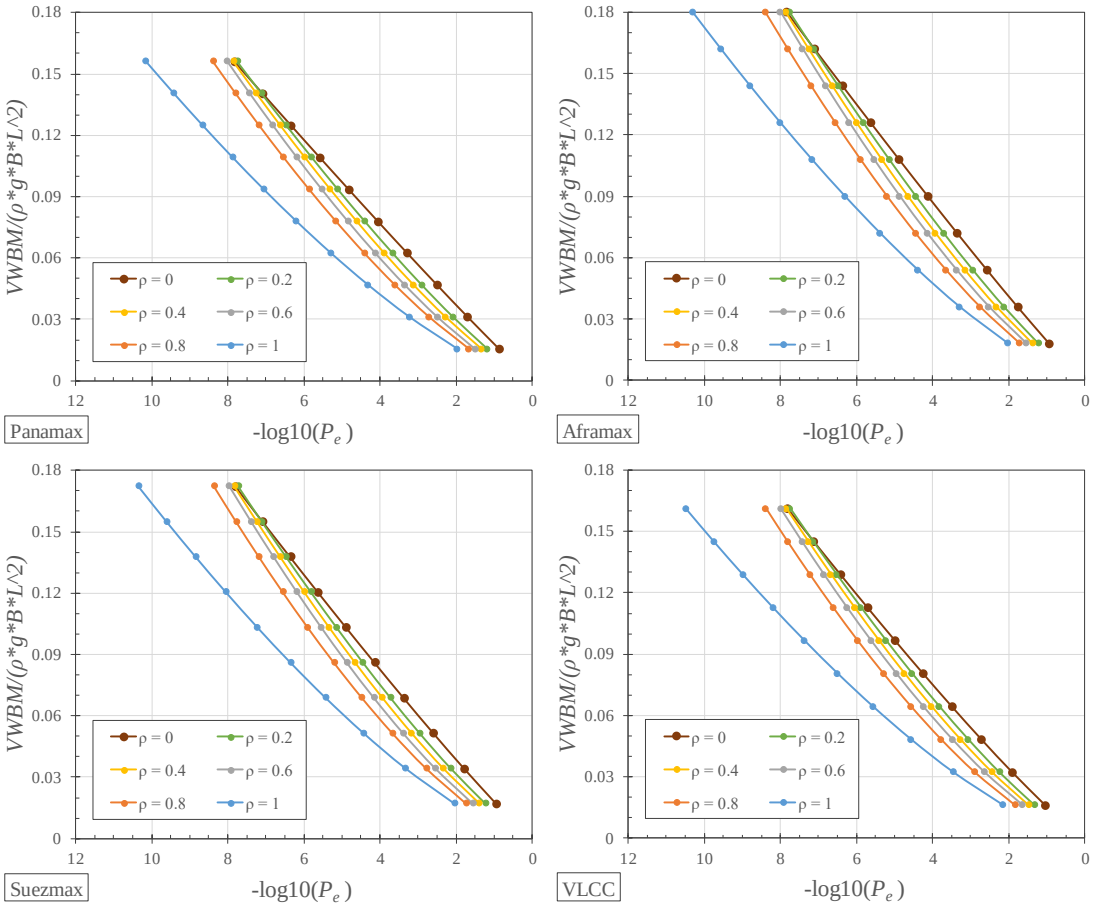

Fig. 5. 2-parameter Weibull distribution of maximum VWBM in respect to correlation coefficient for different tanker sizes.

Weibull scale and shape parameters are presented in Figure 6. There is a clear tendency of reducing both shape and scale parameters with increasing ρ, although it appears that the minimum value the Weibull shape parameter achieves for ρ between 0.7 and 0.8. According to Guedes Soares and Moan (1991), the shape factor is on average 0.95, for uncorrelated long-term VWBM. It may be observed that a similar value is obtained in the present study for ρ=0, but the shape parameter is reduced to about 0.7 as ρ approaches 1.

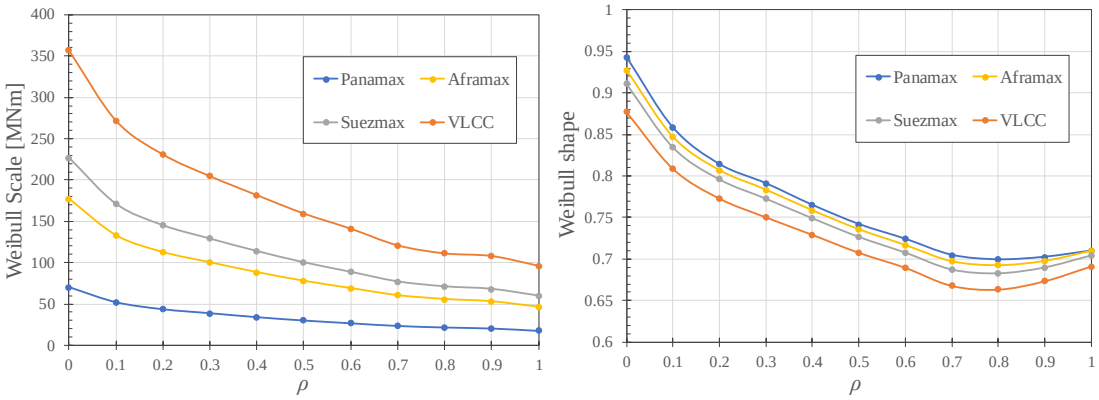

Fig. 6. Weibull scale (left) and shape (right) parameter for VWBM distributions in respect to correlation coefficient for different tanker sizes.

The effect of correlation on the most probable extreme value (MPEV) of VWBM in ship lifetime of 25 years is presented in Figure 7. Results, for various correlation coefficients, are presented relative to the uncorrelated VWBM. It may be seen that MPEV is approximately unaffected by correlation for ρ<0.5, while for higher values of ρ, there is an appreciable reduction of the MPEV. For perfect correlation (ρ=1), MPEV of VWBM is reduced by 30-35%.

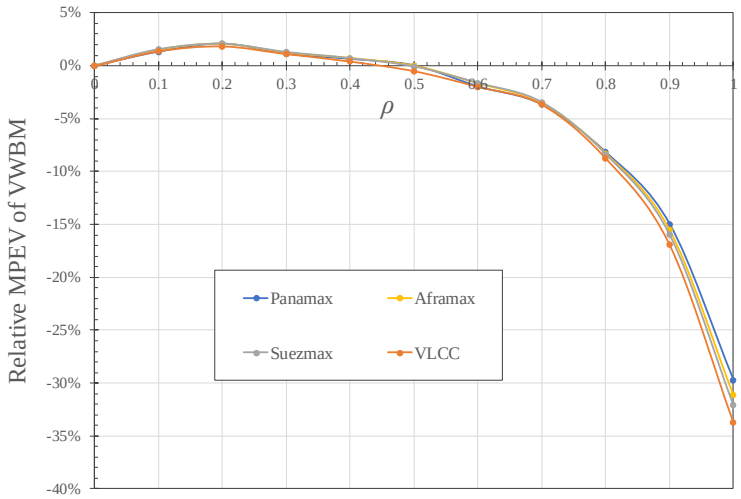

Fig. 7. MPEV of VWBM maximum relative to uncorrelated case in respect to correlation coefficient for different oil tanker sizes.

5. Verification

The system probability calculated by Eq. (5) for unequally correlated members of a series system assumes an equivalent correlation coefficient. It is demonstrated in Figure 7 that for certain values of ρ, VWBMs are considerably reduced. The question that needs to be discussed is what realistic values of ρ are and how they can be calculated. Uninterrupted records of wave data are required for correlation analysis and validation. The ERA5 dataset, used in this paper, is the fifth generation ECMWF (The European Centre for Medium-Range Weather Forecasts) reanalysis, combining model data with observations. The ECMWF version of the third generation WAM (Wave Modeling Project) model is incorporated into data assimilation to obtain high-resolution wave data (Hersbach et al. 2018). Complete ERA5 data covers the period from 1979 until now providing hourly estimates for many quantities, inter alia, ocean-wave data, with a lat-lon grid resolution of approximately 0.36 degrees (ca.

30 km resolution). The route chosen for verification is presented in Figure 8. The selected route passes through quadrants 15 and 16 as already described in Section 2, Figure 1. The significant wave height data for locations along the studied route are extracted from the ERA5 database. Extracted data has been used in correlation analysis where the linear correlation coefficient has been determined between any two points along a route. Also, a histogram of maximum significant wave height during a journey is produced to verify the correlation coefficient used in the previously proposed procedure, described in Section 3.

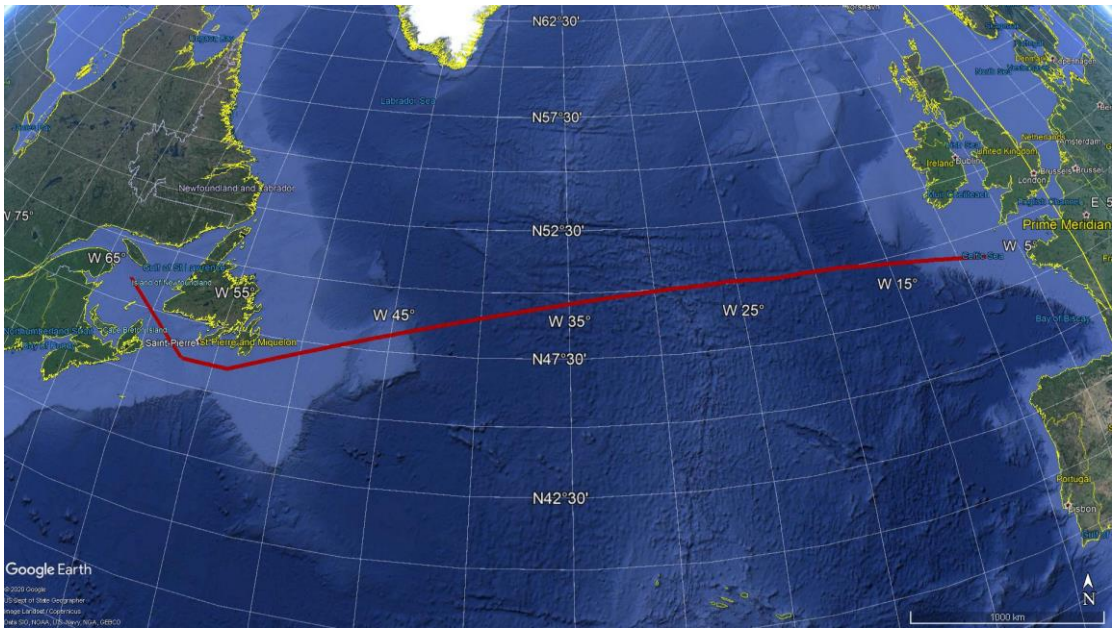

Fig. 8. NA route chosen as reference for verification (earth.google.com/web/).

Pearson's correlation matrix is displayed in Figure 9, showing correlation coefficients between the available significant wave height data from 109 locations along the route. Pearson's correlation coefficient measures the strength and direction of the linear relationship between quantitative random variables. The strength of the relationship between variables i.e. values of the coefficient varies between perfect positive (+1) and perfect negative (–) relationship. As the relationship becomes weaker, the value falls towards 0.

Figure 9 suggests an extremely strong correlation, almost 1, between two adjacent locations. Several following locations have also correlation values over 0.9. The correlation slowly declines as a distance between observed locations moves further away, but not below 0.25. Pearson correlation coefficient, presented below, does not coincide with the correlation coefficient ρ used in the present study, natheless the correlation matrix is calculated to display the presence of a substantial correlation between wave locations along the examined route.

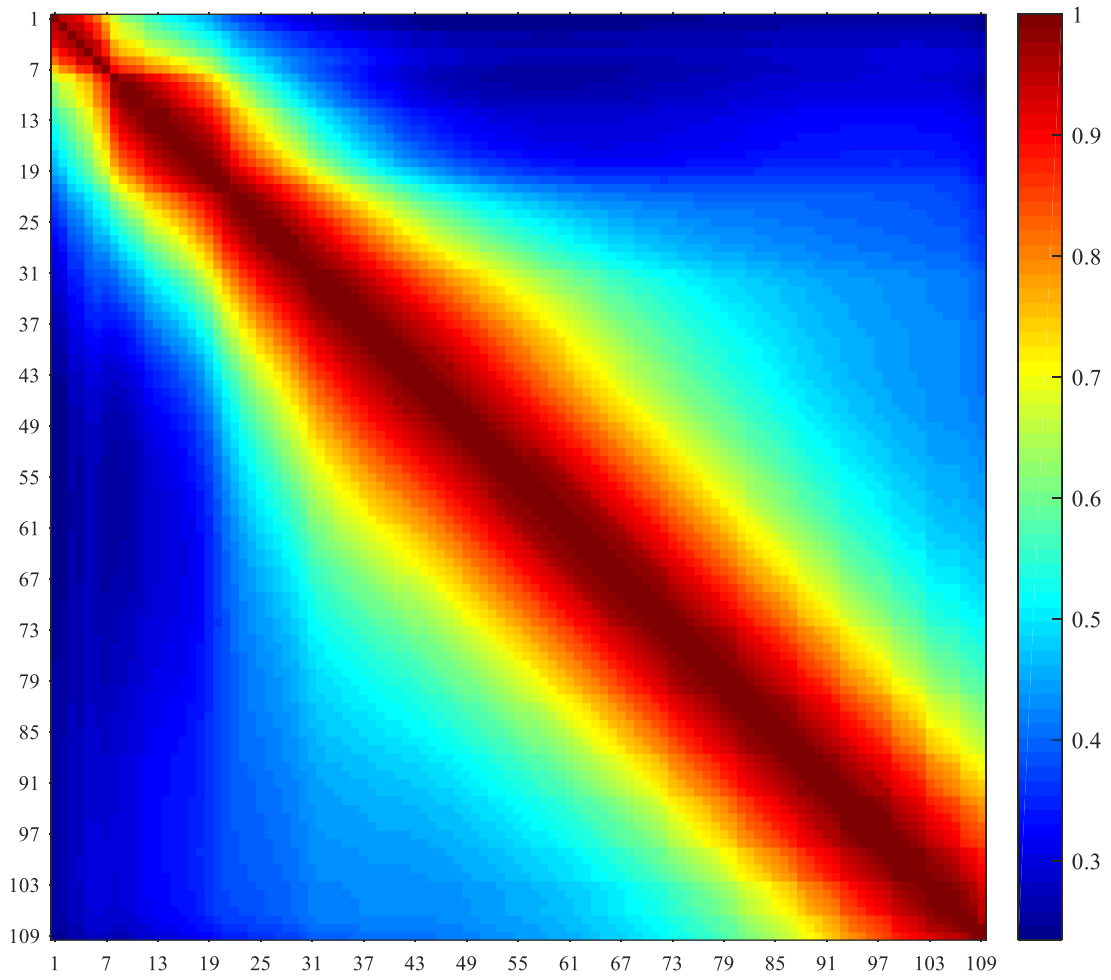

Fig. 9. Pearson's correlation matrix for locations along the route in NA.

The calculation of the equivalent correlation coefficient from the correlation matrix is a complicated task that exceeds the limits of this paper. Therefore, the quantification of the correlation coefficient ρ, used in Eq. (5), is evaluated by comparing the probability density functions presented in Figure 3 with the available ERA5 data. Hourly estimates of wave data are rearranged and filtered to simulate sailing between 109 ERA5 locations, assuming the average timestep of 2 hours between each adjacent location. The timestep is estimated considering the average ship speed (12kn) and the average distance between adjacent locations (approximately 22 NM). Almost 363 000 voyages are simulated based on the ERA5 data from 1979 to 2020. The histogram of extreme significant wave height for the reference period of one journey is created by extracting maximums from each ERA5 dataset representing one voyage. Analyzed data is then compared with the probability density function of H_s calculated varying the ρ from 0 to 1.

The high values of the previously analyzed Pearson's correlation coefficients are suggesting strong dependence between adjacent locations. The comparison presented in Figure 10 indicates that data is best fitted for the ρ around 0.8. Data lay closer to the assumption of perfectly correlated sea states (ρ = 1) than statistically independent ones (ρ = 0). Therefore, a commonly adopted assumption of the statistically independent sea states probably should be revised. One of the possible steps towards the rationalization of the accepted traditional methods is wave scatter diagram modification, as presented in this paper. Also, it would be interesting to link the values of Pearson's correlation matrix with the equivalent correlation coefficient ρ. Unfortunately, one route in one geographical region is not enough to reach a firm conclusion. Hence, similar analysis presents an opportunity for future research.

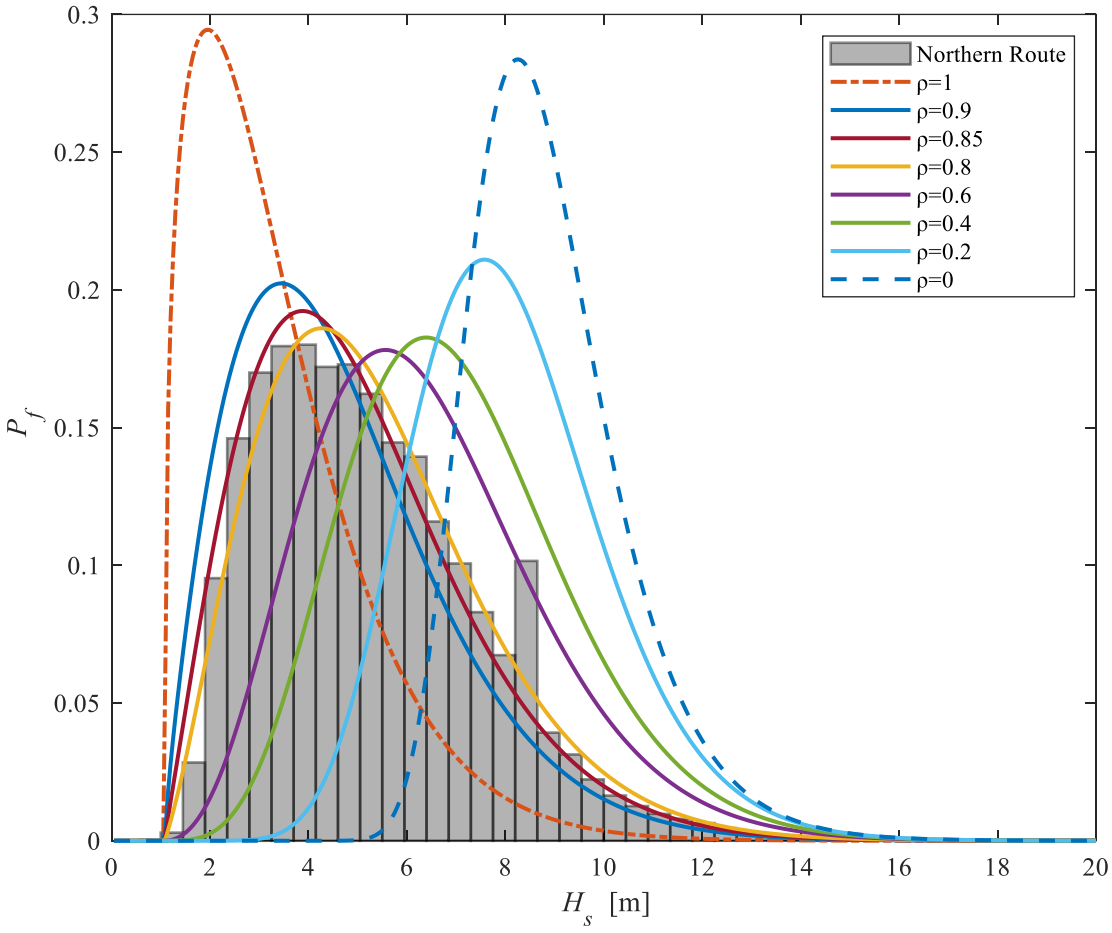

Fig. 10. Probability density functions of extreme significant wave heights compared to ERA5 data for the route in NA.

6. Conclusions

The aim of the study is to improve the IACS NA wave scatter diagram by including the spatial statistical correlation between sea states along the ship's route. The successive sea states that ship encounters along the sailing route in NA are represented by a series of partially correlated events. Standard IACS NA wave scatter diagram is modified to account for this correlation and later used to perform long-term analysis of VWBMs for oil tankers of different sizes. It was found that both the extreme H_s that ships encounter and the extreme VWBM are significantly reduced for large correlation coefficients.

The method is verified by considering data from the ERA5 wave database along the route in the North Atlantic. It was shown that extreme significant wave heights that ship encounters for the reference period on one voyage are lower compared to the results obtained by the commonly used assumption of the statistical independence of sea states along the shipping route. Consequently, for an equivalent correlation coefficient of 0.8, found in the present study, lifetime extreme VWBM may be reduced by about 8%

This finding does not mean that ships could not encounter larger waves, and consequently, higher bending moments. Namely, climate changes due to global warming cause an increase in the frequency and severity of extreme weather events in some geographical regions. Also, rogue waves need to be considered in the design and operation of ships and other marine structures. As different prediction methods are used for these effects, they are not considered in the present study.

The presented method and obtained results can be used by classification societies as a more rational approach for the definition of scatter diagrams intended for reliability-based ship structural design and analysis.

Acknowledgements

This work has been fully supported by Croatian Science Foundation under the project lP-2019-04-2085.

References

Baxevani A, Borgel C, Rychlik I. 2008. Spatial models for variability of significant wave height in world oceans. *International Journal of Offshore and Polar Engineering* 18: 1–7.

Bitner-Gregersen EM, Cramer EH, Løseth R. 1995. Uncertainties of load characteristics and fatigue damage of ship structures. *Marine Structures* 8(2): 97–117.

Bitner-Gregersen EM, Dong S, Fu T, Ma N, Maisondieu C, Miyake R, Rychlik I. 2016. Sea state conditions for marine structures' analysis and model tests. *Ocean Engineering* 119: 309–322.

Bitner-Gregersen EM, Eide LI, Hørte T, Skjong R. 2013. *Ship and Offshore Structure Design in Climate Change Perspective*.

Bitner-Gregersen EM, Gramstad O. 2015. Rogue Waves - Impact on ships and offshore structures, DNV-GL Strategic Research & Innovation Position Paper 05–2015.

Bitner-Gregersen EM 2017. Rethinking Rogue Waves - Towards better modelling insight and action, DNV-GL.

Ćorak M, Parunov J, Guedes Soares C. 2015. Long-term prediction of combined wave and whipping bending moments of container ships. *Ships and Offshore Structures* 10(1): 4–19.

Cramer EH, Hansen PF. 1994. Stochastic modeling of long term wave induced responses of ship structures. *Marine Structures* 7(6): 537–566.

Det Norske Veritas Germanischer Lloyd. 2017. DNVGL-RP-C205: Environmental Conditions and Environmental Loads., Oslo, Norway.

Đigaš A, Ćorak M, Parunov J. 2012. Comparison of Linear Seakeeping Tools For Containerships. Simposyum Theory and Practice of the Naval Achitecture (20; 2012).

De Gracia L, Wang H, Mao W, Osawa N, Rychlik I, Storhaug G. 2019. Comparison of two statistical wave models for fatigue and fracture analysis of ship structures. *Ocean Engineering* 187(March): 106161.

Guedes Soares C. 1996. On the definition of rule requirements for wave induced vertical bending moments. *Marine Structures* 9(3): 409–425.

Guedes Soares C. 1999. On the uncertainty in long-term predictions of wave induced loads on ships. *Marine Structures* 12(3): 171–182.

Guedes Soares C, Moan T. 1991. Model uncertainty in the long-term distribution of wave-induced bending moments for fatigue design of ship structures. *Marine Structures* 4(4): 295–315.

Guedes Soares C, Trovão MFS. 1991. Influence of Wave Climate Modelling on the Long Term Prediction of Wave Induced Responses of Ship Structures. In Price WG, Temarel P, Keane AJ (eds), Dynamics of Marine Vehicles and Structures in Waves, 1–10. Elsevier Science Publishers.

Guedes Soares C, Dogliani M, Ostergaard C, Parmentier G, Pedersen PT. 1996. Reliability Based Ship Structural Design. *Transactions SNAME* 104: 357–389.

Hersbach H, de Rosnay P, Bell B, Schepers D, Simmons A, Soci C, Abdalla S, Alonso-Balmaseda M, Balsamo G, Bechtold P, et al. 2018. *Operational Global Reanalysis: Progress, Future Directions and Synergies with NWP, ERA Report Series*. ECMWF Shinfield Park: Reading, UK.

Hogben N, Dacunha NMC, Oliver GF. 1986. *Global Wave Statistics*. Feltham: British Maritime Technology Ltd.

IACS. 2000. Rec. No. 34. Standard Wave Data (North Atlantic Scatter Diagram).

IACS. 2009. No. 106. IACS Guideline for Rule Development - Ship Structure.

Jensen JJ, Mansour AE. 2002. Estimation of ship long-term wave-induced bending moment using closed-form expressions. *RINA Transactions* 144: 41–55.

Jensen JJ, Mansour AE, Olsen AS. 2004. Estimation of ship motions using closed-form expressions. *Ocean Engineering* 31(1): 61–85.

Katalinić M, Parunov J. 2018. Wave statistics in the Adriatic Sea based on 24 years of satellite measurements. *Ocean Engineering* 158(April): 378–388.

Mansour AE, Preston DB. 1995. Return periods and encounter probabilities. *Applied Ocean Research* 17(2): 127–136.

Michel RK, Osborne M. 2004. Oil Tankers. In Lamb T (ed), Ship Design and Construction, 29.1 – 29.41. New Jersey, USA: SNAME.

Mikulić A, Katalinić M, Parunov J. 2020. The effect of spatial correlation of sea states on predicted extreme significant wave heights along ship sailing routes. In: Marine Technology and Engineering (MARTECH) (in press).

Moan T, Shu Z, Wu M, Amlashi H. 2006. Comparative reliability analysis of ships – considering different ship types and the effect of ship operations on loads. *Transactions SNAME* 114(16–54).

Nitta A. 1995. On D. Faulkner discussion of paper by A. Nitta et al. 'Basis of IACS unified longitudinal strength standard'. vol. 5, no. 1, 1992, 1–21. *Marine Structures* 8(3): 337–339.

Nitta A, Arai H, Magaino A. 1992. Basis of IACS unified longitudinal strength standard. *Marine Structures* 5(1): 1–21.

Parunov J, Senjanović I. 2003. Incorporating model uncertainty in ship reliability analysis. *Transactions - Society of Naval Architects and Marine Engineers* 111: 376–408.

Parunov J, Senjanović I, Pavičević M. 2004. Use of vertical wave bending moment from hydrostatic analysis in design of oil tankers. *International journal of maritime engineering* 146.

Prpić-Oršić J, Parunov J, Šikić I. 2014. Operation of ULCS - real life. *International Journal of Naval Architecture and Ocean Engineering* 6(4): 1014–1023.

Rao SS. 1992. *Reliability-based design*. New York: McGraw-Hill.

Schirmann ML, Collette MD, Gose JW. 2019. Impact of weather source selection on time-and-place specific vessel response predictions. *Trends in the Analysis and Design of Marine Structures - Proceedings of the 7th International Conference on Marine Structures, MARSTRUCT 2019* : 33–41.

Vettor R, Soares CG. 2016. Assessment of the Storm Avoidance Effect on the Wave Climate along the Main North Atlantic Routes. *Journal of Navigation* 69(1): 127–144.

Publication II

Published journal article.

Ocean Engineering 266 (2022) 112738

Contents lists available at ScienceDirect

Ocean Engineering

journal homepage: www.elsevier.com/locate/oceaneng

Uncertainties of wave data collected from different sources in the Adriatic Sea and consequences on the design of marine structures

Maro Ćorak [a], Antonio Mikulić [b], Marko Katalinić [c], Joško Parunov [b,*]

[a] University of Dubrovnik, Maritime Department, Croatia
[b] University of Zagreb, Faculty of Mechanical Engineering and Naval Architecture, Croatia
[c] University of Split, Faculty of Maritime Transportation, Croatia

ARTICLE INFO

Keywords:
Wave data uncertainty
Wave energy potential
Extreme wave loads
Accumulated fatigue damage
Adriatic Sea

ABSTRACT

Uncertainties of wave data sources got increasing attention in the last decades because of their importance for marine structural design and analysis. In the present study, four different wave data sources collected at close geographical locations in the Adriatic Sea are described and compared. Two databases are composed of collected in-situ measurements, while two databases are obtained by hindcasting. The consequences that differences in collected wave data could have on the design of marine structures are presented in three examples: assessment of the wave energy that can be used for selection of wave energy converter, prediction of extreme wave loads for structural strength assessment, and computation of the accumulated fatigue damage. The results indicate surprisingly large differences between wave data contained in the four discussed databases, especially for their extreme values. Consequently, differences in presented application examples are also quite significant. As discussed in the paper, there are various possible reasons for the considerable uncertainties of wave data sources. To better understand and compare the obtained results, wave data from different sources are transformed to refer to the same sea state duration and to the same water depth. Comparative analysis is then performed on the original and transformed data. The novelty of the present study is the quantification of the consequences of the wave data sources uncertainties on the design of marine structures in the Adriatic Sea.

1. Introduction

Accurate knowledge of wave statistics plays a crucial role in the safety analysis of marine structures, having a substantial influence on both their fatigue life prediction and extreme responses. Wave statistical data are collected using different types of long-term measurements, visual observations, and numerical analyses carried out independently or in combination with the prior two methods. Due to various methods employed in their acquisition, wave data can differ even if they refer to the same geographical location. Uncertainty of wave data collected from different sources can have a considerable impact on the design and analysis of marine structures (Bitner-Gregersen et al., 2016, Vettor and Soares, 2016)). Therefore, such uncertainty has become the focus of the interests of the scientific and engineering community in recent years, and it is still not fully quantified today. The importance of wave data selection from multiple sources and their influence on ship responses has been confirmed for the North Pacific by Schirmann et al. (2020) and North Atlantic by Hauteclocque et al. (2020).

According to Bitner-Gregersen et al. (2016), there are several reasons why wave data from different sources may differ even for the same geographical location. One of them is the measurement imperfection of an instrument used to measure a sea state characteristic, which is usually provided by the measuring equipment manufacturer. Estimation uncertainty appears when the quantity used in the comparison is not measured directly but estimated from measured data. A typical example is a determination of the significant wave height from the wave record. Statistical (or sampling) variability is due to the limited number of observations or the existence of time periods with missing data. That variability is usually reflected in the estimated long-term extreme values. When numerical reanalysis is used for generating a wave database, there are uncertainties related to the imperfections and idealizations used in the physical process formulations. Methods and data sources used for the calibration of numerical models may also cause differences in results. All these general uncertainty sources will affect environmental descriptions to a different degree.

The Adriatic Sea is a semi-enclosed sea basin of the Mediterranean

* Corresponding author.
E-mail addresses: mcorak@unidu.hr (M. Ćorak), amikulic@fsb.hr (A. Mikulić), mkatalinic@pfst.hr (M. Katalinić), jparunov@fsb.hr (J. Parunov).

https://doi.org/10.1016/j.oceaneng.2022.112738
Received 16 July 2021; Received in revised form 30 May 2022; Accepted 24 September 2022
Available online 9 October 2022
0029-8018/

Sea with a specific wind–wave climate. It is of elongated, elliptical shape extending from the northwest to the southeast, between the Dinaric and Apennine mountain ranges that influence the dominant winds and wave patterns. Two characteristic winds that reach storm conditions and can cause extreme waves are *bora* (N-NE to E-NE) and *sirocco* (E-SE to SS-E) (Katalinić et al., 2015). Many researchers have been dealing with the analysis of the wave statistics in the Adriatic Sea. Data collected by visual observations of wave heights from seagoing ships during the period of 15 years are analysed in Parunov et al. (2011). The results presented in that research are applicable for ships, while their usage has a large uncertainty for the analysis of offshore structures due to the heavy weather avoidance utilized by ship masters. A more comprehensive wave database analysed is a WorldWaves Atlas (WWA), which has been used for the extreme sea states analysis (Katalinić and Parunov, 2018, 2021). Firstly, a joint probability distribution of significant wave heights and peak spectral periods for three geographical locations along the typical sailing route in the Adriatic and extreme sea states are determined (Katalinić and Parunov, 2018), while later, a more comprehensive wind and wave statistical models are developed for the whole basin (Katalinić and Parunov, 2021). One of the most extensive wind-wave analyses in the northern part of the Adriatic Sea is performed by Pomaro et al. (2017, 2018), where 39 years of directional wave time series at the ACQUA ALTA oceanographic research tower are analysed. They took advantage of an extremely long and unique time series of measured wind and wave data to characterize the local wave climate and describe its relationship with the variability of the atmospheric circulation (Pomaro et al., 2017). Wave energy potential in the Adriatic is studied by Barbariol et al. (2013).

In the present study, a comparison is performed on four validated and recognized databases containing wave data collected from different sources for almost the same location in the north part of the Adriatic Sea. Two datasets are collected by in-situ measurements (ACQUA ALTA and RON), while two databases are obtained by wave hindcasting (WWA and ERA5). ACQUA ALTA database consists of 39 years of directional wave time series recorded since 1979 at the oceanographic research tower (Pomaro et al., 2017). Italian Data Buoy Network RON (Rete Ondametrica Nazionale) project resulted in the wave dataset consisting of measurements on four locations along the western coast of the Adriatic Sea (Liberti et al., 2013). The WWA is developed based on numerical wave modelling hindcast and calibrated by satellite measurements which are in turn validated by in-situ measurements by wave buoys. Records in the WWA are for the present study available for the period from 1992 to 2019 (Katalinić and Parunov, 2021). ERA5 dataset is the fifth generation ECMWF (The European Centre for Medium-Range Weather Forecasts) reanalysis, combining model data with observations, covering the period from 1979 until now (Hersbach et al., 2018; Bencivenga et al., 2012). Obviously, there are many wave datasets available for the Adriatic Sea, but their comparative analysis and uncertainty assessment of consequences on the design of marine structures have not been explored yet.

Therefore, to fill this research gap, a comparative analysis of four stated databases is performed, and the consequences that differences in databases may have on the design of marine structures in the Adriatic Sea are determined. Wave databases are first compared concerning the wave scatter diagrams containing frequencies of occurrence of significant wave height and peak wave period. Except for the visual comparison of scatter diagrams, the annual maxima of significant wave heights are compared. Next, the comparative extreme value analysis is performed to find differences in the long-term extreme significant wave heights.

As the first practical example, consequences of wave data source selection on predicted wave energy potential at the given location are studied by using four different wave scatter diagrams. Discrepancies in the predicted wave energy potentials could result in the choice of different wave energy converters (WEC). For that purpose, diagrams of total available energy for each sea state are created, and the total yearly wave energy potential is calculated for each database. The next example is the uncertainty of the long-term distribution of vertical wave-bending moment of the typical barge that is in permanent service in the concerned geographical region. The most probable extreme wave bending moments for the return period of 20 years resulting from different databases are compared. The last example is the uncertainty of the accumulated fatigue damage of the deck structure of the barge, determined for the period of 20 years for different wave data sources.

Since sea state duration and water depth differ between wave databases and their locations, original wave data are transformed to have equal time resolution and water depth to reduce these discrepancies. Uncertainty assessment is then performed on transformed wave data sets, followed by comparison against the uncertainty of the original data..

The paper is organised as follows. Section 2 presents a description of wave data sources used in the analysis. A comparison of the wave scatter diagrams and the extreme significant wave heights resulting from each wave data source is given in Section 3. Practical consequences of uncertainties on the design of marine structures are provided in Section 4. Discussion with wave transformation to the same water depth and sea state duration is presented in Section 5. The paper closes with conclusions and recommendations.

2. Wave data sources

2.1. ACQUA ALTA database

A database of the in-situ measurements is available from the ACQUA ALTA, an oceanographic research tower located in the north part of the Adriatic Sea, as presented in Fig. 1. The measuring tower is located 16 km off Venice (latitude/longitude: 45.3°/12.5°) at the 16 m depth.

Different wave gauges have been used since the start of the measurements at the ACQUA ALTA research tower. The instrument system has been progressively upgraded and repositioned during maintenance operations, and three different recording periods can be considered. Two pressure transducers were used during the first period (1979–1986). Over the central period (1987–2003), the system was upgraded to three pressure transducers. In the third period (2004 to the present), the pressure transducers have been replaced by echo sounders (Pomaro et al., 2017).

The database is extensively used and reported in the literature. E.g., it is used for a critical analysis of met-ocean conditions leading to a freak wave in 2009 (Cavaleri et al., 2021). A complete set of basic wave parameters is available in open-source format (Pomaro et al., 2018). The database comprises data from 39 years (exactly 438 912 measurements) in 3-h intervals, starting from 1979 to 2017.

Fig. 1. The ACQUA ALTA oceanographic tower years 1970 and 2017). Source (Pomaro et al., 2018).

2.2. RON database

The Italian Data Buoy Network RON project started in 1989 and was continuously running until 2014. On several occasions through the years, measuring locations were added, and the equipment was modernised and upgraded, enabling the acquisition of different types of data needed to define the sea state. In the end, the RON project consisted of 15 oceanographic buoys able to measure significant wave height, peak period, mean period, wave direction, sea surface temperature, wind speed and direction, air temperature, atmospheric pressure, and relative humidity (Liberti et al., 2013). Wave and meteorological records were collected every 30 min and transmitted to shore stations within 15 M via Inmarsat-D+, after which all data were processed in a control centre based in Rome (Liberti et al., 2013). For the present paper, only the location in the north part of the Adriatic Sea, in front of Venice (location 61220), is of interest. It should be noted that results from the analysed RON location must be taken with caution due to the small water depth (17 m) and a relatively small sample of years in which sea state parameters are available. Although measurements at this location started in 2002 and the frequency of measurements is relatively high, almost six years (2005–2010) of data are missing from the dataset, while some of the existing months have very few records available.

2.3. WorldWaves atlas

WorldWaves Atlas (WWA) is developed by Fugro Oceanor, a company dealing with met-ocean analysis for the offshore industry. WWA provides wind and wave data for the global domain from 1979 up to the present. The database is developed by combining numerical wave model hindcast results with the available satellite altimetry data. While satellite altimetry could be considered a more accurate data source, it is extensively verified by buoy in-situ measurements where possible. The data is non-homogenous in space and time, depending on satellite tracks and overflight time (Fig. 2). The space and time homogeneity is thus achieved by underlying the numerical wave model results from the WAM model run at ECMWF (European Centre for Medium range Weather Forecast), i.e., calibrating the numerical model results with an appropriate, available and satellite altimetry data (Katalinić and Parunov, 2018).

Across the Adriatic Sea, 39 uniformly distributed locations across the basin are available at 0.5° lat./long. Resolution. At each location, 12 physical wave and wind parameters are available at 6-h intervals (four per day). Each location contains a total of 38600 records, starting in September 1992 and ending in January 2019.

2.4. ERA 5 database

ERA5 is the fifth generation ECMWF (The European Centre for Medium-Range Weather Forecasts) reanalysis, produced by combining the advanced forecasts modelling and data assimilation systems with vast amounts of observations. For the model data calculation, the ECMWF's Integrated Forecast System (IFS) combines the atmospheric model, the land-surface model (Revised land surface hydrology, HTESSEL), and the third-generation ocean wave model (Wave Modeling Project, WAM).

Complete ERA5 data covers the period from 1979 until now, providing hourly estimates for many atmospheric, land-surface, and ocean-wave climate variables, with a latitude/longitude grid resolution of approximately 0.5°. The location of acquired wave data from the ERA5 dataset coincides with the WWA location, as presented in Fig. 3.

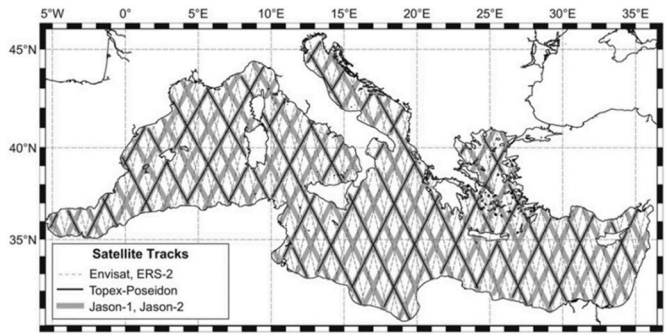

Fig. 2. Satellite tracks over ground. Wave measurement missions over the Mediterranean. Source (Liberti et al., 2013).

3. Comparison of wave databases

Wave databases analysed in the previous section refer to almost the same geographical location. However, there are still some differences between the exact locations where measurements or calibrations are performed that may have consequences on the interpretation of results. The exact positions of measurement points of wave data are given in Fig. 3, where ACQUA ALTA and RON datasets refer to the same location in the shallow waters close to the shore. On the other hand, WWA and ERA5 databases are also available for identical coordinates just 38 km off the aforementioned locations, exposed to open waters with greater water depth but without any natural obstacle between the two. Consequently, both locations have roughly equal fetch in the SE direction from which *sirocco* wind events generate the most severe storms in the Adriatic. However, other wind directions at considered locations have different fetches, which can be the source of uncertainties regarding corresponding waves.

Comparative analysis of previously described wave databases is performed, and the accent is set upon information predominantly used in the design of marine structures, i.e., wave height and period. Firstly, maximum significant wave heights H_s are extracted and compared for overlapping available years from all database sets (1992–2017). Results are presented in Fig. 4 and Table 1, where the maximum significant wave height for the specified timespan reads 5.6 m originating from the WWA database for the year 1993. The maximum wave height for the other two available datasets for that year, ACQUA ALTA and ERA5, read 4.0 m and 3.93 m, respectively.

The overall maximum H_s is registered inside the WWA database, the year 2018, and reads 5.76 m. The maximum H_s by the RON buoy was recorded in 2004, reading 5.01 m. The ACQUA ALTA tower recorded a maximum value of 4.69 m in 1992, while 4.73 m is the ERA5 maximum obtained in 2015. Fairly significant discrepancies between recorded maxima can be observed in the presented records. Hence, a more detailed analysis is performed further below.

A closer look at the daily records reviles that qualitative agreement between time series of H_s in databases is considerably better compared to the discrepancies in maximum H_s. Such comparison is shown in Fig. 5

Fig. 3. The location of analysed wave datasets (ACQUA ALTA tower, WWA, RON buoy and ERA5). Source Google: Earth Pro.

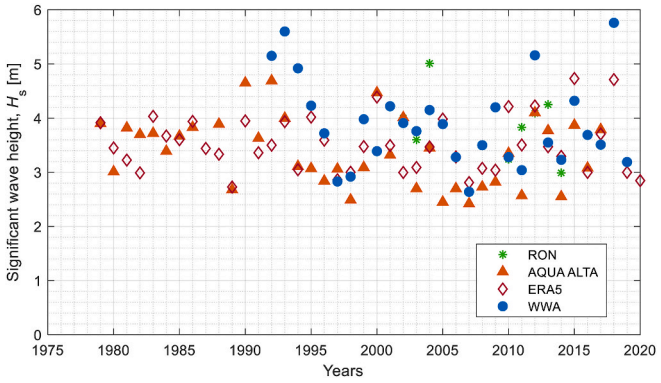

Fig. 4. Maximum yearly significant wave heights recorded in each database.

Table 1
Maximum yearly significant wave height recorded in each database (only years in which at least three databases have records).

Year	$H_{s,max}$, m			
	WWA	ERA5	ACQUA ALTA	RON
1992	5.15	3.50	4.69	–
1993	5.60	3.93	4.00	–
1994	4.92	3.05	3.11	–
1995	4.23	4.02	3.07	–
1996	3.72	3.59	2.84	–
1997	2.83	2.86	3.06	–
1998	2.92	3.00	2.49	–
1999	3.98	3.48	3.09	–
2000	3.39	4.39	4.47	–
2001	4.22	3.49	3.32	–
2002	3.91	3.00	4.01	4.00
2003	3.76	3.09	2.70	3.60
2004	4.15	3.47	3.45	5.01
2005	3.89	3.98	2.45	–
2006	3.28	3.28	2.70	–
2007	2.64	2.81	2.42	–
2008	3.50	3.07	2.73	–
2009	4.20	3.04	2.82	–
2010	3.28	4.21	3.35	3.24
2011	3.04	3.50	2.57	3.83
2012	5.16	4.22	4.10	4.09
2013	3.55	3.47	3.77	4.25
2014	3.23	3.29	2.55	2.99
2015	4.32	4.73	3.87	–
2016	3.69	3.00	3.08	–
2017	3.51	3.71	3.79	–

for months when the maximum H_s is observed in each database. The maximum H_s in the WWA corresponds to January 1993, for the ACQUA ALTA, it is December 1992, whereas February 2015 contains the maximum in the ERA5 dataset. Maximum H_s inside the RON occurred in November 2004, but due to the insufficient number of records, the month with the second largest recorded H_s is presented in Fig. 5 (February 2013). Although large discrepancies were found between maximum H_s from different sources, records clearly show that storms are correctly identified in all cases. Thus, during January 1993 and February 2015, only one severe storm with H_s above 2 m was recorded at each processed location, while during December 1992 and February 2013, three storms at each location with H_s above 2 m were recorded. Although WWA and ERA5 databases are related to the same geographical location, results show rather large discrepancies in recorded maximum significant wave heights H_s. The same can be noticed for in-situ measurements from ACQUA ALTA tower and RON, although the trend of storm predictions is good in all cases.

These differences are even more emphasized in the long-term extreme significant wave height analysis, which is performed by the Annual Maximum Method (Det Norske Veritas, 2019). Hence, the Gumbel distribution is fitted to the annual maxima of significant wave heights using the least square method, as presented in Fig. 6 (Katalinić and Parunov, 2020). Based on the Gumbel parameters, the extreme values of H_s for large return periods are calculated, and the results are presented in Fig. 7. The highest values of extreme H_s are obtained based on records from the RON database, where H_s for the return period of 50 and 100 years reads 6.22 m and 6.76 m, respectively. The lowest values of extreme H_s are obtained from the ERA5 dataset, where H_s for the 50 and 100 years return period reads 4.85 m and 5.14 m, respectively. The predicted extreme values are therefore uncertain and strongly influenced by several factors such as the micro-location, frequency of measurements, data acquisition, calibration method, etc. It should be emphasized that the RON dataset is characterized by statistical uncertainty because of the large time periods with missing data. Another reason for discrepancies between RON and ACQUA ALTA could be the actual ability of the RON floating buoys to accurately follow the free surface, especially in steep waves when non-linear effects are present, and coupling with the mooring line may alter the buoy's dynamics (Bitner-Gregersen et al., 2016).

Discrepancies between ERA5 and WWA databases are particularly interesting since both databases are obtained using similar assumptions and refer to the same geographical location. The calibration method of the numerical wave model, which can be classified as the model uncertainty, could be one of the reasons for these unexpected differences (Bitner-Gregersen et al., 2016). While the basic idea of the calibration process is the same, i.e., to perform regression based on buoys data coupled with altimeter measurements, some details could have been done differently and affected the output. Thus, while altimeter data are assimilated in the ERA5 database to correct the model results at each time step, the altimeter is used only for calibration in other global wave databases. Such an approach tends to underestimate the extremes of the ERA5 dataset, as already found and discussed by Hauteclocque et al. (2020).

Reasons for differences between ACQUA ALTA and WWA databases could also be related to the influence of the shore, as it is known that the global wave datasets are not sufficiently accurate in nearshore areas where an accurate wave prediction would require a more detailed topology and a finer discretisation mesh.

The general source of uncertainty among all databases could also be the time resolution of recorded data (0.5 h, 1 h, 3 and 6 h as explained in previous section) where the calculation and averaging of H_s in different time periods could influence the maximum derived values. This type of uncertainty is classified as the estimation uncertainty (Bitner-Gregersen et al., 2016). Moreover, a general difference between the two locations (ACQUA ALTA/RON and WWA/ERA5) is that waves in shallow water are transformed, resulting in different values of H_s.

Frequencies of occurrence of sea states defined by significant wave height and peak wave period are analysed and presented in the form of scatter diagrams. The WWA scatter diagram contains 38600 sea states, ACQUA ALTA scatter diagram is constructed from 78800 data, while ERA5 contains the largest dataset of 362830 sea states. RON dataset has the highest recording frequency, where sea states are recorded every 30 min, so the scatter diagram is constructed of 103533 sea states. Results are given in Fig. 8, and one can notice that the WWA and the RON scatter diagram have the widest spread of significant wave heights and peak wave periods. Most sea states in the ACQUA ALTA and ERA5 datasets are accumulated between H_s = 0–1.5 m and T_p = 1.5–5 s, while WWA and RON have wave heights located between 0 and 2.5 m for peak periods of 1–6 s. Sea states with the highest probability of occurrence have H_s of 0.25 m and T_p of 2.5 s at ACQUA ALTA, RON, and ERA5 databases, respectively. Results in analysed scatter diagrams are consistent with previously presented records where maximum and extreme H_s are obtained from the most scattered data, i.e., WWA and RON datasets.

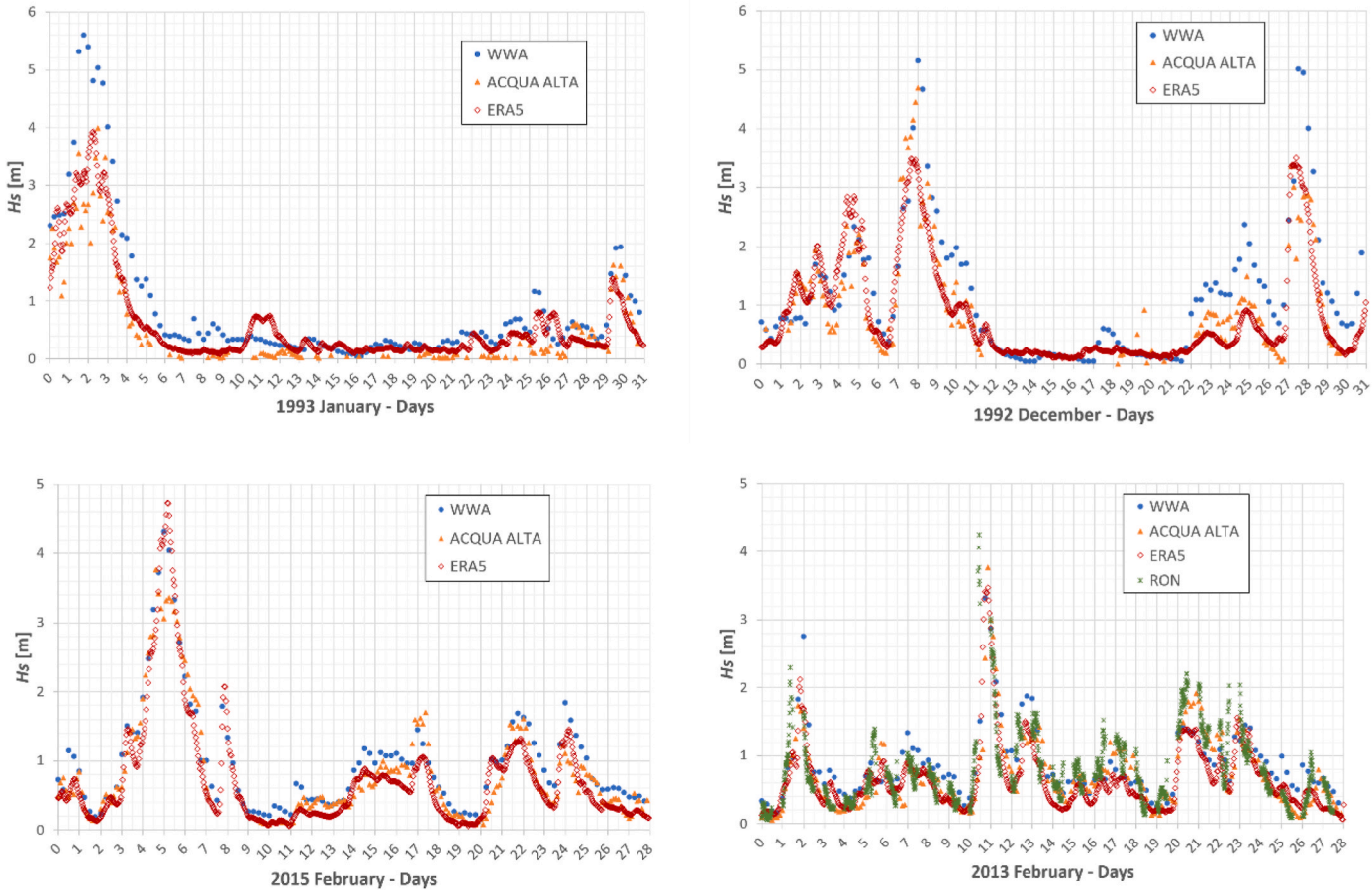

Fig. 5. Time series of H_s for January (1993), December (1992) and February (2015 and 2013) on considered locations.

4. Consequences of uncertainties on the design of marine structures

4.1. Estimation of the wave energy potential

Because of uncertainty in wave data, a different wave energy potential would be estimated, possibly resulting in a selection of different wave energy converters. Simplified expressions based on significant wave height and energy period T_e are used for estimation of the wave power as (Barbariol et al., 2013):

$$P_{dw} = \frac{\rho g^2}{64\pi} \bullet H_{m0}^2 \bullet T_e \tag{1}$$

where the energy period for the Adriatic Sea can be approximated as 0.9 T_p. Total wave energy (MWh/m) potentially produced across all sea states is given by (Barbariol et al., 2013):

$$E_{tot} = \sum_i P_{dwi} \bullet \delta t_i \tag{2}$$

where δt_i is obtained as the product of the probability of occurrence of each sea state and the number of hours in one year.

Diagrams representing available wave energy potential in the northern part of the Adriatic Sea for different wave databases are presented in Fig. 9. For ACQUA ALTA, WWA, and ERA5 datasets, the highest energy potential is achieved during sea states with H_s between 1.0 and 2.0 m and T_p between 4.0 and 6.0 s. RON dataset has a somewhat wider spread of energetic sea states with H_s between 1.0 and 2.5 m and T_p between 4.0 and 7.0 s.

The maximum annual wave energy potential for analysed datasets is presented in Table 2, from which the WWA database could be defined as the most energetic one.

4.2. Calculation of the extreme global wave load from the long-term distribution

Barges for transportation of heavy cargo are frequently operating in the northern part of the Adriatic Sea because of the intensive industrial activities in that region. Therefore, it is of interest for their design and analysis to know extreme wave bending moments that barge may encounter in her lifetime. For that purpose, the barge with the main particulars specified in Table 3 is analysed.

Transfer functions of the vertical wave bending moment at the midship section of the barge, calculated by the closed-for expression proposed by Jensen and Mansour (2002) are shown in Fig. 10. A low forward speed of 5 knots is assumed in the analysis due to expected speed reductions in service during heavy weather conditions.

The long-term distribution of VWBM is calculated by the standard procedure described, e.g., by Ćorak et al. (2015), among others. Ship headings are considered equally probable, while the JONSWAP wave spectrum is used for the description of short-term sea states since it is suggested as an appropriate wave spectrum definition for the Adriatic Sea (Katalinić et al., 2020). The long-term distributions calculated using four different scatter diagrams given in Fig. 8 are shown in Fig. 11.

The most probable extreme values for the return period of 25 years (probability level of 10^{-8}) are provided in Table 4.

From Table 4, one can conclude that the ratio between the highest and the lowest estimated MPEV reads 1.3. Expectedly, extreme values resulting from WWA and RON databases are higher than those resulting from ACQUA ALTA and ERA5.

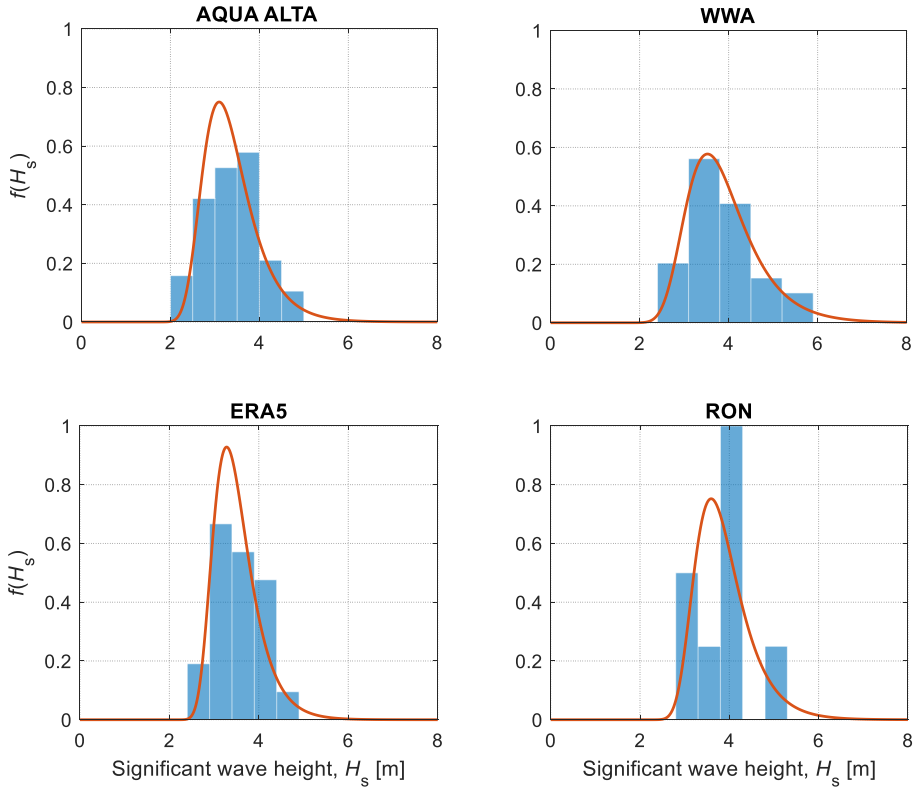

Fig. 6. Gumbel distribution fit on the yearly maxima H_s.

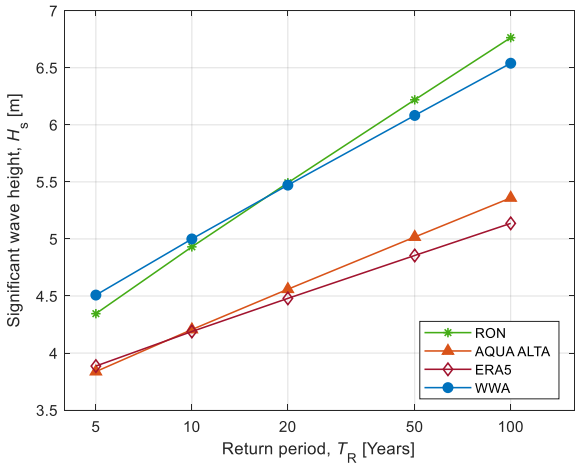

Fig. 7. Extreme significant wave heights for different return periods and for different wave databases.

4.3. Uncertainty in the fatigue life assessment of marine structures

A consequence of the uncertainty in wave data sources on the fatigue life assessment of marine structures is studied in the example of the same barge that was analysed in section 4.2. Fatigue of the main deck is analysed, assuming vertical wave bending moments as the only source of the fluctuating fatigue loading. Section modulus of 6.786 m^3 for the main deck of the barge is assumed. The fatigue analysis is performed according to DNV Rules (Det Norske Veritas, 2010). The standard "D" type of S–N curve is employed together with the stress concentration factor (SCF) of 1.27. Such assumption is equivalent to using the "F" curve without SCF, describing a hot spot at the connection of the main deck longitudinal and web stiffener of the transverse deck girder. The same procedure is employed in Harmonized Common Structural Rules (2012) and by Mansour and Høvem (1994) to analyse the fatigue life of the main deck structures exposed to the fluctuating global VWBM. The following expression is used for fatigue analysis:

$$D = \nu_0 \cdot T_d \left[\frac{q^{m_1}}{\overline{a}_1} \cdot \Gamma\left(\frac{m_1}{h} + 1, \left(\frac{S_1}{q} \right)^h \right) + \frac{q^{m_2}}{\overline{a}_2} \cdot \gamma\left(\frac{m_2}{h} + 1, \left(\frac{S_1}{q} \right)^h \right) \right] \tag{3}$$

where ν_0 is the long-term average response zero-crossing frequency, and T_d is the design life of a barge in seconds. The Weibull scale q and shape h parameter are obtained based on the long-term distribution of the VWBM given in Fig. 11. Afterwards, the stress range level, $\Delta\sigma_0$, is obtained based on Weibull parameters given in Table 5 for a selected number of cycles $n_0$as:

$$q = \frac{\Delta\sigma_0}{(\ln n_0)^{1/h}} \tag{4}$$

Stress range S_1 for which change of slope of S–N curve occurs corresponds to the stress range S_q of the "D" curve from the Harmonized Common Structural Rules (2012).

Results of the fatigue analysis are given in Table 5. It may be seen that the ratio between the largest (RON) and the lowest (ERA 5) accumulated fatigue damage reads 3.3.

5. Discussion

The comparison of wave heights presented in Section 3 suffers from the inconsistency that the time resolution of sea states is not the same. The shortest duration of the sea states is 30 min for the RON database, while the longest reads 6 h for the WWA database. The time resolution of

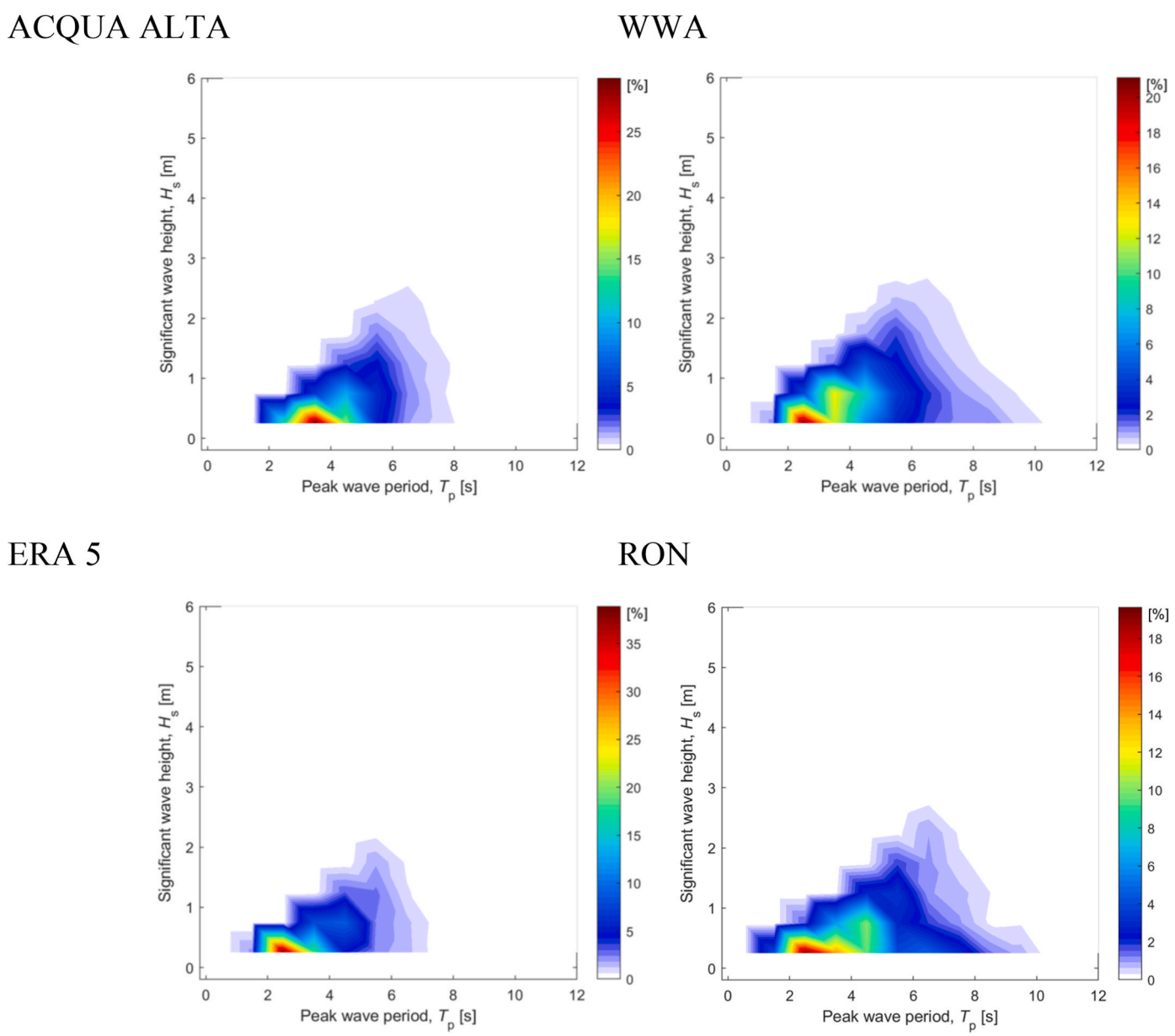

Fig. 8. Scatter diagrams plot for (a) ACQUA ALTA (b) WWA (c) ERA 5 and (d) RON.

the ERA5 and ACQUA ALTA is 1 and 3 h, respectively. Consequently, storm peaks recorded during shorter time intervals may be averaged over longer time periods. This could be particularly important for the Northern Adriatic, where waves generated during *bora* wind dominate. The main characteristic of the *bora* is the high wind speed and short duration (Katalinić and Parunov, 2021). The consequence could be that the height of wind-generated waves changes considerably within a 6-h interval. To account for this effect, the averaging of wave heights is performed for all databases to have the same sea state duration of 6 h. This is done by calculating the statistical average of H_s for all sea states within 6 h. The care is taken that all 6-h intervals refer to the same time for all databases. The averaging will reduce the effect of different time resolutions of sea states among databases. The calculated reduction factor representing averaging of yearly extreme significant wave heights reads 0.92 for ACQUA ALTA and ERA5, while 0.85 for RON.

Another effect that could cause a difference in H_s is the wave deformation while progressing from deep to shallower water. The oceanographic tower and buoys deployed in a limited water depth of 16 m measure already transformed waves, while two numerical wave databases contain deep water waves. To reduce this difference, the wave transformation effect for shallow water is applied to two latter databases. Although the transformation of the wave spectrum for shallow water effects could be performed (Kang et al., 2020), an engineering approach that takes into account the transformation of the deterministic wave is employed (DNV 2019). Wave spectrum is represented by the linear wave with height equal to H_s and period equal to peak spectral period T_p. The main mechanism causing wave transformation is shoaling, which is the wave height modification due to gradual change of the water depth. Other mechanisms of wave transformation, i.e., refraction, reflection, and wave breaking, are not relevant for wave heights considered in the present study. The change of wave height because of the shoaling reads (DNV 2019):

$$\frac{H}{H_0} = K_S = \sqrt{\frac{C_{g,0}}{C_g}} \tag{5}$$

where H is transformed wave height in the shallow water, H_0 is the initial wave height in the deep water, K_S is the shoaling coefficient,

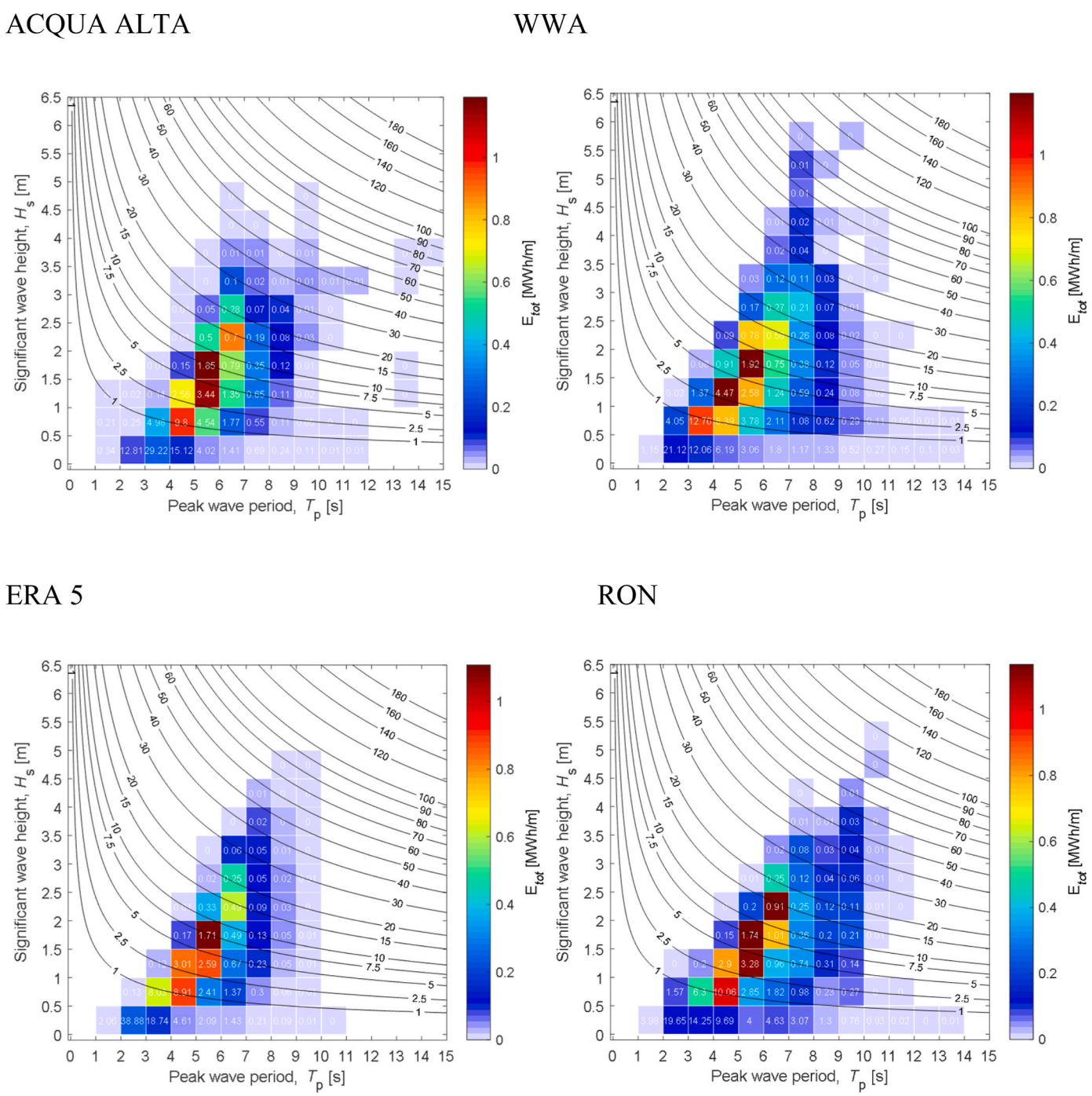

Fig. 9. Wave energy potential diagrams – (E_{tot} is a total potentially produced yearly wave energy for each sea state. Black lines are curves of a constant wave power P (kW/m), while white numbers are the probabilities of occurrence of a sea state (%).) (a) ACQUA ALTA (b) WWA (c) ERA 5 and (d) RON.

Table 2
Total wave energy potential for the location in the Northern Adriatic.

Yearly total wave energy potential E_{tot}, MWh/m			
ACQUA ALTA	WWA	ERA5	RON
11.44	14.39	8.80	12.71

Table 3
The main particulars of the analysed barge.

Lpp, m	*B*, m	*T*, m	*Δ*, t
113.0	36.6	4.50	17210

while $C_{g.0}$ and C_g are wave group velocities in deep and shallow water, respectively. All expressions necessary to calculate shoaling coefficient according to equation (5) can be found in DNV (2019) and are not repeated herein. Basically, from the wave period in the deep water, it is necessary to calculate associated wavelength in deep and shallow water using the dispersion equation. Then the group velocities for deep and shallow water are calculated, and the shoaling coefficient is determined from equation (5).

Peak periods associated with the extreme sea states in the North Adriatic are in the range of 6–9.5 s. Associated wavelengths in deep

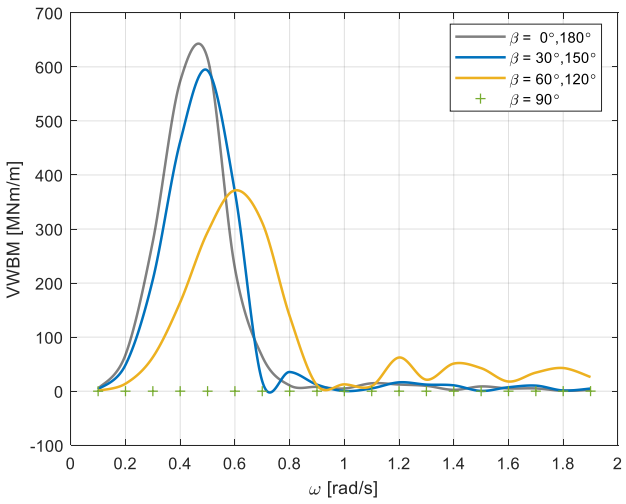

Fig. 10. Transfer functions of VWBM.

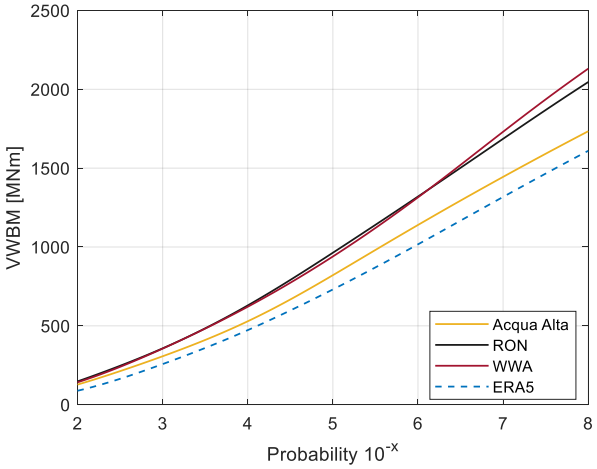

Fig. 11. Long-term distributions of VWBM.

water read 58–105 m. For such wavelengths, 16 m water depth represents intermediate water depth where the wave height because of the shoaling is slightly reduced with respect to the deep water. Only if waves further progress towards shallower water depth, wave heights increase significantly. In the present study, the calculated shoaling coefficient reads 0.92 on average for extreme sea states.

A comparison of yearly maximum H_s, corrected for the effects of time averaging and wave transformation, is presented in Fig. 12.

Yearly extreme H_s are then compared to the ACQUA ALTA database, which is arguably the most accurate wave data source for the location considered. Namely, ACQUA ALTA is a fixed tower that measures waves using well-calibrated instruments, which have been updated with the improvement of the measurement technology through the years (Pomaro et al., 2018). The comparison of statistical properties of differences in yearly maximum H_s with respect to ACQUA ALTA measurements is presented in Table 6 for both original and corrected data.

It may be seen from Table 6 that agreement between RON and ACQUA ALTA is improved when correction for time averaging is employed. The mean value of the difference between ERA 5 and ACQUA ALTA is worse after correction, but the standard deviation of differences is reduced. Finally, the uncertainty of the WWA compared to the ACQUA ALTA is about the same before and after correction. This may be explained by the fact that the reduction for shallow water applied on the WWA is approximately the same as the reduction of time-averaging used on ACQUA ALTA.

Differences in the extreme H_s presented in Table 6 deserve further clarification. It is obvious from Table 6 that numerical wave databases generally overestimate ACQUA ALTA measurements. This could be explained by the effect of sea current that is not included in numerical wave models. Barbariol et al. (2013) analysed the effect of the wave-current interaction in the Gulf of Venice, which corresponds to the ACQUA ALTA location, and found that this effect could reduce the wave height predicted by the numerical wave models. This was explained by the fact that sea currents and *bora*-generated wind waves in the Gulf of Venice propagate in the same direction, causing flattening of wind waves. It should be noted that this effect is noticed only in that location in the Adriatic Sea.

One interesting finding is the difference between two numerical datasets, namely ERA5 and WWA. The recent review of uncertainties in phase-averaged wave spectral models is provided by Bitner-Gregersen et al. (2022). One of the findings is that ERA5 has the tendency to slightly underestimate the extremes. This is confirmed in the present study, as higher extreme values are obtained by WWA compared to the ERA5.

Table 4
The most probable extreme VWBM for the probability level 10^{-8}.

	MPEV of VWBM, MNm			
	ACQUA ALTA	WWA	ERA5	RON
Probability 10^{-8}	1734	2131	1610	2046

Table 5
Barge fatigue results due to different wave data statistics.

	ACQUA ALTA	WWA	ERA5	RON
Weibull Scale parameter	0.52	0.511	0.489	0.519
Weibull Shape parameter, MNm	6.57	7.15	4.29	7.61
Fatigue Damage *D*	0.26	0.42	0.13	0.43

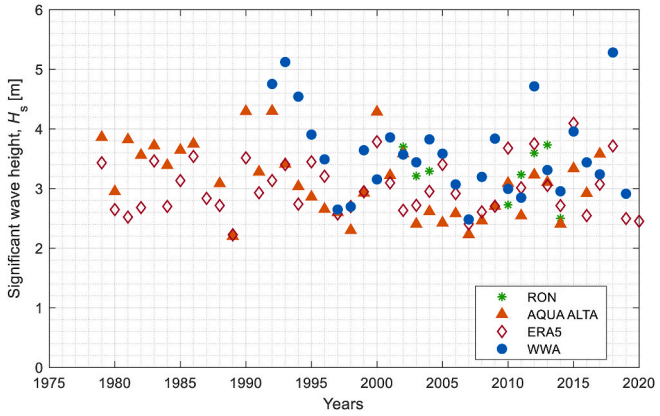

Fig. 12. Maximum yearly significant wave heights after correction for time averaging and wave transformation.

Table 6
Statistics of the differences in yearly maximum H_s between RON, ERA5, and WWA with respect to ACQUA ALTA.

	Original data		Corrected data	
	Mean, m	St. dev., m	Mean	St. dev., m
RON	0.564	0.624	0.376	0.402
ERA 5	0.132	0.571	0.260	0.420
WWA	0.599	0.662	0.597	0.623

6. Conclusions

Four different wave data sources are compared for close locations in the Adriatic Sea: two databases are produced by wave hindcasting, and the other two are obtained by collecting measurements from the fixed locations. The consequences that differences in databases can have on the design of marine structures are presented throughout three examples:

1. uncertainty of the assessment of wave energy that can be used for the selection of wave energy converters,
2. uncertainty in the prediction of extreme wave loads for structural strength assessment,
3. uncertainty in accumulated fatigue damage.

Uncertainties of wave data have the largest consequence on the accumulated fatigue damage of marine structures, where predicted fatigue life based on studied databases can differ by a factor larger than 3. The ratio between the highest and lowest total wave energy potential predicted at the location reads 1.63, while the extreme global wave loads can differ by 30%.

Following conclusions regarding uncertainties in wave data can be drawn:

- Different databases provide similar trends regarding time series of significant wave heights and storm predictions, but their extreme values have greater discrepancies. Differences are persistent even if the equal time resolution is used.
- For practical offshore engineering applications, wave data should be provided for the exact location of a structure, as relatively small geographical distances can produce considerable differences in extremes.
- The WWA database provides conservative extreme values compared to ERA5. Therefore, this database is preferred for practical offshore applications in deep water.
- In the near-shore locations, it is highly recommended to use numerical models that can account correctly for wave-current interaction and shallow water effects.

CRediT authorship contribution statement

Maro Ćorak: analysis, revision, writing original and revised paper. **Antonio Mikulić:** analysis, revision, writing revised paper. **Marko Katalinić:** writing original paper. **Joško Parunov:** Conceptualization, writing revised paper.

Declaration of competing interest

The authors declare that they have no known competing financial interests or personal relationships that could have appeared to influence the work reported in this paper.

Acknowledgements

Work was supported by the Croatian Science Foundation under the project lP-2019-04-2085. World Waves database is provided by Fugro OCEANOR.

References

Barbariol, F., Benetazzo, A., Carniel, S., Sclavo, M., 2013. Improving the assessment of wave energy resources by means of coupled wave-ocean numerical modelling. Renew. Energy 60, 462–471.
Bencivenga, M., Nardone, G., Ruggiero, F., Calore, D., 2012. The Italian data buoy network (RON). Adv. Fluid Mech. IX 74, 321.
Bitner-Gregersen, E.M., Dong, S., Fu, T., Ma, N., Maisondieu, C., Miyake, R., Rychlik, I., 2016. Sea state conditions for marine structures' analysis and model tests. Ocean Eng. 119, 309–322.
Bitner-Gregersen, E., Waseda, T., Parunov, J., Yim, S., Hirdaris, S., Ma, N., Guedes Soares, C., 2022. Uncertainties in long-term wave modelling. Mar. Struct. 84, 103217, 21. https://doi:10.1016/j.marstruc.2022.103217.
Cavaleri, L., Barbariol, F., Bastianini, M., et al., 2021. An exceptionally high wave at the CNR-ISMAR oceanographic tower in the Northern Adriatic Sea. Sci. Data 8, 37. https://doi.org/10.1038/s41597-021-00825-x.
Common Structural Rules, 2012. Harmonized Common Structural Rules for Bulk Carriers and Oil Tankers. IACS.
Ćorak, M., Parunov, J., Guedes Soares, C., 2015. Long-term prediction of combined wave and whipping bending moments of container ships. Ships Offshore Struct. 10, 4–19.
Det Norske Veritas, 2010. Fatigue Assessment of Ship Structures, Classification Notes No.30-7. Det NorskeVeritas.
Det Norske Veritas, 2019. Recommended Practice DNV-Rp-C-205, Environmental Conditions and Environmental Loads. Available online: www.dnv.com.
Hauteclocque, G., Zhu, T., Johnson, M., Bitner-Gregersen, E.H.A., 2020. Assessment of global wave datasets for long term response of ships. In: Proceedings of the ASME 2020 39th International Conference on Ocean, Offshore and Arctic Engineering OMAE 2020, pp. 1–9.
Hersbach, H., de Rosnay, P., Bell, B., Schepers, D., Simmons, A., Soci, C., Abdalla, S., Alonso-Balmaseda, M., Balsamo, G., Bechtold, P., et al., 2018. Operational Global Reanalysis: Progress, Future Directions and Synergies with NWP, ERA Report Series. ECMWF Shinfield Park, Reading, UK.
Jensen, J.J., Mansour, A.E., 2002. Estimation of Ship Long-Term Wave-Induced Bending Moments Using Closed Form Expressions Transactions RINA, pp. 41–55.
Katalinić, M., Parunov, J., 2018. Wave statistics in the Adriatic Sea based on 24 years of satellite measurements. Ocean Eng. 158, 378–388. https://doi.org/10.1016/j.oceaneng.2018.04.009.
Katalinić, M., Parunov, J., 2020. Uncertainties of estimating extreme significant wave height for engineering applications depending on the approach and fitting technique – Adriatic Sea case study. J. Mar. Sci. Eng. 8, 259–278.
Katalinić, M., Parunov, J., 2021. Comprehensive wind and wave statistics and extreme values for design and analysis of marine structures in the Adriatic Sea. J. Mar. Sci. Eng. 9, 522–547.
Kang, H., Chun, I., Oh, B., 2020. New procedure for determining equivalent deep-water wave height and design wave heights under irregular wave conditions. Int. J. Nav. Archit. Ocean Eng. 12, 168–177. https://doi.org/10.1016/j.ijnaoe.2019.09.002. ISSN 2092-6782.
Katalinić, M., Ćorak, M., Parunov, J., 2015. Analysis of wave heights and wind speeds in the Adriatic Sea. In: Gudes Soares, C., Santos, T. (Eds.), Maritime Technology and Engineering. Taylor & Francis Group, London, pp. 1389–1394.
Katalinić, M., Ćorak, M., Parunov, J., 2020. Optimized wave spectrum definition for the Adriatic Sea. Naše more 67 (1), 19–23.
Liberti, L., Carillo, A., Sannino, G., 2013. Wave energy resource assessment in the Mediterranean, the Italian perspective. Renew. Energy 50, 938–949.
Mansour, A., Høvem, L., 1994. Probability-based ship structural safety analysis. J. Ship Res. 38 (4), 329–339.
Parunov, J., Ćorak, M., Pensa, M., 2011. Wave height statistics for seakeeping assessment of ships in Adriatic Sea. Ocean Eng. 38, 1323–1330.
Pomaro, A., Cavaleri, L., Lionello, P., 2017. Climatology and trends of the Adriatic Sea wind waves: analysis of a 37-year long instrumental data set. Int. J. Climatol. 37, 4237–4250.
Pomaro, A., Cavaleri, L., Papa, A., Lionello, P., 2018. 39 years of directional wave recorded data and relative problems, climatological implications and use. Sci. Data 5, 180139. https://doi.org/10.1038/sdata.2018.139.
Schirmann, M.L., Collette, M.D., Gose, J.G., 2020. Significance of wave data source selection for vessel response prediction and fatigue damage estimation. Ocean Eng. 216, 1–15.
Vettor, R., Soares, C.G., 2016. Assessment of the storm avoidance effect on the wave climate along the main North Atlantic routes. J. Navig. 69 (1), 127–144.

Publication III

Preprint of the published journal article.

Bias in estimates of extreme significant wave heights for the design of ship structures caused by neglecting within-year wave climate variability

Antonio Mikulić[a], Joško Parunov[a,*]

[a]*University of Zagreb, Faculty of Mechanical Engineering and Naval Architecture, Ivana Lučića 5, Zagreb 10000, Croatia*

Abstract

The purpose of the study is to examine the effect of within-year wave climate variability on the extreme significant wave heights prediction for the design of ship structures. The significant wave height data used in the study is taken from ERA 5 database for typical locations along frequent shipping routes in the Atlantic and Pacific oceans. For each location, monthly and annual extreme significant wave heights are extracted, and Gumbel distributions are fitted, respectively, using Maximum Likelihood Estimation. Monthly extreme wave heights are then combined, using the method proposed by Carter and Challenor (1981), to account for the effect of intra-annual climate variability on the long-term extremes. Methods are compared for both individual locations and shipping routes. Consequences of the intra-annual climate variability on the extreme vertical wave bending moment are explored, for different shipping routes, comparing the results to IACS rules. It was found that neglecting within-year wave climate variability could lead to the underestimation of long-term extreme significant wave heights and vertical wave bending moments by up to 10%.

Keywords: extreme significant wave heights; seasonal variability; monthly and annual extremes; Gumbel distribution; reliability-based design

1. Introduction

To operate safely and efficiently, ships and offshore structures must withstand extreme ocean wave conditions, where significant wave height represents the main variable in the wave environment description. Therefore, the reliable design of marine structures requires a realistic and accurate prediction of extreme significant wave heights expected during their required lifetime (DNVGL-RP-C205 2017). There are two methods of the wave load calculation for the ultimate strength analysis of marine structures, namely the Design Sea State Method (DSSM) and All Sea State Method (ASSM) (Mansour and Liu, 2008). The former method consists of selecting a design sea state and then performing the analysis of wave loads of marine structure for only that short-term sea condition. The latter method considers all sea states with their probability of occurrence, and then the long-term distribution of wave load is computed, enabling the determination of the most probable extreme value. DSSM is often used in the design of offshore structures, while ASSM is currently recommended by the International Association of Classification Societies (IACS Rec. no.34 2000) for analysis of ship structures. However, even in cases when ASSM is used, knowledge of extreme sea states corresponding to long return periods is useful to describe the severity of the wave environment where marine structure operates. The return period of extreme sea states for the design of offshore structures is very often 50, 100, or even 1000 years, while the return period of sea states for ship structural design reads 25 years.

The extreme significant wave heights are usually calculated using wave statistical data collected on an annual basis, thus neglecting within-year (also called intra-annual) wave climate variability. This question of seasonal variability of the wave climate was originally raised by Carter and Challenor (1981), showing theoretically that neglecting seasonality of the wave climate introduces unconservative bias to the estimated long-term extreme values. The reason why the within-year variability of wave climate has not been accounted for in the analysis of extreme wave heights is that number of observations was not sufficient to fit theoretical probability distribution with enough confidence. This is especially true for wave statistics used for ship structural design as such data are collected by visual observations, suffering from lack of quality and consistency (WMO 1998). However, the situation changed dramatically in the past few decades with the availability of long-term, high-quality wave databases, obtained by hindcasting using numerical wave models as WAM, WAWATCH-III, and SWAN. Such

* Corresponding author.
E-mail address: jparunov@fsb.hr

databases offer the possibility to account for many additional effects, intra-annual climate variability being one of them (Perrault 2021).

Extreme values of surface wave heights in the northern Adriatic are studied by Leder et al. (1998), accounting for monthly variability of wave climate using the approach proposed by Carter and Challenor (1981). Calculated extreme significant wave heights resulted in larger values compared to the extreme values obtained by neglecting that effect. However, the analysis was performed based on the dataset where many of the monthly extremes were missing. Study of the seasonality effect on the extreme wave heights is performed recently by Sartini et. al. (2015) for the Mediterranean Sea. A nonstationary model based on a time-dependent version of the Generalized Pareto Distribution (GPD)-Poisson point process model has been implemented and applied to model extreme wave heights. Seasonal changes of significant wave heights in shelf seas around India are studied by Kumar et al. (2018) based on wave hindcast data. A seasonal extreme value analysis of North Sea storm conditions using a statistically rigorous and physically reasonable approach is presented by Hansen et al. (2020). The simplified approach based on time-dependent, generalized extreme value (GEV) models and classical regression is proposed to estimate correlated extreme significant wave heights and wind velocities accounting for seasonality (Calderón-Vega et al. 2020).

Data from the ERA5 wave database is used in the present study. Typical locations along shipping routes in the Atlantic and Pacific oceans are selected. For each location, annual extreme significant wave heights for each month are extracted, and Gumbel distribution is fitted, enabling a theoretical estimate of the long-term monthly extreme values. The method of Carter and Challenor (1981) is then employed to estimate long-term overall annual extreme values from monthly extremes. Results are compared to the commonly used yearly long-term extreme values, obtained by fitting the Gumbel distribution to the overall annual extremes. The comparison is conducted for individual locations and routes, thus also considering the effect of the wave climate variation along the shipping route. Finally, consequences of the intra-annual climate variability on the extreme vertical wave bending moment (VWBM) are assessed using the design sea state method for different shipping routes.

The present paper is in line with the current efforts by major class societies for the revision of the global wave data for ship strength analysis (de Hauteclocque et al. 2020). Namely, the current standard for wave statistics to be used in ship design is still defined in IACS Rec. no.34 (2000), despite big progress that has been achieved in wave modeling in the last two decades. Additionally, the present study contributes to the joint efforts of two leading research associations, ISSC and ITTC, to quantify and reduce uncertainties associated with wave data and models currently used in the design and operation procedures of ships and offshore structures (Bitner-Gregersen et al. 2016).

The paper is structured into 6 sections and Appendix. After the introduction in Section 1, Section 2 describes chosen North Atlantic and Pacific routes. It also offers an introduction to the ERA5 wave database and data source characteristics. The research methodology is introduced in Section 3. Gumbel distribution is fitted to the sorted data and later used to calculate extremes for the specific return period. A portion of the results, substantial to the research, are presented in Section 4, while the rest are given in the Appendix. 5. The effect of the wave climate variation along shipping routes and consequences on the extreme vertical wave bending moments (VWBM) are demonstrated in subsection 4.1 and 4.2 respectively. Results are further commented on and discussed in Section 4.1. Section 6 provides recommended future steps and conclusions.

2. Wave data and shipping routes

The significant wave height data used in the presented analysis is a high-resolution hindcast, extracted from ERA 5 database accounting for waves generated and directly affected by local winds and the ones generated by the wind at a different location and time, also called swell. ERA5 is the fifth generation ECMWF (The European Centre for Medium-Range Weather Forecasts) reanalysis, produced combining advanced forecasts modeling and data assimilation systems with vast amounts of observations (Hersbach et al. 2018). For the model data calculation, the ECMWF's Integrated Forecast System (IFS) combines the atmospheric model, the land-surface model (Revised land surface hydrology, HTESSEL), and the third-generation ocean wave model (Wave Modeling Project, WAM). Complete ERA5 data covers the period from 1979 until now, providing hourly estimates for many atmospheric, land-surface, and ocean-wave climate variables, with a lat-lon grid resolution of approximately 0.5 degrees.

Two frequent shipping routes (northern and southern) are selected for each North Atlantic and Pacific Ocean (Mansour and Preston 1995) as representative for different wave severity. The Northern shipping route in the North Atlantic is the great circle route, connecting ports in North Europe and Great Lakes, having some of the most extreme weather conditions in the world. The Southern route is the "low-powered" shipping lane between

Gibraltar and Houston (Figure 1). The Northern route in the Pacific is the great circle route between San Francisco and Yokohama, while the Southern route connects the same locations by way of Honolulu, Hawaii (Figure 2).

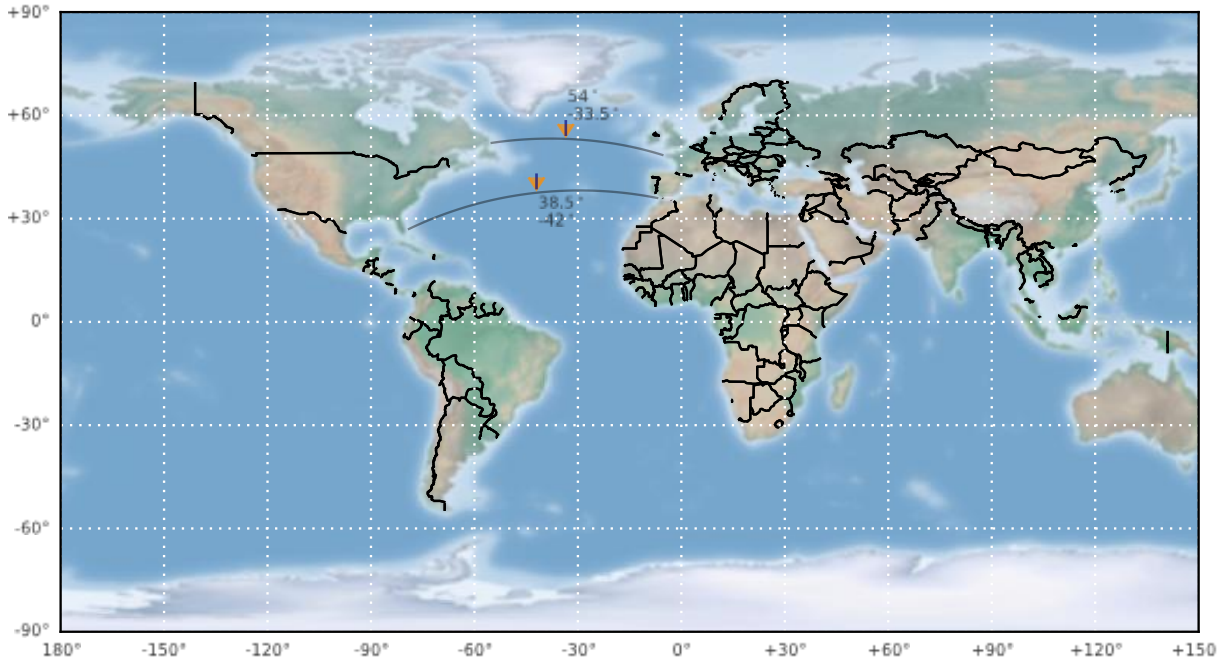

Fig. 1. Northern and Southern shipping route and analyzed mid-locations in North Atlantic.

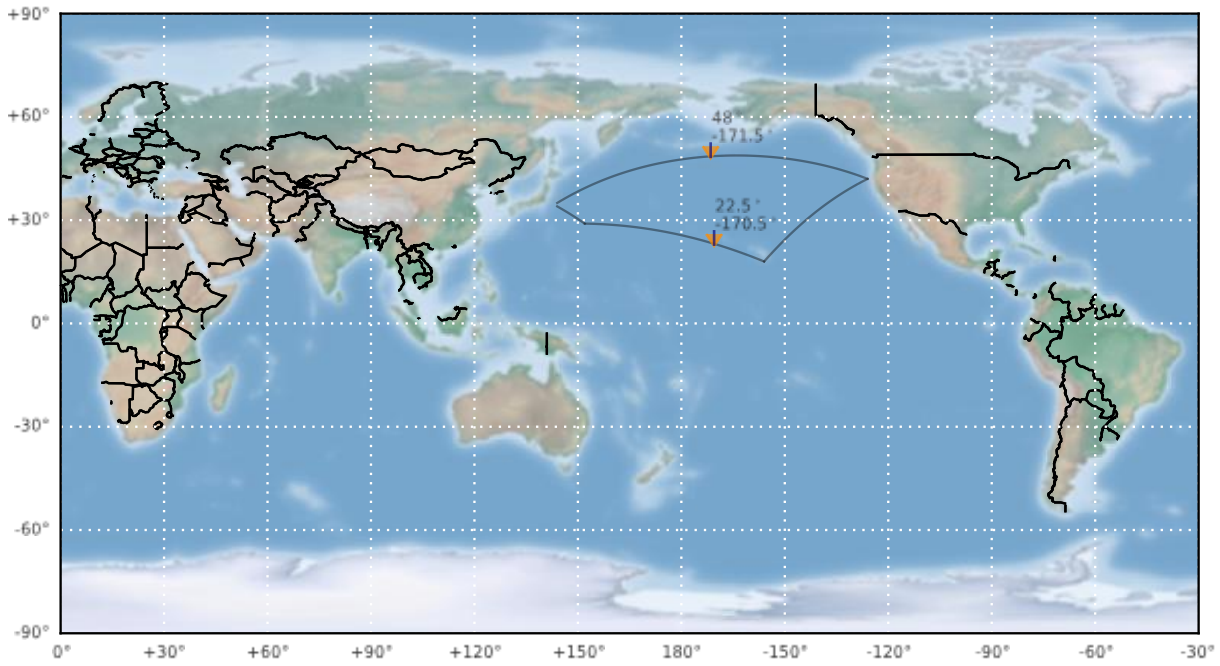

Fig. 2. Northern and Southern shipping route and analyzed mid-locations in North Pacific.

Locations in the middle of each route are considered representative for the shipping routes and therefore further analyzed in the present study. Locations and routes are labelled in order of appearance:

1. location in the middle of Northern route in North Atlantic: 54° N 33.5° W

2. location in the middle of Southern route in North Atlantic: 38.5° N 42° W
3. location in the middle of Northern route in North Pacific: 48° N 171.5° W
4. location in the middle of Southern route in North Pacific: 22.5° N 170.5° W

3. Methodology

The annual extreme significant wave heights are extracted for each month, throughout every year available, at defined locations. According to the recommendations of DNVGL-RP-C205 (2017), a year is defined from July of the concerned year to the June of the following year. Out of 42 years of available data, the research considers only complete and uncorrupted data available throughout the whole year. Although the size of clean data differed between locations, an equal timeframe of 36 years from July 1979 to June 2015 is used for all locations for the sake of better comparison and consistency. The lowest and the highest recorded annual extreme significant wave height for each month in the period of availability of the ERA5 database is shown in Figure 3.

The maximum annual significant wave height data is usually described using Gumbel extreme value probability density function and cumulative distribution given as respectively:

$$f_{H_s}(x) = \frac{1}{B} \cdot e^{-\left(\frac{x-A}{B} + e^{-\left(\frac{x-A}{B}\right)}\right)} \tag{1}$$

$$F_{H_s}(x) = e^{-e^{-\left(\frac{x-A}{B}\right)}} \tag{2}$$

where A and B are respectively location and scale parameters of the Gumbel distribution. Fitting of Gumbel distribution is performed by the Maximum Likelihood Method (MLE), using the '*Nelder-Mead*' simplex algorithm provided by *scipy.optimize* package in Python (Virtanen et al. 2020). The obtained parameters A and B are presented in Table 1. It should be noted that parameter A represents the most probable annual extreme significant wave height either for each month or for the whole year. Histograms and fitted Gumbel distributions are shown in the Appendix, both on a monthly and yearly basis, for each of the selected midway locations.

The distribution of extremes during the year may be calculated from the monthly distributions, using the expression proposed by Carter and Challenor (1981):

$$P_{H_s}\left(X < x\right) = \prod_{i=1}^{12} F_i(x) \tag{3}$$

Equation (3) assumes that monthly extremes $F_i\ (x)$ are independent, which is considered as a reasonable assumption. Furthermore, it is necessary to introduce the return period $T(x)$, defined as the mean period (in years) between the occurrence of two values equal or higher than x. So, the probability that x will be exceeded in any year is given as:

$$\frac{1}{T(x)} = 1 - F(x) \tag{4}$$

When $F(x)$ is calculated for different return periods $T(x)$, corresponding return significant wave heights are easily obtained from the Gumbel distribution (2). It should be noted that, unless distributions of monthly extremes are identical, the resulting distribution from Equation (3) is not Gumbel distribution. Therefore, quintiles of distribution and return values are to be obtained numerically using probabilities given by Equation (4).

4. Results

Violin plots of monthly extremes for all locations are given in Figure 3. Graphs display minimum, maximum, and mean values, with the addition of a rotated kernel density plot on each side, picturing how values are distributed. It may be seen from Figure 3 that the highest waves are recorded in the Northern North Atlantic, occurring in December and January. In the Southern North Atlantic, the highest significant wave heights are recorded in December and February. It is intersecting to notice that in summer months, August and September, rather severe sea states are found, with significant wave heights almost equal to those in winter months. That is probably because of hurricanes appearing in the Southern North Atlantic at the end of the summer season. In the Northern part of the North Pacific, the highest annual significant wave heights are recorded from October to March. Extreme values are between those recorded in the Northern and Southern North Atlantic. The mildest wave climate is found for the location on the Southern route in the North Pacific.

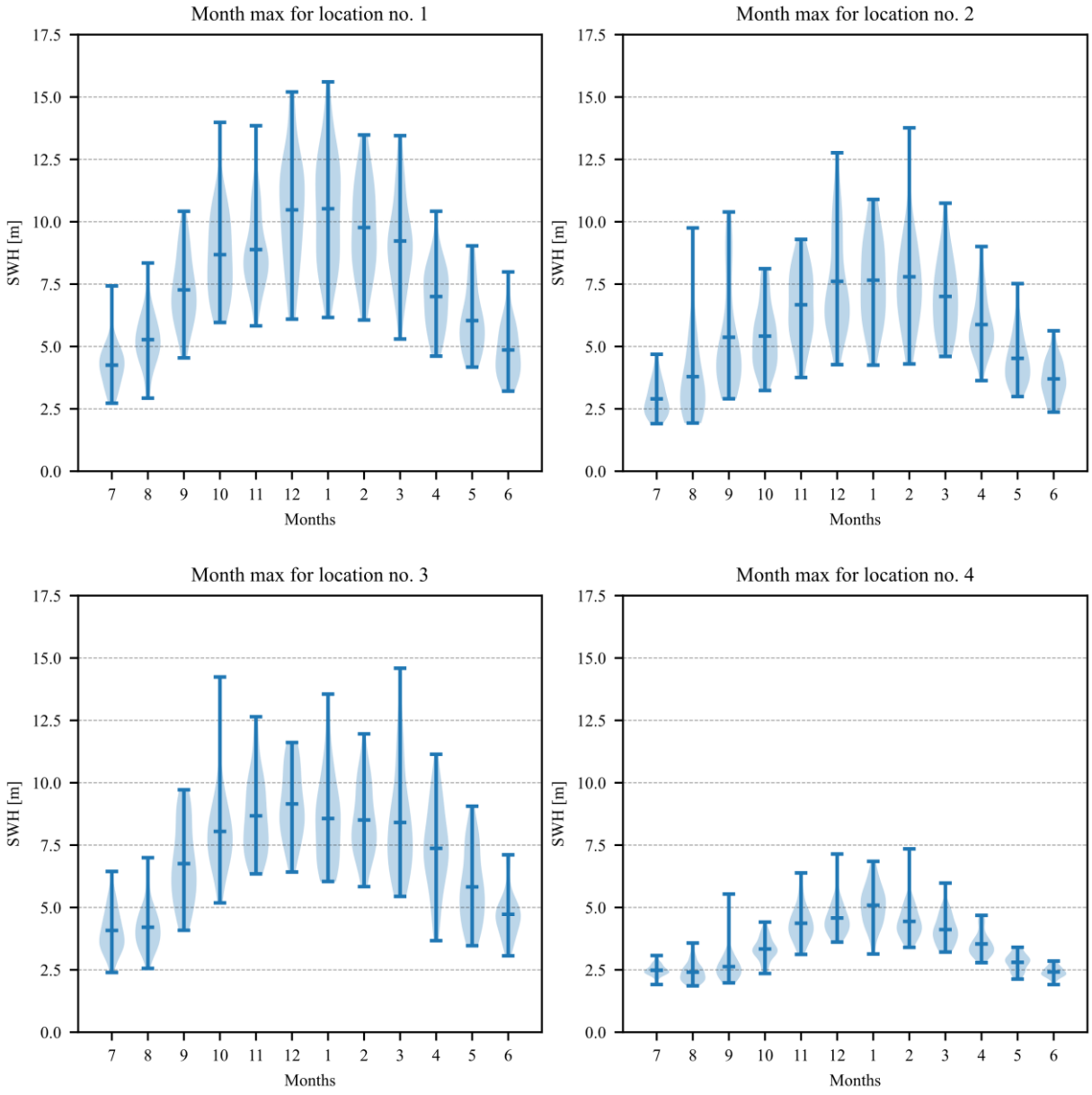

Fig. 3. Violin plot of monthly significant wave height extremes for all four locations.

Parameters of the Gumbel distribution fitted to monthly and yearly extremes are presented in Table 1. The most probable extreme significant wave height, represented by Gumbel parameter *A* is the highest during winter months, especially December and January suggesting that most yearly extremes occur in those months. Northern locations have higher values compared to the Southern ones. The values presented in Table 1 correlate with the

previous figure. The last row corresponds to the Gumbel distribution parameters fitted to the extreme values determined on a yearly basis.

Table 1. Gumbel parameters A and B for each month and a whole year.

Month	Locations							
	Loc. 1		Loc. 2		Loc. 3		Loc. 4	
	A	*B*	*A*	*B*	*A*	*B*	*A*	*B*
7	3.85	0.73	2.59	0.53	3.67	0.75	2.37	0.23
8	4.75	1.04	3.09	1.08	3.81	0.72	2.23	0.29
9	6.57	1.29	4.45	1.41	5.99	1.38	2.41	0.34
10	7.85	1.46	4.80	1.07	7.32	1.30	3.10	0.45
11	8.15	1.32	5.95	1.37	7.95	1.23	4.03	0.59
12	9.37	2.10	6.69	1.55	8.46	1.28	4.28	0.49
1	9.45	1.98	6.79	1.60	7.72	1.44	4.67	0.82
2	8.85	1.70	6.85	1.64	7.80	1.28	4.13	0.52
3	8.35	1.67	6.28	1.29	7.45	1.59	3.83	0.50
4	6.36	1.19	5.34	0.97	6.50	1.68	3.32	0.36
5	5.43	1.04	4.05	0.79	5.12	1.24	2.63	0.32
6	4.34	0.90	3.32	0.69	4.28	0.79	2.31	0.21
Year	11.92	1.42	9.13	1.34	10.28	1.28	5.20	0.60

A comparison of return significant wave heights obtained by employing Equation (2) (C&C method) and return values from Gumbel distributions fitted to the yearly extreme values (last row in Table 1) is presented in Figure 4. Values from Gumbel yearly extremes are lower in all cases. For all locations, those differences are intensified with the increase of the return period. Differences between Gumbel yearly extremes and values obtained by the C&C method are also decreased as extremes are more uniformly distributed throughout the year. As expected from the results in Figure 3, location 1 has the highest and location 4 has the lowest predicted extreme value.

Table 2. Significant wave height, for monthly and yearly 25 years return period

Month	Locations			
	Loc. 1	Loc. 2	Loc. 3	Loc. 4
7	6.19	4.29	6.06	3.10
8	8.06	6.56	6.11	3.16
9	10.71	8.97	10.40	3.51
10	12.52	8.23	11.48	4.54
11	12.37	10.33	11.90	5.92
12	16.10	11.65	12.54	5.86
1	15.78	11.92	12.34	7.30
2	14.30	12.09	11.89	5.80
3	13.69	10.41	12.54	5.43
4	10.16	8.43	11.87	4.48
5	8.75	6.59	9.10	3.66
6	7.20	5.53	6.81	2.99
Year	16.45	13.42	14.38	7.11
Year C&C	17.93	13.96	14.93	7.46

A comparison of extreme significant wave height for the return period of 25 years, which is the reference return period for the analysis of ship structures, is given in Table 2 for each of the four analyzed locations. Except for location 4, predicted extremes for each month are lower than the yearly predictions. For location 1, the yearly prediction difference between the C&C method and conventional extreme value estimate on an annual basis is around 9%, while for all other locations difference is approximately halved.

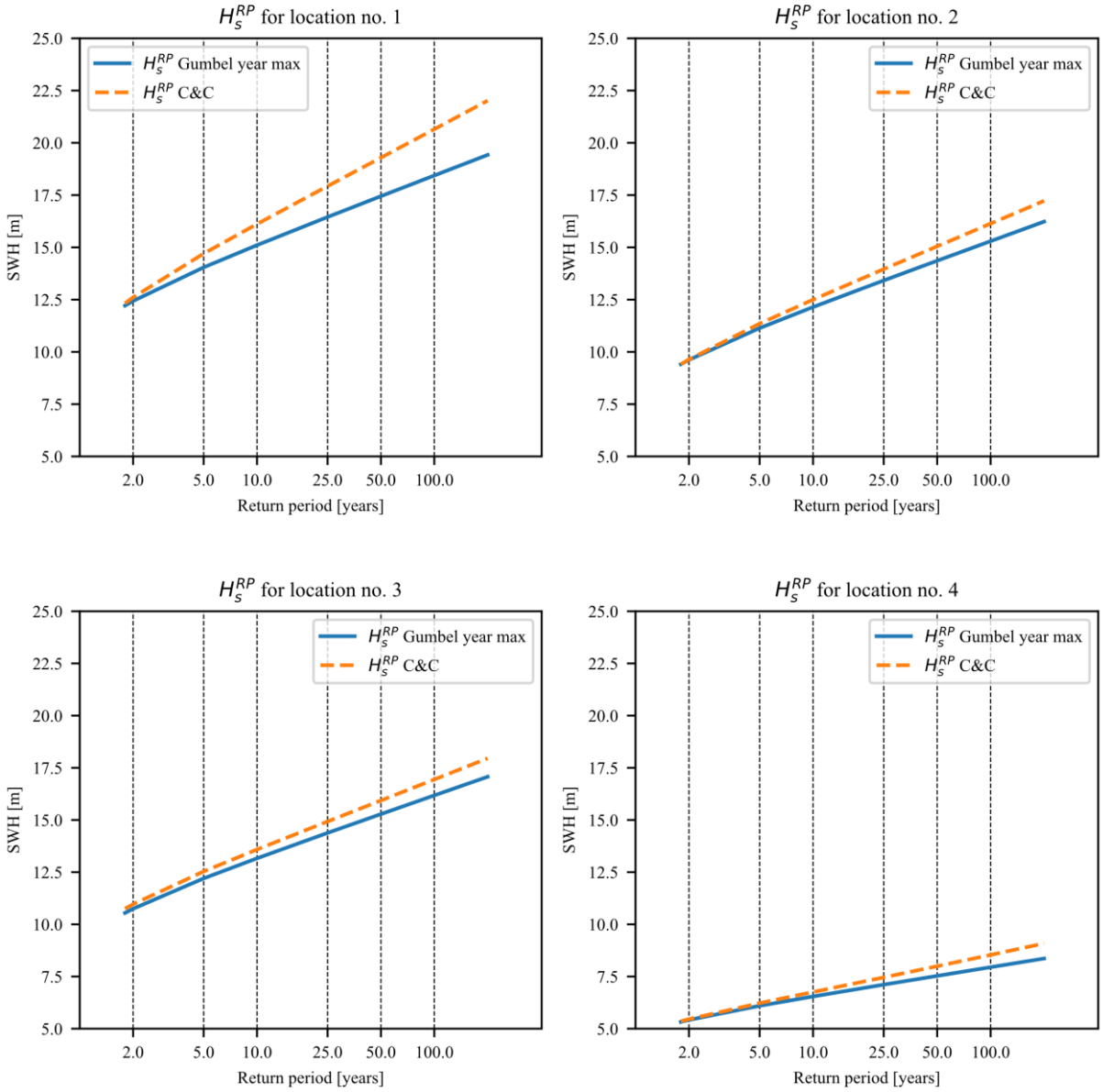

Fig. 4. The distribution of the return SWHs for four mid-locations.

4.1. The effect of the wave climate variation along the shipping route

The results presented in Section 3 are obtained for a single location at the midway of each route. As such, results are more appropriate for offshore structures than for ocean-going ships. To obtain results relevant for the desing and analysis of ships, 7 equally spaced locations along each of the routes given in Figures 1 and 2 are considered.

The resulting extreme value distribution along the shipping route is obtained by statistically combining extreme value distributions at individual locations:

$$P_{H_s,route}\left(X < x\right) = \prod_{j=1}^{N} P_{H_s,j}^{\frac{1}{N}} \tag{5}$$

The extreme value distributions $P_{Hs,j}$ $(X<x)$ is defined by Equation (3) for specific location j along the route. The total number of locations reads $N = 7$ for each route. Equation (5) implicitly includes the assumption that the extreme sea states along the shipping route are statistically independent. This assumption seems reasonable, as the distance between locations is rather large. The effect of statistical correlation of sea states along the route can be considered using the method described by Mansour and Preston (1995) and Mikulić et al. (2021). Another assumption inherent in Equation (5) is that ship spends equal time at each of 7 equally spaced locations that also looks as a reasonable assumption.

The distribution of the return SWHs along the routes is presented in Figure 5. A similar trend is noticeable, with some differences when considering only mid-point location and whole shipping route. It is interesting to notice that three routes display milder conditions than mid-locations, while southern route in North Pacific suggest a tougher environment than the mid-point.

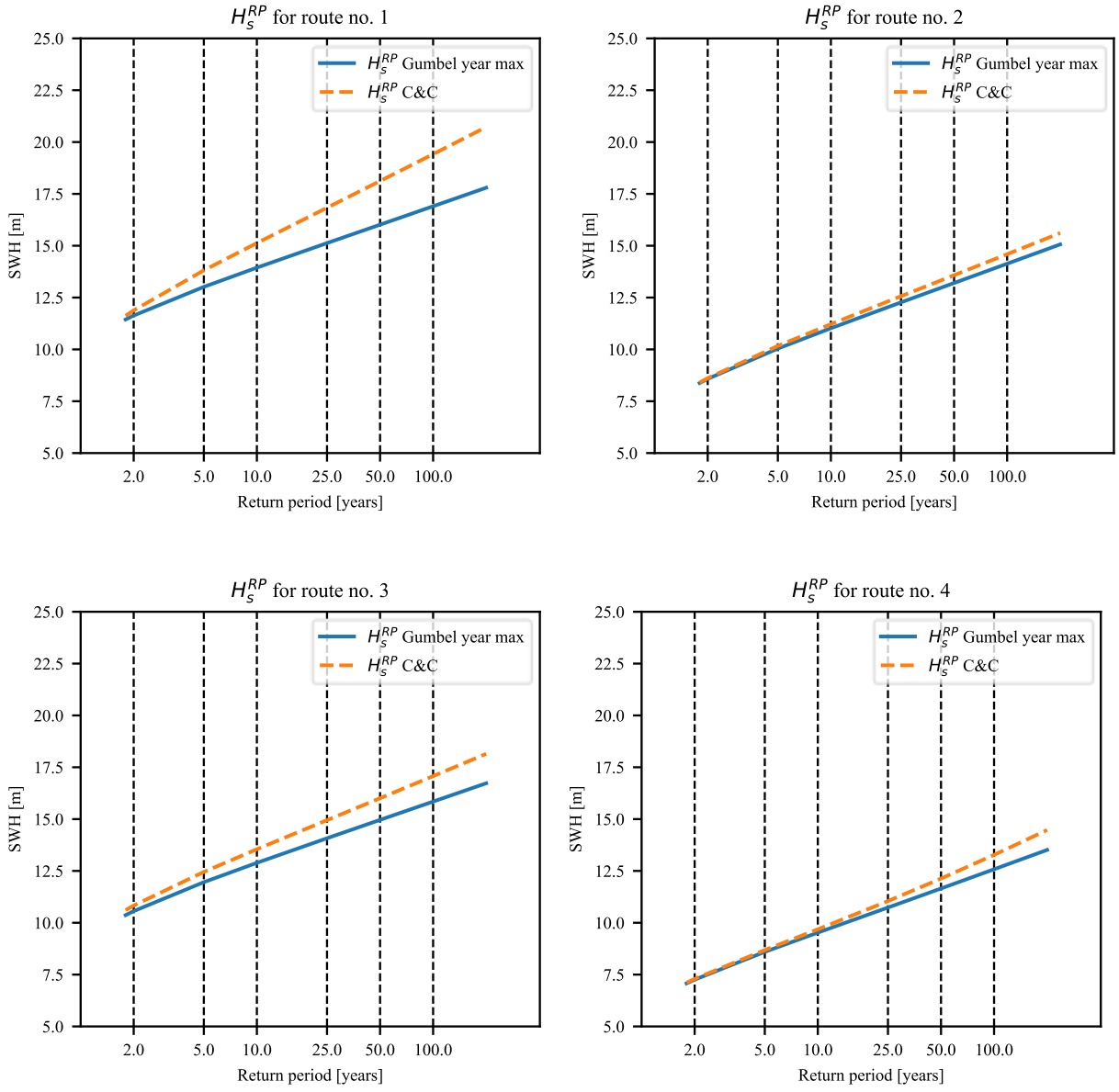

Fig. 5. The distribution of the return SWHs for four shipping routes.

The resulting extreme significant wave heights for the return period of 25 years, relevant for the design of ship structures, are given in Table 3. Extreme values given in Table 3 are obtained using yearly values and C&C method for individual locations along routes and then combined using Equation (4) to obtain extreme values along

the whole shipping route. Finally, Equation 3 is employed to obtain the most probable extreme value for the return period of 25 years.

Table 3. The most probable significant wave height (in m), for 25 years return period along shipping routes

Method	Route			
	1	2	3	4
Year	15.13	12.27	14.08	10.73
Year C&C	16.83	12.57	14.95	11.05

The comparison of the results presented in Table 3 with those from the bottom rows of Table 2, suggests that for 25 years return period, North Atlantic routes (no. 1 and 2) have 6-10% (1.1 to 1.4 m) lower SWH values compared to their midway locations. The values for the Northern North Pacific route have negligible difference (0-2%) in contrary to the Southern route in the North Pacific with around 50% higher values. Southern route in the North Pacific (Route 4) is the longest and has the biggest latitude difference between mid-location and the rest of the route that can explain this discrepancy. Regardless, it is a clear conclusion that results from the one location is not sufficient to represent the whole shipping route.

4.2. Consequences on the extreme vertical wave bending moments

Consequences of the intra-annual climate variability on the extreme VWBM on different shipping routes are assessed using the DSSM (Mansour and Liu 2008). The method is based on the assumption that extreme wave loads in ship lifetime are achieved on given short-term sea state of certain duration that ship can encounter with some low probability. Design sea states used in the present analysis are those given in Table 3. Associated mean zero-crossing wave periods are determined based on SWH (H_S) using Equation (6).

$$\mu = E\left[\ln T_Z\right] = a_0 + a_1 H_S^{\,a_2} \tag{6}$$

Coefficients a_0, a_1, and a_2 are defined in DNVGL-RP-C205 (2017) depending on the operating area. The short-term most probable linear VWBM is calculated using closed-form expressions for transfer functions derived by Jensen et al. (2004). Duration of the short-term sea state is assumed to be 3 hours. Minimum cruising speed of 5 knots is assumed in such extreme sea conditions. Also, assumptions that ship is sailing in head seas is adopted, which is reasonable assumption considering that in extreme conditions ship master usually turns ship in head waves to avoid excessive rolling.

Four oil tankers of different sizes (Panamax, Aframax, Suezmax, and VLCC) are considered at each route. The average dimensions of different classes of the oil tanker are given by Michel and Osborne (2004) while block coefficient C_b is assumed to be 0.8 in all cases.

Extreme VWBM is compared to the IACS Rule VWBM, prescribed in the IACS UR-S11 (2021). Linear IACS Rule VWBM is calculated as an average between sagging and hogging VWBM. The ratio of the VWBM calculated by direct analysis and IACS Rule linear VWBM is presented in Table 4.

Results from Table 4 indicate IACS rules comprehend VWBM return values obtained from annual distributions, as they should since IACS rule VWBM refer to unrestricted voyage. Further, it seems Rules have almost sufficient safety margin to cover the effects of intra-annual wave climate variability, since only Aframax class on route 1 is exceeding the IACS rule VWBM. As it could be seen before, northern routes have higher values of VWBM having Route 1 as the highest and Route 4 as the lowest extreme value.

Table 4. The ratio of linear VWBM by direct analysis and IACS Rules for oil tankers of different class

Ship class	Route 1		Route 2		Route 3		Route 4	
	Yearly	C&C	Yearly	C&C	Yearly	C&C	Yearly	C&C
Panamax	0.86	0.93	0.73	0.74	0.83	0.87	0.67	0.68
Aframax	0.95	**1.04**	0.79	0.81	0.90	0.96	0.70	0.72
Suezmax	0.90	0.99	0.73	0.75	0.84	0.89	0.63	0.65
VLCC	0.81	0.91	0.64	0.66	0.73	0.79	0.53	0.55

5. Discussion

Various distributions have been used for fitting wave heights with some success over the years. The most often used are Log-normal, Weibull 3-parameter, and Gumbel distribution (WMO 1998). A comparison of three distributions fitting yearly extremes and corresponding return SWH functions for location 1 is shown in Figure 6. Gumbel distribution visibly yields the most conservative results. The resulting SWH for 25 years reads 16.45 for Gumbel distribution suggesting more than 1m higher than Log-normal value and 1.5m higher than the extreme value obtained from Weibull 3P distribution. Poor fit of Log-normal distribution is obvious in Figure 6 that is also reported in WMO (1998). Weibull 3P is flexible, and since 3 parameters are used, a good fit is provided in Figure 6. However, this distribution is mostly used for fitting the upper tail of all data points rather than for fitting just their maximum values. Among these distributions, Gumbel is the only one theoretically confirmed as the asymptotic distribution of extreme values. It has been the most often used distribution of maximum wave heights when a sufficient number of maxima are available, and it is recommended by the Classification Society for fitting annual extreme significant wave heights (DNVGL-RP-C205 2017). Based on these arguments, Gumbel distribution is adopted for fitting extreme significant wave heights in the present study.

Maximum Likelihood Method is adopted for fitting parameters of the Gumbel distribution, although it should be mentioned that the choice of the fitting method can also result in different extreme value prediction that is not considered herein (Katalinić and Parunov 2020).

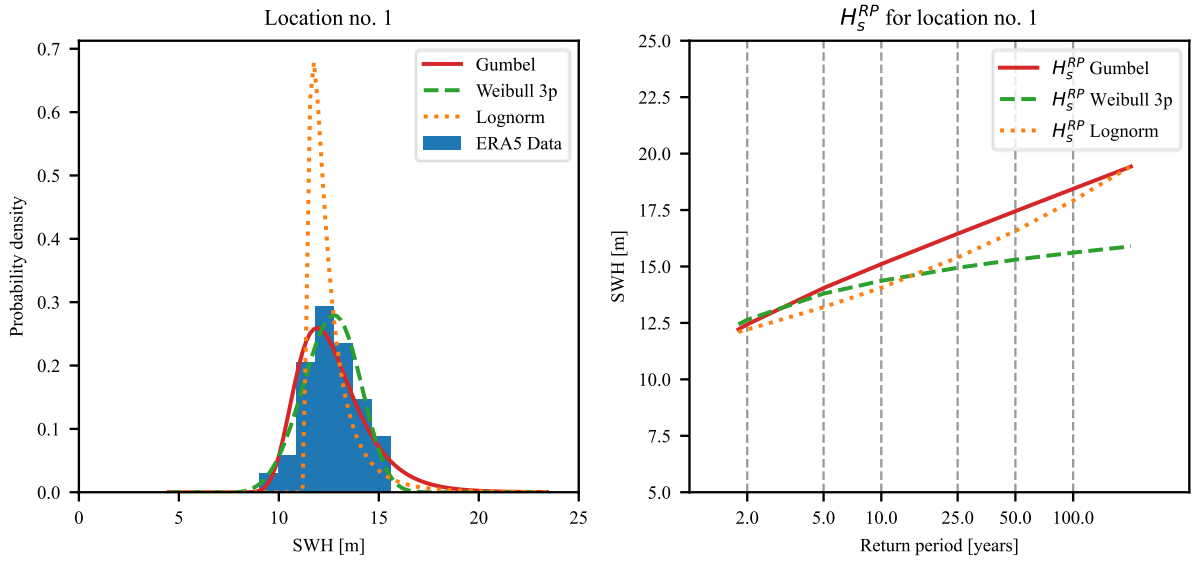

Fig. 6. Influence of different distribution fitted to the yearly annual extremes for location no. 1. (Left – probability density functions; Right – the most probable significant wave heights for different return periods)

The influence of the intra-annual wave climate variability on return significant wave heights is obvious from results presented in Section 4, especially for the Northern North Atlantic mid-location, where the return value calculated by the C&C method exceeds those calculated based on yearly extremes by almost 1.5 m. For all locations and routes, the return value calculated from the product of monthly extremes exceeds those from yearly extremes, indicating that the conventional assumption that extreme wave heights are evenly distributed throughout

the year is unconservative. Obtained results have theoretical proof that the return value obtained from annual distribution is less than the exact value obtained from compound distributions if proportional sampling is used (Carter and Challenor 1981). Proportional sampling is when the number of sampling from one division is proportional to the duration of that division. In the present case of almost uninterrupted data contained in the ERA5 database, this assumption of proportionality is obviously satisfied. Therefore, differences in return values presented in Figure 4 and Table 2 are expected and supported by the theory.

The underlying assumption for return value calculation by fitting the extreme distribution to the annual extreme values is that monthly data are identical for different months. As may be seen from Figure 3, this assumption is inappropriate as there are large differences between monthly extreme wave heights. Therefore, the application of extreme distribution to the annual extremes is theoretically inconsistent that causes an error in estimating return values.

Extreme wave loads for ultimate strength analysis of ships are obtained using wave data obtained from visual wave observations collected in the Global Wave Statistics (GWS, Hogben et al. 1986). Since most ships are designed for global, unrestricted service, the North Atlantic (NA) has been chosen as the operational area reference for calculating extreme wave loads on ship structures. IACS proposed a standard IACS NA wave scatter diagram, containing 100 000 observations, obtained by Monte Carlo simulation using the joint probability distribution of significant wave heights and mean zero-crossing periods, combining distributions of different wave zones in NA (DNV 2017). IACS NA wave scatter diagram is obtained on an annual basis by neglecting a monthly variability of the wave climate. Consequently, return significant wave heights contained in IASC NA wave scatter diagram could be unconservative, as shown by the results presented in Section 4.

It should be mentioned, however, that this simplification of neglecting intra-annual variability is just one of several, often contradictory assumptions used in the IACS procedure for calculating extreme wave loads on ships (IACS Rec. no.34 2000). For example, the effect of neglecting spatial correlation among sea states along the shipping route is to reduce extreme values, as shown by Mikulić et al. (2021). On the contrary, the unconservative aspect of the currently used wave scatter diagram is related to the global warming, increasing the return significant wave height in NA (Bitner-Gregersen et al. 2016).

6. Conclusions

Conventionally, extreme significant wave heights for long return periods in the design of marine structures are determined from yearly extreme values by fitting Gumbel distribution. Such an approach is theoretically inconsistent, as Gumbel distribution is the asymptotic extreme-value distribution only in the case when extreme values are identically distributed throughout the year. Such assumption is, however, rarely satisfied and, therefore, it is necessary to consider the consequence of within-year variability on estimate return significant wave heights.

The aim of the presented study is to quantify the bias in the extreme significant wave heights prediction for design of ship structures caused by neglecting within-year wave climate variability. The analysis is based on the extreme significant wave heights at locations along typical shipping routes extracted from ERA 5 database. The extreme significant wave height data for each month and the whole year are fitted by Gumbel distribution using the Maximum Likelihood Estimate method. Yearly extreme values considering within-year climate variability are calculated from monthly extremes by the method proposed in Carter and Challenor (1981). The extreme values at discrete locations are then combined statistically to obtain distribution of extreme significant wave height along typical commercial shipping routes.

It is found that the effect of neglecting intra-annual wave climate variability is to underestimate extreme significant wave heights at individual locations and along shipping routes by up to 10%. This difference is increasing with the variability of monthly extreme value distributions through the year. If considered, the effect of within-year variability consequently causes an increase of long-term extreme vertical wave bending moments on ships. Although it was found that ICAS Rule wave beding moment possibly comprehends this effect, it is advised to account for intra-annual variability in the analysis of extreme wave heights and corresponding extreme wave loads for ultimate limit state design of ships structures.

Acknowledgements

This work has been fully supported by Croatian Science Foundation under the project lP-2019-04-2085.

References

Bitner-Gregersen EMEM, Dong S, Fu T, Ma N, Maisondieu C, Miyake R, Rychlik I. 2016. Sea state conditions for marine structures' analysis and model tests. *Ocean Engineering* 119: 309–322.

Calderón-Vega F, García-Soto AD, Mösso C. 2020. Correlation of concurrent extreme metocean hazards considering seasonality. *Applied Sciences (Switzerland)* 10(14).

Carter DJT, Challenor PG. 1981. Estimating return values of environmental parameters. *Quarterly Journal of the Royal Meteorological Society* 107(451): 259–266.

Det Norske Veritas Germanischer Lloyd. 2017. DNVGL-RP-C205: Environmental Conditions and Environmental Loads., Oslo, Norway.

Hansen HF, Randell D, Zeeberg AR, Jonathan P. 2020. Directional–seasonal extreme value analysis of North Sea storm conditions. *Ocean Engineering* 195(September 2019): 106665.

de Hauteclocque G, Zhu T, Johnson M, Austefjord H, Bitner-Gregersen E. 2020. Assessment of global wave datasets for long term response of ships. Proceedings of the International Conference on Offshore Mechanics and Arctic Engineering - OMAE (2A-2020 vols).

Hersbach H, de Rosnay P, Bell B, Schepers D, Simmons A, Soci C, Abdalla S, Alonso-Balmaseda M, Balsamo G, Bechtold P, et al. 2018. Operational global reanalysis: progress, future directions and synergies with NWP. (27).

Hogben N, Dacunha NMC, Oliver GF. 1986. *Global Wave Statistics*. Feltham: British Maritime Technology Ltd.

IACS. 2000. Rec. No. 34. Standard Wave Data (North Atlantic Scatter Diagramm).

IACS. 2021. UR S11 Longitudinal Strength Standard. 1–31.

Jensen JJ, Mansour AE, Olsen AS. 2004. Estimation of ship motions using closed-form expressions. *Ocean Engineering* 31(1): 61–85.

Katalinić M, Parunov J. 2020. Uncertainties of estimating extreme significantwave height for engineering applications depending on the approach and fitting technique-adriatic sea case study. *Journal of Marine Science and Engineering* 8(4).

Kumar VS, Joseph J, Amrutha MM, Jena BK, Sivakholundu KM, Dubhashi KK. 2018. Seasonal and interannual changes of significant wave height in shelf seas around India during 1998–2012 based on wave hindcast. *Ocean Engineering* 151(May 2016): 127–140.

Leder N, Smirčić A, Vilibić I. 1998. Extreme values of surface wave heights in the northern Adriatic. *Geofizika* 15: 1–13.

Mansour AE, Liu D. 2008. *Strength of ships and ocean structures*. Edited by JR Paulling. Jersey City, NJ, USA: Society of Naval Architects and Marine Engineers.

Mansour AE, Preston DB. 1995. Return periods and encounter probabilities. *Applied Ocean Research* 17(2): 127–136.

Michel RK, Osborne M. 2004. Oil Tankers. In Lamb T (ed), Ship Design and Construction, 29.1-- 29.41. New Jersey, USA: SNAM0E.

Mikulić A, Katalinić M, Ćorak M, Parunov J. 2021. The effect of spatial correlation of sea states on extreme wave loads of ships. *Ships and Offshore Structures* 0(0): 1–11.

Perrault DE. 2021. Probability of Sea Condition for Ship Strength, Stability, and Motion Studies. *Journal of Ship Research* 65(1): 1–14.

Sartini, L.; Cassola, F.; Besio G. 2015. Extreme waves seasonality analysis: An application in the Mediterranean Sea. *Journal of Geophysical Research: Oceans RESEARCH* 120: 6266–6288.

Virtanen P, Gommers R, Oliphant TE, Haberland M, Reddy T, Cournapeau D, Burovski E, Peterson P, Weckesser W, Bright J, et al. 2020. SciPy 1.0: Fundamental Algorithms for Scientific Computing in Python. *Nature*

Methods 17: 261–272.

World Meteorological Organization. 1998. *GUIDE TO WAVE ANALYSIS AND FORECASTING*, (2nd edition). Geneva, Switzerland: Secretariat of the World Meteorological Organization.

Appendix Histograms of extreme significant wave heights and fitted Gumbel distributions

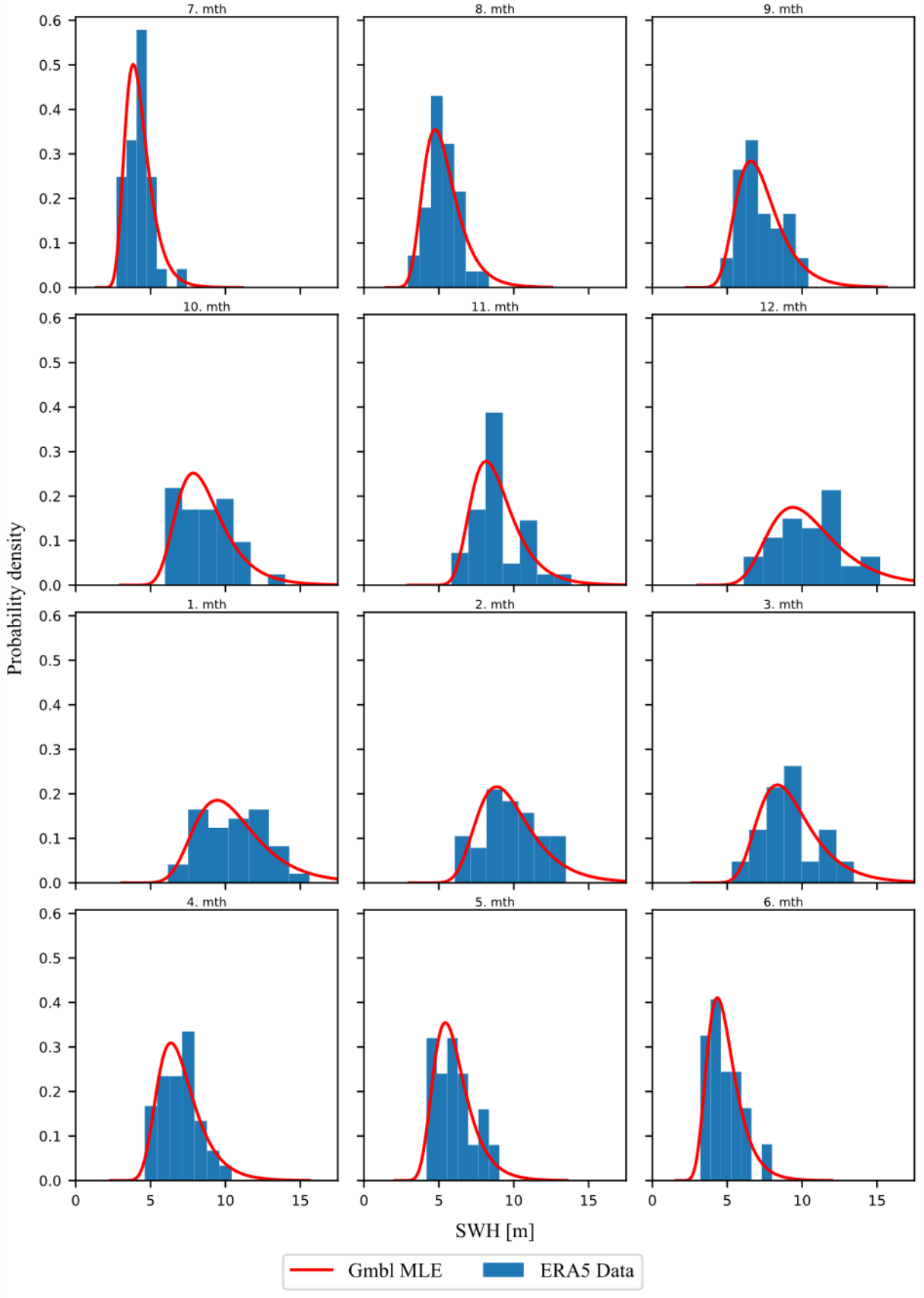

Fig. A1. Histogram of annual extremes for each month at location in the Northern North Atlantic.

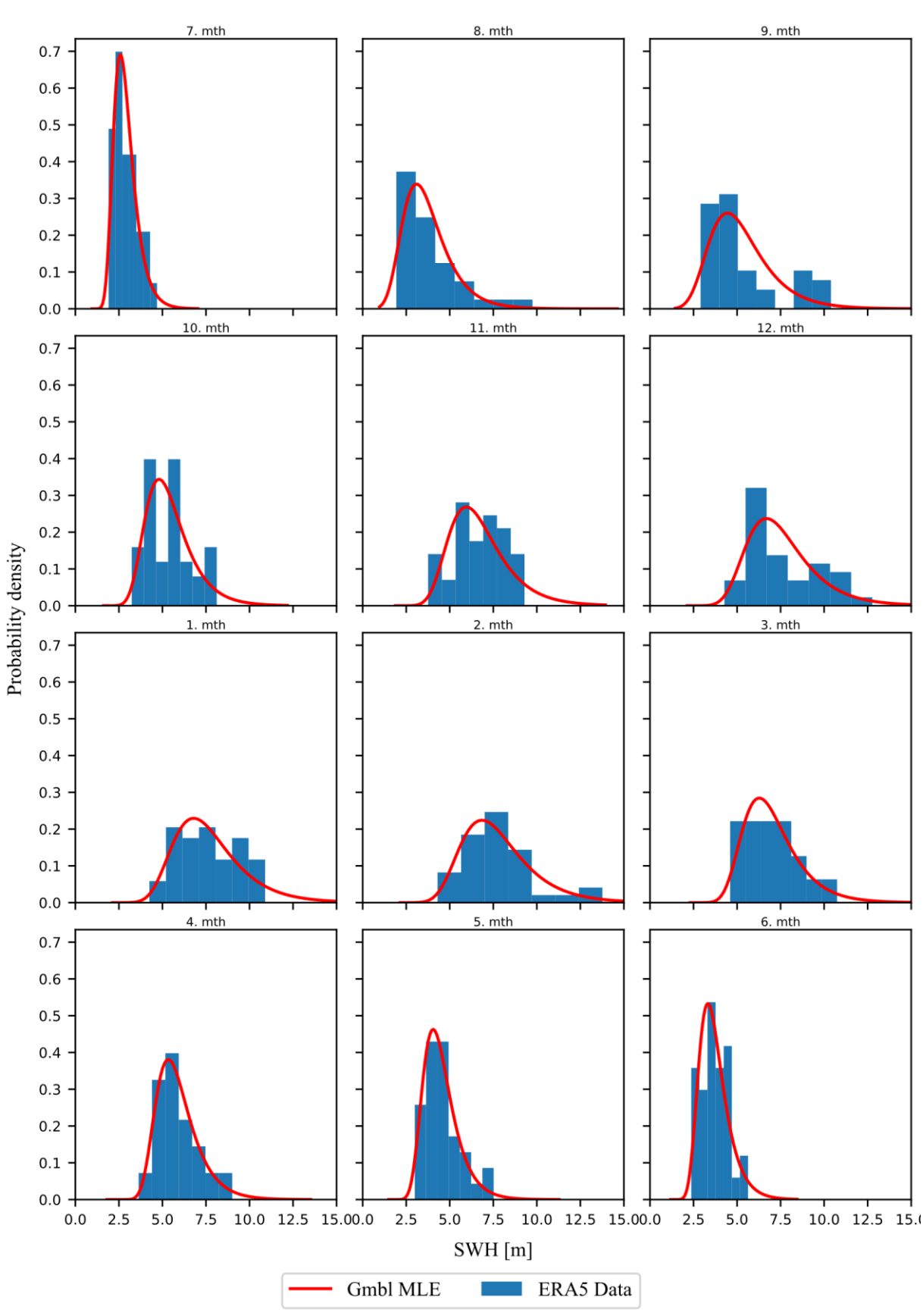

Fig. A2. Histogram of annual extremes for each month at location in the Southern North Atlantic.

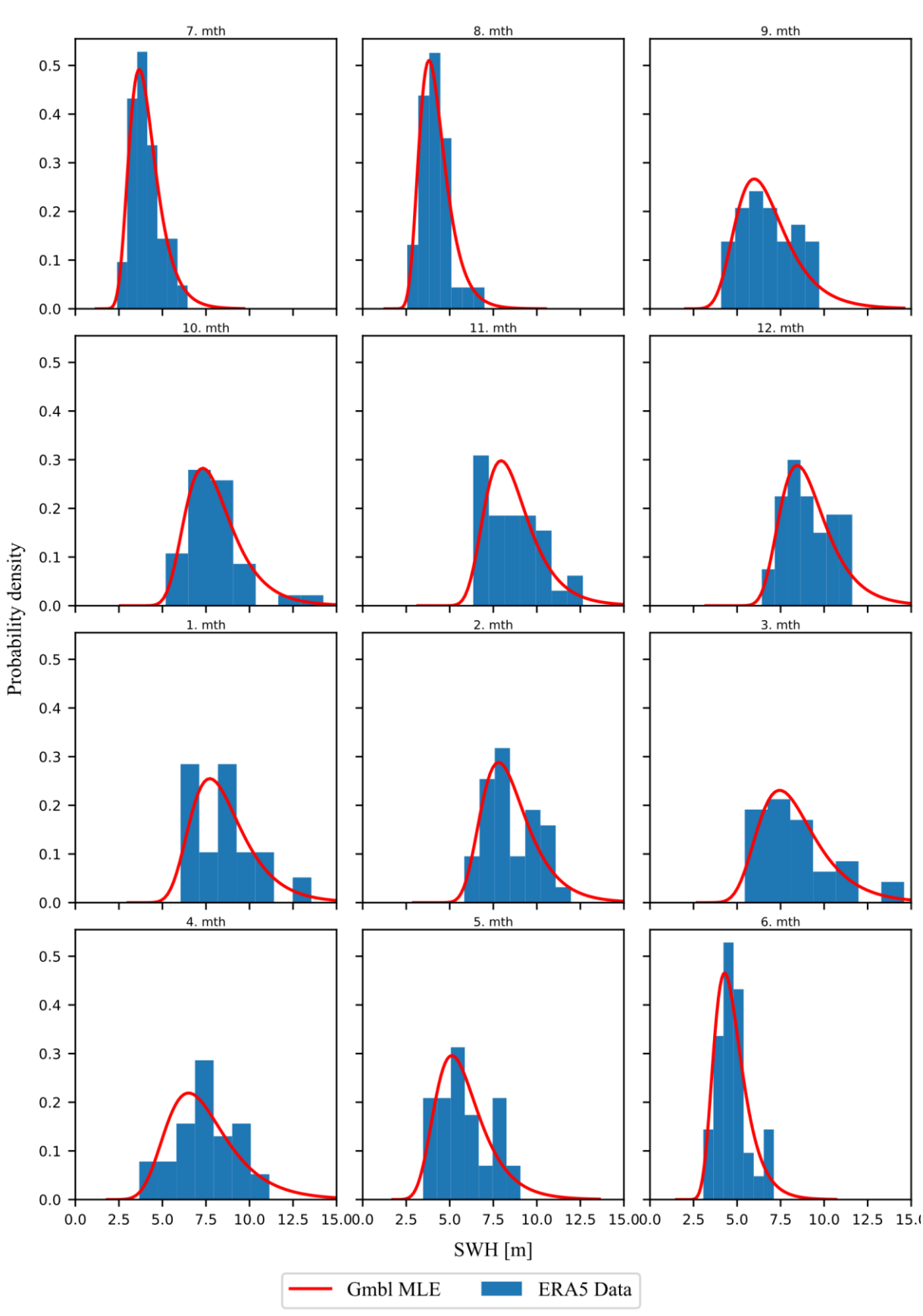

Fig. A3. Histogram of annual extremes for each month at location in the Northern North Pacific.

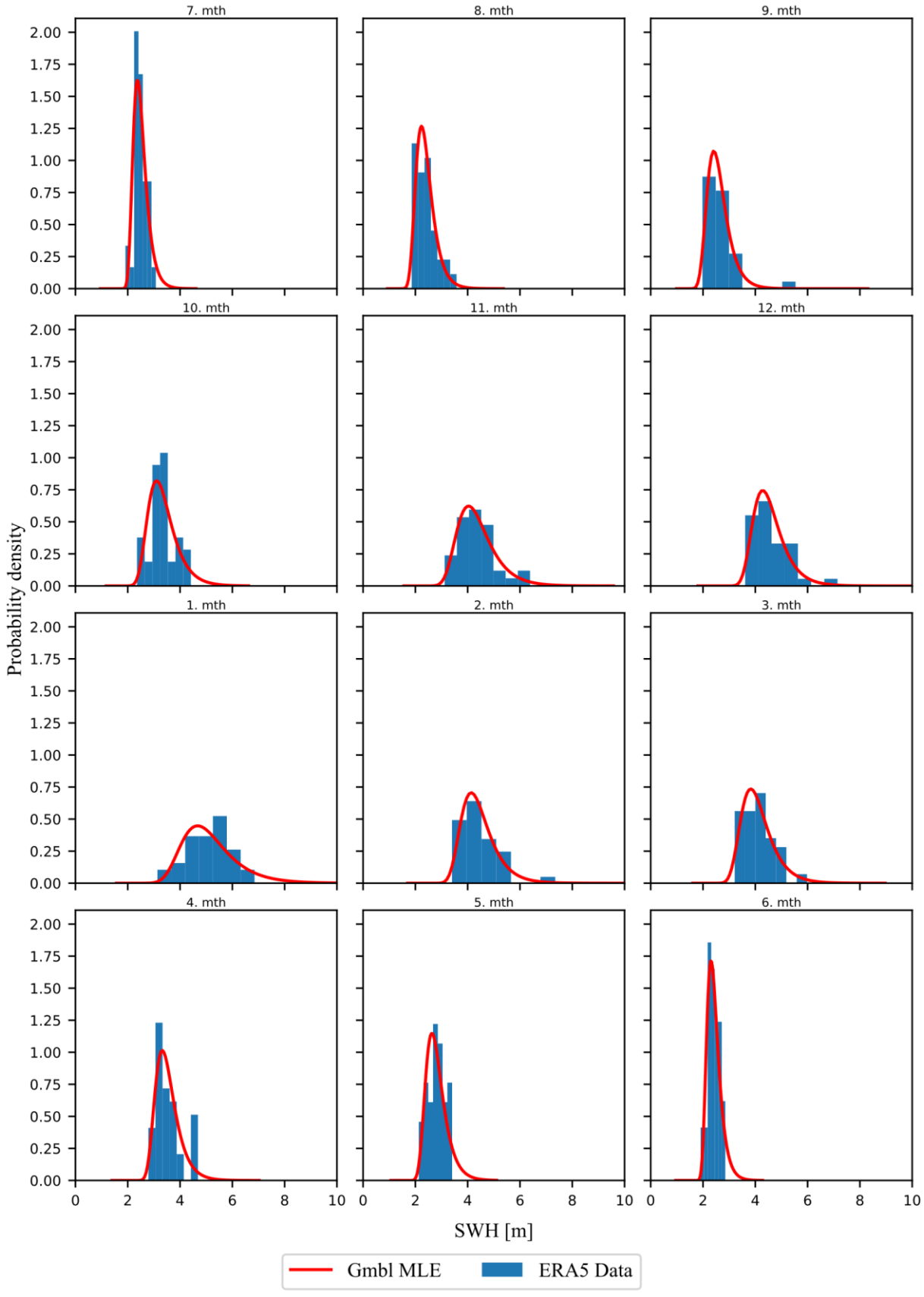

Fig. A4. Histogram of annual extremes for each month at location in the Southern North Pacific.

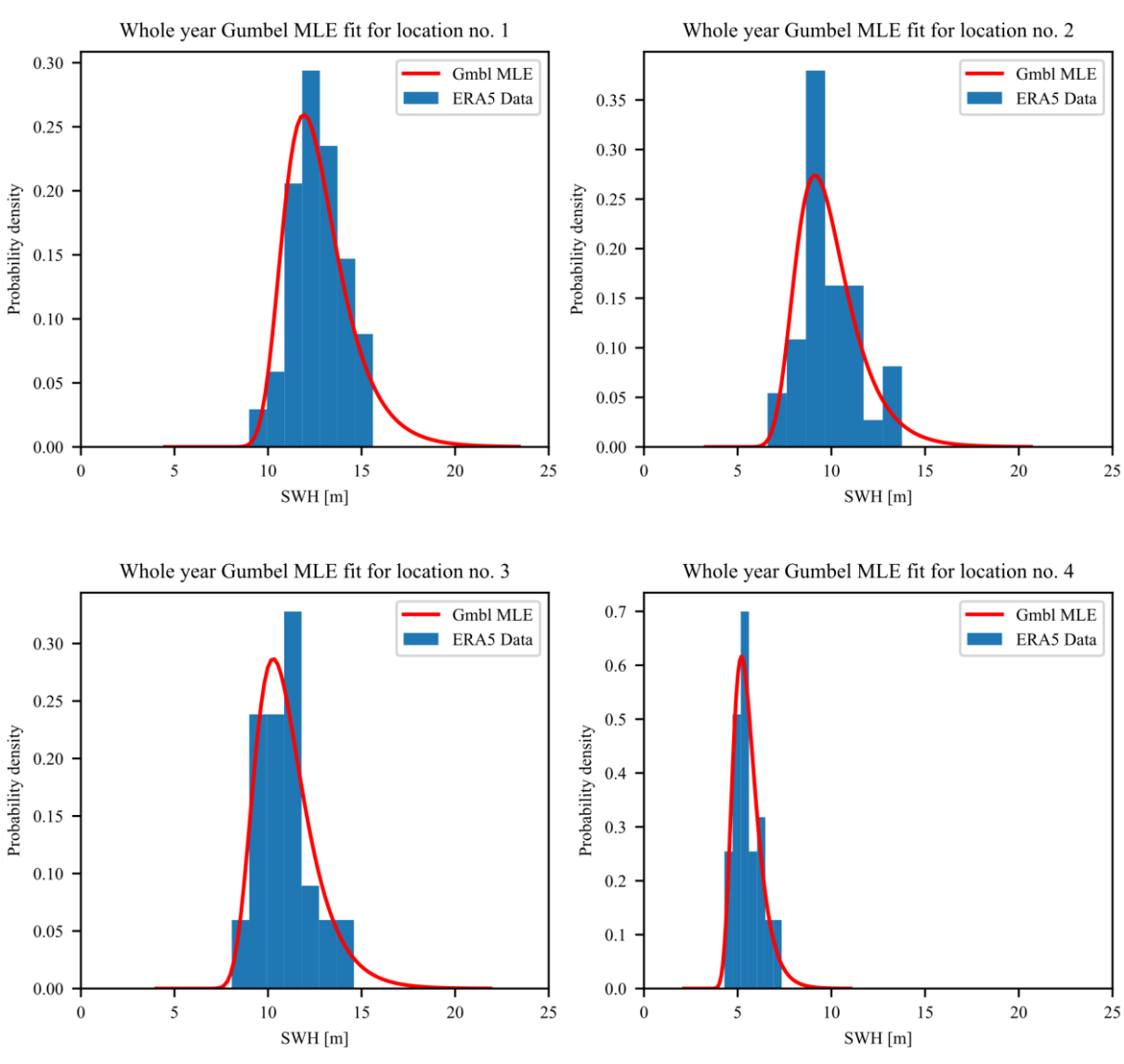

Fig. A5. Yearly annual extremes for all four locations.

Publication IV

Published journal article.

Journal of *Marine Science and Engineering*

MDPI

Article

A Wave Directionality and a Within-Year Wave Climate Variability Effects on the Long-Term Extreme Significant Wave Heights Prediction in the Adriatic Sea

Antonio Mikulić * and Joško Parunov *

Faculty of Mechanical Engineering and Naval Architecture, University of Zagreb, Ivana Lučića 5, 10000 Zagreb, Croatia

* Correspondence: antonio.mikulic@fsb.hr (A.M.); josko.parunov@fsb.hr (J.P.)

Abstract: The extreme significant wave height predictions often neglect within-year wave climate variability and wave directionality. Depending on a geographical region, local wind patterns and year climate variability could have an influence on the long-term prediction of waves. The Adriatic Sea having two dominant wind patterns of different characteristics, *Bura* and *Jugo*, is a great example for the case study. The 23-year hindcast wave data used in the presented study is extracted from the WorldWaves database. Based on wind and wave data, annual extreme significant wave heights generated by different wind patterns and for different months are fitted by Gumbel distribution using maximum likelihood estimation. Combined long-term extremes are then predicted by calculating system probability. It was found that considering the wave directionality, and especially the seasonality of wave climate, leads to a larger prediction of extreme significant wave heights. The extreme value prediction considering wave directionality on average yields 4% larger significant wave heights, while considering within-year climate variability leads to, on average, 8% larger extremes compared to the predictions when both effects are neglected.

Keywords: significant wave height; long-term probability; wind direction; wave directionality effects; seasonal variability effects; monthly maxima; directional maxima; annual maxima; Adriatic Sea

Citation: Mikulić, A.; Parunov, J. A Wave Directionality and a Within-Year Wave Climate Variability Effects on the Long-Term Extreme Significant Wave Heights Prediction in the Adriatic Sea. *J. Mar. Sci. Eng.* **2023**, *11*, 42. https://doi.org/10.3390/jmse11010042

Academic Editor: Achilleas Samaras

Received: 1 December 2022
Revised: 21 December 2022
Accepted: 22 December 2022
Published: 28 December 2022

1. Introduction

Throughout the years, significant wave height (SWH) has become the most important variable in engineering practices for the wave environment description. Prediction accuracy is important for performance and design optimization within many marine-related industries, such as shipbuilding, offshore, renewable energy, aquaculture, etc.

For the analysis of extreme wave loads, two methods are recommended by [1]. The design sea state method (DSSM) performs wave loads analysis on a selected short-term sea state condition called design sea state, while the all sea state method (ASSM) calculates the most probable extreme value considering the probability of occurrence of all sea states. The former method is usually used in the design of offshore structures, while the latter is recommended for the analysis of ship structures by the International Association of Classification Societies (IACS) [2].

A return period, also known as a recurrence interval, is often used to determine extreme sea states. In the case of marine structures, it is an average time or estimated average time between the occurrences of the extreme sea states. The theoretical return period between occurrences is the inverse of the average frequency of occurrence. Ships are designed considering a 25-year return period, which grows to 100 for offshore structures, while for some coastal defense systems like dams, it starts from 1000 years and above.

The main aim of the present study is to define extreme SWHs that may be used in the context of DSSM. Traditionally, these extreme values are determined by using annual extreme values without considering within-year variability or wave directionality.

Therefore, the research investigates using maxima for each month or each wave prevailing direction to estimate long-term extreme SWHs instead of using only annual maxima (AM). As the creation of surface waves in the Adriatic is predominantly influenced by two winds of completely different characteristics [3], it is useful to investigate the seasonality and directionality effect on long-term predictions.

A within-year wave climate variability was first questioned in [4], demonstrating theoretical proof that long-term extreme values estimated, neglecting seasonality of the wave climate, introduce unconservative bias. Using the approach proposed by Carter and Challenor (C–C) in [4] to account for monthly variability, extreme SWHs in the northern Adriatic is examined in [5]. The study shows that neglecting seasonality effects leads to smaller extreme SWH values for a given return period. The main drawback of these analyses is that they were performed based on the dataset where many of the monthly extremes were missing. Complete datasets containing many years of uninterrupted wave measurements are required to obtain a reliable prediction of long-term extremes.

The effect of within-year wave climate variability on the design of ship structures is examined in [6]. Consequences of the extreme vertical wave bending moment (VWBM) are explored along frequent shipping routes in the Atlantic and Pacific Oceans and compared to IACS rules. Neglecting within-year wave climate variability could lead to the underestimation of long-term extreme SWHs and VWBMs by up to 10%.

The pioneering research of wave statistics in the Adriatic region was performed by Tabain in [7] and later revised and updated in [8], developing the most commonly used Tabain's wave spectrum. Tabain's spectrum is a single-parameter modification of the JONSWAP spectrum based on the limited number of wave measurements and observations from merchant and meteorological ships.

A collection of wave data from visual observation across the Adriatic is collected inside the *Atlas of Climatology of the Adriatic Sea* [9] published by the Republic of Croatia Hydrographic Institute. The data obtained by observations from the merchant and meteorological ships from 1949–1970 is presented in the form of wave roses. Around 15 years of wave observations from [9] are fitted using the three-parameter Weibull distribution in [10] to develop extreme wave statistics. However, the data from [9] suffers from uncertainties due to the lack of extremes caused by heavy weather avoidance and visual wave observation inaccuracies. The term visual wave observation refers to observations taken by trained officers from voluntary observing ships (VOS) and should not be confused with highly accurate optical measurements, like stereo cameras from fixed offshore installations [11]. There is a general concern that VOS wave data are less reliable than in-situ and remotely sensed wave measurements because of their low accuracy and insufficient sampling [12] (Gulev, 2003).

Except for visual observations, wave data are obtained by measurements from fixed wave buoys, radars, lasers, stereo cameras, etc. [13]. Wave buoys and oceanographic towers are considered reference measurement sources regarding accuracy. For application on ship structures, however, they have drawbacks as they are located outside main shipping routes and quite often appear to be out of service for an extended period. A rare example of uninterrupted long-term wave measurements from a fixed oceanographic tower is Acqua Alta in the North Adriatic Sea [14]. Within the RON project (The Italian Data Buoy Network), four wave buoys along the western Adriatic coast off the cities of Monopoli, Ortona, Ancona, and Venezia, were operational during the period between 2009 and 2014, with occasional breaks due to failure or service intervals [15].

The extreme SWHs are usually evaluated using wave statistical data accumulated on an annual basis incorporating all directions, thus neglecting within-year (also called intra-annual) wave climate variability and directionality effects. Until long-term, high-quality hindcast wave databases became available, the number of observations had been insufficient to confidently fit the theoretical probability distribution to monthly or directional maxima, namely for the ship design, since the visual observations were the main data source suffering from a lack of quality and consistency. Currently, several long-term

hindcast wave databases are available for the Adriatic, such as ERA5, the fifth generation ECMWF (The European Centre for Medium-Range Weather Forecasts) reanalysis, or the WorldWaves atlas (WWA) developed by Fugro Oceanor.

Comparative analysis of wave data from different formerly described sources (Acqua Alta, RON, ERA5, and WWA) is performed in [16] for the location in the North Adriatic, close to Venice, where long-term databases are available. Different data sources provide similar time series trends of SWHs and storm predictions, but the extreme values have larger discrepancies. Rather large uncertainties of wave data sources have the greatest consequences on fatigue life prediction. Since the WWA database is found to be conservative, it is recommended for practical engineering applications in deep water compared to ERA5, while for the near-shore region, it is recommended to use models accounting for wave–current interaction and shallow water effects.

Wave statistics based on WWA are developed by [17] for one location in the middle of the Adriatic Sea. The model includes three-parametric Weibull distribution as the marginal distribution of SWH and the log-normal distribution as the conditional distribution of peak wave periods, while the relation between wind speed and wave height is established by regression analysis. The analysis is further extended in [18] to all 39 grid points in the Adriatic basin while replacing the regression analysis with a conditional distribution of wind speed. The same WWA database was also used for the operability analysis of a passenger ship sailing through the Adriatic [19] and for the assessment of wind and wave energy potential in the Adriatic [20].

There are many works discussing the evolution of wave motion in the Adriatic Sea with deterministic models. Benetazzo et al. [21] studied expected changes in wind and wave severity for the period 2070–2099. The wind field computed by a high-resolution regional climate model (RCM) is used to force the SWAN spectral wave model. The performed statistical analysis is compared to the simulation results for 1965–1994. Although increases in the wave severity were found locally, a milder future wave climate in the Adriatic was predicted compared to the present climate. A similar conclusion was drawn by [22], running the high-resolution RCM over the Adriatic Sea. Future projections generally confirmed the tendency to a decreasing energy trend, with more extreme events in the northern part of the Adriatic. The important practical aspect was the identification of potential storms, allowing researchers to focus on extreme events and avoiding the need to run entire climatological wave simulations. Deterministic wave simulations, based on climate models, could represent the future trend in the design and analysis of marine structures. However, these models are still not recognized and included in the procedures for the computation of extreme wave and wind loads on marine structures by relevant institutions and classification societies. Probabilistic predictions based on past measurements are still the recommended procedure [1]. Therefore, the focus of the present study is on a probabilistic rather than a deterministic model.

The motivation for the study was born because almost all previous analyses for the Adriatic considered the AM method, thus neglecting directional and seasonal effects. Only the study by Leder et al. [5] quantified the seasonality effect on long-term SWHs prediction. However, the analysis was performed based on the fragmented dataset where more than a third of the monthly extremes were missing and had to be estimated from the wind data using quadratic regression. The surface wave creation in the Adriatic, however, is predominantly influenced by two winds of completely different characteristics [3]. Therefore, it would be very useful to question the directionality effect on long-term predictions.

The aim of the presented research is to develop and compare statistics of the extreme significant wave height in the Adriatic region obtained by considering wind patterns, within-year climate variability and neglecting both. Yearly maxima are extracted for each direction and month, and extreme value distributions are fitted. System probability, i.e., the C–C method, is applied to determine combined extreme significant wave heights. Obtained extreme values are then compared to the ones calculated by neglecting both effects. The calculations are done for the whole Adriatic Sea.

The research is described and presented through five sections and an Appendices A and B. After the Introduction, Section 2 first describes the case study, available dataset, landscape, and climate of the Adriatic region. The second subsection of Section 2 describes the methodology used for the computation of extreme values. The underlined results are presented in Section 3, while the remainder is provided in the Appendices A and B. The fourth section is reserved for a discussion, followed by conclusions and future steps.

2. The Case Study and Methodology

2.1. The Adriatic Sea

2.1.1. Characteristics of Wind and Wave Climate

With an average width of around 200 km, winds in the Adriatic are limited by fetch. The creation of surface waves in the Adriatic is dominated by two winds of completely different characteristics. The north-eastern wind *Bura* and south-eastern *Jugo*, thus, also creating consequently different waves. Although the strongest winds blow from the north-east, having shorter fetch results in the wave spectrums is typical for partially developed sea states. The longest fetch is obviously along the basin, corresponding with southeast winds yielding the highest recorded wave heights of 10.87 m. More than 1000 islands along the east coast shelter the wave influence in that near-shore region, while relatively small sea depths are present in the northern part of the basin and could influence the wave characteristics. The bathymetric map of the Adriatic Sea is shown in Figure 1.

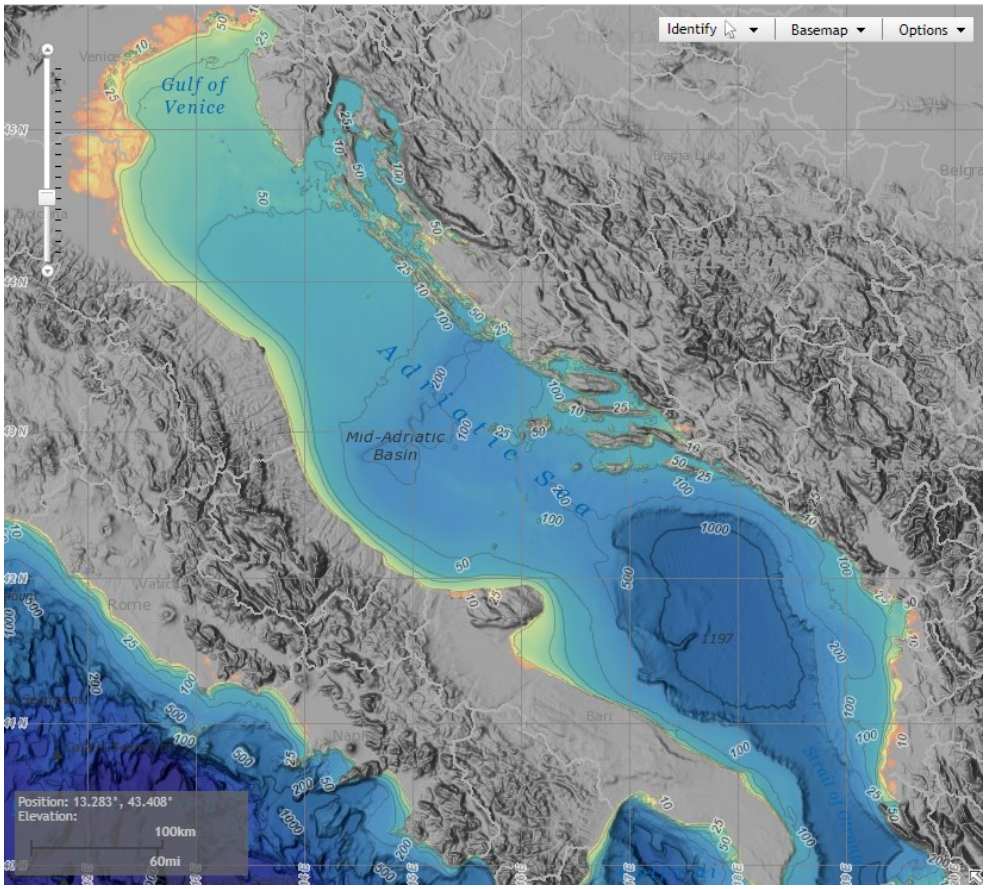

Figure 1. The Adriatic Sea is located in the central-north part of the Mediterranean Sea. Surrounded by the mountain ranges Apennine in the west and Dinaric in the east, the basin stretches for more than 800 km from the shallower northwest to the deeper southeast, where the Strait of Otranto connects with the rest of the Mediterranean Sea. Depth contours or isobaths outline basin bathymetry offering an insight into seafloor terrain—source: https://maps.ngdc.noaa.gov/viewers/bathymetry/ (accessed on 30 November 2022).

Jugo (E–SE to SS–E, Italian sirocco) is a strong and warm southeast wind that comes with a lot of rain. Blowing through the whole year, it is more common in the south of the Adriatic, which is characterized by strong winds and rough seas. *Jugo* reaches its peak strength after two to three days of persistent blowing and usually lasts days. Sometimes, however, especially during the winter season, it can last up to a week.

A very cold, dry wind *Bura* (N–NE to E–NE, Italian bora) blows from the northeast over the coastal Dinaric Mountains slopes. Characterized by violent gusts, it brings accelerating cold air that meets the seawater with great force, spreading it in the shape of a fan. With powerful blows and rapid changes of direction, *Bura* generates short but very high waves with a lot of foam and spray [3].

Lebić is a south-western wind blowing mostly during the winter and usually announced by above-average tides. Although short in duration, it can generate rough waves while also carrying abundant rainfall. *Maestral* is a constant, humid, and mostly thermal summer wind blowing from the northwest. As a regular wind of moderate strength, it is very convenient for sailing. The main wind patterns in the Adriatic Sea are presented on the lower left part of the map in Figure 2.

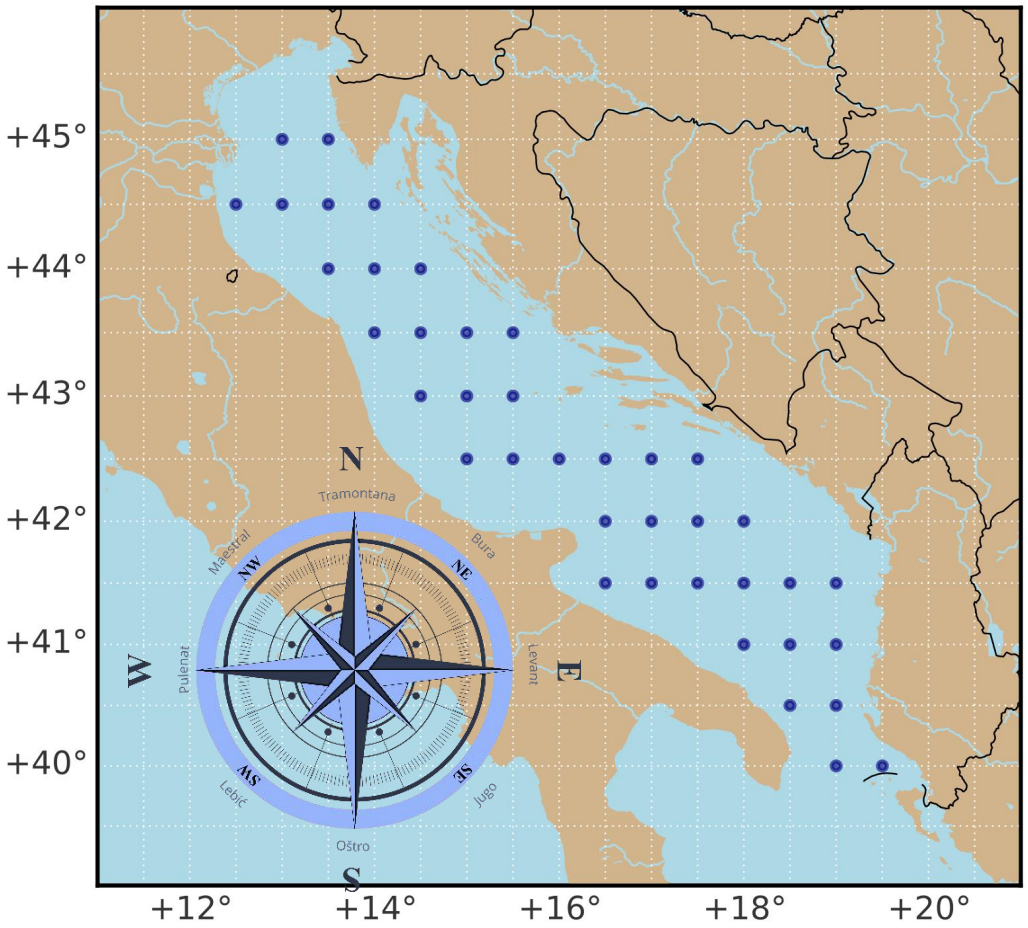

Figure 2. The Adriatic Sea map. The offshore grid of 39 blue dots denotes available locations for wave data extraction from the WWA database. Lat-lon grid resolution is 0.5 degrees. Almost all defined points are at the same time calibration points close to the satellite tracks. The wind rose is presented in the lower-left corner of the map.

The surface wave creation in the Adriatic is dominated by *Bura* and *Jugo*, having entirely distinct characteristics and creating different waves. Wave statistics in Adriatic are thus far mostly developed regardless of the wind pattern. Hence, the paper attempts to provide more detailed insights in that regard.

2.1.2. Wave Data

The study is conducted based on data extracted from the World Wave atlas (WWA). The WWA is the collective name for a series of comprehensive high-resolution atlases developed by Fugro Oceanor, providing wind and wave climate statistics/data for any region worldwide. The data derived from the European Centre for Medium-Range Weather Forecasts (ECMWF) wave models are calibrated by Fugro Oceanor against satellite altimetry measurements gathered from eight different satellite missions: Geosat (1986–1989), Topex (1992–2002), Topex/Poseidon (2002–2005), Jason (2002–2008), Geosat Follow-On (2000–2008), EnviSat (2002–2010), Jason-1s (2009–2012), and Jason-2 (2008–on-going). The WWA database for the Adriatic covers a period of 23 years from 1997 until 2020 in 6 h intervals giving a total of 33,600 records per parameter at each location. Data are available at a lat-lon grid resolution of 0.5 degrees creating the offshore grid of 39 points across the Adriatic, as shown in Figure 2. Available data include wind speed and direction, integral spectral wave parameters (e.g., significant wave height, peak spectral period, mean wave period), and wave direction for wind waves and swell, considered separately and combined, offering, in total, 12 wind and wave parameters.

The WWA model data are calibrated against the long-term satellite data in order to provide bias-free homogeneous long-term model data of the highest quality. Thus, representing a state-of-the-art comprehensive and systematic source of wave data as input to coastal models and studies for the Adriatic region.

2.2. Methodology

For each location where data is available, the procedure runs as presented in the flow chart in Figure 3. The procedure is performed separately for wave directionality and intra-annual variability. The basic steps of the analysis are:

1. Extracting empirical extreme values from the database;
2. Fitting theoretical extreme value distribution to the empirical data;
3. Combining individual distributions in the system probability distribution;
4. Calculating a long-term extreme value from the system probability distribution.

Each step is described in more detail below.

A time series of SWH data and mean wave direction (MWD) is extracted from the WWA database serving as model input. Through filtering and sorting, two separate subsets of SWH maxima are extracted from 23 years of data. The seasonality is studied through 12 months, while for directionality, 4 main directions are chosen as follows:

1. *Bura*—mean direction 45°, N–E;
2. *Jugo*—mean direction 135°, S–E;
3. *Lebić*—mean direction 225°, S–W;
4. *Maestral*—mean direction 315°, N–W.

For the seasonality study, monthly maxima (MM) are extracted for every year available, resulting in a subset of 12 records of MM easily visualized as a matrix containing 23 rows (years) and 12 columns (months), named MM23 $\times$ 12. Similarly, directional maxima (DM) are extracted, resulting in a subset of size 23 $\times$ 4 (4 directions) named DM23 $\times$ 4. The AM are easily obtained using any of these 2 datasets and extracting a maximum value for a given year, i.e., getting a maximum value of a row. The year is defined as the period from summer to summer, starting 1st July, not the calendar year, as recommended in [1].

The maximum SWHs are described using type-I generalized extreme value distribution, also known as Gumbel distribution. The probability density function (PDF) (1) and cumulative distribution (2) are defined as (DNV, 2017):

$$f_{H_s}(x) = \frac{1}{B} e^{-((\frac{x-A}{B}) + e^{-(\frac{x-A}{B})})} \quad (1)$$

$$F_{H_s}(x) = e^{-e^{-(\frac{x-A}{B})}} \quad (2)$$

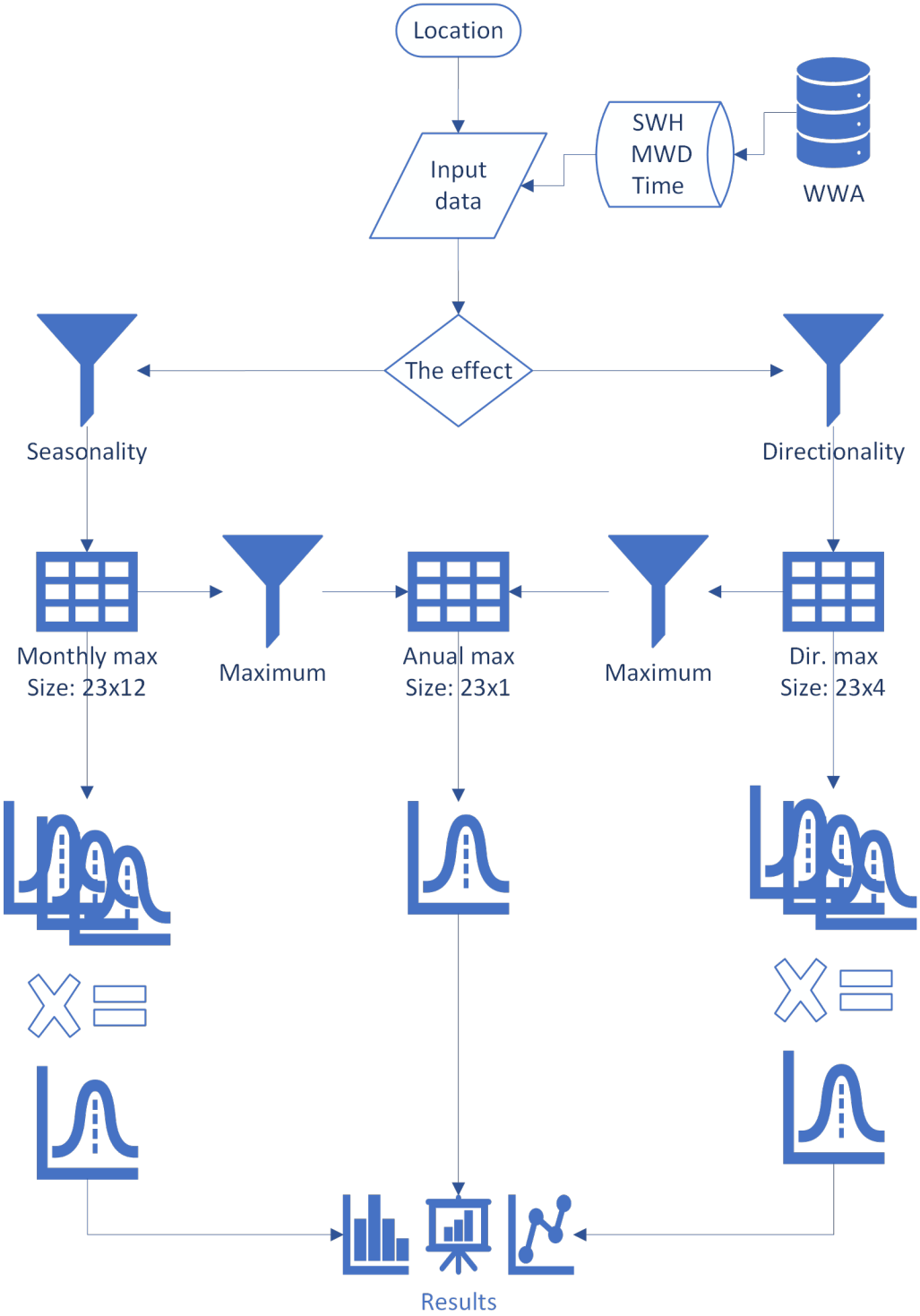

Figure 3. The flow chart of the presented approach.

Parameter A, although called the location parameter, in this context represents the most probable extreme SWH, and B is the scale parameter. Gumbel PDF is fitted to 12 records of MM, 4 records of DM, and AM. Fitting of Gumbel distribution is performed by the maximum likelihood method (MLE), utilizing the scipy.stats package in Python [23]. From individual distributions of directional or monthly maxima, combined 'annual maxima' is calculated by the C–C method, using Equation (3) [4].

$$P_{H_s}(X < x) = \prod_{i=1}^{N} F_i(x) \quad (3)$$

The C–C method assumes cumulative distributions $F_i(x)$ to be independent, while N represents the total number of months or directions. For the prediction of long-term extremes, the return period $T(x)$ is defined as the mean period (in years) between the occurrence of two values equal to or higher than x. For different return periods $T(x)$, the probability is calculated, and corresponding return SWHs are easily obtained from the CDFs defined in Equations (2) and (3). Unless distributions of directional or monthly extremes are identical, the resulting distribution from Equation (3) is not Gumbel distribution. Thus, results must be calculated numerically. Obtained values are then compared, and the results are presented in the next section.

3. Results

The extreme SWHs summarized in Figures 4 and 5 are calculated for the return periods of 25 and 100 years, respectively, at 39 locations across the Adriatic. The dashed lines on the upper graph represent the extreme value resulting from the system probability approach (C–C method, Equation (3)). The blue dashed line accounts for different directions combining probability distributions of DM, while the orange dashed line combines probability distributions of MM. The red line displays results from the conventional method using AM, neglecting both effects. Lower graphs on both figures highlight deviations of C–C using DM and MM from the AM. Locations on the left side of the graphs in Figures 4 and 5 correspond to the southern part of the Adriatic Sea, moving to the locations in the northern Adriatic as we move to the right side of the graphs. The exact position of locations could be easily identified using the map presented in Figure 2.

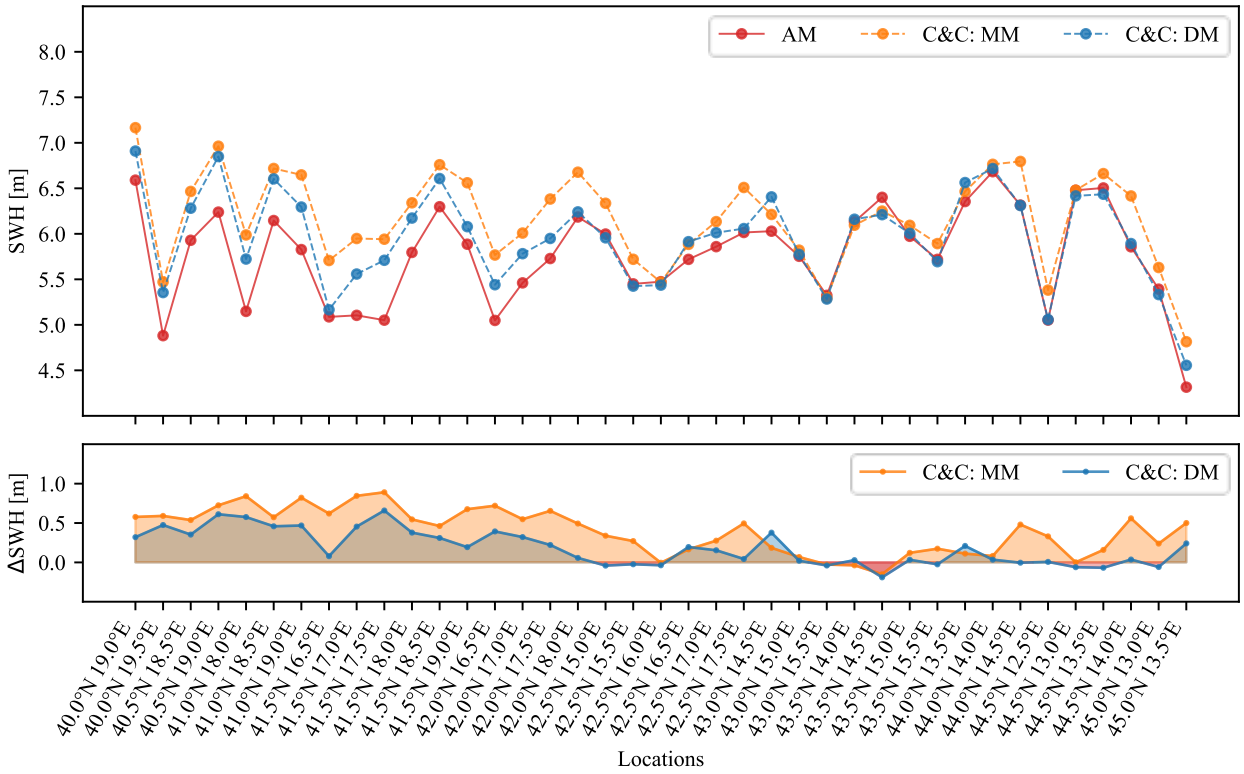

Figure 4. The extreme SWHs for the return period of 25 years. The blue dashed line represents long-term predictions calculated using system probability distribution obtained by the C–C method combining probability distributions of DM. The orange dashed line combines distributions of MM. The red line represents the conventional method using AM, neglecting both effects. Moving from left to right on the horizontal axis corresponds to moving across locations from southeast to northwest. The lower graph displays the differences between the given C–C and the AM approach.

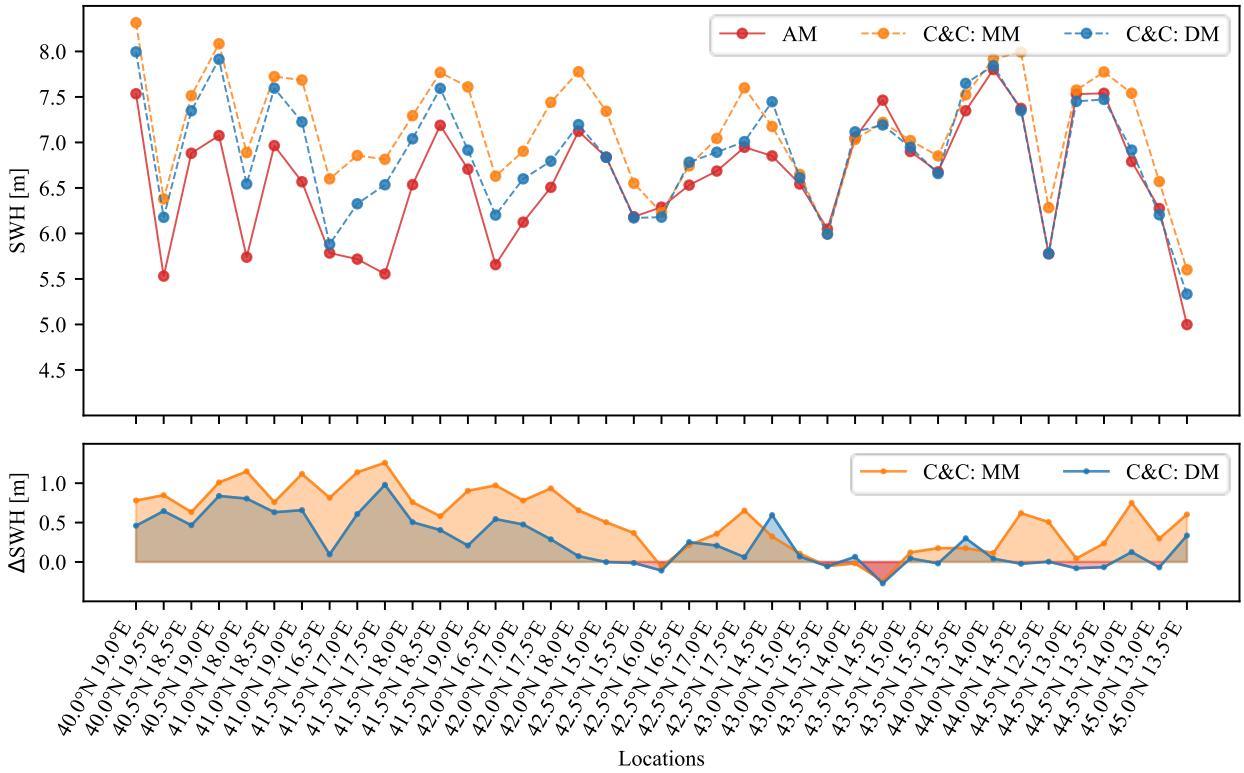

Figure 5. The extreme SWHs for the return period of 100 years. The blue dashed line represents long-term predictions calculated using system probability distribution obtained by the C–C method combining probability distributions of DM. The orange dashed line combines distributions of MM. The red line represents the conventional method using AM, neglecting both effects. Moving from left to right on the horizontal axis corresponds to moving across locations from southeast to northwest. The lower graph displays the differences between the given C–C and the AM approach.

Relations between extreme values from C–C and AM are qualitatively similar for both months and directions. Throughout locations, C–C MM produces the most conservative results for almost all locations, with few exceptions where it is equal to or slightly exceeded by the other two. These exceptions occur in the middle part of the Adriatic, where the wave climate is the mildest. The C–C DM produces evidently smaller differences, offering predictions close to AM for almost half of the studied locations. Extending the return period from 25 to 100 years only amplifies differences while trends remain unchanged. For both return periods, southern locations observe higher differences, yielding the highest values for 41.5° N 17.5° E. The lowest deviations are displayed for locations in the middle Adriatic (43.0° N 15.5° E), whereas for some locations, C–C MM and DM predict SWHs even lower than the standard AM approach. Several locations are found in the northern Adriatic where *Bura* has the highest influence yielding results equal to or higher than the AM, from which location 44.0° N 13.5° E is further analyzed.

Detailed results of the three locations mentioned in the previous paragraph are displayed in Figures 6 and 7. Directional effects are exhibited in Figure 6a, plotting the extreme SWHs at different return periods for each direction, C–C, and AM approach. Dispersion of the DM is described in Figure 6b using box plots, where white circles represent the AM that occurred in each direction. Similarly, the within-year climate variability effects are examined in Figure 7. The predicted extreme SWHs at different return periods are compared between individual months, C–C, and the AM approach. Box plots are based on MM, and the white circles herein represent the AM that occurred each month.

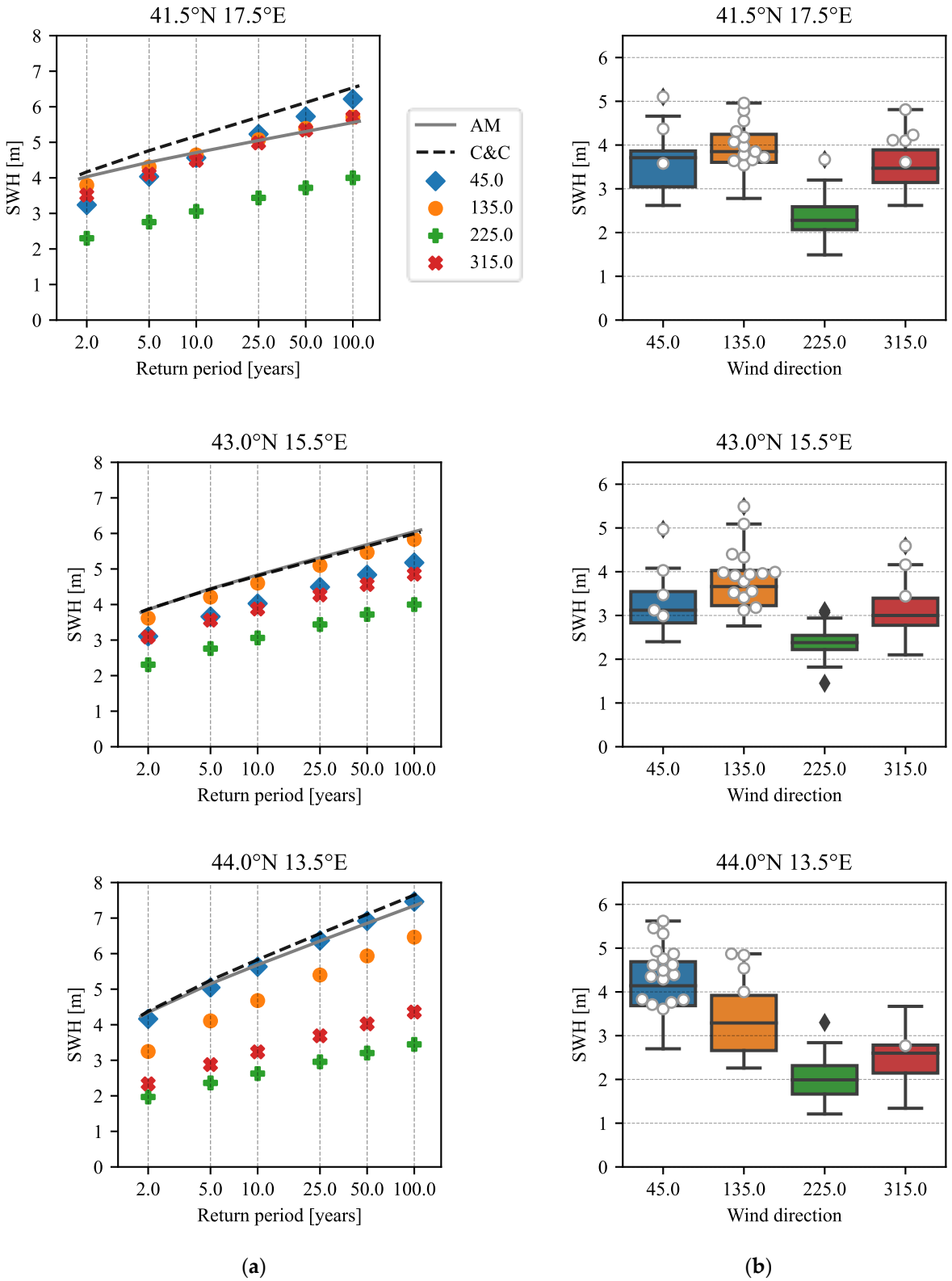

Figure 6. Directionality effect for three characteristic locations: (**a**) The extreme SWHs calculated based on different return periods. Markers represent results from individual directions, while the dashed black line displays values obtained by the C–C approach combining DM; (**b**) Box plot describing the dispersion of maxima that occurred in a given direction. White circles highlight the values that are also the annual maxima that occurred in a given direction.

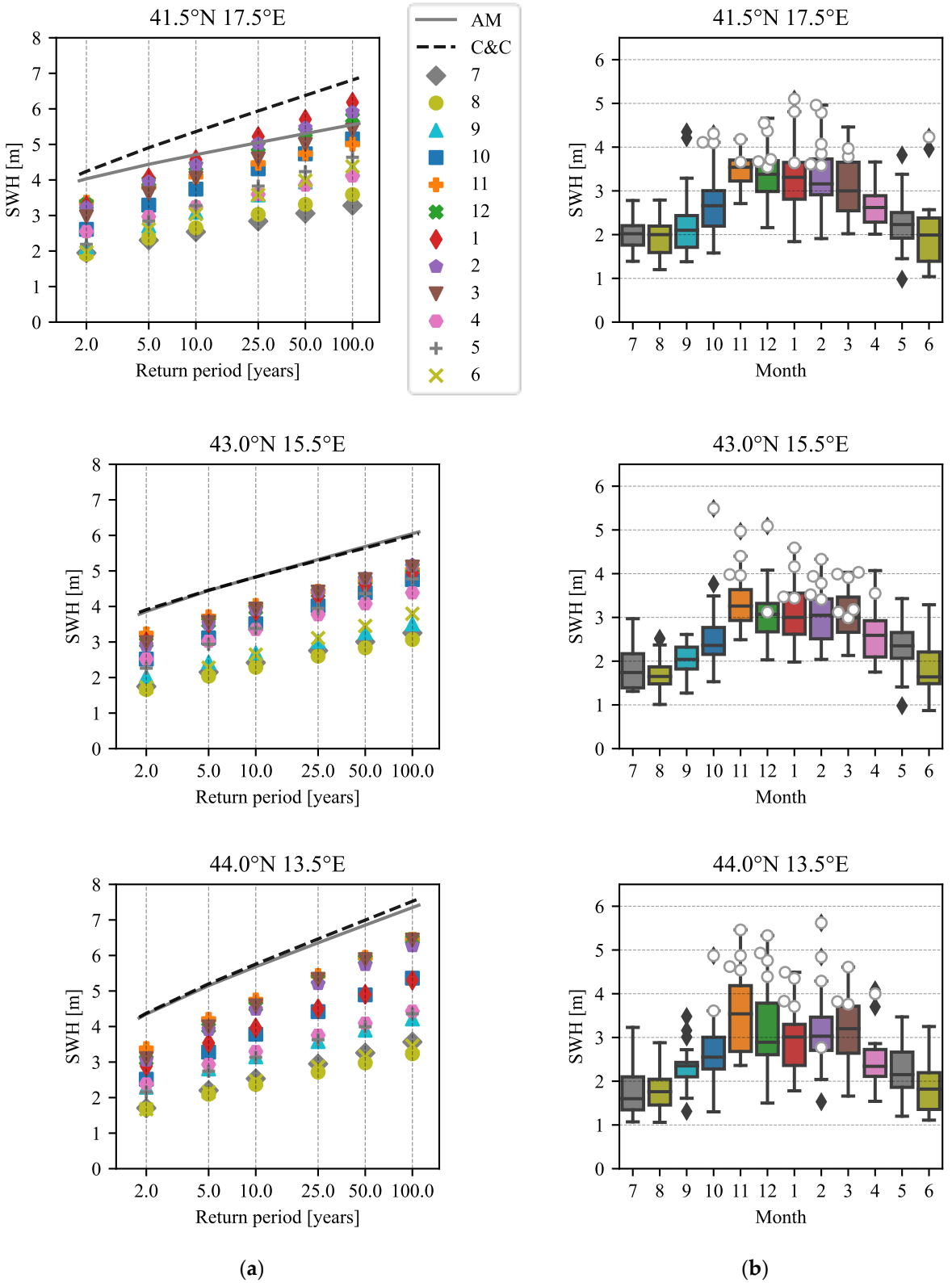

Figure 7. Seasonality (Within-year climate variability) effect for three characteristic locations: (**a**) The extreme SWHs calculated based on different return periods. Markers represent results from individual months, while the dashed gray line displays values obtained by the C–C approach combining MM; (**b**) Box plot describing the dispersion of maxima that occurred in a given month. White circles highlight the values that are also the annual maxima that occurred in a given month.

Directionality effects across the Adriatic Sea are also examined in Figure 8, revealing the distribution of the number of yearly maxima across four studied directions. Analysis suggests domination of *Bura* waves in the north and along the west coast of the Adriatic, while *Jugo* dominates the remaining locations across the basin. In the southernmost locations, close to the Strait of Otranto, there is a strong influence of the Ionian Seas, causing a mixture of different wind and wave systems. Consequently, in those locations, it could be that extreme waves are not predominantly influenced by *Jugo* or *Bura*.

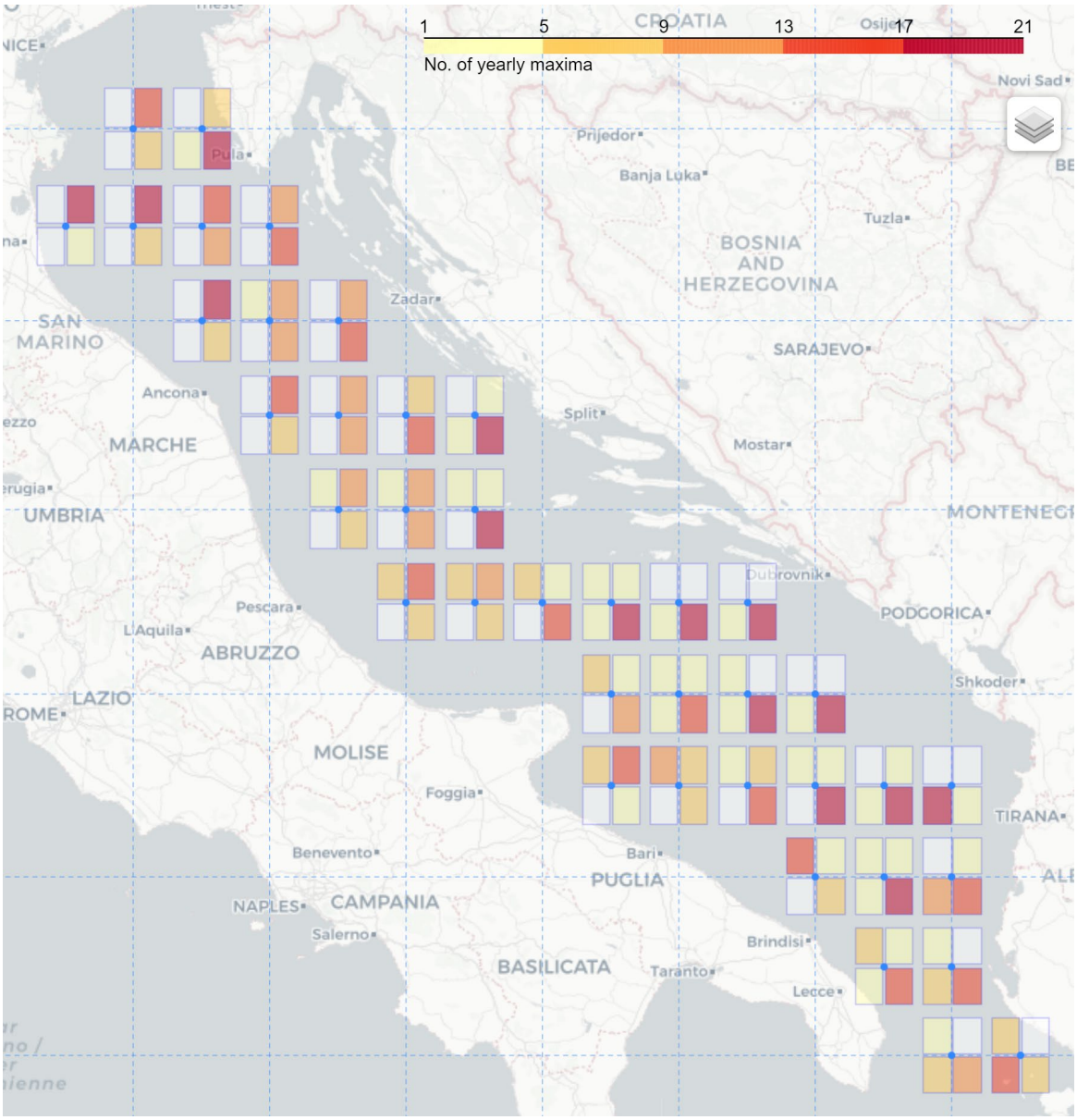

Figure 8. Distribution of yearly maxima from four main quadrants across the Adriatic Sea. Each location is represented by a blue dot and four quadrants suggesting the direction of the waves. The color scale presented in the upper left corner indicates the number of yearly maxima that occurred in a direction.

4. Discussion

Results presented in Figure 8 are direct consequences of the wind and terrain properties, as the Adriatic is encompassed by the Apennines to the West, the Alps to the north, and the Dinarides to the East. *Jugo*, being a strong wind with the longest fetch, expectedly generates the highest waves through the Adriatic basin. Waves generated by *Bura* prevail

in the north, alongside the western coast, where it had some time and length to develop some rough seas. Although having longer fetch, *Maestral*, due to moderate power and short duration, evidently cannot produce any significant influence except in a few locations in the southwest. *Lebić*, as a wind of short duration, while also having a shorter fetch, can hardly produce waves higher than the previous three winds. Therefore, only a few locations in the south, already outside the Adriatic Sea, are observing higher impact from that direction due to influence from the rest of the Mediterranean.

Blowing through the whole year, it is more common in the south of the Adriatic, which is characterized by strong winds and rough seas. *Jugo* reaches its peak strength after two to three days of persistent blowing and usually lasts up to days. Sometimes, however, especially during the winter season, it can last up to a week.

A very cold, dry wind *Bura* (N–NE to E–NE, Italian bora) blows from the northeast over the coastal Dinaric Mountain slopes. Characterized by violent gusts, it brings accelerating cold air that meets the seawater with great force, spreading it in the shape of a fan. With powerful blows and rapid changes of direction, *Bura* generates short but very high waves with a lot of foam and spray [3].

In the uppermost graph in Figure 6, for location 41.5° N 17.5° E, there are at least three wind systems influencing extreme values of significant wave heights, i.e., *Bura*, *Jugo*, and *maestral*. As seen in the uppermost Figure 6a, for return periods of 25 years and higher, predictions from three directions overshoot AM predictions, therefore, confirming a high difference in the C–C approach. As seen from Figures 5 and 6, these relatively large differences between the AM and C–C methods are characteristic of the southern locations close to the Strait of Otranto.

A large overestimation of the C–C method compared to the AM for location 41.5° N 17.5° E is also evident for MM in the uppermost Figure 7a. Comparably, December, January, and February overshoot the AM approach for the same return periods, while AM are almost evenly distributed from October–March. It is interesting to observe in the uppermost right graph in Figure 7 that some extreme events occur outside the October–March season, which is characteristic of *maestral*. This spread of extreme event occurrence throughout the year is the likely reason for differences between the C–C and AM method.

Location 43.0° N 15.5° E (middle graphs in Figures 6 and 7) in the middle Adriatic displays slightly less scattered values between distributions of both DM and MM. Namely, for a DM, *Jugo* is clearly a predominant wind pattern, regarding both the number of extremes and their values. Therefore, no difference between the AM and the C–C methods is observed. However, the explicit dominance regarding the number of extremes or their values is not displayed by any particular month. Only a somewhat lower dispersion between monthly predictions of the three analyzed locations can be exhibited (Figure 7b), resulting in almost equal values from both AM and the C–C method, i.e., negligible within-year climate variability effect.

In the northern part of the Adriatic Sea, location 44° N 13.5° E (the lowest graphs in Figures 6 and 7), the C–C predictions slightly exceed the AM predictions. *Bura* exerts a significant influence on both the frequency of occurrence and values of extremes. *Jugo* produces several annual extremes but with obviously lower values and frequency of occurrence. Encountering the dominance of a particular month is much harder as the influence is almost evenly distributed from November up till March. However, a general trend can be observed in Figures 4 and 5, where discrepancies between the C–C and the AM method are being reduced as we move from the south towards the north Adriatic.

Additional graphs are presented in Appendix A, comparing extremes obtained for individual directions (Figure A1) and months (Figure A2) with extremes obtained by AM and C–C methods. For a substantial number of locations, extremes for individual directions and months exceed those obtained by the AM method. However, these results never exceed the predictions obtained by the C–C method, representing a safe and conservative envelope of individual results. This exceedance of AM is the most frequent for individual directions and the return period of 100 years.

It is well known that both choices of the theoretical extreme value distribution and fitting method may influence the prediction. The choice of Gumbel extreme value distribution is based on the recommendations of the classification societies for fitting annual extreme SWHs [1]. The choice is also confirmed by a comparative analysis of three extreme value distributions performed in [6], where it was found that the Gumbel distribution is the most appropriate. Histograms and fitted extreme value distributions are shown in Appendix B, Figure A3, for three locations analyzed in Section 3. Fitting distributions for individual wave directions and months are presented in Figure A3 sides, respectively. Appropriate fitting is observed for most cases. In some rare instances, e.g., for September for loc. 43.0° N 15.5° E (middle graphs in Figure A3, Appendix B), fitting is not adequate as the tail of the distribution function likely overestimates extremes.

However, the shape of the histogram is such that other probability distribution and fitting methods would hardly improve this fitting. It should be mentioned that the present study includes a large number of directions, months, and locations, aiming to draw the conclusion from the whole dataset. In such a case, it would be rather inconvenient to fit different distributions with different methods on a case-by-case basis.

The general discussion about the accuracy of wave data contained in the wave databases is given in [13], where some effects like the quality of the wind forcing model, scarcity of the satellite altimeter data, and the resolution in space and time are emphasized as highly important. The comparison performed in [15] has found that extreme heights in storm conditions predicted by the WWA are higher compared to the ERA5 reanalysis database, hence supporting the usage of WWA, confirming the statement in [13] that ERA5 tends to underestimate extreme wave heights.

The study presents results of the extreme value analysis of wave heights in the Adriatic Sea by considering simultaneously physically similar processes, i.e., waves generated by *bora* and waves generated by *Jugo* for directional analysis and waves generated in each month for within-year variability analysis. The main advantage of the proposed method lies in having directional and seasonal maxima that, as we could observe, can sometimes exceed the ones derived from the whole dataset. Also, extreme values obtained by system probability, i.e., combining distributions from individual directions, are always conservative. The approach is slightly more complex than the conventional analysis and requires a large dataset containing many years of uninterrupted records with high temporal resolution. Since a lot more fitting is performed compared to the conventional method, the proposed methodology is more sensitive considering distribution fitting uncertainty.

The method presented is general and can be employed for any location where long-term continuous data about sea states are available from either measurements or numerical reanalysis. It is of particular interest to investigate the applicability of the method to the North Atlantic, which is the design wave environment for ship structures. Although wave databases are considered in the development of the design wave climate, the effects of wave directionality and inter-annual variability are currently not considered in ship structural design, which means that wave data are probabilistically considered on an annual basis without considering the variability of wave conditions through the months [24]. The effect of the intra-annual variability in the North Atlantic is analyzed by [6], where a moderate increase of design significant wave height is obtained. Wave directionality is also currently not considered, and it is assumed that waves from all directions are equally probable. The effect could be potentially important, as indicated by [25]. Namely, the dominant storm conditions in the North Atlantic are storms being generated in the regions around Newfoundland, which then travel across the ocean towards the Azores islands and Portugal. For ships crossing from Europe towards the USA, the storms will be on the starboard side, but in the other direction, the storms would be on the port side of the ships. Therefore, it would be reasonable to investigate this effect in the North Atlantic for implementation in ship design. It is to be mentioned that results obtained for the Adriatic Sea should not be mapped to other regions, as wave generation processes occurring in the Adriatic basin are

peculiar and strongly controlled by the relationship between basin geometry and variations in wind intensity and directions.

5. Conclusions

Extreme significant wave height statistics are developed for the Adriatic region by considering wind patterns and within-year climate variability. Results are based on the WorldWaves database, containing 23 years of continuous wave records. The analysis of extreme values is based on the system probability method proposed by Carter and Challenor [4]. Results are compared to the ones neglecting wind directionality and wave climate seasonality effects, suggesting the following:

- *Bura* is the wind pattern generating extreme wave heights in the north part of the Adriatic and along the west coast. Across the remaining part of the Adriatic Sea, *Jugo* is a dominating wind pattern. The only exception is the southernmost part of the Adriatic, where extreme waves may be generated by other wind patterns;
- The extreme value prediction considering wave directionality is, on average, 4% larger compared to the predictions when this effect is neglected;
- The extreme values predictions from individual directions can overshoot the ones derived from the whole dataset, i.e., by neglecting directionality. However, extreme values obtained by system probability, combining distributions from individual directions, are always conservative;
- The yearly maxima predominantly occur inside one or two directions, *Bura* in the north and along the west coast, and *Jugo* across the remaining part of the basin. The importance of wave directionality is increased near the Strait of Otranto because of the influence of other wind and wave patterns from the Ionian Sea;
- The extreme value prediction considering within-year climate variability appears as a more important effect, leading to, on average, 8% larger extremes compared to the prediction when this effect is neglected;
- Similar to the wave directionality, the within-year climate variability effect is more influential in the southern part of the Adriatic;
- The study reveals that neglecting wave directionality and within-year wave climate variability effects for the Adriatic Sea, in general, leads to an underestimation of the long-term extreme SWHs. Therefore, it is recommended to consider these effects when defining extreme environmental conditions for the design and analysis of marine structures operating in the Adriatic Sea.

Author Contributions: Conceptualization, A.M. and J.P.; methodology, A.M. and J.P.; software, A.M.; validation, A.M.; formal analysis, A.M.; investigation, A.M.; resources, A.M.; data curation A.M.; writing—original draft preparation, A.M.; writing—review and editing, A.M. and J.P.; visualization, A.M.; supervision, J.P.; project administration, J.P.; funding acquisition, J.P. All authors have read and agreed to the published version of the manuscript.

Funding: This work has been fully supported by Croatian Science Foundation under the project lP-2019-04-2085.

Institutional Review Board Statement: Not applicable.

Informed Consent Statement: Not applicable.

Data Availability Statement: Not applicable.

Acknowledgments: This work has been fully supported by Croatian Science Foundation under the project lP-2019-04-2085. The WorldWaves data are provided by Fugro OCEANOR AS.

Conflicts of Interest: The authors declare no conflict of interest. The funders had no role in the design of the study; in the collection, analyses, or interpretation of data; in the writing of the manuscript; or in the decision to publish the results.

Appendix A

Comparison of maxima for individual directions and months with maxima obtained by AM and C–C method.

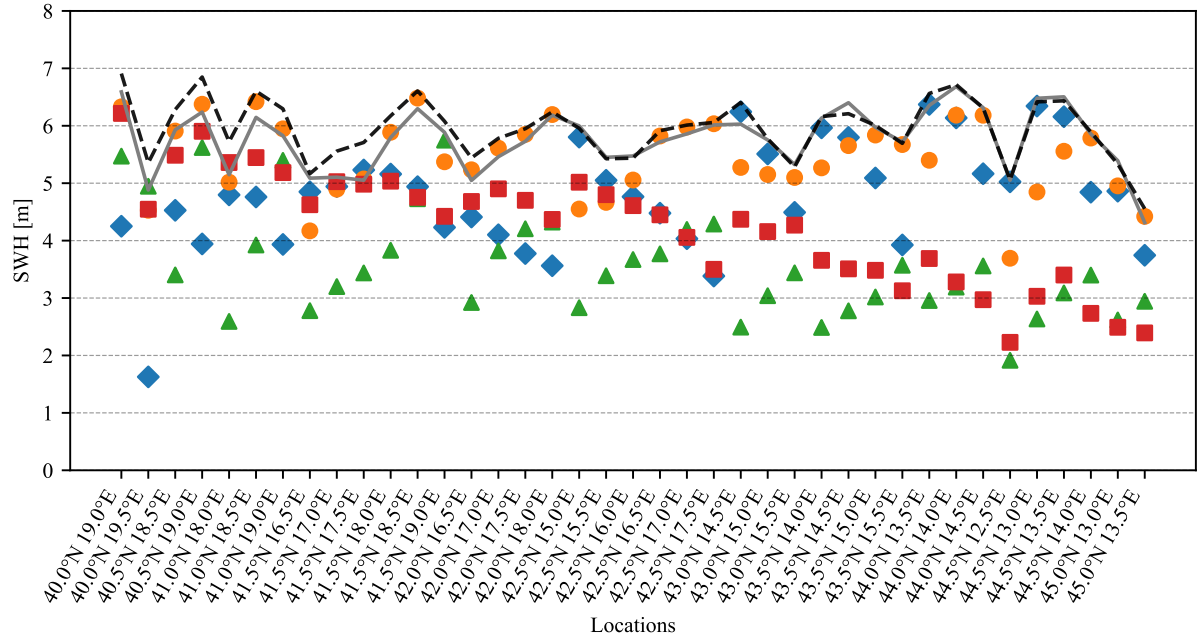

(**a**)

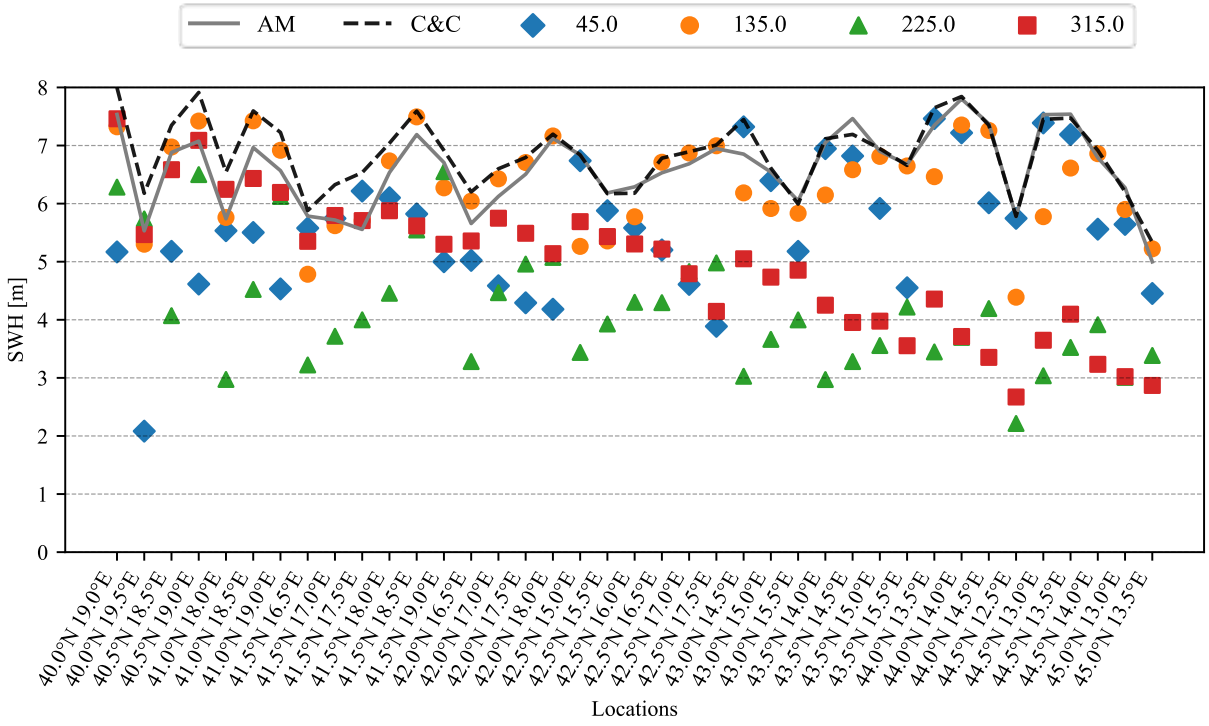

(**b**)

Figure A1. The extreme SWHs predictions calculated based on the return period: (**a**) 25 years; (**b**) 100 years. Markers represent results from individual directions, while the dashed gray line displays values obtained by the C–C approach combining DM.

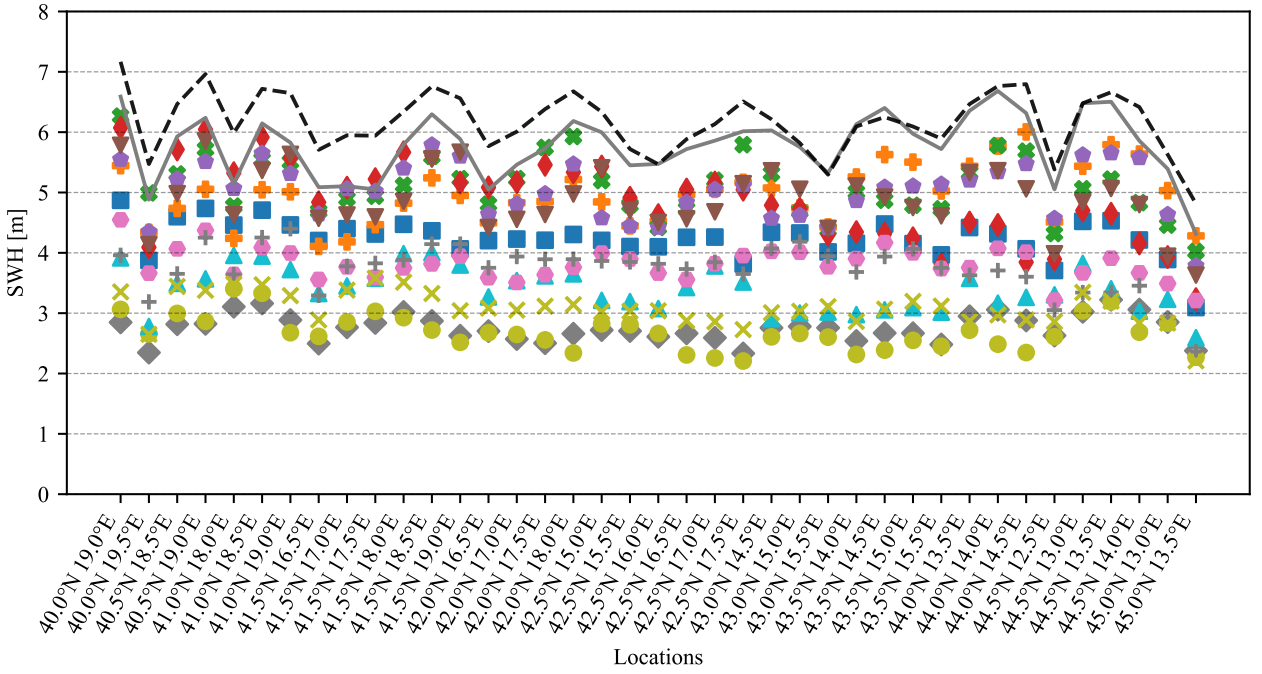

(a)

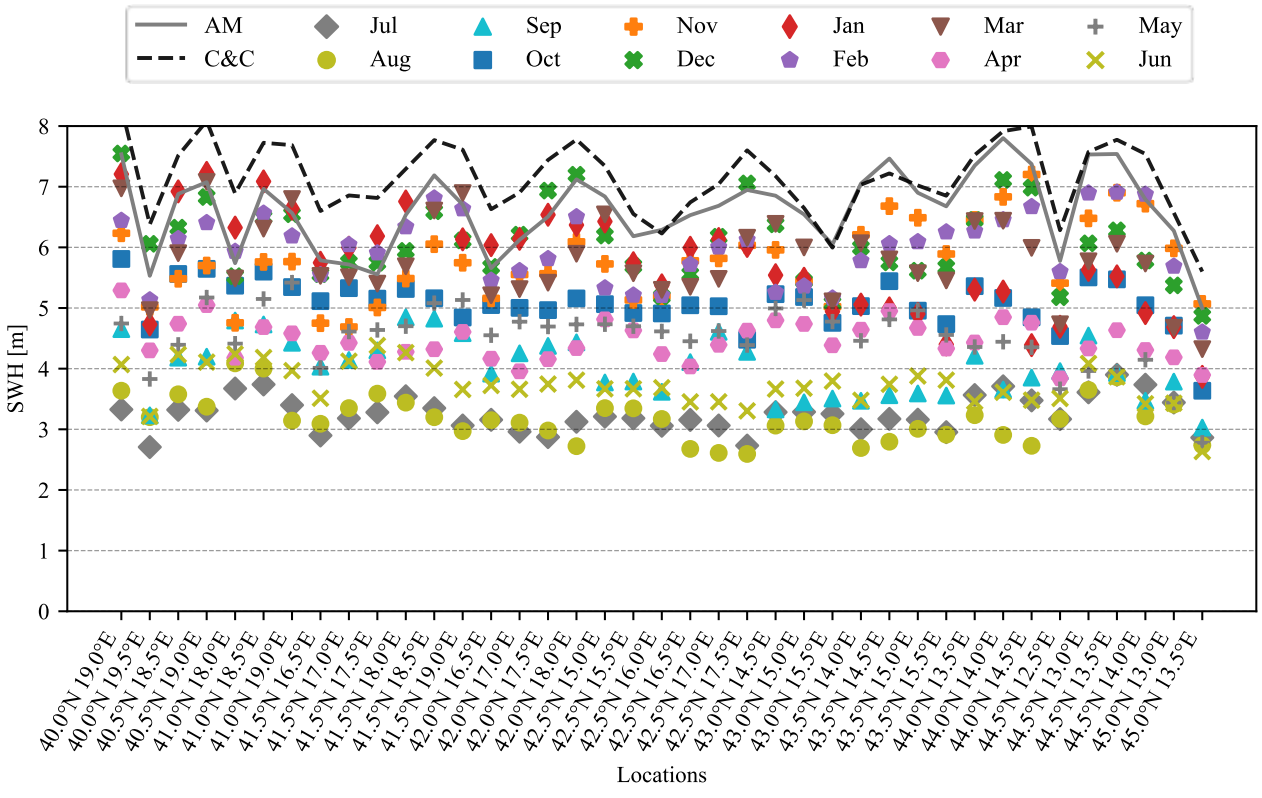

(b)

Figure A2. The extreme SWHs predictions calculated based on the return period: (**a**) 25 years; (**b**) 100 years. Markers represent results from individual months, while the dashed gray line displays values obtained by the C–C approach combining MM.

Appendix B

Histograms and probability density plots of fitted Gumbel distributions for three characteristic locations: (a) Directional maxima; (b) Monthly maxima.

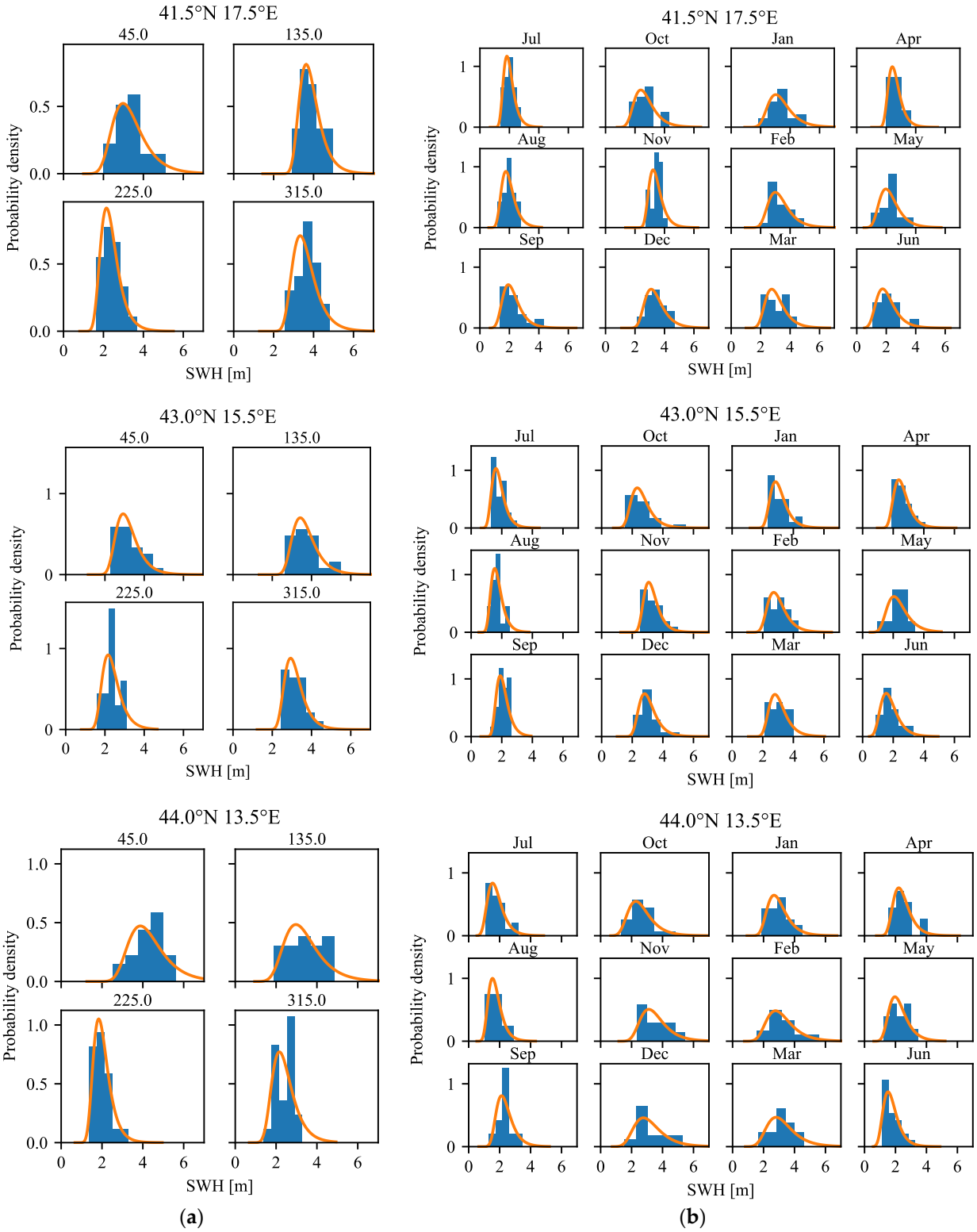

Figure A3. Histograms of SWH maxima and PDF plots of fitted Gumbel distributions for three characteristic locations: (**a**) Directional maxima; (**b**) Monthly maxima.

References

1. Det Norske Veritas. *Recommended Practice DNV-RP-C205: Environmental Conditions and Environmental Loads*; Det Norske Veritas: Oslo, Norway, 2019.
2. IACS. *Rec. No. 34. Standard Wave Data (North Atlantic Scatter Diagramm)*; IACS: London, UK, 2000.
3. Mikulić, A.; Parunov, J. Dependence of the Long-Term Extreme Significant Wave Heights on the Wave Directionality: The Adriatic Sea Case Study. In *Sustainable Development and Innovations in Marine Technologies: Proceedings of the 19th International Congress of the International Maritime Association of the Mediterranean (IMAM 2022), Istanbul, Turkey, 26–29 September 2022*; Ergin, S., Soares, C.G., Eds.; CRC Press: London, UK, 2022; p. 474. ISBN 9781003358961.
4. Carter, D.J.T.; Challenor, P.G. Estimating Return Values of Environmental Parameters. *Q. J. R. Meteorol. Soc.* **1981**, *107*, 259–266. [CrossRef]
5. Leder, N.; Smirčić, A.; Vilibić, I. Extreme Values of Surface Wave Heights in the Northern Adriatic. *Geofizika* **1998**, *15*, 1–13.
6. Mikulić, A.; Parunov, J. Bias in Estimates of Extreme Significant Wave Heights for the Design of Ship Structures Caused by Neglecting Within-Year Wave Climate Variability. *Ships Offshore Struct.* **2022**, 1–14. [CrossRef]
7. Tabain, T. The Proposal for the Standard of Sea States for the Adriatic. *Brodogradnja* **1974**, *25*, 251–258.
8. Tabain, T. Standard Wind Wave Spectrum for the Adriatic Sea Revisited (1977–1997). *Brodogradnja* **1997**, *45*, 303–313.
9. HHI. *Klimatološki Atlas Jadranskog Mora (1949.–1970.)*; HHI: Split, Croatia, 1979.
10. Parunov, J.; Ćorak, M.; Pensa, M. Wave Height Statistics for Seakeeping Assessment of Ships in the Adriatic Sea. *Ocean Eng.* **2011**, *38*, 1323–1330. [CrossRef]
11. Benetazzo, A.; Fedele, F.; Gallego, G.; Shih, P.-C.; Yezzi, A. Offshore Stereo Measurements of Gravity Waves. *Coast. Eng.* **2012**, *64*, 127–138. [CrossRef]
12. Gulev, S.K.; Grigorieva, V.; Sterl, A.; Woolf, D. Assessment of the Reliability of Wave Observations from Voluntary Observing Ships: Insights from the Validation of a Global Wind Wave Climatology Based on Voluntary Observing Ship Data. *J. Geophys. Res. Ocean.* **2003**, *108*, 3236. [CrossRef]
13. Bitner-Gregersen, E.M.; Waseda, T.; Parunov, J.; Yim, S.; Hirdaris, S.; Ma, N.; Soares, C.G. Uncertainties in Long-Term Wave Modelling. *Mar. Struct.* **2022**, *84*, 103217. [CrossRef]
14. Pomaro, A.; Cavaleri, L.; Papa, A.; Lionello, P. 39 Years of Directional Wave Recorded Data and Relative Problems, Climatological Implications and Use. *Sci. Data* **2018**, *5*, 1–12. [CrossRef]
15. Bencivenga, M.; Nardone, G.; Ruggiero, F.; Calore, D. The Italian Data Buoy Network (RON). *WIT Trans. Eng. Sci.* **2012**, *74*, 321–322. [CrossRef]
16. Ćorak, M.; Mikulić, A.; Katalinić, M.; Parunov, J. Uncertainties of Wave Data Collected from Different Sources in the Adriatic Sea and Consequences on the Design of Marine Structures. *Ocean Eng.* **2022**, *266*, 112738. [CrossRef]
17. Farkas, A.; Parunov, J.; Katalinić, M. Wave Statistics for the Middle Adriatic Sea. *J. Marit. Transp. Sci.* **2016**, *52*, 33–47. [CrossRef]
18. Katalinić, M.; Parunov, J. Comprehensive Wind and Wave Statistics and Extreme Values for Design and Analysis of Marine Structures in the Adriatic Sea. *J. Mar. Sci. Eng.* **2021**, *9*, 522. [CrossRef]
19. Petranović, T.; Mikulić, A.; Katalinić, M.; Ćorak, M.; Parunov, J. Method for Prediction of Extreme Wave Loads Based on Ship Operability Analysis Using Hindcast Wave Database. *J. Mar. Sci. Eng.* **2021**, *9*, 1002. [CrossRef]
20. Farkas, A.; Degiuli, N.; Martić, I. Assessment of Offshore Wave Energy Potential in the Croatian Part of the Adriatic Sea and Comparison with Wind Energy Potential. *Energies* **2019**, *12*, 2357. [CrossRef]
21. Benetazzo, A.; Fedele, F.; Carniel, S.; Ricchi, A.; Bucchignani, E.; Sclavo, M. Wave Climate of the Adriatic Sea: A Future Scenario Simulation. *Nat. Hazards Earth Syst. Sci.* **2012**, *12*, 2065–2076. [CrossRef]
22. Bonaldo, D.; Bucchignani, E.; Ricchi, A.; Carniel, S. Wind Storminess in the Adriatic Sea in a Climate Change Scenario. *Acta Adriat.* **2017**, *58*, 195–208. [CrossRef]
23. Virtanen, P.; Gommers, R.; Oliphant, T.E.; Haberland, M.; Reddy, T.; Cournapeau, D.; Burovski, E.; Peterson, P.; Weckesser, W.; Bright, J.; et al. SciPy 1.0: Fundamental Algorithms for Scientific Computing in Python. *Nat. Methods* **2020**, *17*, 261–272. [CrossRef]
24. de Hauteclocque, G.; Maretic, N.V.; Derbanne, Q. Hindcast Based Global Wave Statistics. *Appl. Ocean Res.* **2023**, *130*, 103438. [CrossRef]
25. Parunov, J.; Soares, C.G.; Hirdaris, S.; Wang, X. Uncertainties in Modelling the Low-Frequency Wave-Induced Global Loads in Ships. *Mar. Struct.* **2022**, *86*, 103307. [CrossRef]

Publication V

Published journal article.

Journal of *Marine Science and Engineering*

MDPI

Article

Environmental Contours in the Adriatic Sea for Design and Analysis of Marine Structures

Antonio Mikulić * and Joško Parunov *

Faculty of Mechanical Engineering and Naval Architecture, University of Zagreb, Ivana Lučića 5, 10000 Zagreb, Croatia

* Correspondence: antonio.mikulic@fsb.hr (A.M.); josko.parunov@fsb.hr (J.P.)

Abstract: The environmental contours represent an approach for defining extreme environmental conditions, resulting in extreme responses of marine structures with a given return period. Over the past decade, an increasing number of studies have been developed dealing with the methods for defining environmental contours and enhancing their practical application in different marine environments. In the present study, environmental contours describing significant wave heights and peak wave periods are created for the Adriatic Sea. This small semi-enclosed sea basin within the Mediterranean Sea encounters increasing maritime and offshore activities. Considering also a great but still unused potential for the installation of renewable energy facilities, the main motives for the presented study are concluded. The environmental contours are established based on 24 years of hindcast wave data extracted from the WorldWaves database. Joint distributions consisting of the marginal distribution of significant wave height and conditional distributions of peak wave periods are used as a basis for the creation of environmental contours using the IFORM and ISORM methods. Return periods of 1 year, 25 years, and 100 years are considered relevant for the marine operation, design of ships, and offshore structures, respectively. A possibility of environmental contour practical application to the calculation of global wave loads upon ship structures is presented. Based on the uncertainty assessment performed, conservative environmental contours for the whole Adriatic are also presented.

Keywords: environmental contours; IFORM; ISORM; global wave loads; significant wave height; peak wave period; return period

Citation: Mikulić, A.; Parunov, J. Environmental Contours in the Adriatic Sea for Design and Analysis of Marine Structures. *J. Mar. Sci. Eng.* **2023**, *11*, 899. https://doi.org/10.3390/jmse11050899

Academic Editors: Nikolaos Skliris and Robert Marsh

Received: 20 March 2023
Revised: 16 April 2023
Accepted: 19 April 2023
Published: 23 April 2023

1. Introduction

Several approaches are presented in Det Norske Veritas (DNV) recommendations [1] to describe the extreme value distribution of wave conditions. Alongside design sea state and extreme individual wave height, as already well-established procedures, is the currently intensely researched environmental contour (EC) approach. It is a method applied to approximate and visually present long-term extreme sea states and responses.

Although a more precise estimation of the long-term structural responses can be obtained by integrating the product of the short-term response distribution, and the long-term joint distribution of the environmental conditions, the so-called "full long-term analysis" [2], the EC method is considerably less computationally demanding. Additionally, considering the ability to be incorporated within well-established structural design methodologies, compliant with instituted guidelines [1,3,4], the EC method is commonly used to get a first estimate or even as a complete replacement for a full long-term analysis.

While it can be applied for predictions over some large sea areas (e.g., ship structural analysis [5]), it is mostly used to make predictions for a specific site for coastal and offshore applications such as offshore oil and gas platforms and renewable energy structures [6]. Renewable energy applications, e.g., wave energy converters [7–9] or wind farms [10,11],

have been extensively investigated in the literature, particularly over the past few years following global goals of decarbonization and sustainability.

Various approaches for deriving an EC from a metocean dataset have been proposed in the literature. The process generally includes the estimation of the joint distribution of the environmental variables and contour construction based on the defined joint distribution. A joint distribution can be defined by global hierarchical models [12], copula models [13], non-parametric models (for example, kernel density estimates) [11,14], or conditional extremes models [15]. Additionally, a method for the estimation of model parameters can vary between maximum likelihood estimation (MLE), method of moments (MOM), or least squares fit (LSQ), weighted or not.

The contour construction methods can be classified based on the variable space used for creation and associated exceedance probability. The EC can be created in standard normal space (inverse first-order reliability method (IFORM) [16], inverse second-order reliability method (ISORM) [17], and inverse directional simulation [15]) or directly in physical variable space (direct sampling (DS) method [18], direct IFORM [19], and highest density contour (HDC) method [20]). Based on a target exceedance probability, EC can be evaluated based on marginal exceedance probability or total exceedance probability [21].

Probably the most commonly applied approach is the inverse first-order reliability method (IFORM), proposed by Winterstein [16]. The IFORM utilizes Rosenblatt transformation on the joint distribution of environmental variables and linearizes the failure surface at the design point. Therefore, depending on the true nature of the failure surface, IFORM can underestimate the return values. Modification of the failure surface towards the second-order approximation (a circle for 2D cases) is proposed by Chai and Leira [17], suggesting the inverse second-order reliability method (ISORM). The only difference in contour creation between the two approaches, assuming an equal joint model is used, occurs within reliability index β values. The ISORM yields higher values, therefore resulting in more conservative contours.

The first comprehensive overview of EC methods in general, with a special dedication to structural reliability analysis applications, is given by Ross et al. [22]. The paper describes different approaches to estimating the joint distribution of environmental variables and corresponding EC based on that distribution. The recommendation as to when and how they should be used is proposed at the end. A comparison framework for evaluating ECs of extreme sea states is developed by Eckert et al. [23]. This paper develops generalized metrics for comparing the performance of contour methods to one another among study sites. These metrics were developed to evaluate the accuracy, physical validity, and aggregated temporal performance. By applying these metrics, users can compare and select the best contour method to predict extreme sea states at a certain location for a given application. Another detailed benchmark on the robustness of EC methods and sampling uncertainty was carried out by Haselsteiner et al. [24]. The results showed significant discrepancies in both maximum significant wave height (H_s) predictions and the amount of data points occurring outside of a given contour caused by variability from different joint distribution models and different contour construction methods. The choice of joint distribution appears to have more impact.

The pioneering research of wave statistics in the Adriatic region was performed by Tabain in [25,26], developing wave histograms and specific wave spectrum (Tabain's spectrum) as a single parameter modification of the JONSWAP spectrum relevant for the Adriatic. Tabain's spectral and statistical description of waves was created based on the limited number of wave measurements and observations from merchant and meteorological ships. A collection of wave data from visual observation across the Adriatic [27] was later used in [28] to develop extreme wave statistics using the three-parameter Weibull distribution. However, the data from [27] suffered from uncertainties due to the lack of extremes caused by heavy weather avoidance and visual wave observation inaccuracies. Recently, the long-term, high-quality hindcast wave database, the WorldWaves Atlas (WWA), developed by Fugro Oceanor, has been used for environmental description in

the Adriatic. Comparative analysis performed in [29] indicated that WWA is conservative compared to other databases available for the Adriatic. The WWA has been extensively used across different recent studies in the Adriatic, for example, the wave loads and operability analysis [30], the extreme value analysis [31], and renewable energy potential [32].

The aim of the present study is to develop ECs for the Adriatic Sea, the semi-enclosed sea basin within the Mediterranean Sea with increasing maritime and offshore activities. Two methods for environmental contours are compared, as well as different location parameters of the marginal distribution of wave heights, contributing thus to the uncertainty analysis of the long-term description of the marine environment, as the present concern of the international research community [33]. The practical application of EC is presented in the example of the short-term extreme vertical wave bending moments on oil tankers of different sizes sailing in the Adriatic. The present study is carried out for the whole Adriatic basin, representing the continuation of the research on the environmental description in the Adriatic for different types of marine applications, e.g., wave loads on damaged ships [34]. ECs presented in the paper enable engineers and decision makers a quick and reliable estimate of marine structures loading during marine operations planning and for preliminary design of ships and offshore structures in the Adriatic.

The research is presented through 5 sections and an Appendix A. After the Introduction, Section 2 is divided into two subsections. The first presents the available dataset and offers a brief description of the wave climate of the Adriatic region. The second subsection of Section 2 gives an overview of the methodology used in the computation. The results are presented in Section 3. The fourth section is reserved for a discussion, followed by corresponding conclusions, given in the last section. The environmental contours for 39 locations covering the whole Adriatic are presented in Appendix A.

2. Wave Data and Methodology

2.1. Wave Data in the Adriatic Sea

The study is performed based on 24 years of wave data extracted from the World Wave Atlas (WWA) produced by Fugro OCEANOR. The WWA is the collective name for a series of comprehensive high-resolution wind and wave climate atlases, providing statistics and data for any region worldwide. The data derived from the European Centre for Medium-Range Weather Forecasts (ECMWF) wave models are calibrated by Fugro OCEANOR [35–37] against satellite altimetry measurements gathered from eight different satellite missions: Geosat (1986–1989), Topex (1992–2002), Topex/Poseidon (2002–2005), Jason (2002–2008), Geosat Follow-On (2000–2008), EnviSat (2002–2010), Jason-1s (2009–2012), and Jason-2 (2008–on-going).

The available data for the Adriatic region cover a latitude–longitude grid resolution of 0.5 degrees, offering 39 accessible locations presented in Figure 1. A total of 12 wind and wave parameters are available from 1997 until 2020 at each location. Covering a 24-year period at 6 h intervals, the dataset provides a total of 33,600 records per parameter. Available data include wind speed and direction, integral spectral wave parameters (e.g., H_s, peak wave period (T_p), mean wave period), and wave direction for wind-waves and swell, considered separately and combined. The WWA model data calibrated against the satellite data represent a state-of-the-art comprehensive and systematic source of wave data as input to studies in the Adriatic region [29].

Located in the central-north part of the Mediterranean Sea, surrounded by the Apennine in the west and Dinaric mountain ranges in the east, the Adriatic Sea stretches from the shallower northwest to the deeper southeast, with an average width of around 200 km. The surface wave creation is predominantly influenced by the northeastern wind *bura* and southeastern *jugo*. Although the strongest winds blow from the northeast, the longest fetch coincides with southeast winds yielding the highest recorded wave heights of 10.87 m.

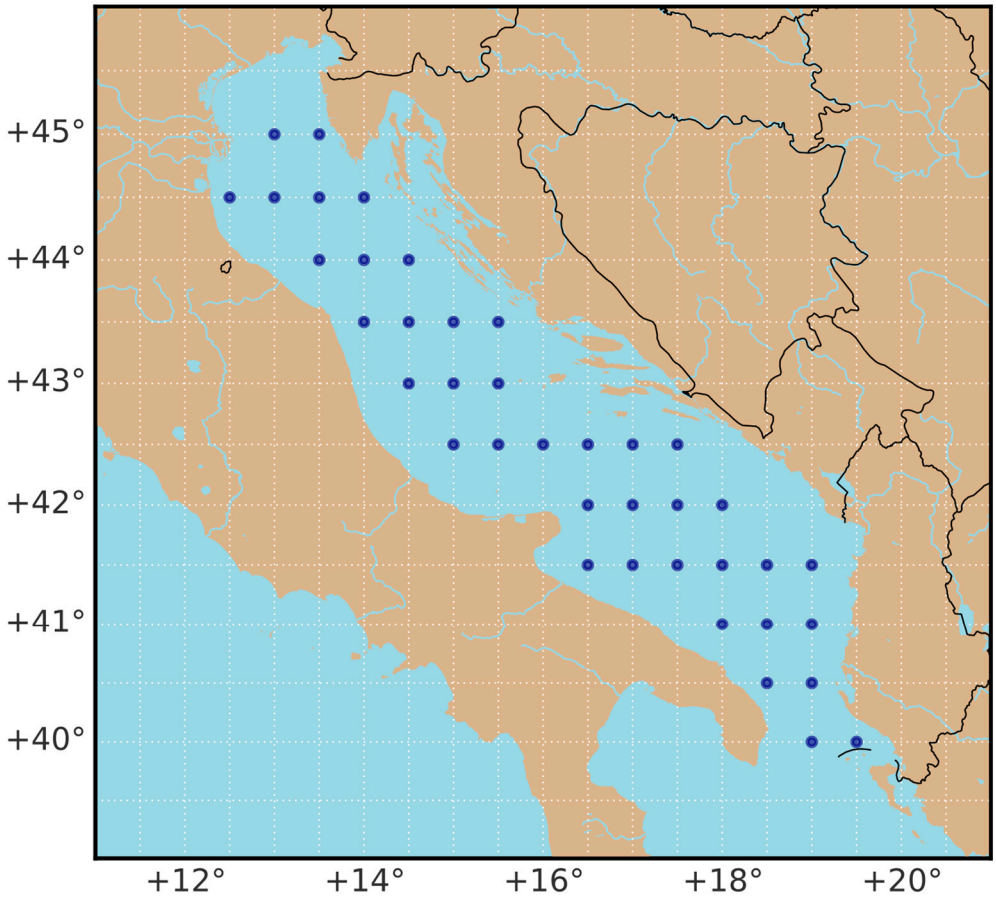

Figure 1. The offshore grid of 39 available data points from the WWA for the Adriatic Sea.

2.2. Methodology

Statistical modeling is the first step in an EC creation carried out by constructing the joint environmental model of sea state variables of interest. The joint model used in the presented study (1), the so-called hierarchical conditional model, factorizes the joint density into the product of a marginal PDF $f_{H_s}(h)$ describing the distribution of H_s and a conditional PDF $f_{T_p|H_s}(t|h)$ describing the T_p.

$$f_{H_sT_p}(h,t) = f_{H_s}(h) f_{T_p|H_s}(t|h) \tag{1}$$

In Equation (1), H_s and T_p indicate random variables, while h and t represent their realizations. The three-parameter Weibull distribution (2) is used for the marginal PDF of H_s where α, β, and γ represent the scale, shape, and location parameters.

$$f_{H_s}(h) = \frac{\beta}{\alpha} \cdot \left(\frac{h-\gamma}{\alpha}\right)^{\beta-1} \cdot \exp\left(-\left(\frac{h-\gamma}{\alpha}\right)^{\beta}\right) \tag{2}$$

The conditional PDF of T_p is modeled by a lognormal distribution as described as in (3).

$$f_{T_p|H_s}(t|h) = \frac{1}{\sigma(h)t\sqrt{2\pi}} \cdot \exp\left(-\frac{[ln(t)-\mu(h)]^2}{2\sigma(h)^2}\right) \tag{3}$$

The mean value $\mu(h)$ and standard deviation $\sigma(h)$ of $ln(T_p)$ are conditional on H_s as follows:

$$\mu(h) = E[ln(T_p)] = a_0 + a_1 h^{a_2} \sigma(h) = Var[ln(T_p)] = b_0 + b_1 h^{b_2} \tag{4}$$

The parameters of the distributions are determined by applying the maximum likelihood estimate (MLE) method on the available data for all locations.

The second part undertakes the contour construction based on the obtained joint distribution. Two chosen approaches IFORM and ISORM typically assume some type of hierarchical model as defined before. The IFORM is the most applied EC method in offshore engineering. Using the Rosenblatt transformation, the joint distribution of environmental variables is transformed to independent standard normal variables, $\mathbf{u} = \{u_1, u_2\}$, for the presented case:

$$u_1 = \Phi^{-1}(F_{H_s}(h))u_2 = \Phi^{-1}\Big(F_{T_p|H_s}(t|h)\Big) \tag{5}$$

where Φ^{-1} is the standard univariate normal CDF, while $F_{H_s}(h)$ and $F_{T_p|H_s}(t|h)$ are marginal CDF of H_s and conditional CDF of T_p, respectively. Probability of failure P_f is then calculated in the standard normalized U-space

$$1 - P_f = \int_{G_U(\mathbf{u})\leq 0} \Phi(\mathbf{u}) d\mathbf{u} \tag{6}$$

where $\Phi(\mathbf{u})$ denotes the PDF of standard univariate normal distribution. To solve the equation, the IFORM method assumes a linear approximation to the failure surface $G_U(\mathbf{u})$ at the design point. The distance from the U-space origin to the design point, referred to as the reliability index (β_F for the IFORM), can then be calculated as (7) suggests.

$$\beta_F = \Phi^{-1}\Big(1 - P_f\Big) \tag{7}$$

The linearization of the failure surface has no a priori physical backing. Therefore, the assumption should be supported on a case-by-case basis. To overcome possible underestimation of the linearization, the ISORM approach assumes a quadratic failure surface. Instead of a tangent (hyper-)plane at the design point, Chai and Leira [17] propose a (hyper-)sphere passing through the design point and centered at the origin of the U-space. The reliability index β_S for the ISORM approach can be calculated using (8).

$$\beta_S = \sqrt{\chi_n^{-1}\Big(1 - P_f\Big)} \tag{8}$$

where χ_n^{-1} represents the inverse CDF of the chi-square distribution with n degrees of freedom, corresponding to the number of environmental variables n = 2. The failure probability is defined by a given sea state duration τ and return period T_R.

$$P_f = \frac{\tau}{T_R \cdot 365.25 \cdot 24} \tag{9}$$

A return period, also known as a recurrence interval, is frequently used to determine extreme events. In the case of marine structures, it is an average time or an estimated average time between the occurrences of the extreme sea states, i.e., extreme responses. The theoretical return period between occurrences is the inverse of the average frequency of occurrence. Ships are designed considering a return period of 25 years, which raises to 100 for offshore structures. Based on the reliability index for the prescribed return period, the circle is established in U-space.

$$\sqrt{{u_1}^2 + {u_2}^2} = \beta \tag{10}$$

Finally, the EC is obtained by transforming the circle from the U-space into a contour in the environmental parameter space using the inverse Rosenblatt transformation (11).

$$h_s = F_{H_s}^{-1}(\Phi(u_1))t_p = F_{T_p|H_s}^{-1}(\Phi(u_2)) \tag{11}$$

The ECs are produced for two return periods of 25 and 100 years, applying both the IFORM and ISORM approach through a Python script generated by combining several well-defined libraries, *virocon* [38,39] and *MHKiT* [40]. Results are displayed and compared for representative locations in the Adriatic.

To determine maximum responses corresponding with the ECs, the contours of the most probable extreme VWBM at midship in short-term conditions are produced relative to the value of VWBM required by the International Association of Classification Societies (IACS) Rules [41]. Transfer functions of VWBM at midship are calculated using the semi-analytical approach proposed and validated by Jensen and Mansour [42], which is particularly useful in conceptual studies such as the present one. The approach approximates a ship hull by a pontoon of equal length, equivalent breadth, and draught, while speed and block coefficient are accounted for through correction factors. The response spectrum of VWBM is computed as a product of a wave spectrum and a square modulus of a transfer function. The most probable extreme amplitude of the VWBM (M_w^*) is calculated by the following expression:

$$M_w^* = \sqrt{2{\sigma_R}^2 \ln(N_C)} \tag{12}$$

where ${\sigma_R}^2$ is the response variance, obtained as the zeroth spectral moment, and N_C is the number of response cycles occurring through a sea state duration.

The response analysis is performed on four classes of oil tankers, Panamax, Aframax, Suezmax, and VLCC, representing the actual size range of oil tankers operating worldwide. The average dimensions of a typical ship, i.e., a class representative presented in Table 1, are provided in [43]. A reduced ship speed of 5 knots is recommended for the evaluation of the design wave loads for strength assessment [44].

Table 1. Main dimensions of four representative oil tankers representing the range of actual sizes.

Ship Class	Length [m]	Breadth [m]	Draught [m]
Panamax	174.4	31.4	11.3
Aframax	229.7	41.9	13.1
Suezmax	260.8	45.8	15.9
VLCC	318.6	58.4	21.1

Therefore, in the present study, ships sailing in head waves with a low forward speed of 5 knots are considered. Consistently with sea state resolution in the WWA database, 6 h is selected as the short-term sea state duration. The results of the analysis are presented in the following section together with the EC.

3. Results

Joint hierarchical models are fitted to data for all 39 locations as a base for contour creation. The 25- and 100-year contours have been created applying both IFORM and ISORM approaches. Three locations from the Adriatic sub-basins exhibiting above-average H_S estimates are chosen as representative of the south (41.5° N 18.5° E), central (43.0° N 14.5° E), and north (44.5° N 13.0° E) Adriatic. A comparison of contour creation methods is displayed in Figure 2a. A 100-year contour is distinguished with a dashed line, while a full line signifies a 25-year return period. Orange and gray differentiate the IFORM and ISORM approaches, respectively, while blue circles represent hindcast wave data. The goodness of fit of marginal Weibull PDF of H_s is presented on the left, Figure 2b. Except for small deviations at the highest quantiles, a rather good fit is obtained. For central and north location Q-Q plots in Figure 2b, fitted marginal distributions of H_s seem to slightly underestimate the highest value, while for the southern part, the contrary happens. As expected, ISORM displays more conservative results yielding the largest variations at the marginal values, i.e., peaks of H_s and T_p. At the extremes, ISORM predicts around 20% higher H_s. Out of 23 years of datapoints, most fall inside the 25-year IFORM contour. However, a slight underestimation of IFORM is evident due to some high H_s data left

outside the contour. Therefore, the ISORM contour is used in further response analysis and presentation.

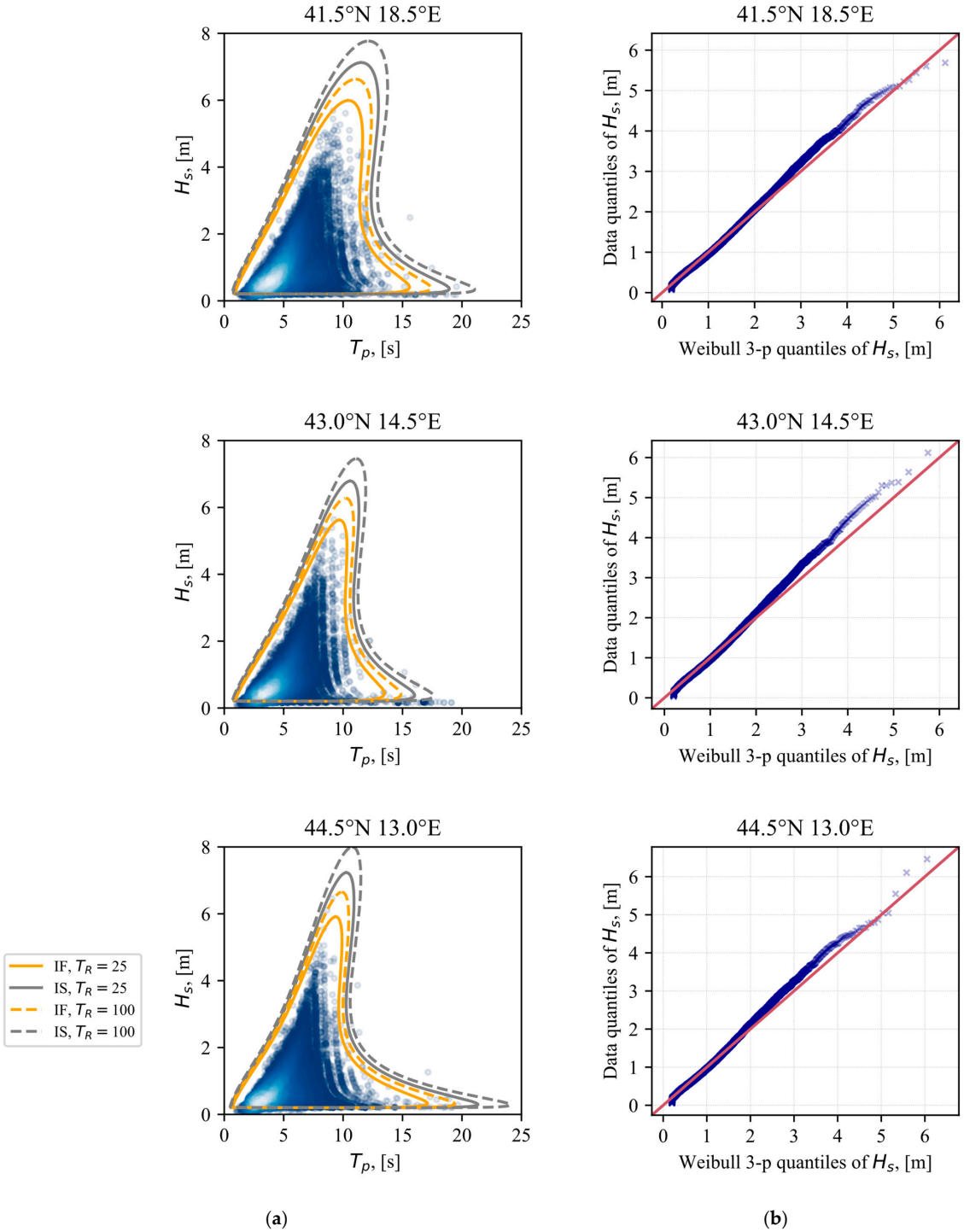

Figure 2. A comparison of EC for three characteristic locations: (**a**) The comparison of IFORM and ISORM corresponding 25-year and 100-year contours; (**b**) Q–Q plot comparing H_s data to the corresponding fitted Weibull distribution.

The results combining ISORM EC and contours of VWBM ratio are presented in Figures 3 and 4. The contours represent the percentage of the most probable extreme VWBM compared to the linear IACS Rule VWBM. The ECs reach the highest extreme VWBM ratio of almost 60% for the Panamax tanker at the southern location (upper left

graph in Figure 3). At the same location, the relative VWBM for Aframax ship is slightly lower. Expectedly, with increasing the size of the oil tanker, the VWBM contours shift to the right side of the graph, i.e., towards the higher T_p, reducing VWBM relative to the IACS value. It is interesting to notice that the periods of sea states in the North Adriatic are lower, reducing relative VWBM.

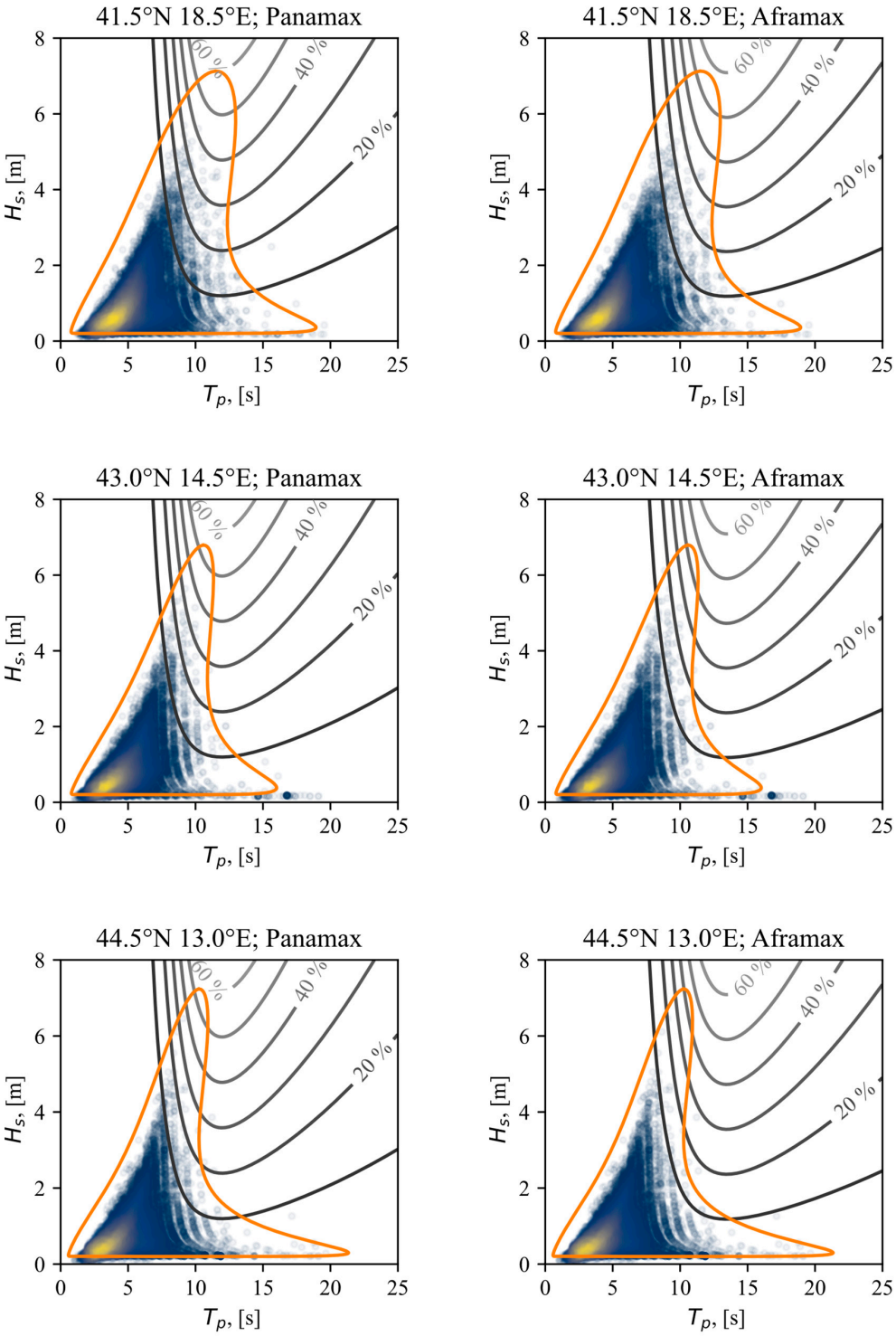

Figure 3. The ISORM 25-year contour (orange) in comparison to VWBM contours (gray) of oil tankers for three characteristic locations: (**a**) Panamax contours; (**b**) Aframax contours.

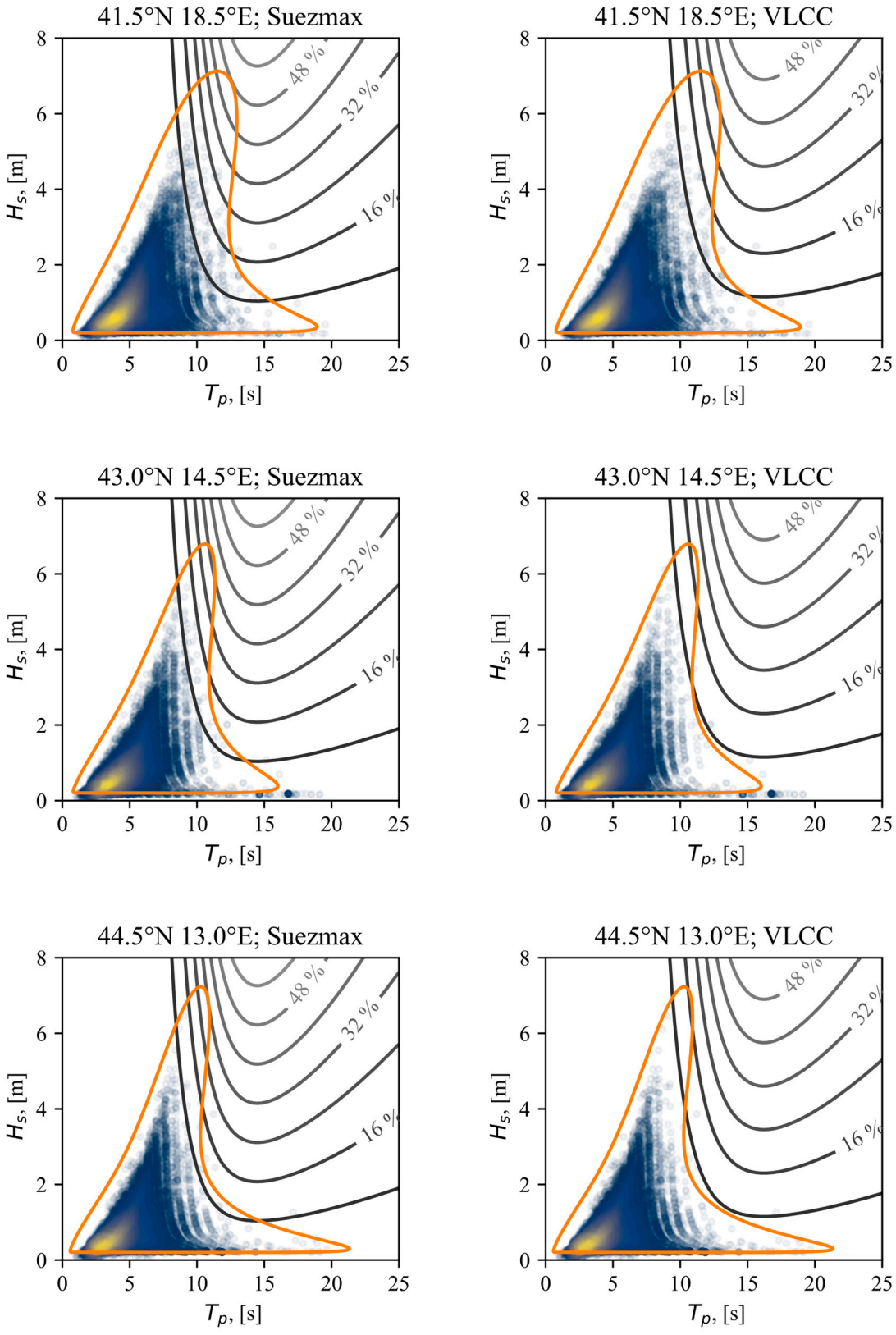

Figure 4. The ISORM 25-year contour (orange) in comparison to VWBM contours (gray) of oil tankers for three characteristic locations: (**a**) Suezmax contours; (**b**) VLCC contours.

4. Discussion

The shape of environmental contours in the Adriatic is similar in all three locations, although in the southern part of the Adriatic (upper row in Figure 3, 41.5° N), it may be noticed that the region encompassed by EC corresponding to the highest significant wave heights is wider compared to the other locations. This indicates that the response of marine structures should be investigated for the range of wave periods, while in the central and north Adriatic, the peak wave period corresponding to the extreme wave height is almost unique. Additionally, depending on the ship type, the maximum response does not always occur for a single maximum H_s but rather for the range of H_s–T_p pairs, thus suggesting the use and implementation of ECs in extreme long-term response analysis.

In all cases, there is an "elongated tail" of EC at low significant wave heights, extended toward large wave periods. Particularly long waves of a small height and long period could be ignored as their influence on the response of marine structures is negligible.

Although the current study has not explored other contour methods and joint models, generated contours seem to describe data well. There is a slight underestimation from IFORM, whereas overestimation of the ISORM contour on the other end may be noticed. The conservative trends of the ISORM approach are supported by a plain overview of the presented Equations (7) and (8) for reliability index calculations. There are also in line with the results and conclusions published in the literature [17]. However, the ECs are sensitive to the initial joint probability distribution. The location parameter γ is the most uncertain when fitting the Weibull 3P distribution. Namely, the physical interpretation of this parameter is the minimum significant wave height representing permanent sea activity. A comparison of IFORM and ISORM ECs for various choices of γ is shown in Figure 5, where large uncertainty may be observed. The reason for these discrepancies s in the fitting of the tail of the marginal distribution of H_S, which may be seen in the Q-Q plots presented in Figure 6. One can conclude from Figures 5 and 6 that the Weibull 2P (Weibull 3P with location parameter equal to zero, $\gamma = 0$) distribution is completely inappropriate as the long-term distributions of H_S lead to unconservative ECs.

As the Adriatic is a semi-enclosed sea basin with rather low extreme significant wave heights, the extreme VWBM of oil tankers is not approaching the IACS Rule VWBM. Namely, Rule VWBM is intended for ocean-going ships with unrestricted service. Nevertheless, for smaller ships (Panamax tankers, in the present case), extreme VWBM in short-term sea conditions could reach 60% of the IACS Rule value. This ratio is decreased with increasing ship size. There is also a slightly larger extreme VWBM in the southern part of the Adriatic compared to other locations, although the difference between locations is generally not significant.

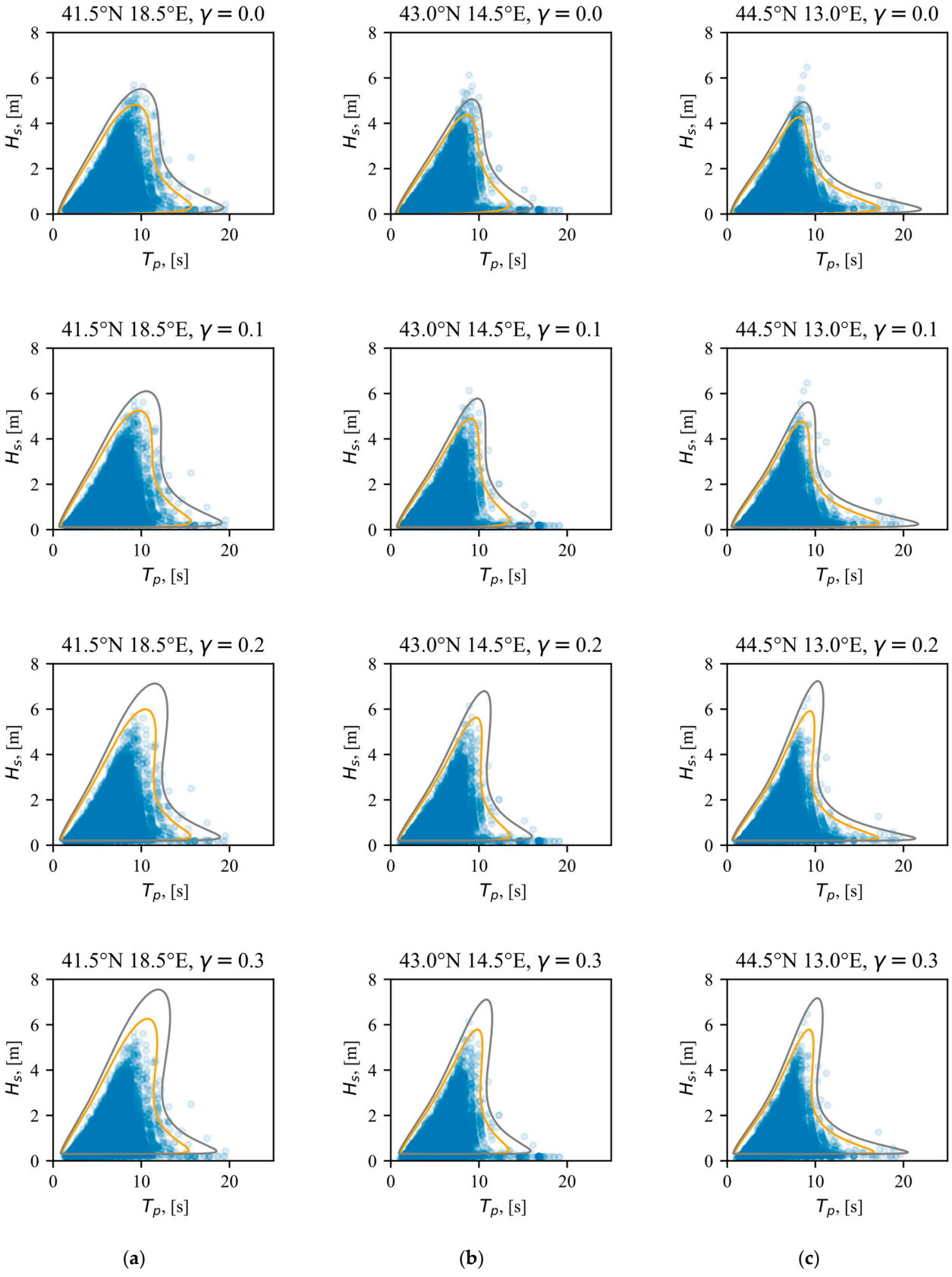

Figure 5. The 25-year IFORM (orange) and ISORM (gray) contour based on a different variation of joint model parameters, i.e., varying location parameter γ for locations: (**a**) south (41.5° N 18.5° E), (**b**) central (43.0° N 14.5° E), and (**c**) north (44.5° N 13.0° E) Adriatic.

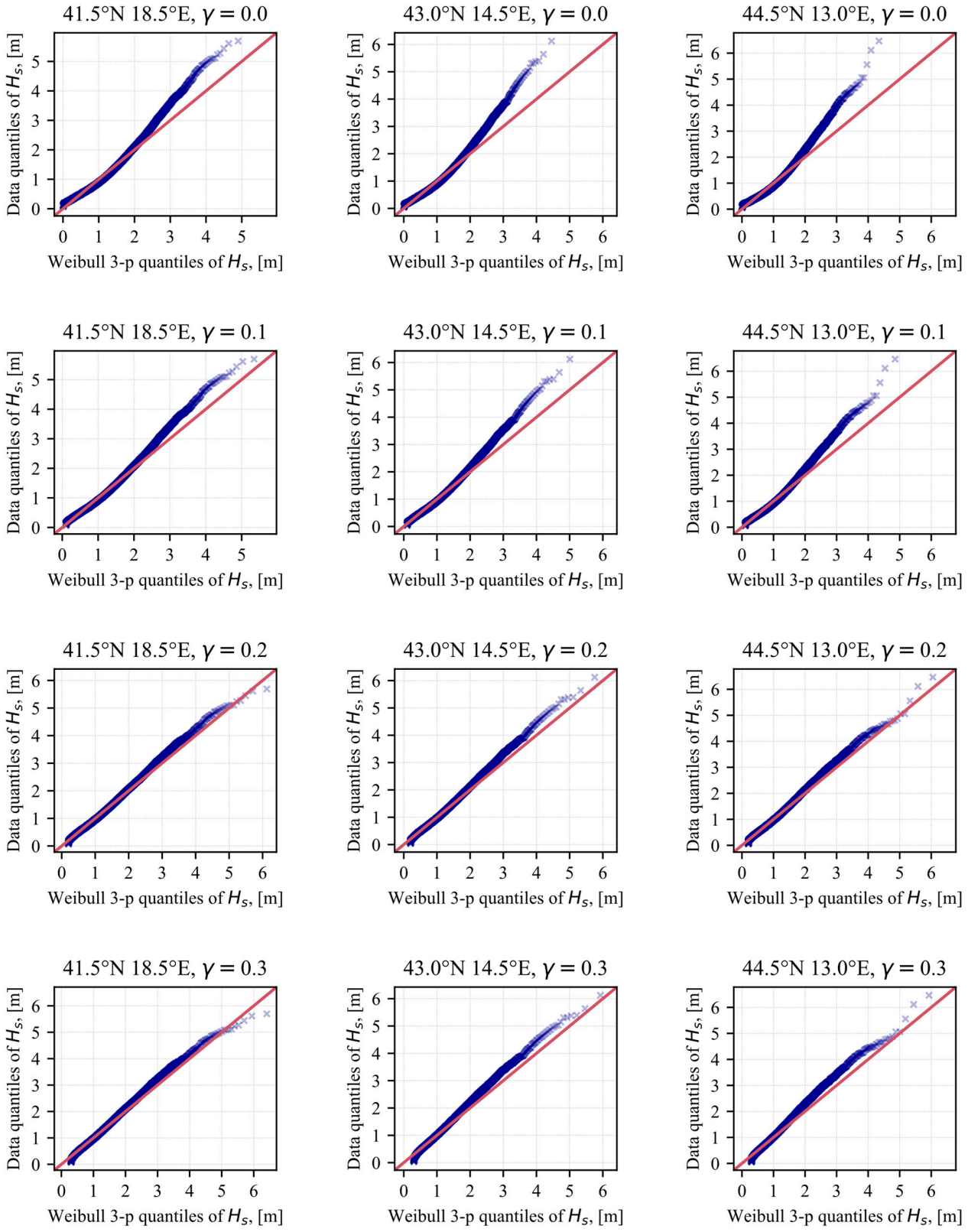

Figure 6. The Q–Q plots illustrate a comparison of H_s data to the corresponding fitted Weibull distribution. Influence of location parameter variation γ on joint model fit for locations: (**a**) south (41.5° N 18.5° E), (**b**) central (43.0° N 14.5° E), and (**c**) north (44.5° N 13.0° E) Adriatic.

5. Conclusions

The development of environmental contours (ECs) for the semi-enclosed basin of the Adriatic Sea is presented in the paper. The ECs are obtained based on the joint probability distribution of significant wave heights and peak wave periods using data contained in the WorldWaves database. The joint probability distribution used in the study consisted of the Weibull 3P marginal distribution of H_s and the log-normal conditional distribution of T_P.

By comparing ECs obtained using IFORM and ISORM methods, it was found that the latter leads to the conservative estimate of extreme sea states for the same choice of the joint probability distribution parameters. It is also found that ECs are highly sensitive to the joint probability model, especially to the selection of the location parameter γ of Weibull 3P distribution.

The application of ECs is shown through the example of extreme short-term vertical wave bending moments on oil tankers of different sizes, where ECs can be used to identify wave conditions leading to the largest extreme values. Although global wave loads on ships in the Adriatic are generally not approaching IACS Rule values, the benefit of using ECs is clearly shown, as they include not only extreme H_S but also a range of wave steepness that may influence ship global wave-induced response.

As a result of the study, ECs for all 39 locations in the Adriatic are presented in Appendix A for three characteristic return periods of 1, 25, and 100 years. The 1-year ECs are used for planning marine operations in the Adriatic, e.g., transportation of heavy cargoes or installation of offshore platforms, while those for return periods of 25 and 100 years are useful for the design of ships and offshore structures, respectively. Although more detailed information for specific locations is required for commercial purposes, presented contours may be used for preliminary identification of extreme sea states.

Author Contributions: Conceptualization, A.M. and J.P.; methodology, A.M. and J.P.; software, A.M.; validation A.M.; formal analysis, A.M.; investigation, A.M.; resources, A.M.; data curation A.M.; writing—original draft preparation, A.M.; writing—review and editing, A.M. and J.P.; visualization, A.M.; supervision, J.P.; project administration, J.P.; funding acquisition, J.P. All authors have read and agreed to the published version of the manuscript.

Funding: This work has been fully supported by Croatian Science Foundation under the project lP-2019-04-2085.

Institutional Review Board Statement: Not applicable.

Informed Consent Statement: Not applicable.

Data Availability Statement: Not applicable.

Acknowledgments: This work has been fully supported by the Croatian Science Foundation under the project lP-2019-04-2085. The WorldWaves data are provided by Fugro OCEANOR AS.

Conflicts of Interest: The authors declare no conflict of interest. The funders had no role in the design of the study; in the collection, analyses, or interpretation of data; in the writing of the manuscript; or in the decision to publish the results.

Appendix A

The ECs based on the ISORM for all 39 locations in the Adriatic are presented in following figures for characteristic return periods of 1, 25, and 100 years.

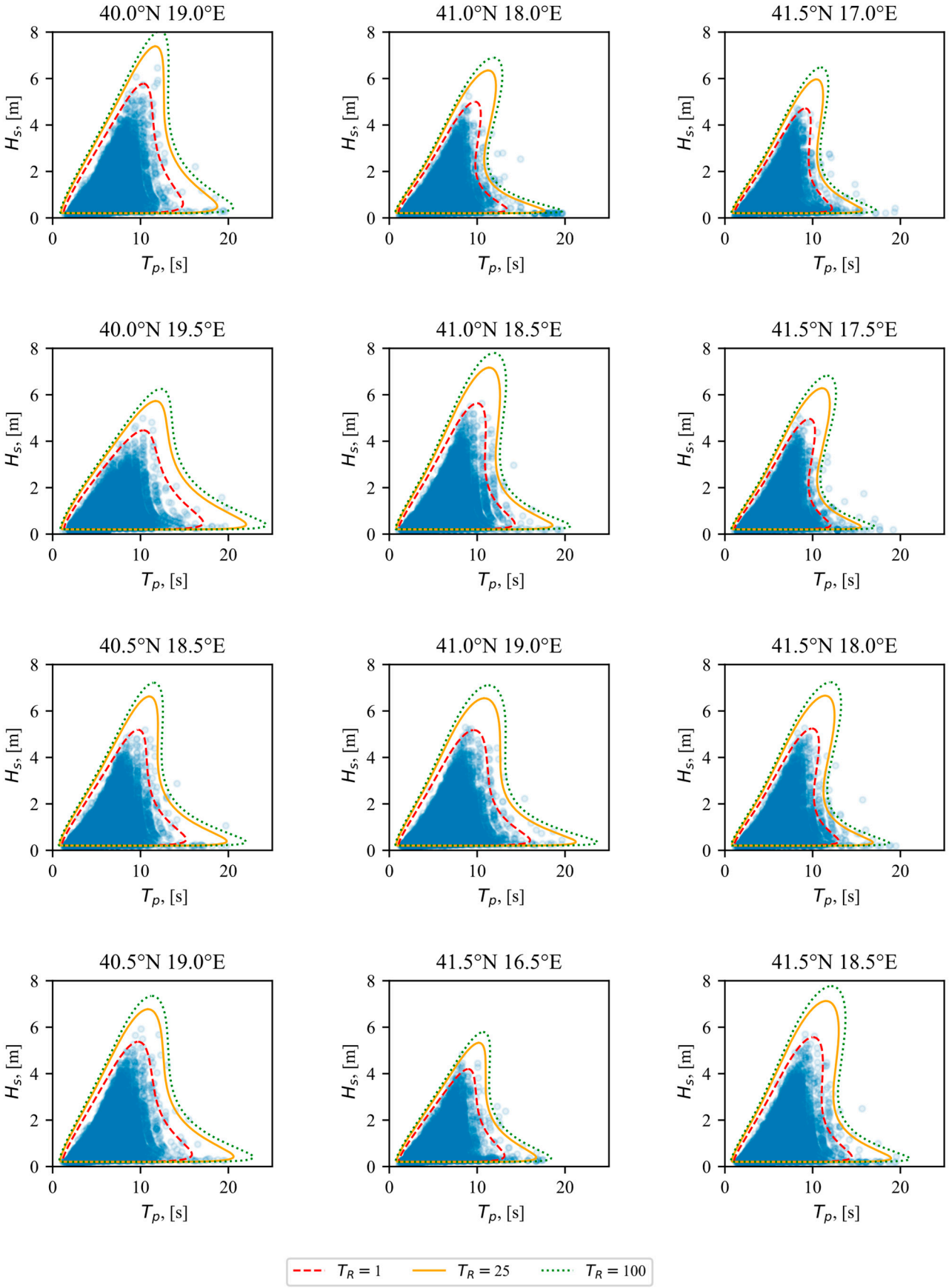

Figure A1. The ISORM ECs for characteristic return periods of 1, 25, and 100 years, pt.1.

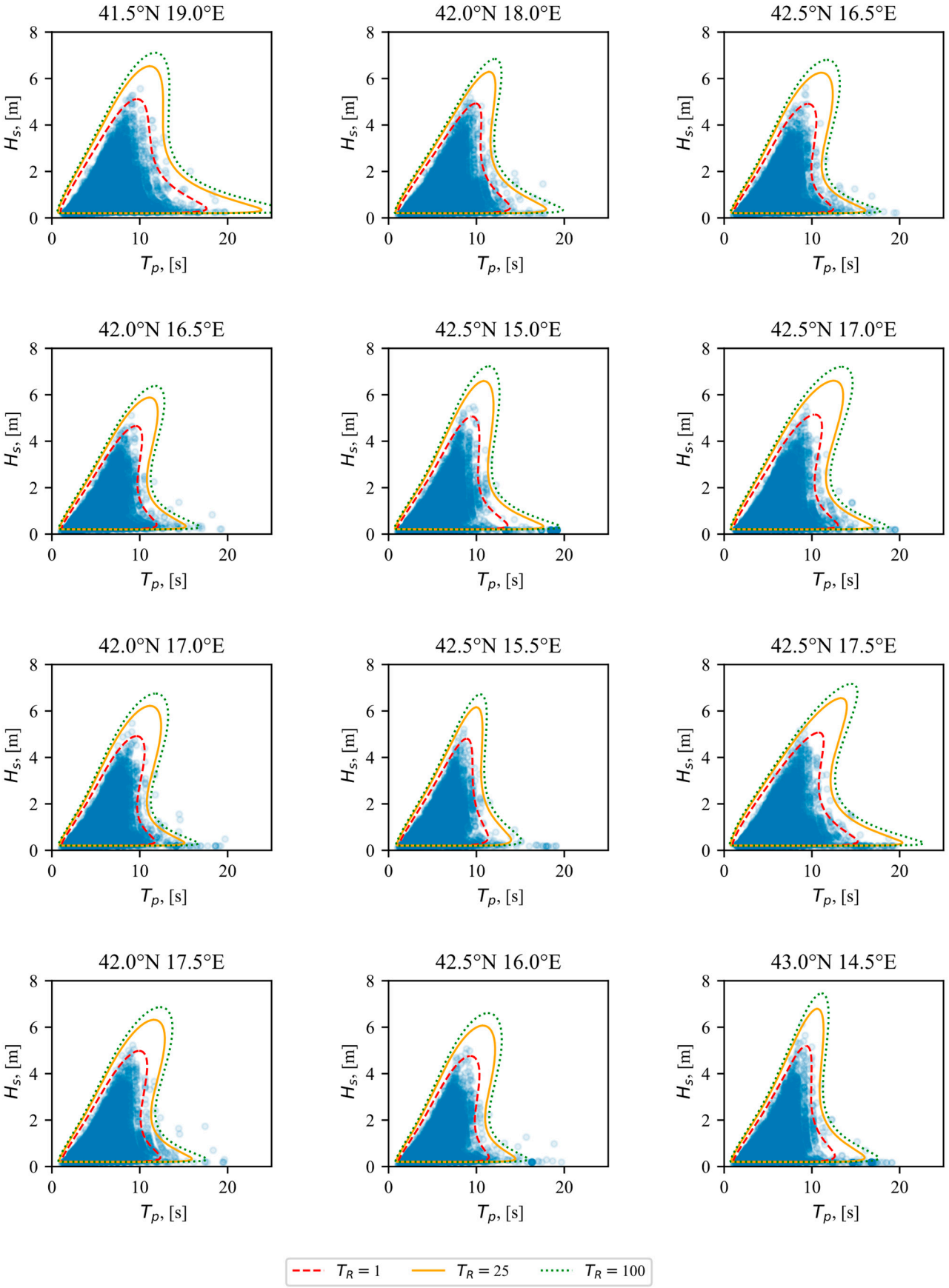

Figure A2. The ISORM ECs for characteristic return periods of 1, 25, and 100 years, pt.2.

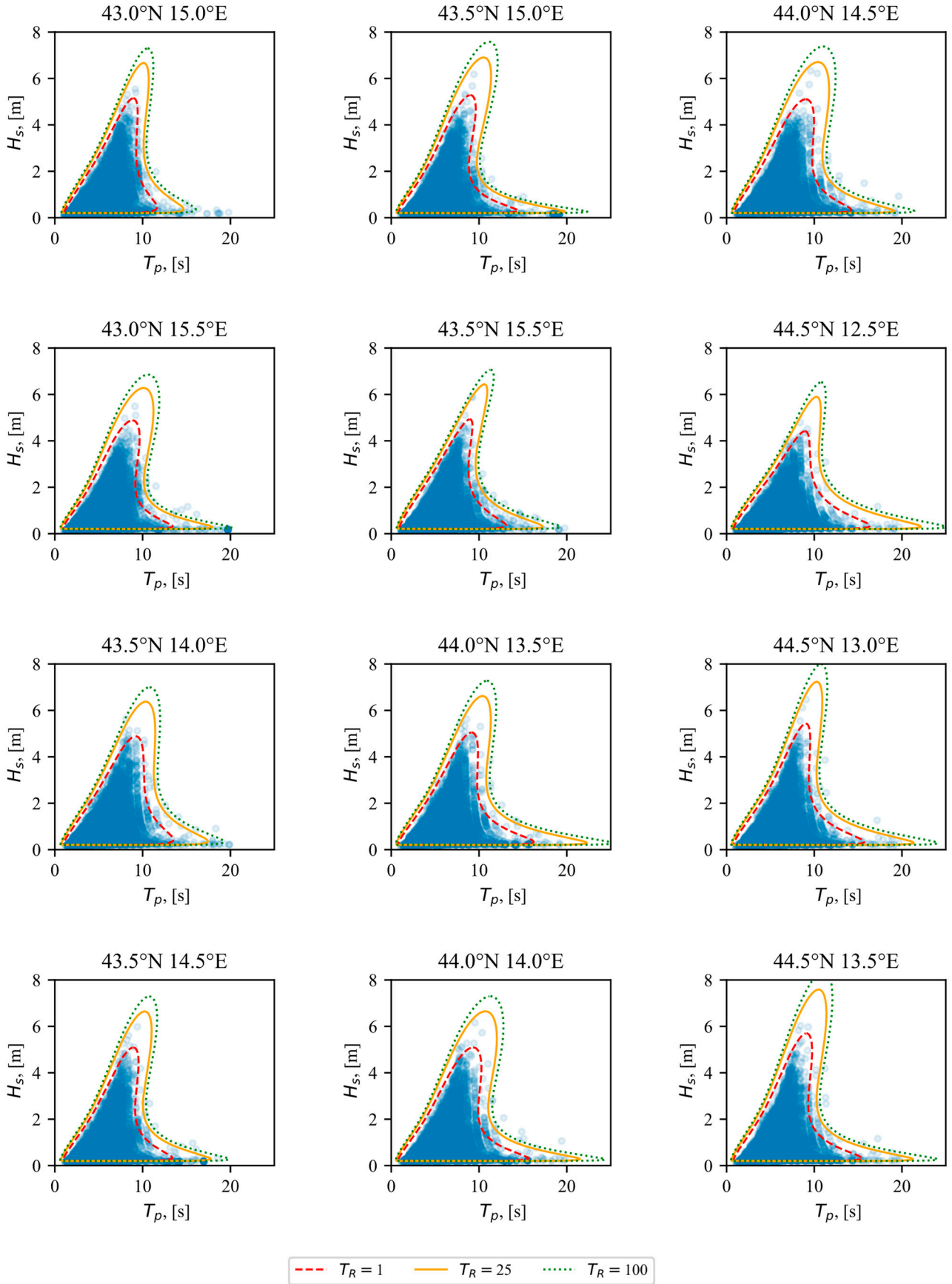

Figure A3. The ISORM ECs for characteristic return periods of 1, 25, and 100 years, pt.3.

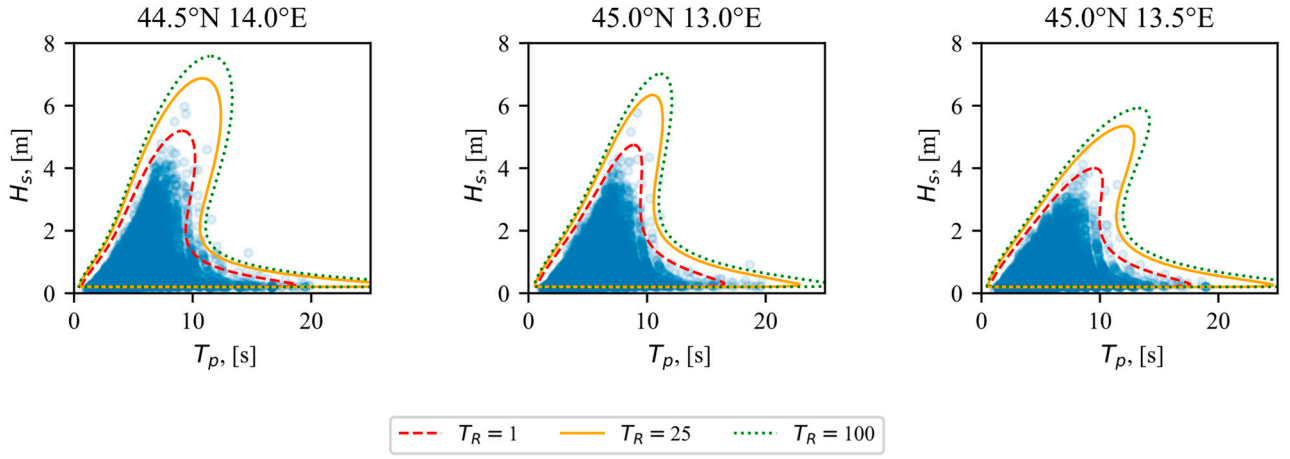

Figure A4. The ISORM ECs for characteristic return periods of 1, 25, and 100 years, pt.4.

References

1. Det Norske Veritas. *Recommended Practice DNV-RP-C205: Environmental Conditions and Environmental Loads*; Det Norske Veritas: Oslo, Norway, 2019.
2. Guedes Soares, C. Long Term Distribution of Non-Linear Wave Induced Vertical Bending Moments. *Mar. Struct.* **1993**, *6*, 475–483. [CrossRef]
3. *ISO 19901-1:2015*; Petroleum and Natural Gas Industries, Specific Requirements for Offshore Structures: Part 1: Metocean Design and Operating Considerations. International Organization for Standardization: Geneva, Switzerland, 2005.
4. *NORSOK Standard N-003*; Edition 3Actions and Action Effects. Norwegian Technology Standards Institution: Oslo, Norway, 2017.
5. Baarholm, G.; Moan, T. Application of Contour Line Method to Estimate Extreme Ship Hull Loads Considering Operational Restrictions. *J. Ship Res.* **2001**, *45*, 228–240. [CrossRef]
6. Wrang, L.; Katsidoniotaki, E.; Nilsson, E.; Rutgersson, A.; Rydén, J.; Göteman, M. Comparative Analysis of Environmental Contour Approaches to Estimating Extreme Waves for Offshore Installations for the Baltic Sea and the North Sea. *J. Mar. Sci. Eng.* **2021**, *9*, 96. [CrossRef]
7. Harnois, V.; Thies, P.R.; Johanning, L. On Peak Mooring Loads and the Influence of Environmental Conditions for Marine Energy Converters. *J. Mar. Sci. Eng.* **2016**, *4*, 29. [CrossRef]
8. Neary, V.S.; Ahn, S.; Seng, B.E.; Allahdadi, M.N.; Wang, T.; Yang, Z.; He, R. Characterization of Extreme Wave Conditions for Wave Energy Converter Design and Project Risk Assessment. *J. Mar. Sci. Eng.* **2020**, *8*, 289. [CrossRef]
9. Katsidoniotaki, E.; Nilsson, E.; Rutgersson, A.; Engström, J.; Göteman, M. Response of Point-Absorbing Wave Energy Conversion System in 50-Years Return Period Extreme Focused Waves. *J. Mar. Sci. Eng.* **2021**, *9*, 345. [CrossRef]
10. Vanem, E.; Hafver, A.; Nalvarte, G. Environmental Contours for Circular-Linear Variables Based on the Direct Sampling Method. *Wind Energy* **2020**, *23*, 563–574. [CrossRef]
11. Haselsteiner, A.; Ohlendorf, J.-H.; Thoben, K.-D. Environmental Contours Based on Kernel Density Estimation. *arXiv* **2017**. [CrossRef]
12. Bitner-Gregersen, E.M. Joint Met-Ocean Description for Design and Operations of Marine Structures. *Appl. Ocean Res.* **2015**, *51*, 279–292. [CrossRef]
13. Montes-Iturrizaga, R.; Heredia-Zavoni, E. Environmental Contours Using Copulas. *Appl. Ocean Res.* **2015**, *52*, 125–139. [CrossRef]
14. Eckert-Gallup, A.; Martin, N. Kernel Density Estimation (KDE) with Adaptive Bandwidth Selection for Environmental Contours of Extreme Sea States. In Proceedings of the OCEANS 2016 MTS/IEEE, Monterey, CA, USA, 19–23 September 2016; pp. 1–5.
15. Jonathan, P.; Ewans, K.; Randell, D. Non-Stationary Conditional Extremes of Northern North Sea Storm Characteristics. *Environmetrics* **2014**, *25*, 172–188. [CrossRef]
16. Hirdaris, S.E.; Bai, W.; Dessi, D.; Ergin, A.; Gu, X.; Hermundstad, O.A.; Huijsmans, R.; Iijima, K.; Nielsen, U.D.; Parunov, J.; et al. Loads for Use in the Design of Ships and Offshore Structures. *Ocean Eng.* **2014**, *78*, 131–174. [CrossRef]
17. Chai, W.; Leira, B.J. Environmental Contours Based on Inverse SORM. *Mar. Struct.* **2018**, *60*, 34–51. [CrossRef]
18. Bang Huseby, A.; Vanem, E.; Natvig, B. A New Approach to Environmental Contours for Ocean Engineering Applications Based on Direct Monte Carlo Simulations. *Ocean Eng.* **2013**, *60*, 124–135. [CrossRef]
19. Derbanne, Q.; de Hauteclocque, G. A New Approach for Environmental Contour and Multivariate De-Clustering. In Proceedings of the ASME 2019 38th International Conference on Ocean, Offshore and Arctic Engineering, Glasgow, UK, 9–14 June 2019; Volume 3.
20. Haselsteiner, A.F.; Ohlendorf, J.-H.H.; Wosniok, W.; Thoben, K.-D.D. Deriving Environmental Contours from Highest Density Regions. *Coast. Eng.* **2017**, *123*, 42–51. [CrossRef]

21. Mackay, E.; Haselsteiner, A.F. Marginal and Total Exceedance Probabilities of Environmental Contours. *Mar. Struct.* **2021**, *75*, 102863. [CrossRef]
22. Ross, E.; Astrup, O.C.; Bitner-Gregersen, E.; Bunn, N.; Feld, G.; Gouldby, B.; Huseby, A.; Liu, Y.; Randell, D.; Vanem, E.; et al. On Environmental Contours for Marine and Coastal Design. *Ocean Eng.* **2020**, *195*, 106194. [CrossRef]
23. Eckert, A.; Martin, N.; Coe, R.G.; Seng, B.; Stuart, Z.; Morrell, Z. Development of a Comparison Framework for Evaluating Environmental Contours of Extreme Sea States. *J. Mar. Sci. Eng.* **2021**, *9*, 16. [CrossRef]
24. Haselsteiner, A.F.; Coe, R.G.; Manuel, L.; Chai, W.; Leira, B.; Clarindo, G.; Guedes Soares, C.; Hannesdóttir, Á.; Dimitrov, N.; Sander, A.; et al. A Benchmarking Exercise for Environmental Contours. *Ocean Eng.* **2021**, *236*, 109504. [CrossRef]
25. Tabain, T. The Proposal for the Standard of Sea States for the Adriatic. *Brodogradnja* **1974**, *25*, 251–258.
26. Tabain, T. Standard Wind Wave Spectrum for the Adriatic Sea Revisited (1977–1997). *Brodogradnja* **1997**, *45*, 303–313.
27. Hydrographic Institute of Republic of Croatia. *Atlas of the Climatology of the Adriatic Sea*; HHI: Split, Croatia, 1979. (In Croatian)
28. Parunov, J.; Ćorak, M.; Pensa, M. Wave Height Statistics for Seakeeping Assessment of Ships in the Adriatic Sea. *Ocean Eng.* **2011**, *38*, 1323–1330. [CrossRef]
29. Ćorak, M.; Mikulić, A.; Katalinić, M.; Parunov, J. Uncertainties of Wave Data Collected from Different Sources in the Adriatic Sea and Consequences on the Design of Marine Structures. *Ocean Eng.* **2022**, *266*, 112738. [CrossRef]
30. Petranović, T.; Mikulić, A.; Katalinić, M.; Ćorak, M.; Parunov, J. Method for Prediction of Extreme Wave Loads Based on Ship Operability Analysis Using Hindcast Wave Database. *J. Mar. Sci. Eng.* **2021**, *9*, 1002. [CrossRef]
31. Katalinić, M.; Parunov, J. Comprehensive Wind and Wave Statistics and Extreme Values for Design and Analysis of Marine Structures in the Adriatic Sea. *J. Mar. Sci. Eng.* **2021**, *9*, 522. [CrossRef]
32. Farkas, A.; Degiuli, N.; Martić, I. Assessment of Offshore Wave Energy Potential in the Croatian Part of the Adriatic Sea and Comparison with Wind Energy Potential. *Energies* **2019**, *12*, 2357. [CrossRef]
33. Bitner-Gregersen, E.M.; Waseda, T.; Parunov, J.; Yim, S.; Hirdaris, S.; Ma, N.; Guedes Soares, C. Uncertainties in Long-Term Wave Modelling. *Mar. Struct.* **2022**, *84*, 103217. [CrossRef]
34. Parunov, J.; Rudan, S.; Ćorak, M. Ultimate Hull-Girder-Strength-Based Reliability of a Double-Hull Oil Tanker after Collision in the Adriatic Sea. *Ships Offshore Struct.* **2017**, *12*, S55–S67. [CrossRef]
35. Barstow, S.; Mørk, G.; Lønseth, L.; Schjølberg, P.; Machado, U.; Athanassoulis, G.; Belibassakis, K.A.; Gerostathis, T.; Stefanakos, C.; Spaan, G. WORLDWAVES: Fusion of Data from Many Sources in a User-Friendly Software Package for Timely Calculation of Wave Statistics in Global Coastal Waters. In Proceedings of the 13th International Offshore and Polar Conference and Exhibition, ISOPE2003, Honolulu, HI, USA, 25–30 May 2003; pp. 136–143.
36. Barstow, S.; Mørk, G.; Lønseth, L.; Schjølberg, P.; Machado, U.; Athanassoulis, G.; Belibassakis, K.A.; Gerostathis, T.; Stefanakos, C.; Spaan, G. WORLDWAVES: High Quality Coastal and Offshore Wave Data within Minutes for Any Global Site. In Proceedings of the OMAE03 22nd International Conference on Offshore Mechanics and Arctic Engineering, Cancun, Mexico, 8–13 June 2003.
37. Barstow, S.; Mørk, G.; Lønseth, L.; Mathisen, J. WorldWaves Wave Energy Resource Assessments from the Deep Ocean to the Coast. *J. Energy Power Eng.* **2011**, *5*, 730–742.
38. Haselsteiner, A.F.; Lehmkuhl, J.; Pape, T.; Windmeier, K.-L.; Thoben, K.-D. ViroCon: A Software to Compute Multivariate Extremes Using the Environmental Contour Method. *SoftwareX* **2019**, *9*, 95–101. [CrossRef]
39. Haselsteiner, A.F.; Windmeier, K.-L.; Ströer, L.; Thoben, K.-D. Update 2.0 to "ViroCon: A Software to Compute Multivariate Extremes Using the Environmental Contour Method". *SoftwareX* **2022**, *20*, 101243. [CrossRef]
40. Klise, K.; Pauly, R.; Ruehl, K.M.; Olson, S.; Shippert, T.; Morrell, Z.; Bredin, S.; Lansing, C.; Macduff, M.; Martin, T.; et al. MHKiT (Marine and Hydrokinetic Toolkit)—Python [Computer Software]. 2020. Available online: https://github.com/MHKiT-Software/MHKiT-Python (accessed on 18 April 2023).
41. IACS. *IACS International Association of Classicfication Societies*; IACS: London, UK, 2019; pp. 1–13.
42. Jensen, J.J.; Mansour, A.E. Estimation of Ship Long-Term Wave-Induced Bending Moment Using Closed-Form Expressions. *RINA Trans.* **2002**, *144*, 41–55.
43. Michel, R.K.; Osborne, M. Oil Tankers. In *Ship Design and Construction*; Lamb, T., Ed.; SNAME: Jersey City, NJ, USA, 2004; pp. 29.1–29.41.
44. IACS. *Rec. No. 34. Rev.2 Standard Wave Data (North Atlantic Scatter Diagramm)*; IACS: London, UK, 2022.